UNIVERSITY OF NATAL

SCHOOL OF GEOLOGICAL AND COMPUTER SCIENCES

THE AHLMANNRYGGEN GROUP, WESTERN DRONNING MAUD LAND, ANTARCTICA.

By

Samantha Perritt

B.Sc. (Honours)

Submitted in fulfilment of the academic
requirements for the degree of
Doctor of Philosophy in the
Department of Geology,
University of Natal
Durban

November 2001

This thesis represents original work by the author and has not otherwise been submitted in any form for any degree or diploma to any tertiary institution. Where use has been made of the work of others, it is duly acknowledged in the text.

Samantha Helen Perritt

"At the bottom of this planet lies an enchanted continent in the sky... Sinister and beautiful she lies in her frozen slumber, her billowy white robes of snow weirdly luminous with amethysts and emeralds of ice, her dreams iridescent ice halos around the sun and moon, her horizons painted with pastel shades of pink, gold, green and blue. Such is Antarctica..."

Admiral Richard E. Byrd (1947)

ABSTRACT

The Mesoproterozoic Ritscherflya Supergroup forms an extensive volcano-sedimentary cover succession on the Archaean Grunehogna Province of western Dronning Maud Land, Antarctica. The oldest, predominantly sedimentary deposits of this cover succession are exposed across the Borgmassivet and southern Ahlmannryggen mountain ranges, and are collectively assigned to the Ahlmannryggen Group. A revised lithostratigraphy places exposures from these two regions in separate subdivisions, with three formations being recognised in the Ahlmannryggen (Pyramiden, Schumacherfjellet and Grunehogna Formations) and four formations being defined for the Borgmassivet (Veten, Framryggen, Högfonna and Bråpiggen Formations). Deposition of these successions occurred in a combination of fluvial braid-plain and braid-delta plain environments, with exposures in the Ahlmannryggen and Borgmassivet regions representing contemporaneous sedimentation in different portions of the same basin, under similar conditions.

The development of the Ahlmannryggen Group basin is attributed to flexing associated with continental collision during the assembly of Rodinia. Collision and accretion of a continental island arc terrain (the Maudheim Province) along the southern margin of the Grunehogna Province is considered responsible for flexural subsidence and the development of a peripheral foreland basin. The Ahlmannryggen Group represents 'molasse' stage infilling of this basin, with sedimentation being dominated by a combination of transverse and longitudinal drainage systems entering a depo-centre located to the east/southeast of the presently exposed succession.

Detritus entering the basin was sourced either directly or indirectly from at least seven different terrains, aged *ca.* 1135Ma, *ca.* 1335Ma, *ca.* 1600-1700Ma, *ca.* 2000-2100, *ca.* 2645Ma, *ca.* 2400-2900Ma and *ca* 2900-3300Ma, according to U/Pb detrital zircon SHRIMP analysis. The source terrains included the Maudheim Province, basement granites of the Grunehogna Province, an older sedimentary terrain dominated by a banded ironstone association, at least two further magmatic provinces and two metamorphic terrains. Of these source terrains, only the Maudheim Province and Grunehogna Province basement granites are presently exposed in western Dronning Maud Land.

The subsequent development of large-scale buckle folds and extensive brittle deformation within the Grunehogna Province cover rocks is attributed to the formation of a regionally extensive sinistral strike-slip system during NNW-SSE Pan-African compression, and can be correlated to structures exposed in the Maudheim Province and northern Mozambique. It is proposed that this strike-slip system developed in response to escape tectonics operating during a late stage of Gondwana amalgamation, as a result of the Ross Orogeny, and the suturing of East and West Antarctica.

ACKNOWLEDGMENTS

This project was made possible through the logistical support and generous funding provided by the Department of Environmental Affairs and Tourism – Directorate: Antarctica and Islands. Thanks must go to many people involved in the South African National Antarctic Programme, with special acknowledgment of the assistance provided by the personnel of 22 Squadron of the South African Air Force and members of the SANAE 37, 38 and 39 teams. Special thanks also to Andre Hattingh, Sam Oosthuizen and Henry Valentine for the excellent logistical organisation of the field seasons. Experienced field operation managers Rick Lewis and Ian Manson, who passed on a wealth of practical knowledge and ensured a safe conclusion to both the `98-`99 and `99-`00 seasons, are gratefully acknowledged.

Special thanks must go to Prof Mike Watkeys, for his enthusiastic supervision and endless encouragement and motivation. Dr Greg Whitmore, many thanks for your assistance, advice and support. I am deeply indebted to Mawson Croaker, not only for his assistance in the field, but also for the wealth of constructive advice that he has provided. The success of this project was in no small part as a result of his interest and support. Dr Richard Armstrong of the Australian National University is gratefully acknowledged for the help he provided during collaborative geochronological work on detrital zircon suites. Thanks must also go to the technical staff of the geology department, Mukesh Seyambu, Pat Suthan and Roy Seyambu, for their assistance during sample preparation.

Many thanks to the remaining staff members and other post-graduate students in the department for their interest and encouragement. In particular, thanks to Benardo and Claire for putting up with numerous interruptions and discussions. Rio and Charl – a thousand thanks for the constant interest, support, distraction and motivation. Lastly, a special thank-you must go to the members of my family, their continued support during the years of both undergraduate and post-graduate study is greatly appreciated.

CONTENTS

SECTION A

1-INTRODUCTION
2-REGIONAL GEOLOGY
3-LITHOSTRATIGRAPHY

Overview:
Section A is designed to give the reader a general introduction to the regional geology of the study area and the nature of the investigation undertaken by the author. A detailed stratigraphic revision is also presented so that the observations described in the following sections can be placed in their correct geological context.

1. INTRODUCTION

The Ahlmannryggen Group, first described by Roots (1953), represents the lower clastic deposits of a volcano-sedimentary cover succession referred to as the Ritscherflya Supergroup, which extends across the Borgmassivet and Ahlmannryggen regions of western Dronning Maud Land (WDML), Antarctica (Figure 1.1). Despite good exposure, the lithotectonic status of the Ahlmannryggen Group within the crustal framework of WDML has remained controversial since it was first described.

The importance of the Ahlmannryggen Group lies in its loosely constrained Mesoproterozoic age (Moyes *et al.*, 1995a; Moyes and Harris, 1996) and the fact that it provides a unique record of basin evolution during the ~1200-1000Ma event recorded in WDML, Mozambique and KwaZulu Natal. The low metamorphic grade and relatively mild deformation of the Ahlmannryggen Group have resulted in a remarkably well preserved succession, providing an ideal opportunity to examine the nature of this episode of tectonism from a cratonic perspective and allows for the refining of models of local plate assembly. The Ahlmannryggen Group also records a number of post-depositional deformation events, suggesting that the Borgmassivet and Ahlmannryggen mountain ranges represent a crucial area for investigating the nature of both the ~1200-1000Ma ("Kibaran") and ~500Ma ("Pan-African") episodes in WDML. Attempts to unravel the intricacies of these events within the highly deformed basement rocks of Dronning Maud Land are often frustrated by the cryptic nature of the superimposed deformation events and the inherent difficulties in interpreting geochronological data from high grade poly-metamorphic terrains (Groenewald *et al.*, 1995; Jackson, 1997).

The geology of the Borgmassivet and Ahlmannryggen regions assumes further prominence in the light of uncertainties regarding the nature of the underlying Archaean basement, which has alternatively been interpreted as an isolated microplate (Barton *et al.*, 1987) or a fragmented extension of the Kaapvaal Craton (Groenewald *et al.*, 1995). Plate reconstructions based on palaeomagnetic data and marine geophysical evidence reveal that the Grunehogna Province and Kaapvaal-Zimbabwe Cratons were juxtaposed from the mid Proterozoic until the Mesozoic (Peters, 1989; Hodgkinson, 1989; Gose *et al.*, 1997; Martin and Hartnady, 1986) (Figure 1.2). The tectonic evolution of WDML during the amalgamation of the supercontinents of Rodinia and Gondwana is therefore closely linked to that of southern Africa.

Despite the fundamental importance of the Ahlmannryggen Group in understanding the crustal evolution of WDML, the stratigraphy, sedimentary environments, age, provenance, structural deformation and tectonic setting are not well understood. This study integrates diverse geological data sets, in order to more accurately constrain the evolution, tectonic setting and deformation of the Ahlmannryggen sedimentary basin.

1.1 PURPOSE AND AIMS

This project arose from the lack of comprehensive studies on the 1200-1000Ma Ritscherflya Supergroup and the poor understanding of the lithotectonic status of the Ahlmannryggen Group. The research was designed to partly fulfil Study Four of the previous SANAP Earth Science five year plan: Characterisation of the Mesoproterozoic to Palaeozoic evolution of western Dronning Maud Land (Krynauw *et al.*, 1996).
The project aims to:

- determine the lithostratigraphy, sediment-ology and provenance of the Ahlmannryggen Group in order to decipher the depositional environments and tectonic setting of the Ahlmannryggen sedimentary basin and further elucidate the geological evolution of WDML;
- determine if the Ahlmannryggen Group can be correlated with other sedimentary successions cropping out in southern Africa (with specific reference to the Umkondo Group of Zimbabwe and Mozambique); and
- elucidate the tectonic styles associated with Pan-African(?) deformation of the Grunehogna Province, and thus allow extrapolation and comparison with adjacent Pan-African terrains.

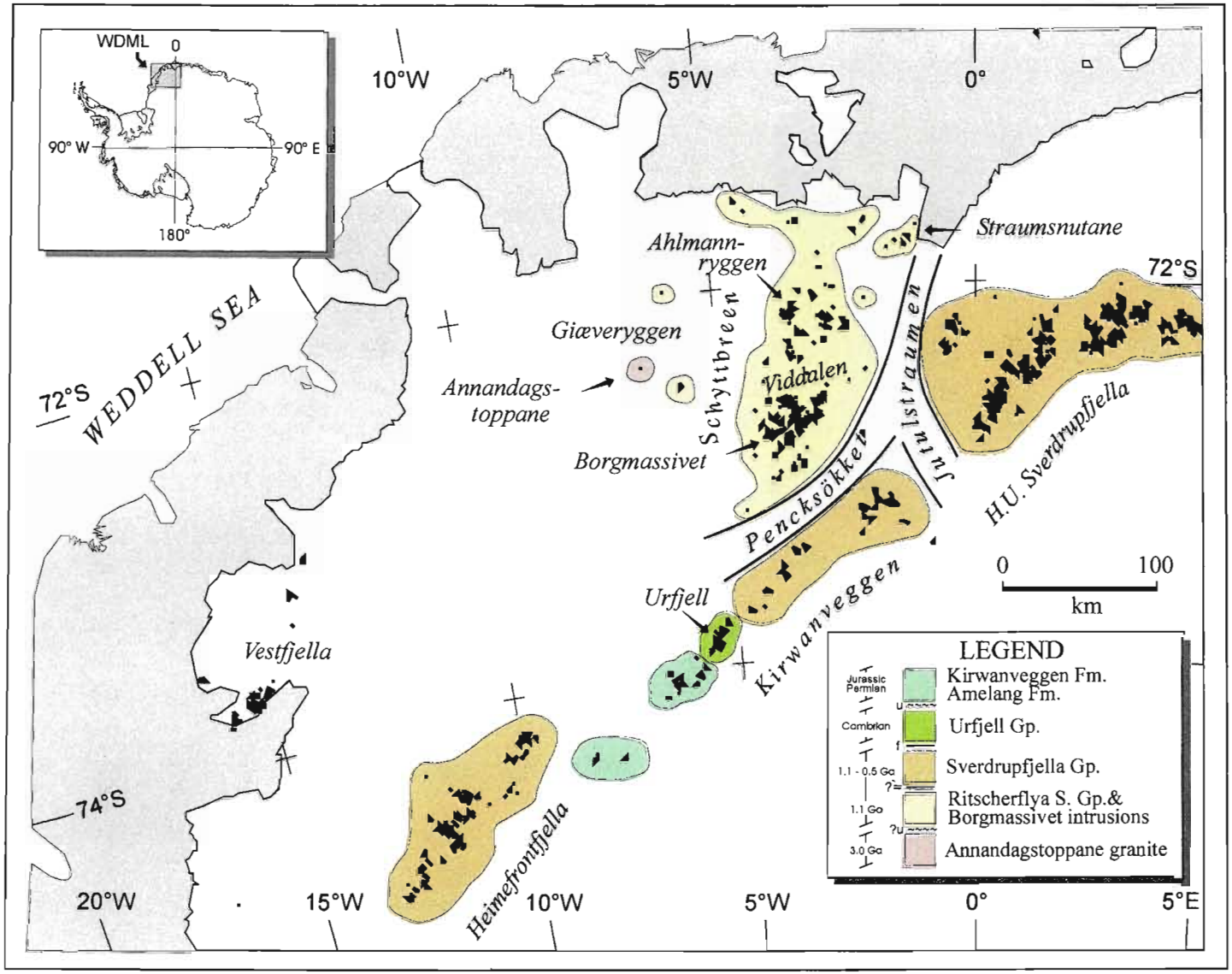

Figure 1.1: Location and regional geology map of western Dronning Maud Land (modified from Jackson, 1997). WDML is dominated by two distinct provinces, the Ahlmannryggen-Borgmassivet Block (Grunehogna Province) and the Heimefrontfjella-Kirwanveggen-Sverdupfjella Belt (Maudheim Province), which are separated by a major physiographic discontinuity along the Jutulstraumen and Pencksökket Glaciers. The Ahlmannryggen Group is exposed in the Borgmassivet and southern Ahlmannryggen regions, as well as at isolated localities in the Giæveryggen.

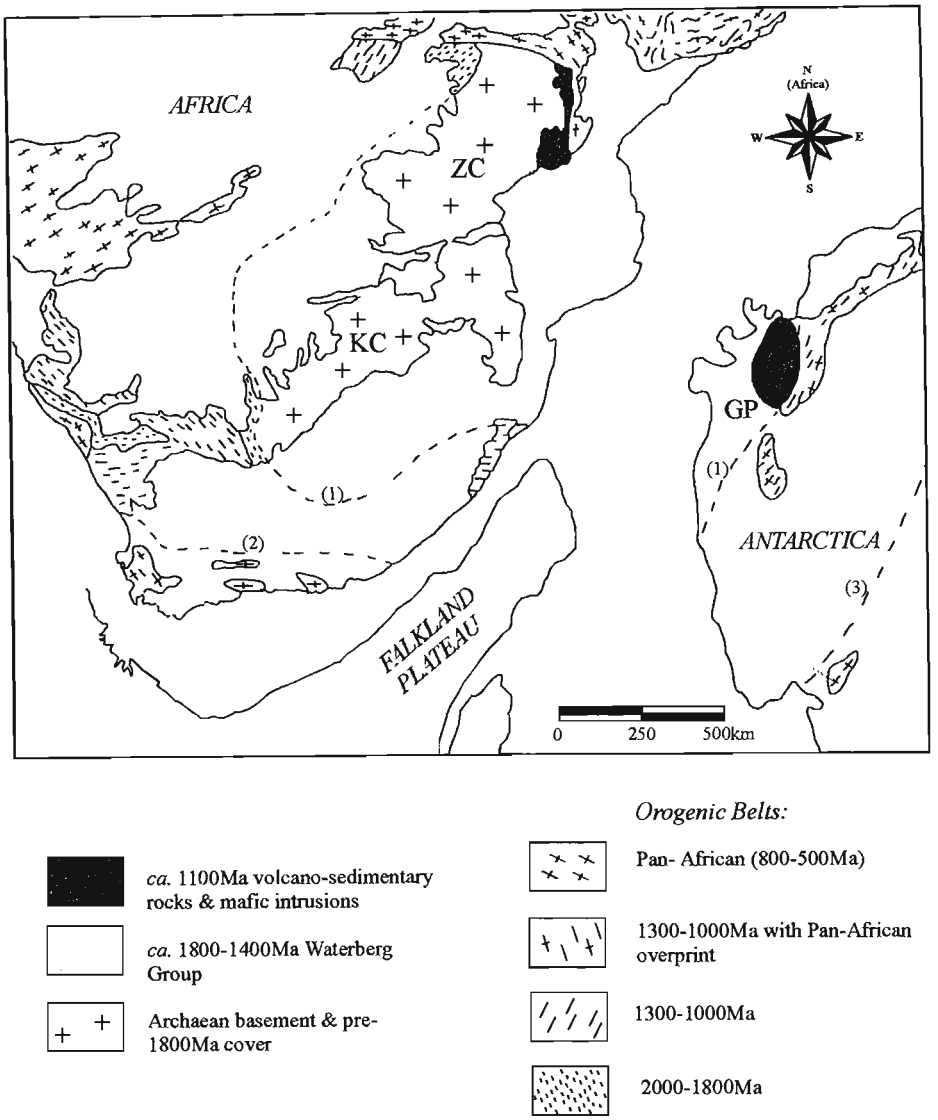

Figure 1.2: Plate reconstructions based on palaeomagnetic data and marine geophysical evidence reveal that the Grunehogna Province (GP) was juxtaposed with the Kaapvaal and Zimbabwe Cratons (KC, ZC) between the mid Proterozoic and the Mesozoic (restored to pre-Mesozoic-drift positions after De Wit *et al.*, 1988). The Ahlmannryggen Group forms the oldest exposed sequence in the Grunehogna Province cover rocks, and provides for an ideal opportunity to refine models of local plate assembly. [Inferred tectonic boundaries-after Hanson *et al.*, 1998: (1)-edge of Archaean cratonic basement, (2)-boundary between Namaqua-Natal belt and Pan-African orogen in southern Africa, (3)-possible Pan-African suture in Antarctica.]

In order to achieve the aims of this research project, the following work objectives needed to be completed:

- mapping of the Ahlmannryggen Group exposures and the regional geology of the Ahlmannryggen and Borgmassivet, in order to accurately define the lithostratigraphy of the regions.
- detailed sedimentological analysis involving the construction of sedimentary logs and lateral profiles, to aid the definition of lithofacies, facies associations and architectural elements in order to elucidate the depositional environments of the Ahlmannryggen Group.
- sampling for the purpose of major and trace element whole-rock geochemistry, U/Pb detrital zircon Sensitive High Resolution Ion Micro-Probe (SHRIMP) analysis and petrology in order to understand the provenance of the Ahlmannryggen Group and elucidate possible source terrains and the tectonic setting.
- structural analysis in order to determine the nature of the deformation affecting the Ahlmannryggen Group, and the tectonic relationship of the Ahlmannryggen Group to the rest of WDML.
- development of a tectonic model for the evolution of the Ahlmannryggen Group and Grunehogna Province, integrating sedimentology, provenance, geochronology and structural data sets.

1.2 LOCATION AND PHYSIOGRAPHY

The Ahlmannryggen Group is exposed as isolated nunataks and groups of nunataks in the Ahlmannryggen and Borgmassivet regions (Figure 1.1, 1.3a, b, Map 1). The Ahlmannryggen forms a broad, north-easterly trending ridge bordered by the Jutulstraumen glacier to the east and the Schyttbreen glacier on the west. Rock outcrops are scarce, and occur as scattered nunataks and groups of nunataks, occupying approximately 2% of the area. In general, the snow surface slopes to the north, descending from some 1400m in the south-eastern part to about 100m at its junction with the ice shelf. This slope is also reflected by the summit levels of the nunataks, which decrease from 1800 m in the south, to less than 200m in the north. The erosion of the nunataks in the Ahlmannryggen is typically alpine, and exposed surfaces are shattered, leading to scarp recession and the formation of cirques. Ultimately, this results in the development of knife-edged arêtes and pyramidal horns, the best example of which is the Matterhorn-like Istind, the highest and most prominent peak in the Ahlmannryggen, 1838m above mean sea level (Wolmarans and Kent, 1982).

The Ahlmannryggen is separated from the adjoining Borgmassivet by the east-northeast trending Viddalen ice stream, a tributary of the Jutulstraumen. The Borgmassivet has a much higher proportion of exposed rock than the Ahlmannryggen, almost 10%. It comprises an area of some 1500km^2, in which the nunataks are generally closely spaced, flat-topped mesas. They are higher than those of the Ahlmannryggen and are characterised by sheer walls towering as much as 1000m above the surrounding ice. Here the mountains are shaped mainly by scarp recession, rather than cirque recession as in the Ahlmannryggen. In the Borgmassivet, the thick sills that intrude the rocks of the Ritscherflya Supergroup have exercised a more obvious control on the topography than in the Ahlmannryggen. These sills are more resistant to frost weathering, with the result that many of the mountains are table-like, with their tops defined by intrusions (Wolmarans and Kent, 1982).

The Ahlmannryggen Group exposures range between 30km and 160km south of the South African Antarctic Base, SANAE IV, and access to the nunataks is by skidoo and foot. This study is based on fieldwork in the Borgmassivet and Ahlmannryggen carried out during the 1998/1999 and 1999/2000 Austral summer seasons, under the auspices of the South African National Antarctic Programme (SANAP).

1.3 PREVIOUS INVESTIGATIONS

During the period 1949 to 1952, the Norwegian-British-Swedish Antarctic expedition explored much of WDML and produced the first topographic and geological maps based on aerial photographs and overland traverses. Roots and Reece were the geological personnel on this expedition, and they assigned the sedimentary succession exposed west of the Jutul glacier

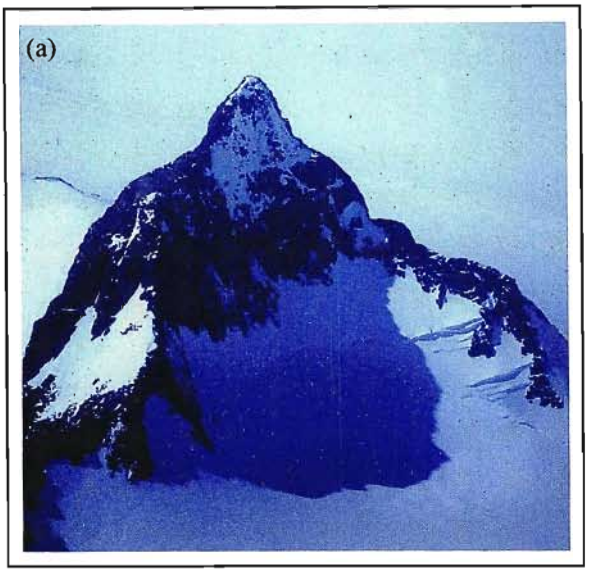

Figure 1.3: (a) The 200m high SE face of the Matterhorn-like peak of Istind Nunatak in the eastern Ahlmannryggen. Nunataks in the Ahlmannryggen region are characterised by knife-edged arêtes and pyramidal horns due to alpine-like erosion.

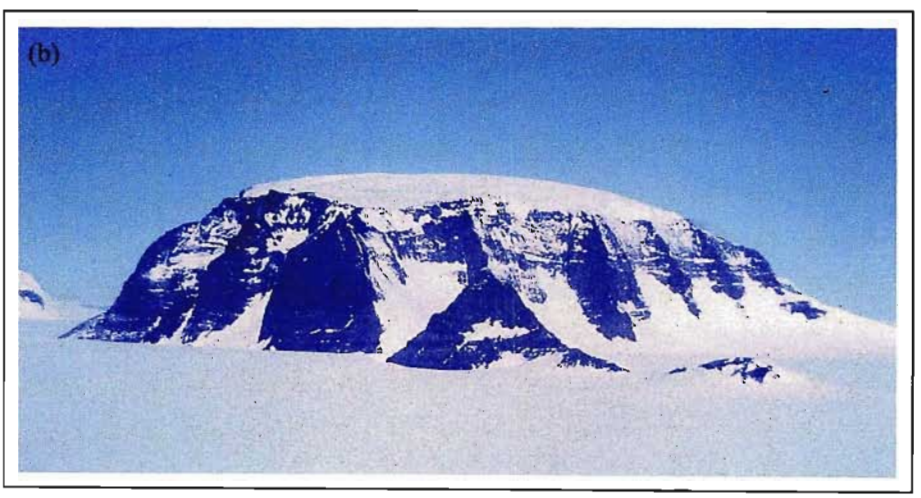

Figure 1.3: (b) The nunataks in the Borgmassivet are preferentially shaped by scarp recession and are often capped by thick sills. As a result, the nunataks tend to form flat-topped mesas with shear walls, as seen at Domen, a peak in the central Borgmassivet that rises 540m above the Raudbergdalen glacier.

(present day Jutulstraumen) to an Ahlmannrygg Group (Roots, 1969).

South African research in WDML prior to 1976 concentrated on the Grunehogna Province and the Kirwanveggen escarpment, but soon expanded to include the H. U. Sverdrupfjella (e.g. Grantham, 1992, Groenewald, 1995). In the late 1960's, concurrent investigations were carried out by De Ridder (1970) and Neethling (1970) on the Ahlmannryggen Group in the Borgmassivet and Ahlmannryggen regions respectively. Neethling (1970) described a sedimentary succession with a mainly continental depositional setting, varying initially from shallow water marine to subaerial at the time of closure; while De Ridder (1970) envisaged a large, shallow flood plain affected by occasional episodes of transgression and regression. Detailed work on the Grunehogna cluster of nunataks was also carried out during the late 1960's by Aucamp (1972), who favoured a deltaic depositional environment for the sedimentary rocks exposed in the area. Bredell (1977) expanded on Aucamp's work during 1970-1971, to include most of the exposures in the Ahlmannryggen area. In 1982, Wolmarans and Kent published a summary of all past research done in WDML, and proposed the currently accepted stratigraphic subdivisions for the Ritscherflya Supergroup. Subsequent investigations of the Ahlmannryggen Group were carried out by Ferreira and Swanepoel (1983 to 1985), in the Ahlmannryggen and Borgmassivet areas respectively. Ferreira (1986) retained the stratigraphic subdivisions of Wolmarans and Kent (1982), but proposed the existence of a regressive depositional cycle from marine to braided and meandering river environments. Swanepoel (1988) only recognised fluvial deposits and proposed dramatic revisions to Wolmarans and Kent's (1982) stratigraphic subdivisions.

Concurrent to the investigations of the sedimentary Ahlmannryggen Group, detailed research was also conducted on the volcanic lithologies of the Jutulstraumen Group (Watters *et al.*, 1991) and the extensive mafic sills of the Borgmassivet Suite (Krynauw, 1986; Krynauw *et al.*, 1987, 1991).

This study is designed to resolve the many conflicting ideas regarding the nature of the Ahlmannryggen basin and provide a new perspective on the tectonic evolution of the region. The various analytical techniques and methods used to meet the aims of the study are described in Appendix 1.

2. OUTLINE OF THE REGIONAL GEOLOGY

2.1 INTRODUCTION

Western Dronning Maud Land consists broadly of two distinct geological terrains (Figure 1.1). To the west is a relatively undisturbed Proterozoic volcano-sedimentary succession overlying Archaean basement granites – the Grunehogna Province (Krynauw, 1996a), while to the east there are the poly-cyclically deformed high-grade metamorphic rocks of the Proterozoic H.U. Sverdrupfjella, Kirwanveggen and Heimefrontfjella, which constitute the Maudheim Province (Groenewald *et al.*, 1991). The boundary between these two provinces is masked by the Jutulstraumen and Pencksökket glaciers.

The Maudheim Province exhibits a complex tectonothermal history. Models proposed for the crustal evolution of this province indicate that the terrain formed in volcanic island arc to retro-arc marginal basin settings (Grantham *et al.*, 1995; Groenewald *et al.*, 1995; Jacobs *et al.*, 1996). Widespread zircon crystallisation ages of 1.2Ga to 1.1Ga are interpreted to represent the age of the island arc (Harris, 1999), while two orogenic episodes, at 1135-900Ma and 550-450Ma respectively, are recognised (Jacobs *et al.*, 1996; Jackson, 1997; Board, 2001).

Exposures occurring in the Grunehogna Province are in marked contrast to those of the high-grade belt. The region to the west of the Jutulstraumen-Pencksökket glacial divide is dominated by a well preserved cratonic cover succession (Ritscherflya Supergroup) overlying Archaean basement granites (Wolmarans and Kent, 1982).

This study focuses on the Ahlmannryggen Group of the Ritscherflya Supergroup, the oldest exposed succession in the cover succession and one of four lithotectonic units recognised in the Grunehogna Province. The lithologies and field relationships of the different tectonic units in the Grunehogna Province are examined in this section, and form the basis for later discussions and conclusions.

The four lithotectonic units recognised in the Grunehogna Province include (Figure 2.1):

- the *ca.* 3000Ma Annandagstoppane basement granite;
- the Mesoproterozoic Ritscherflya Supergroup;
- the *ca.* 1000Ma(?) Borgmassivet Suite; and
- occasional mafic Jurassic dykes.

2.2 BASEMENT GRANITE

The Annandagstoppane basement granite was first discovered by Russian geologists during the 1960's. The granite is exposed at three nunataks in WDML, and comprises medium- to coarse-grained granite crosscut by veins of pegmatite and graphic granite (Barton *et al.*, 1987). It is typically undeformed, and shows the development of crude layering, which Krynauw (1996a) attributed to crystal-size variations. Hydrothermal alteration is variably developed, and has affected only certain minerals in any phase. According to Barton *et al.* (1987), the results of Rb-Sr and Pb whole rock and mineral isotopic analysis suggests that:

- the granite was emplaced between 3115-2945Ma ago,
- the Sr isotopes were nearly homogenised on a whole rock scale at ~2823Ma, by hydrothermal alteration, and
- the intrusion of a gabbro phase at ~1200Ma reset the Rb-Sr system in biotite.

Barton *et al.* (1987) inferred that the granite is of S-type because it is per-aluminous, has a high SiO_2 content, lacks hornblende and sphene, and contains accessory monazite and muscovite. According to Krynauw (1996a), one of the main problems regarding the interpretation of the Annandagstoppane granite is the extremely small outcrop area (~10 000m^2), in relation to its importance in terms of correlation with the Kaapvaal Craton.

Rather than calling the region the Grunehogna Craton, Krynauw (1996a) proposed that the term Grunehogna Province be used, reflecting the uncertainty regarding the nature of the basement underlying most of the area.

Two contrasting origins have been proposed for the Grunehogna Province; it is considered to represent either an isolated microplate (Barton *et al.*, 1987) or a fragmented extension of the

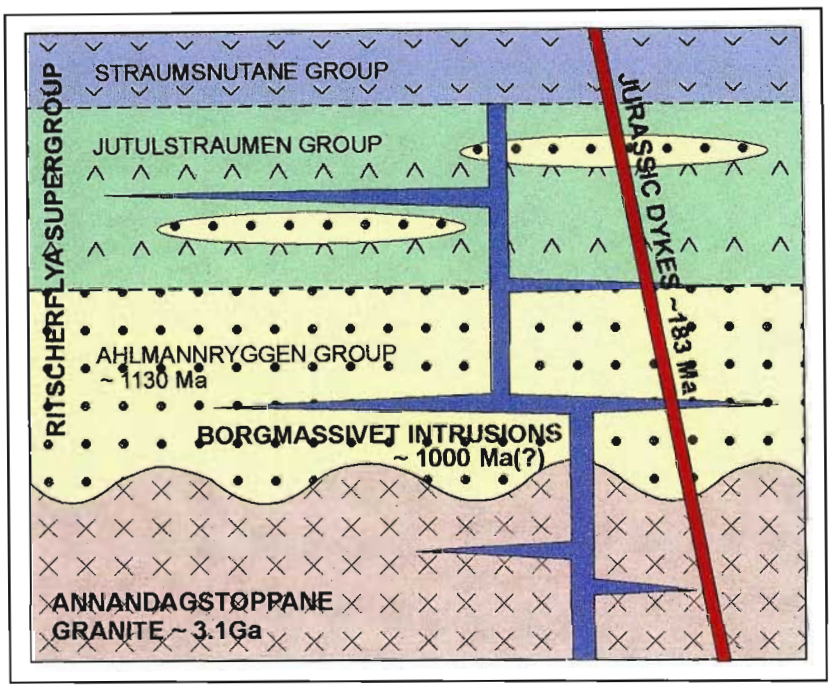

Figure 2.1: Inferred relationships between the four lithotectonic units exposed in the Grunehogna Province of WDML. The Ritscherflya Supergroup is considered to unconformably overlie the Annandag-stoppane Granite, although the contact is not exposed. The lower Ahlmannryggen Group is a predominantly sedimentary sequence, while the overlying Jutulstraumen Group is dominated by volcaniclastics with minor intercalated sedimentary units. The Borgmassivet Suite consists of the Borgmassivet intrusions and basalts of the Straumsnutane Group, which are considered consanguineous on the basis of geochemical data. Rare mafic dykes of Jurassic age cross-cut the Ritscherflya Supergroup.

Kaapvaal Craton of southern Africa (Wolmarans and Kent, 1982, Krynauw *et al.*, 1991, Groenewald *et al.*, 1995). Both these interpretations are based on an extremely limited exposure of basement granite in the Giaeverryggen area of WDML.

Barton *et al.* (1987) suggested that the granite is unlike any other granite of this age documented in southern Africa or East Antarctica, and speculated that the Grunehogna Province originated as a micro-continent. According to Groenewald *et al.* (1995), the uniqueness of the granite is equivocal as Barton *et al.* (1987) based their interpretation on limited geochemical and petrographic data (10 samples) and the Annandagstoppane granite may in fact share certain similarities with granites in the Barberton Mountain Land area of South Africa. As such, the Grunehogna Province may alternatively be regarded as a fragment of the Kaapvaal Craton.

An Archaean age for the granite was first suggested by Halpern (1970) who determined a model Rb-Sr whole rock age of approximately 2960Ma. These results were supported by the findings of Barton *et al.* (1987), who reported whole rock Pb-Pb data indicating an age of 2937 ±84Ma, although the most linear fit gave a slightly older age of 3111 ±78Ma. Moyes and Barton (1990) reported Rb-Sr data from eight muscovite separates which gave a weighted average model age of 2942 ±21Ma, essentially indistinguishable from the Pb-Pb whole rock data, whereas the Rb-Sr whole rock data gave an errorchron age of 2818 ±98Ma. They interpreted the latter age as indicating that the granite was non-isochemically affected by some event at this time. Two biotite separates gave Rb-Sr model ages of 1250Ma and 1083Ma, which were interpreted to reflect resetting events.

2.3 RITSCHERFLYA SUPERGROUP

The Ritscherflya Supergroup extends across the Ahlmannryggen and Borgmassivet mountain ranges of the Grunehogna Province, with an isolated exposure also recorded from Giaeverryggen to the west. As a result of extensive snow / ice cover, the nature of the relationship of the volcano-sedimentary Ritscherflya Supergroup to the granite exposed at Annandagstoppane is entirely based on assumptions regarding the nature of intermediate to mafic sills and dykes which intrude both the Archaean granite and the Ritscherflya Supergroup (Krynauw, 1996).

The Ritscherflya Supergroup has traditionally been divided into a lower, predominantly sedimentary succession (Ahlmannryggen Group), and an upper, mainly volcanic succession (Jutulstraumen Group). This currently accepted stratigraphy of the Ritscherflya Supergroup is outlined in Wolmarans and Kent (1982), however a three-fold subdivision within the supergroup provides a more accurate representation of the nature of this cover succession. Currently, thick basaltic to andesitic lava flows exposed in the Straumsnutane region (located to the NE of the Ahlmannryggen, Figure 1.1) are assigned to the Straumsnutane Formation, forming the uppermost succession in Wolmarans and Kent's Jutulstraumen Group. Yet, on geochemical grounds, these extrusions are correlated with extensive tholeiitic sills which intrude the sediments of the Ahlmannryggen Group and the volcaniclastics of the underlying formations in the Jutulstraumen Group (Krynauw *et al.*, 1991), and are regarded as representing a distinct magmatic event. It is therefore proposed that these lavas be assigned to a separate group in order to reflect their contrasting mode of formation -the Straumsnutane Group (Figure 2.1).

Extensive revisions to the litho-stratigraphy of the Ahlmannryggen Group are also recommended, and are discussed in detail in the following chapter (Chapter 3).

2.3.1 The Ahlmannryggen Group

The rocks of the lower Ahlmannryggen Group (Figure 2.2a) crop out in the Borgmassivet and southern Ahlmannryggen regions, with limited exposure also recorded by Krynauw (1986) from Forstefjell in the Giaeverryggen. This sedimentary succession is sandstone to fine-grained/mudstone dominated, with minor gravel deposits, and provides a record of deposition in continental braided fluvial and delta-plain settings. The lithostratigraphy, sedimentology, provenance, structure and tectonic setting of the Ahlmannryggen Group are reported in detail in the following sections of this thesis.

2.3.2 The Jutulstraumen Group

The revised Jutulstraumen Group comprises a succession of sedimentary breccia deposits and

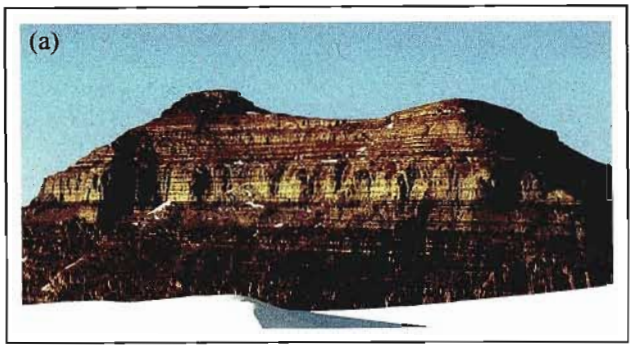

Figure 2.2:(a) The Ahlmannryggen Group is a sandstone to fine-grained dominated sequence. The exposure on the southern face of Nunatak 1885 in the central Borgmassivet is typical of many of the Ahlmannryggen Group outcrops, which are often characterised by laterally persistent, alternating units of sandstone and mudstone. The cliff face is about 180m high. (Photo locality- S face of Nunatak 1885).

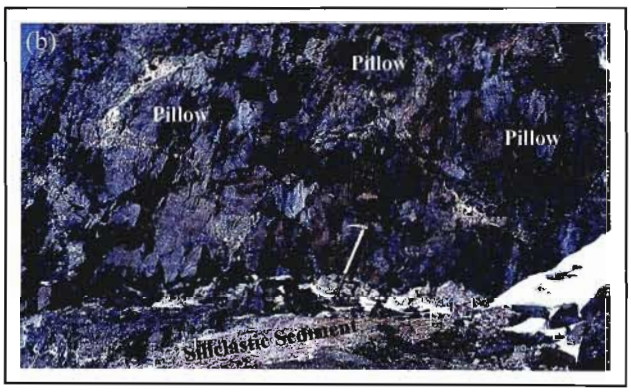

Figure 2.2:(b) The Straumsnutane Group (revised from Wolmarans and Kent, 1982) is dominated by subaerial basaltic to andesitic lava flows, in which pillow structures and rare intercalated siliclastic units are preserved, suggesting the presence of localised bodies of water (the ice axe is approximately 75cm long). (Photo locality- N face of Snökallen, Straumsnutane).

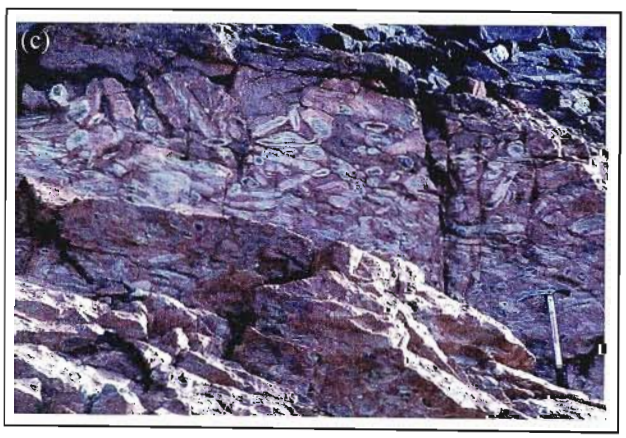

Figure 2.2:(c) Sills of the Borgmassivet Suite intruded wet, unconsolidated or partially lithified sediments at shallow crustal levels (Krynauw *et al.*, 1988). The resulting sediment-sill interaction zone is characterised by numerous ovoid bodies and vugs, with one of the most striking exposures occurring at Grunehogna, in the central Ahlmannryggen. (Photo locality- SE face of Grunehogna Peak 1285).

tuffs, overlain by arenites and interbedded agglomerates and tuffs. Watters *et al.* (1991) considered these successions to be alluvial fan deposits associated with active fault scarps. Three formations are assigned to the Group (revised from Wolmarans and Krynauw, 1981; Wolmarans and Kent, 1982):

- the Fassetfjellet Formation, forming an isolated exposure at Fassetfjellet in the north-eastern to central Borgmassivet; and
- the Tindeklypa and Istind Formations, which together form the Viddalen Subgroup, and occur in the eastern Ahlmannryggen.

2.3.3 The Straumsnutane Group

The revised Straumsnutane Group comprises a succession of basaltic to basaltic-andesite lava flows with minor intercalated siliciclastic beds (Figure 2.2b). The isolated and relatively sparse exposures inhibit detailed stratigraphic discrimination, and the full extent of the succession is unknown. An estimated 850m is exposed, but neither the upper nor lower contacts have been identified, and this must be regarded as a minimum estimate (Watters *et al.*, 1991). Although the lava flows were emplaced in a dominantly subaerial environment, the presence of bodies of water is reflected by the local occurrence of pillow lava, hyaloclastite beds and rare tuffaceous sedimentary layers exhibiting ripple marks and desiccation structures (Watters *et al.*, 1991; Groenewald *et al.*, 1995).

2.3.4 Age

The Ritscherflya Supergroup apparently accumulated during the mid-Proterozoic, although absolute age data for individual units are sparse, principally due to a lack of suitable samples for isotopic analysis and pervasive hydrothermal alteration (Barton *et al.*, 1987). The sediments are commonly metamorphosed to the muscovite-chlorite or quartz-albite-epidote-biotite grade of the greenschist facies of regional metamorphism, and frequently show evidence of contact metamorphism adjacent to intrusives.

Moyes *et al.* (1995a) analysed sediments from Grunehogna Nunatak (the Grunehogna Formation) and reported a Sr T_{chur} average age of 1129Ma, which was interpreted as reflecting the time of deposition or diagenesis of the sediment, based on work by McCulloch and Wasserburg (1978). A 1080Ma average of Rb-Sr and Sm-Nd dates was interpreted as an approximation of the consolidation or lithification age. A significantly older Nd T_{chur} age of ~1808Ma was taken as being indicative of the average age of the crust from which the sediments were derived, assuming a bulk earth composition. However, Moyes *et al.* (1995a) indicated that the T_{dm} ages of ~2171Ma may be a more accurate reflection if a depleted source is considered. Moyes and Harris, (1996) determined a 1136 ±2Ma Pb-Pb evaporitic zircon age for a volcaniclastic unit exposed at Bråpiggen (from the Bråpiggen Formation - this study). Whole rock Sm-Nd results gave a wide scatter, but apparently 5 samples were more closely grouped about a line equivalent to an age of 1003 ±192Ma.

Although primarily undertaken to aid provenance studies, Sensitive High-Resolution Ion Micro-Probe (SHRIMP) analysis of three samples from the Ahlmannryggen Group confirms a *ca.* 1135Ma maximum age for the upper portions of the succession. Unfortunately, the minimum age of the Ritscherflya Supergroup is relatively poorly constrained due to the lack of precise chronological controls for the Borgmassivet Suite. Contamination and pseudo-isochrons have resulted in a wide range of ages being reported for the sills (Borgmassivet Intrusions), varying from 1802 ±100Ma to 767 ±49Ma (Moyes *et al.*, 1995a), while reported ages for the extrusives (Straumsnutane Group) range from 1115 ±37Ma to 465 ±16Ma (Peters *et al.*, 1991).

2.3.5 Structure

Compared to the adjacent high-grade metamorphic Maudheim Province, which has been subjected to a number of superimposed ductile deformation events (Groenewald *et al.*, 1995; Grantham *et al.*, 1995), the deformation affecting the Grunehogna Province is relatively mild, being confined to brittle deformation and gentle folding. Consequently, the region is often referred to as undisturbed or undeformed (e.g. De Ridder, 1970; Grantham and Hunter, 1991; Krynauw, 1996a,b; Moyes *et al.*, 1993). This is not the case, and the deformation and its significance are described in detail in Section C3.

2.4 BORGMASSIVET SUITE

The extensive and widespread Borgmassivet intrusions (described in detail by Krynauw *et al.*, 1988, 1990, 1991, 1994; Watters *et al.*, 1991; Peters *et al.*, 1991) form most of the outcrops in the northern parts of the Grunehogna Province.

The Borgmassivet intrusions occur as sills up to 400m thick and layered bodies of unknown lateral and vertical extent. Lithologies include quartz gabbro, gabbronorite, and granophyric quartz monzogabbro. The sills are generally concordant with the sedimentary units of the Ritscherflya Supergroup, but locally may exhibit a crosscutting relationship. Minor volumes of granite also occur locally.

Previously, these intrusions were subdivided into the Robertskollen and Nils Jorgennutane Suites. However, Krynauw *et al.* (1990) recommended that these subdivisions be dropped in favour of an all-inclusive term, the Borgmassivet Suite. The Borgmassivet Suite includes the Borgmassivet Intrusions (all the mid-Proterozoic intrusions in the Ritscherflya Supergroup) and the basalts of the (revised) Straumsnutane Group. The minor granites, representing small-scale products of anatectic melting of wet sediments adjacent to the Borgmassivet intrusives, are termed the Grunehogna Granites by Krynauw *et al.* (1990).

On the basis of the contact relations and petrography of reconstituted sediments, Krynauw *et al.* (1988) concluded that some sills intruded wet, unconsolidated or partially lithified sediments at shallow crustal levels (Figure 2.2c). Virtually instantaneous fluidisation within the peripheral sediment-sill interaction zones destroyed the sedimentary structures, and heating of the peripheral zone resulted in partial melting within the hydrous system.

The geochemisty of the Borgmassivet Suite, which exhibits tholeiitic and minor calc-alkaline characteristics, is described in detail by Krynauw *et al.* (1991), Watters *et al.* (1991) and Peters *et al.* (1991). Coherence of geochemical data suggests that the magmas from which the Borgmassivet intrusions and basalts of the Straumsnutane Group solidified, were consanguineous. According to Krynauw *et al.* (1991), the geochemical patterns resemble those for continental tholeiites, such as the Karoo basalts of South Africa, the Kirkpatrick basalts from southern Victoria Land and the Sudbury Complex, although tholeiitic island arc suites cannot be excluded.

The intrusions provide a considerable range of ages in the Rb-Sr system, which initially led to confusion about the age of the sediments in which they are emplaced. Continued research using Sm-Nd, Rb-Sr and Pb-Pb systematics has led to provisional conclusions that the mafic magmatism occurred at *ca.* 1000Ma (Moyes *et al.*, 1995a). All older ages are attributed to isotopic pseudo-isochrons caused by crustal contamination and hydrothermal alteration (Krynauw *et al.*, 1991; Moyes *et al.*, 1993; Moyes *et al.*, 1995a). Nevertheless, a *ca.* 1000Ma age conflicts with the 1080Ma lithification age proposed by Moyes *et al.* (1995a) for the sediments of the Ahlmannryggen Group. If the sills intruded wet, unconsolidated or partially lithified sediments, as described by Krynauw *et al.* (1988), a pre- 1080Ma age is implied, and the younger *ca.* 1000Ma age must be considered unreliable.

A pre- 1080Ma age for the Borgmassivet Suite would also accord with its proposed correlation with the Umkondo dolerites of Mozambique-Zimbabwe (Swanepoel, 1995), dated at 1105Ma by Hanson *et al.* (1998) and Wingate (2001).

2.5 JURASSIC DYKES

Mafic dykes have intruded the rocks of the Ritscherflya Supergroup, as well as the Borgmassivet Suite, throughout the Ahlmannryggen and Borgmassivet. The dykes range in width from 30cm to 30m, generally dip steeply and, based on their orientation, have probably intruded along pre-existing joints and fractures. The dykes are usually fine-grained, with chilled margins and are doleritic to olivine doleritic in composition. They are considered to be Jurassic in age (Aucamp, 1972; Wolmarans and Kent, 1982; Peters *et al.*, 1991) and can be correlated with the extensive Karoo and Ferrar dolerites, which exhibit a well-constrained age of 183Ma (Encarnación *et al.*, 1996; Duncan *et al.*, 1997).

3. LITHOSTRATIGRAPHY OF THE AHLMANNRYGGEN GROUP

3.1 INTRODUCTION

The currently accepted stratigraphy of the Ahlmannryggen Group is outlined by Wolmarans and Kent (1982), and is based on a synthesis of previous work. However, there was, and still is, considerable controversy surrounding the stratigraphic subdivision, due to the widely spaced nature of the outcrops, a lack of prominent marker horizons, difficulty in accessing exposures and possible block faulting of the region. The problem is compounded by that fact that past researchers have tended to concentrate on exposures located in either the Borgmassivet or the Ahlmannryggen (separated by the 10km wide Viddalen glacier), and have then attempted to broadly apply these locally derived stratigraphic subdivisions to the entire area. This approach contravenes the basic principles of lithostratigraphy (e.g. Hedberg, 1976), which indicate that successions which lack any visible physiographic link should be assigned different unit names, in spite of certain similarities. Possible correlations between the Borgmassivet and Ahlmannryggen can only be identified once separate lithostratigraphies have been established.

The present study considered exposures in both the Ahlmannryggen and Borgmassivet areas, and revealed that none of the previous stratigraphic subdivisions are applicable for the entire Ahlmannryggen Group. To rectify this situation, an alternative stratigraphy will be proposed, intended to incorporate successions exposed in both regions. It is necessary to present this new interpretation of the stratigraphy here in the introductory section to ensure that geological observations described in subsequent sections can be placed in their correct geological context. Figure 3.1 summarises and correlates past stratigraphic subdivisions, while a more detailed description is included in Appendix 2.

3.2 PROPOSED STRATIGRAPHY FOR THE AHLMANNRYGGEN GROUP

The proposed stratigraphic revisions are based on a combination of lithostratigraphic, structural and sedimentological criteria. Only a brief description of the key lithostratigraphic features of each formation is given here, as detailed discussions regarding sedimentological and structural characteristics are included in Sections B and C. The proposed new stratigraphy is summarised and compared to the currently accepted stratigraphy of Wolmarans and Kent (1982) in Figure 3.2.

3.3 PROPOSED STRATIGRAPHY FOR THE AHLMANNRYGGEN REGION

Three conformable(?) formations have been defined for exposures of the Ahlmannryggen Group encountered in the Ahlmannryggen area. These include a lower Pyramiden Formation (>600m), a middle Schumacherfjellet Formation (*ca.* 390m) and an upper Grunehogna Formation (>500m). Summaries of the lithostratigraphic characteristics and distribution of the different formations are shown in Figures 3.3 – 3.5 and Map 1 (rear pocket).

3.3.1 Pyramiden Formation

The Pyramiden Formation (Figure 3.3) was initially placed in the Lower Borg Formation of the Ahlmannrygg Group by Roots (1969), but was given formation status shortly thereafter by Neethling (1970). Since then, the Pyramiden Formation has been consistently recognised as the basal formation of the Ahlmannryggen Group, despite the fact that the upper and lower contacts of the formation are not exposed. This study advocates the retention of this formation, which appears to structurally, and presumably stratigraphically, underlie the Schumacherfjellet Formation, but suggests that the currently accepted distribution should be revised.

As summarised in Wolmarans and Kent (1982), the Pyramiden Formation has been recognised at Pyramiden (the type locality), Sphinksen and Knallen, an isolated cluster of nunataks at the head of the Viddalen, the glacier that separates the Ahlmannryggen from the Borgmassivet (Map 1). Other small exposures correlated with the Pyramiden Formation have been described from Babordsranten and Kjölrabbane Peak 1611 (Bredell, 1977) and Trioen (Neethling, 1970). Bredell advocated the inclusion of exposures occurring at Nashornet, Viddalskollen and

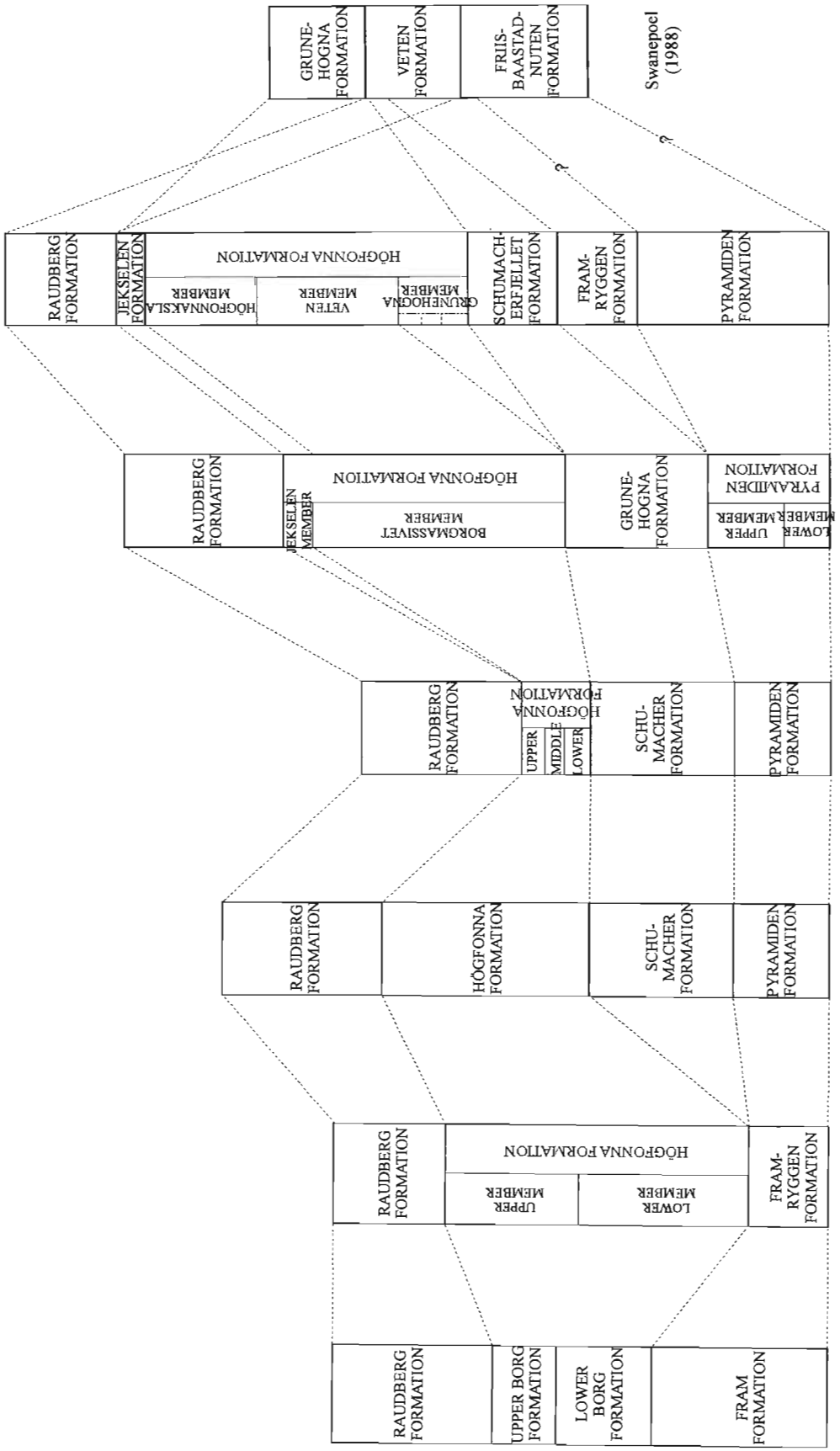

Figure 3.1: Summary and correlation of previous stratigraphic subdivisions for the Ahlmannryggen Group.

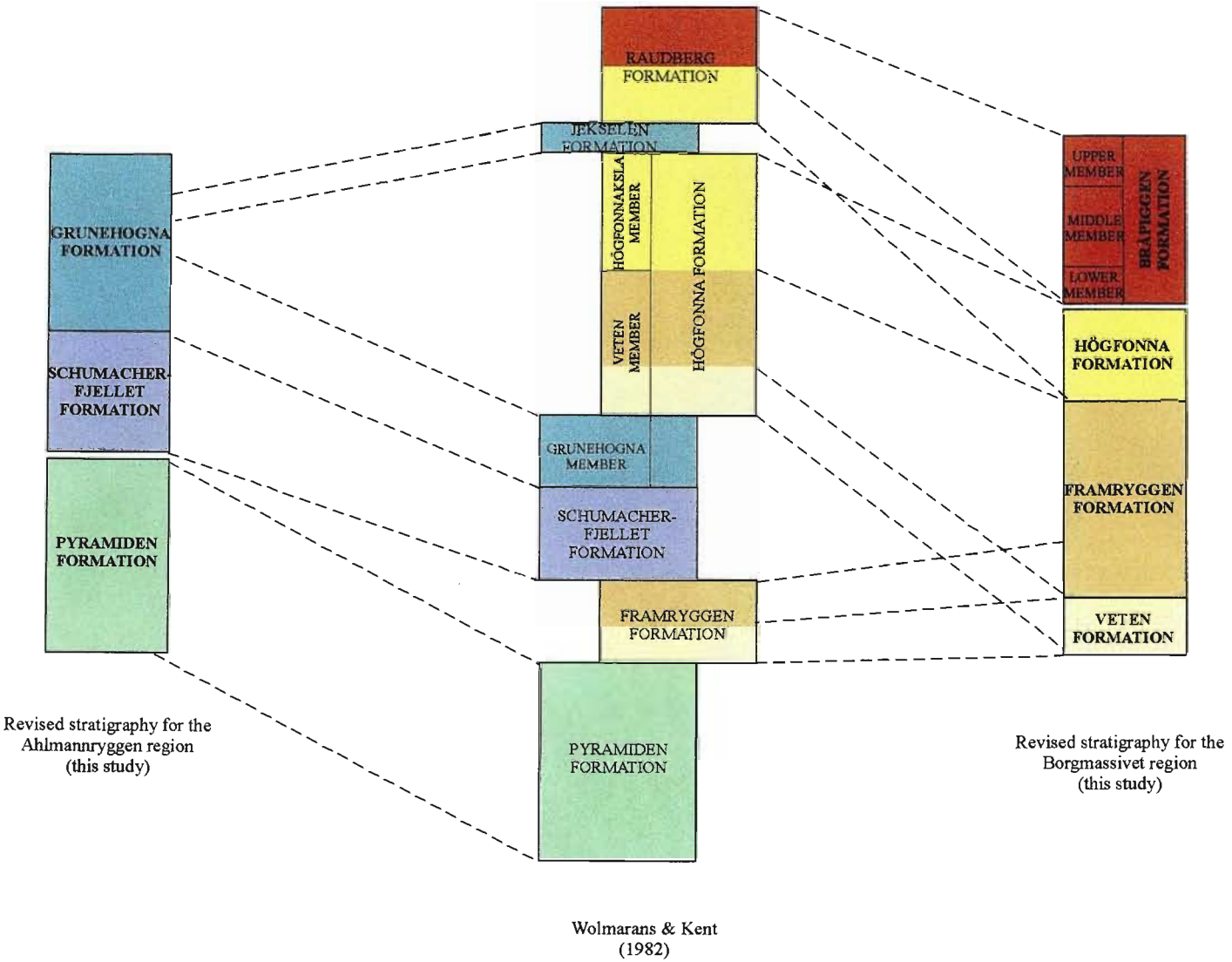

Figure 3.2: Proposed stratigraphic revisions for the Ahlmannryggen Group in the Ahlmannryggen and Borgmassivet regions and comparison with the currently accepted stratigraphy of Wolmarans and Kent (1982).

LEGEND FOR DETAILED
LITHOSTRATIGRAPHIC SECTIONS

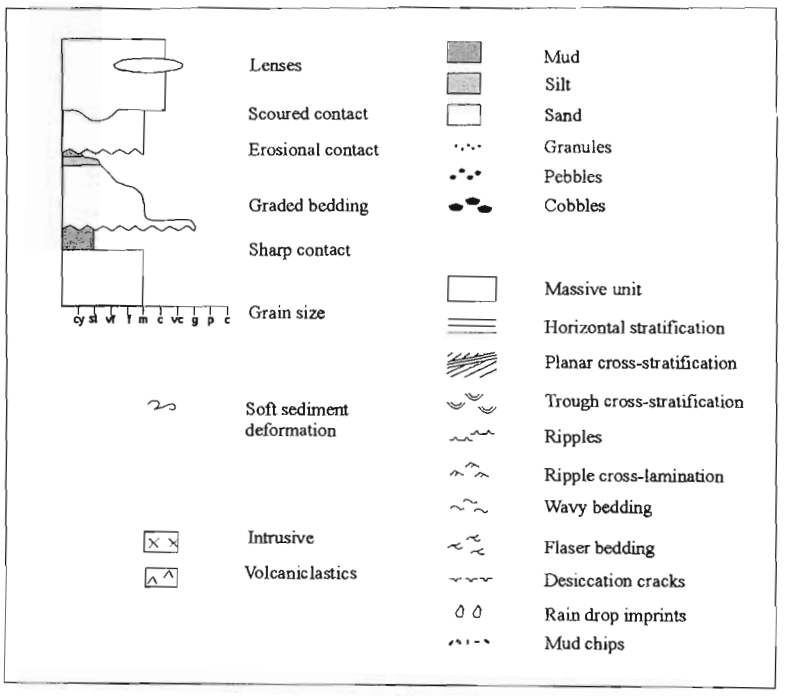

LEGEND FOR GENERAL
LITHOSTRATIGRAPHIC SECTION

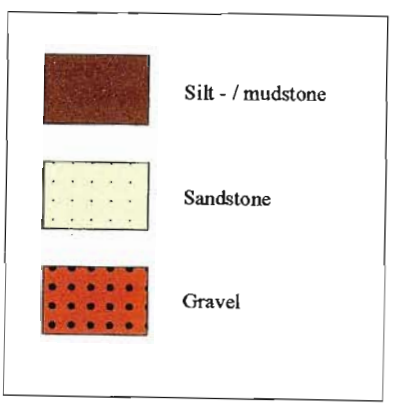

Legends for Figures 3.3-3.9: detailed and simplified lithostratigraphic sections.

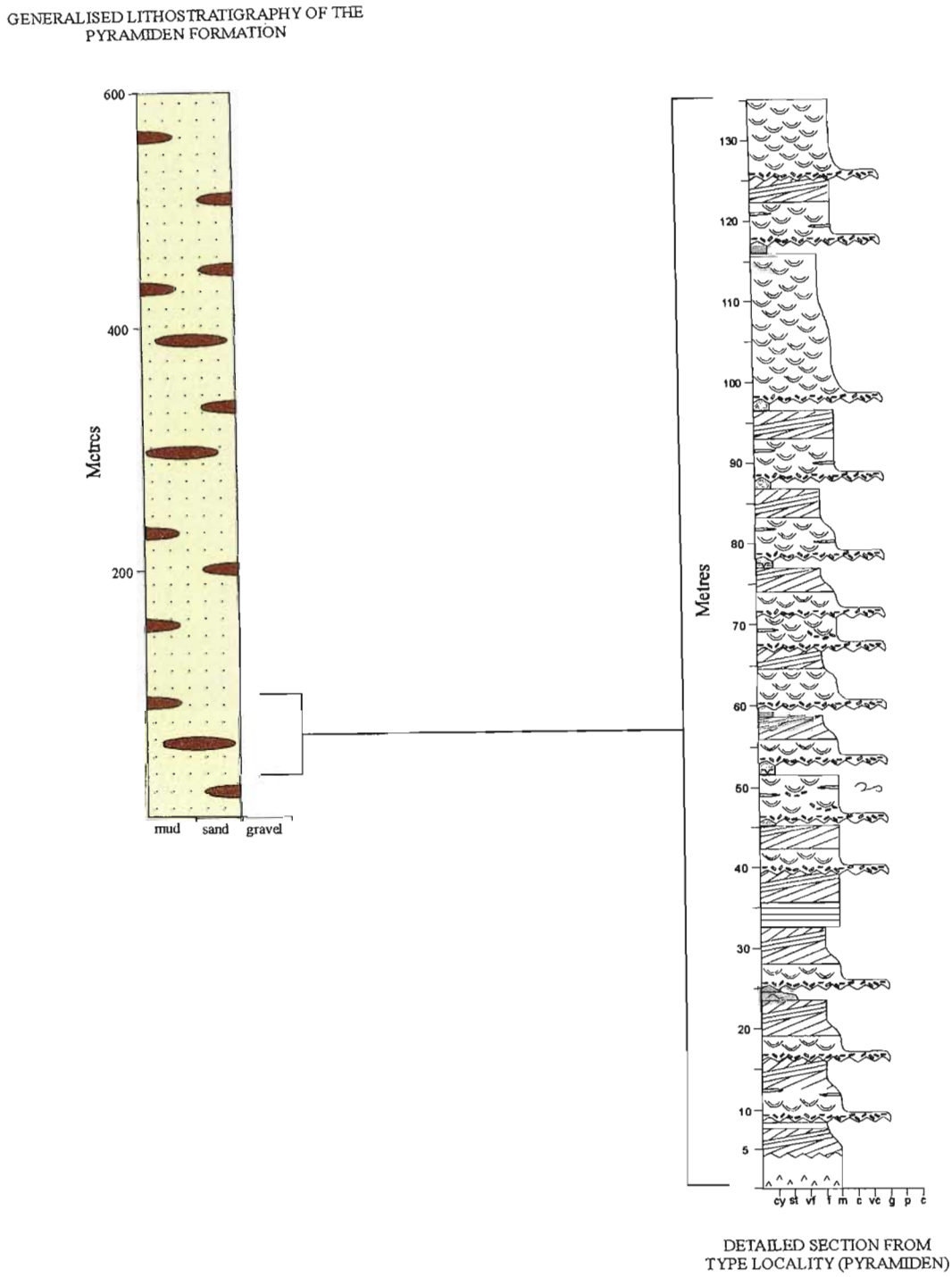

Figure 3.3: Detailed and generalised lithostratigraphy of the Pyramiden Formation, a sandstone dominated sequence characterised by trough and planar cross-stratification. Note: the intraformational mud-chip conglomerates are not included on the simplified log. The legends for both logs are shown on page 17.

Nashornkalvane, a series of nunataks situated along a north-east trending ridge at the confluence of the Viddalen and Jutulstraumen glaciers, some 60km east of the type locality. However, detailed examination of these exposures revealed no similarity to the lithostratigraphic characteristics typical of the Pyramiden Formation, and they were instead found to correlate more closely with the Schumacherfjellet and Grunehogna Formations, and as a result, have been excluded from the Pyramiden Formation.

The Pyramiden Formation is characterised by the presence of greenish grey sandstone units dominated by medium- to large-scale trough and planar cross-beds, in which mudstone rip-up clasts are a common feature. Fine-grained, dark grey mudstone units are also present, and tend to occur as isolated lenses and layers of limited lateral extent. Overall, exposures of the Pyramiden Formation tend to exhibit a moderate degree of lateral variability, with individual units displaying variable thicknesses, and often pinching out laterally. Other notable features include the presence of desiccation cracks, raindrop imprints, ripple marks and the presence of minor extraformational gravel deposits.

The thickest exposed succession (some 600m) occurs at the type locality, but in light of the fact that neither the upper nor lower contacts are exposed, this can only be regarded as a minimum estimate of the overall thickness of the Pyramiden Formation.

3.3.2 Schumacherfjellet Formation

This study is in agreement with Wolmarans and Kent (1982), who suggested that because of priority and acceptance by use, Neethling's (1970) terminology should be retained for this succession, albeit in the slightly changed form of 'Schumacherfjellet' Formation.

The occurrence of the Schumacherfjellet Formation is restricted to the Ahlmannryggen, where it is widely distributed. In addition to exposures at Schumacherfjellet, Grunehogna (type locality), Lyftingen, Babordsranten, Kjollrabbane, Styrbordsknatten, Ovenuten, Flarjuvnutane, Flarjuven and Klumpane, as summarised in Wolmarans and Kent (1982), successions consistent with the lithostratigraphy of the Schumacherfjellet Formation were also found to exist at Veslekletten and Nashornkalvane. As previously mentioned, Bredell (1977) advocated the inclusion of successions exposed at Nashornkalvane in the Pyramiden Formation, however these exposures were found to correlate more closely with the Schumacherfjellet Formation.

The lithostratigraphy and distribution of the Schumacherfjellet Formation has been summarised in Figure 3.4 and Map 1. The Schumacherfjellet Formation is characterised by alternating units of light coloured (yellowish grey to cream) sandstone and dark coloured (brown to black to purple) mudstone. Trough cross-bedding is common in the sandstones, while the fine-grained units display abundant small-scale structures such as horizontal lamination, ripple cross-lamination and wavy bedding. The proportion of sandstone to mudstone varies markedly through the succession, but throughout the formation, the units consistently displayed a high degree of lateral persistence and an absence of extraformational gravel. The contact between individual sandstone and mudstone units is often gradational, and soft-sediment deformation is common. Mudstone rip-up clasts may be present in the sandstone units, while rare desiccation cracks were noted in some of the mudstone units.

The base of the Schumacherfjellet Formation is not exposed, and the estimated thickness of 390m must be regarded as a minimum. The conformable upper contact of the Schumacherfjellet Formation with the overlying Grunehogna Formation is exposed at Grunehogna Peak 1285, and a small unnamed nunatak to the south-west, where it represents one of the few exposed contacts between formations of the Ahlmannryggen Group.

3.3.3 Grunehogna Formation

The Grunehogna Formation is restricted to the Ahlmannryggen region, but has generally been included as a member within the Högfonna Formation, a subdivision originally defined from exposures in the Borgmassivet. Therefore, in keeping with the attempt to define a separate stratigraphy for the two regions, it is considered appropriate to establish a subdivision specific to the Ahlmannryggen, and it is recommended that the Grunehogna member defined by Wolmarans and Kent (1982) be upgraded to form the Grunehogna Formation (Figure 3.5, Map 1).

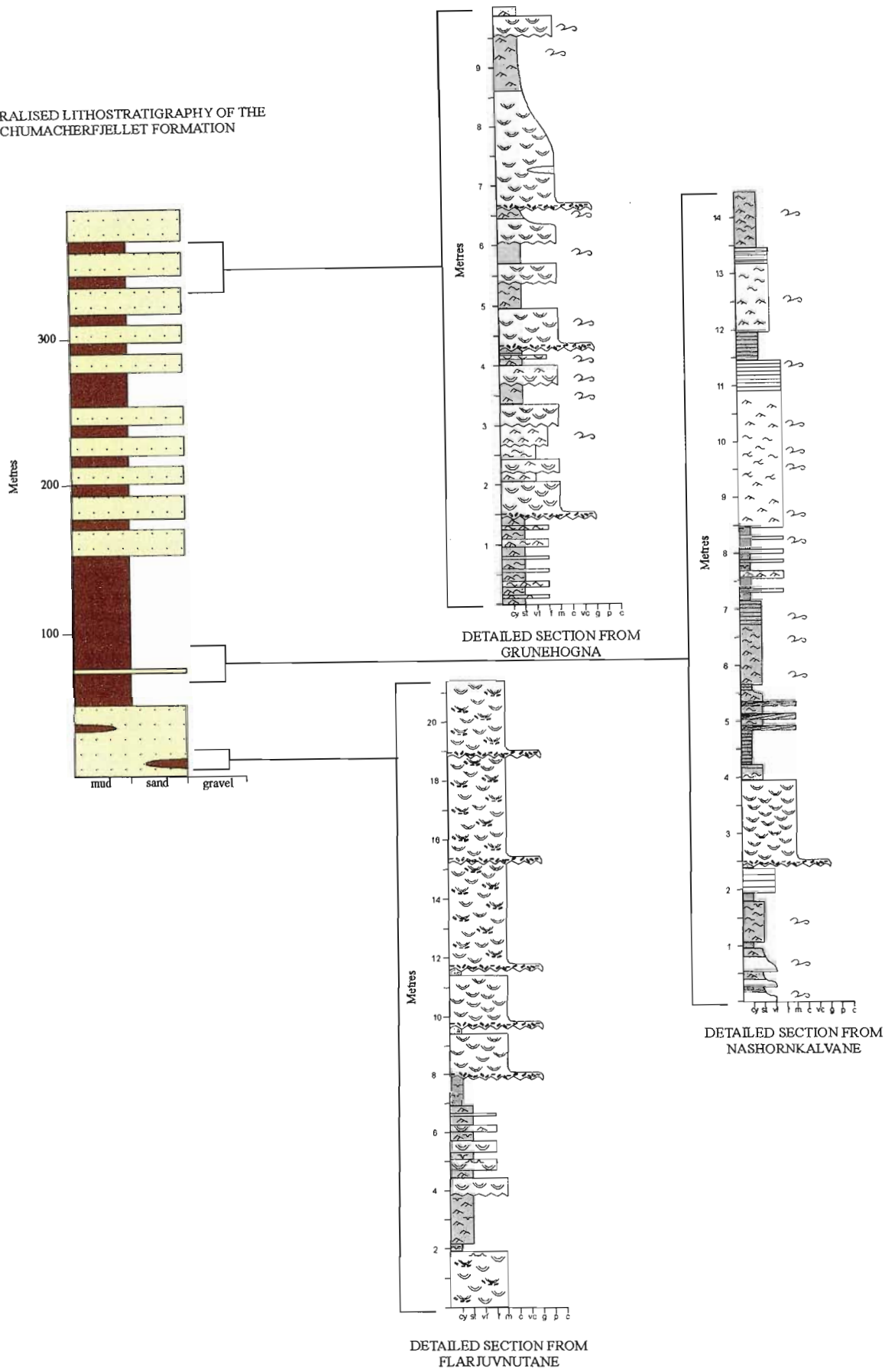

Figure 3.4: Generalised and detailed lithostratigraphy of the Schumacherfjellet Formation, a formation characterised by alternating units of light coloured sandstone and dark mudstone. Legends are shown on page 17.

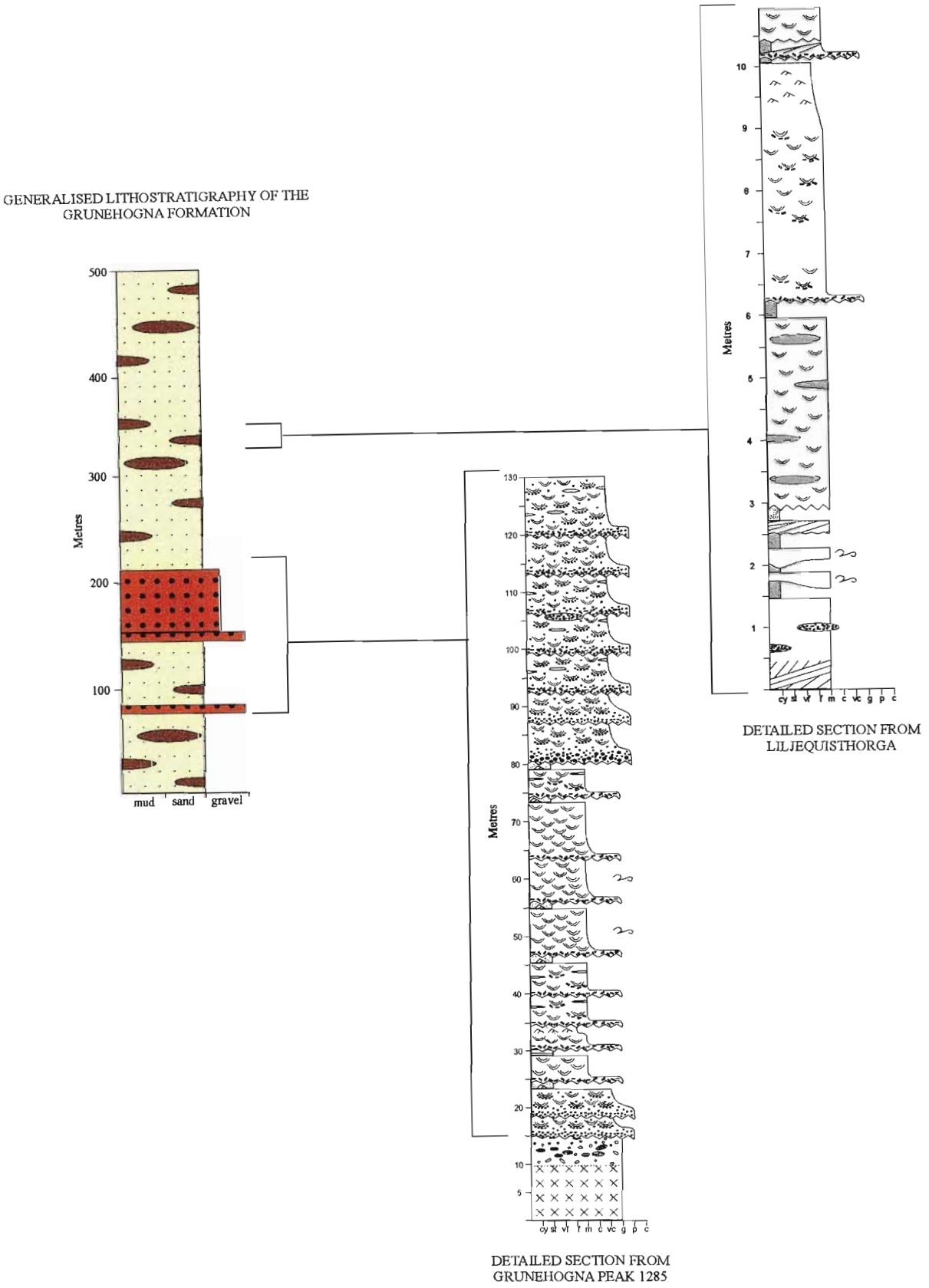

Figure 3.5: Generalised and detailed lithostratigraphy of the Grunehogna Formation, a sandstone to gravel dominated sequence exposed in the central to eastern Ahlmannryggen. Note: the intraformational mud-chip conglomerates are not included on the simplified log. The legends for both logs are shown on page 17.

The type locality for the Grunehogna Formation is exposed at Grunehogna Peak 1285, with correlations occurring at Liljequisthorga, Schumacherfjellet and Snöhetta. As previously mentioned, a conformable lower contact with the underlying Schumacherfjellet Formation is exposed at Grunehogna, however, nowhere is the upper contact of the formation exposed, and it is therefore only possible to provide a minimum estimate of 500m for the thickness of the sequence. Wolmarans and Kent (1982) included exposures at Jekselen within a separate formation, the Jekselen Formation. These outcrops occur as detached blocks or large xenoliths within the Borgmassivet Intrusions, and display similar lithostratigraphic characteristics to exposures at Grunehogna and Liljequisthorga. No evidence could be found that would warrant the inclusion of these exposures in a separate subdivision, and as such, it is suggested that they be included within the Grunehogna Formation. Bredell (1977) advocated the inclusion of successions exposed at Nashornet and Viddalskollen in the Pyramiden Formation, however, based on sedimentological characteristics, these exposures were found to correlate more closely with the Grunehogna Formation, and have been included here.

The Grunehogna Formation is dominated by trough cross-bedded, reddish coloured sandstone units which contain thin layers of purple to red-brown mudstone. Extraformational gravel units containing brilliant red jasper are common. All the units display a high degree of lateral variability, and where present, the fine-grained deposits tend to occur as isolated layers and lenses of limited lateral extent. The lower 210m (exposed at Peak 1285) displays a general coarsening-upwards trend, and changes from being dominated by sandstone units in the first 140m to being characterised by gravel deposits for the overlying 70m. The succession subsequently reverts to sandstone dominated for the remaining 290m. The mudstone units tend to display ripple cross-lamination, and occasionally exhibit desiccation cracks. Soft-sediment deformation is relatively common.

Two prominent gravel units, at 80m and at 140m, have previously been used to subdivide the succession into informal units. However these units are not laterally persistent and therefore should not be used as a basis for further subdivision of the formation. Accordingly, it is recommended that the three informal units defined by Aucamp (1972), and retained by Wolmarans and Kent (1982) be discarded.

3.4 PROPOSED STRATIGRAPHY FOR THE BORGMASSIVET REGION

Four formations are proposed for exposures of the Ahlmannryggen Group encountered in the Borgmassivet area. Unfortunately, the isolated nature of the exposures results in it being unclear as to whether or not these units are conformable. They consist of a lower Veten Formation (>175m), a Framryggen Formation (*ca.* 600m), overlain by a Högfonna Formation (*ca.* 300m) and an upper Bråpiggen Formation (>490m). Summaries of the lithostratigraphic characteristics and distribution of the different formations are shown in Figures 3.6 - 3.9 and Map 1.

3.4.1 Veten Formation

Past researchers have tended to include this succession within the Högfonna Formation (Figure 3.1, Appendix 2). However, Wolmarans and Kent (1982) recognised that the distinctive characteristics of this sequence justified a more detailed subdivision, and advocated the creation of a separate member (the Veten member) within their Högfonna Formation. Considering the distinctive nature of this succession, it is recommended that this approach should be taken one step further, and the Veten member upgraded to the Veten Formation. The distribution and thickness of the Veten Formation varies from that of the original Veten member, as Wolmarans and Kent (1982) included part of the overlying succession in their Veten member.

The type locality for the Veten Formation (Figure 3.6, Map 1) consists of the lower 120m of the sequence exposed at Veten Nunatak. The formation also includes units exposed at Fingeren, Söyla, Domen, Nålegga, Knappane and at the base of Pilarryggen (lower 140m). Based on descriptions by De Ridder (1970), the lower 70m of a 250m thick succession exposed at Borga can also be correlated with the Veten Formation. Wolmarans and Kent (1982) had included the entire succession exposed at Veten (some 470m) in their Veten member. However, the upper 330m of strata display a markedly different lithostratigraphy, which correlates closely with the type locality for the overlying

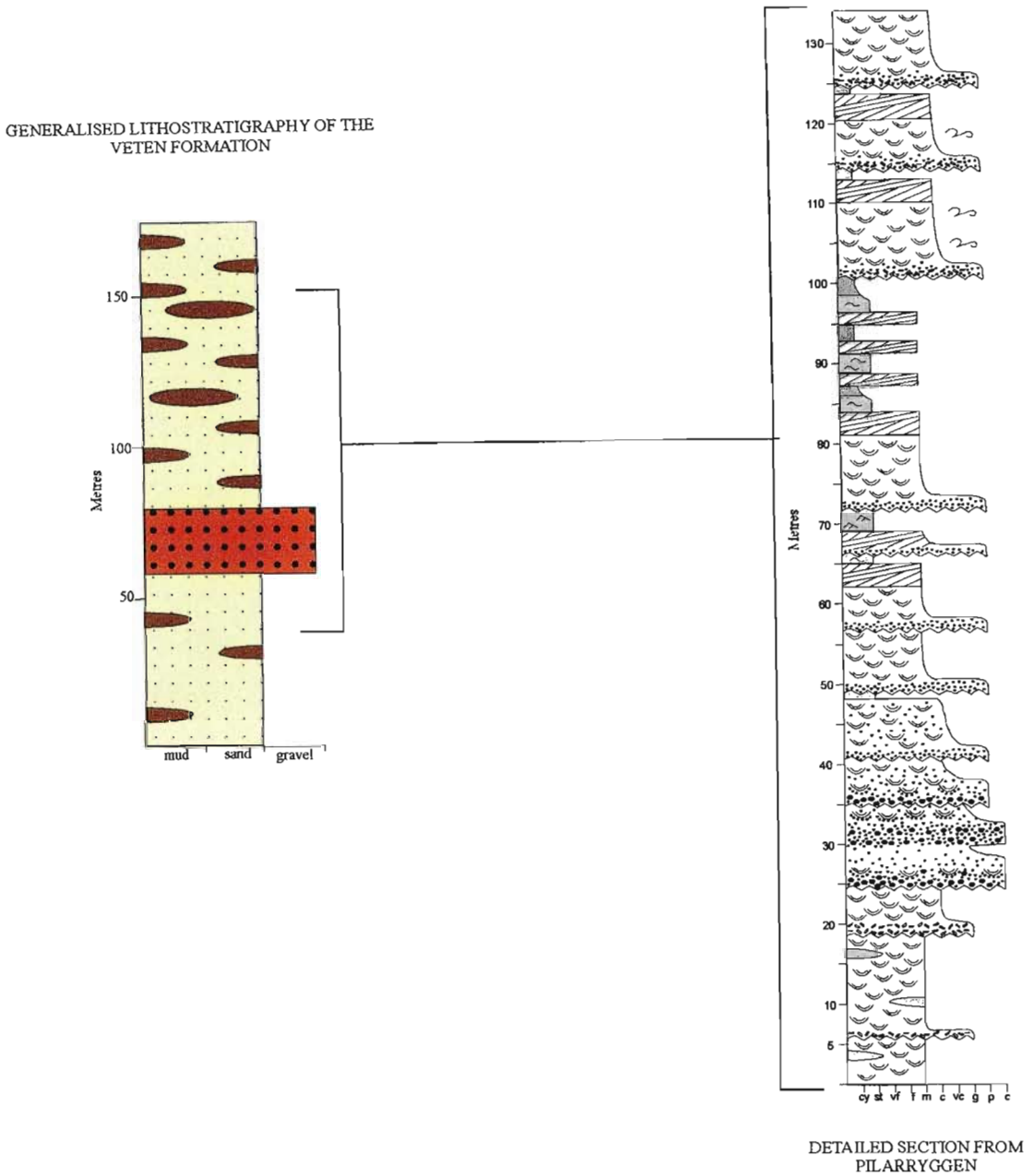

Figure 3.6: Generalised and detailed lithostratigraphy of the Veten Formation, a sandstone to gravel dominated sequence containing the oldest exposed strata in the Borgmassivet. Note: the intraformational gravel units are not included on the simplified log. The legends for both logs are shown on page 17.

Framryggen Formation, and as a result, have been excluded from the Veten Formation.

The lithostratigraphic characteristics of the Veten Formation (>175m) have been summarised in Figure 3.6. The lower 60m of the exposed succession is characterised by the presence of brown to grey to greyish-green, trough and planar cross-bedded sandstones, commonly containing mudstone rip-up clasts. Subordinate black to purplish-brown mudstone beds are also present. The succession subsequently passes into a 10m to 15m thick section dominated by extraformational gravel deposits. The remainder of the formation (some 50 to 100m) consists of a combination of sandstone and mudstone beds, in which the fine-grained units are often well developed and may occur in packages up to 10m thick. All units within the Veten Formation exhibit a relatively high degree of lateral variability, with the mudstone units commonly occurring as impersistent layers and lenses.

The lower contact of the Veten Formation is not exposed, and as such the estimated thickness of 175m must be regarded as a minimum. The conformable upper contact with the overlying Framryggen Formation is exposed at Veten and at Pilarryggen.

3.4.2 Framryggen Formation

The 'Fram' Formation was first recognised by Roots (1969), who considered it to be the lowermost succession of his Ahlmannrygg Group. This formation was retained by De Ridder, in the slightly altered form 'Framryggen Formation', but was discarded in subsequent stratigraphic revisions based on successions exposed in the Ahlmannryggen region (Neethling, 1970, Aucamp, 1972 and Bredell, 1977). The formation was re-established by Wolmarans and Kent (1982), who advocated a stratigraphic position between the Pyramiden and Schumacherfjellet Formations, both of which occur exclusively in the Ahlmannryggen region. This is an example of the confusion that has resulted from trying to determine an overall stratigraphy based on localised research, and from attempting to combine successions exposed in the two different regions into one stratigraphic system.

It is agreed here that the Framryggen Formation (Figure 3.7, Map 1) should be recognised as a subdivision within the Ahlmannryggen Group, but only within the Borgmassivet region, and its currently accepted relative stratigraphic position requires revision. The type locality for the Framryggen Formation occurs at Framryggen Nunatak, with correlative successions exposed at Stridbukken, Möteplassen, Kjellbergnuten, Framrabben, Nunataks 1810, 1885 and 1910 south of Borga, as well as at Veten and Pilarryggen, where a conformable contact with the underlying Veten Formation is exposed. Based on descriptions by Swanepoel (1988) a conformable upper contact with the overlying Högfonna Formation is possibly exposed at Kjelbergnuten.

The lower 250m of the formation is dominated by purplish-brown to black mudstone units with abundant small-scale sedimentary structures, including ripple cross-lamination, wavy bedding, and horizontal lamination. This fine-grained succession is overlain by approximately 80m of coarser-grained deposits characterised by grey to greenish-grey, planar and trough cross-bedded sandstones. Rare gravel deposits were also noted. This overlying, sandstone-dominated succession shows a gradual fining-upwards trend, with a progressive vertical increase in the proportion of fine-grained deposits and a corresponding decrease in the proportion of sandstone, until the succession is once again dominated by mudstone, for a thickness of 40m. This fining-upwards cycle is repeated in the upper *ca.* 300m of the Framryggen Formation. Mudstone rip-up clasts are often present in the sandstone units, and soft-sediment deformation is common. Desiccation cracks and raindrop imprints were also noted in the fine-grained units.

Overall, the *ca.* 600m thick Framryggen Formation is a fine-grained dominated succession in which most units tend to exhibit a high degree of lateral continuity, and individual beds can often be traced for several kilometres, along the full extent of an exposure.

3.4.3 Högfonna Formation

Past stratigraphic subdivisions have tended to split a lithostratigraphically very similar set of successions into two different formations, namely the Raudberg Formation and the Högfonna Formation (Figure 3.1, Appendix 3). Exposures in the Borgmassivet region previously assigned to either the upper part of the Högfonna Formation (Högfonnaksla member of Wolmarans and Kent, 1982) or the lower part of the

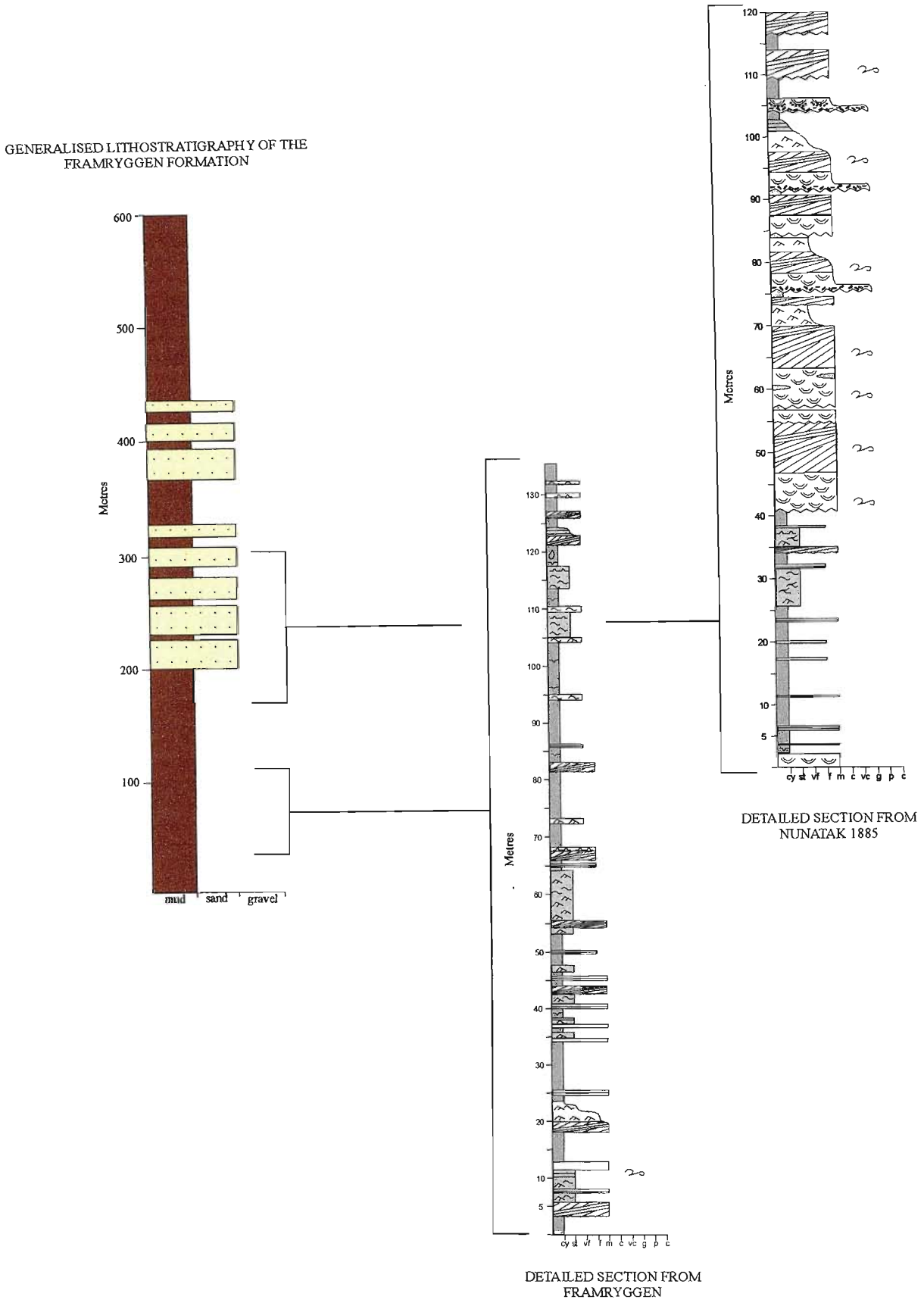

Figure 3.7: Generalised and detailed lithostratigraphy of the Framryggen Formation, which is characterised by alternating laterally continuous layers of dark coloured mudstone and light coloured sandstone, with the former dominating the overall sequence. Legends are shown on page 17.

Raudberg Formation, can be correlated lithostratigraphically and structurally. These successions have therefore been combined into a single formation, named the Högfonna Formation. The terminology is retained due to its acceptance by use and because the type locality for the formation occurs at Högfonnaksla, the northern most ridge of Högfonna Nunatak.

The Högfonna Formation (Figure 3.8, Map 1) is found at Högfonna, the type locality, as well as Raudberget, Ovebratten, and Mana. Examination of sedimentary logs constructed by Swanepoel (1988) suggests that exposures may also occur at Vindegga and Kjellbergnuten. Other localities previously included in the Högfonna and Raudberg Formations, namely Bråpiggen, Friis-Baastadnuten, Huldreslottet and Ryvingen, display markedly different lithostratigraphic features, and are included in the overlying Bråpiggen Formation. Wolmarans and Kent (1982) also included exposures occurring at the lower part of Fassetfjellet in their Högfonna Formation. However, these sediments are apparently closely associated with lavas and volcaniclastics of the overlying Jutulstraumen Group (outcrop is virtually inaccessible) suggesting that the exposures should be excluded from the Ahlmannryggen Group.

The Högfonna Formation is dominated by dark grey to red coloured, cross-bedded sandstone containing abundant mudstone rip-up clasts. At Högfonnaksla, trough cross-bedded sandstones dominate the lower 200m of the succession, and display an overall coarsening-upward trend. This is followed by an approximately 100m thick succession characterised by extraformational gravel deposits. A similar coarsening-upwards succession, dominated by trough cross-bedded sandstone, is also encountered at Raudberget, Högfonna Peak 2130 and Mana. The more southerly exposures of the Högfonna Formation, including Vindegga, Kjellbergnuten, Ovebratten, and to a lesser extent Mana, display successions characterised by a slightly different lithostratigraphy. At these exposures, planar cross-bedded sandstones dominate, or occur in combination with trough cross-bedded sandstones. Subordinate red to purplish mudstone beds occur as thin layers and lenses and often exhibit desiccation cracks.

Despite these variations, all exposures investigated in this study were found to have a number of features in common, including the dominance of sandstone units, a relatively high degree of lateral variability and the presence of minor mudstone units. Other notable characteristics include the presence of isolated pyroclastic units, abundant soft-sediment deformation and abundant heavy mineral laminae. As the upper contact with the overlying Bråpiggen Formation is not exposed, only a minimum estimate of *ca.* 300m can be given for the overall thickness of the formation.

3.4.4 Bråpiggen Formation

Exposures occurring at Huldreslottet, Ryvingen, Friis-Baastadnuten and Bråpiggen comprise a succession that structurally and stratigraphically overlies the Högfonna Formation, to which the name Bråpiggen Formation has been assigned (Figure 3.9, Map 1). These exposures had previously been included in either the Högfonna or Raudberg Formation by Wolmarans and Kent (1982), but have been separated on the basis of their distinctly different lithostratigraphy. The Bråpiggen Formation can be subdivided into three members.

3.4.4.1 Lower Member

The Lower member of the Bråpiggen Formation is exposed at Huldreslottet, and the lower part of Ryvingen and Friis-Baastadnuten, and is characterised by *ca.* 130m of laterally persistent, mudstone units displaying abundant small-scale sedimentary structures (ripple cross-lamination, wavy bedding and horizontal lamination). Thin, subordinate sandstone beds are also present, and tend to display either trough or planar cross-stratification. Desiccation cracks were also noted.

3.4.4.2 Middle Member

Exposures assigned to the Middle member of the Bråpiggen Formation occur in the upper part of Ryvingen and Friis-Baastadnuten, and the lower part of Bråpiggen. The Middle member conformably overlies the Lower member, and is characterised by an overall fining-upwards succession. At Friis-Baastadnuten, trough cross-bedded sandstones, with minor examples of planar cross-bedded sandstone and extraformational gravel dominate the lower 160m, while the succession at Ryvingen is characterised by planar cross-bedded sandstone only. In both exposures, mudstone beds form only a minor proportion of the succession. A progressive increase in the proportion of mudstone is noted in the upper 80m of the

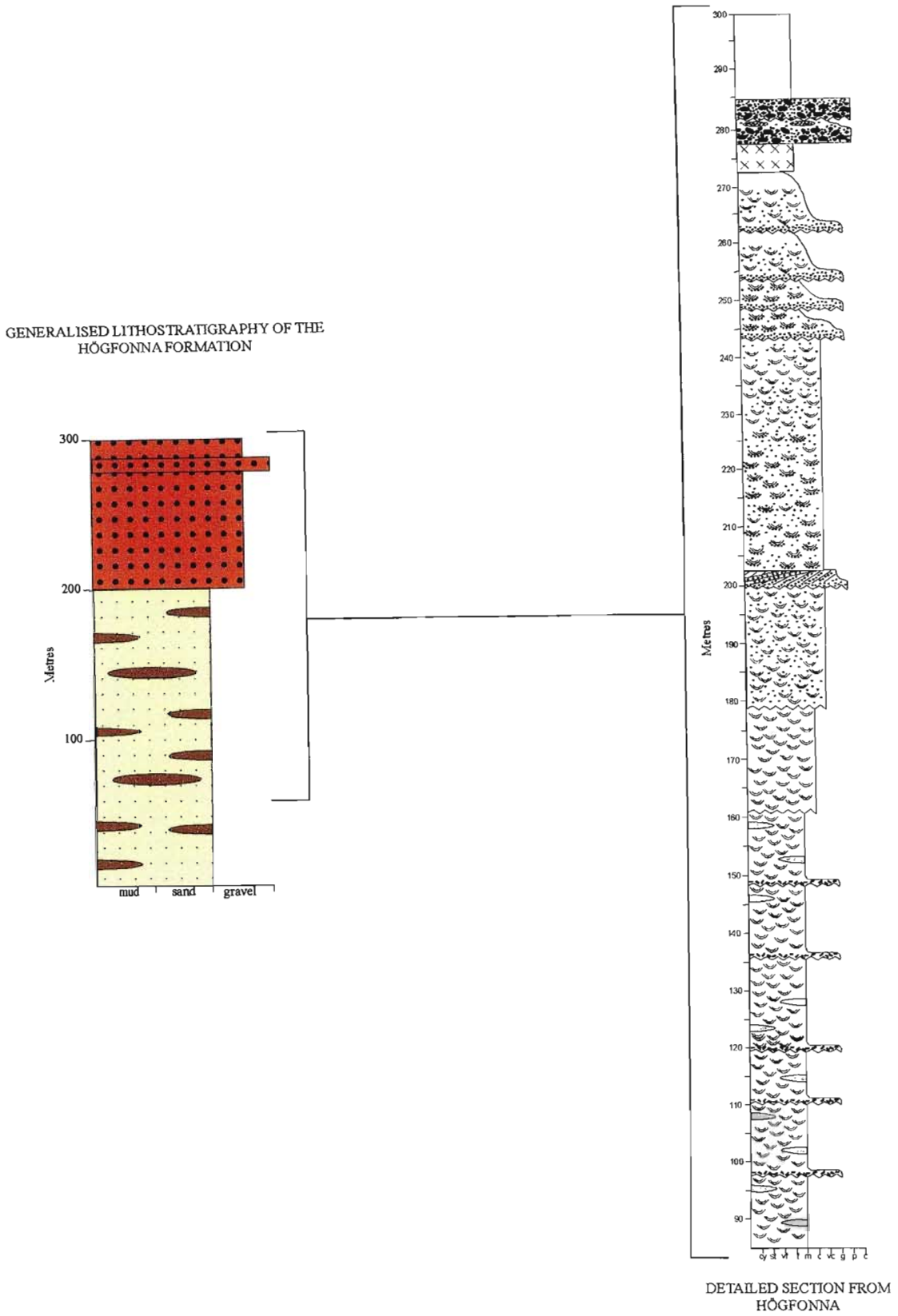

Figure 3.8: Generalised and detailed lithostratigraphy of the Högfonna Formation, a sandstone to gravel dominated sequence exposed in the central Borgmassivet. Note: intraformational mud-chip conglomerates are not included on the simplified log. Legends for both logs are shown on page 17.

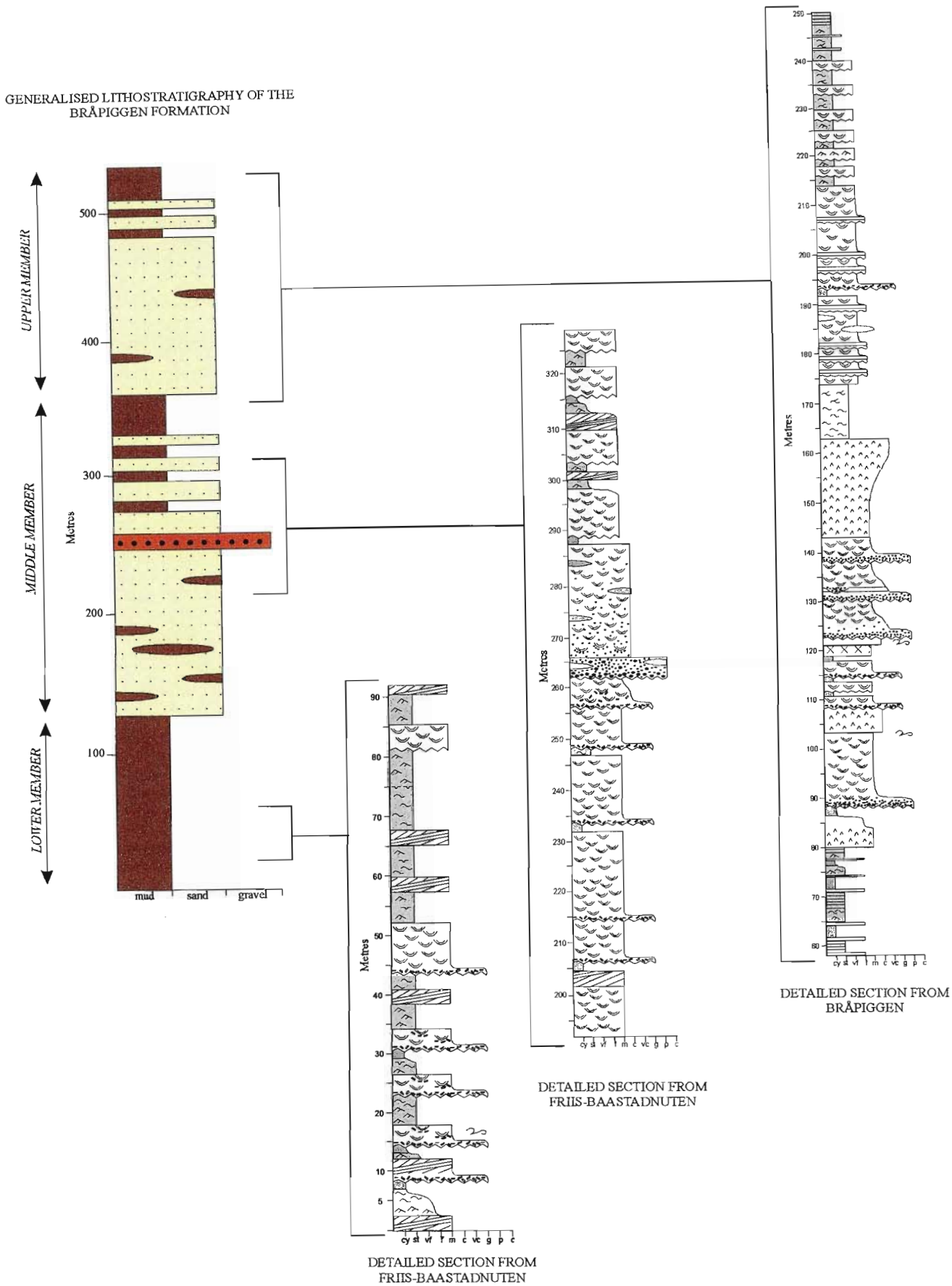

Figure 3.9: Generalised and detailed lithostratigraphy of the Bråpiggen Formation, which can be subdivided into three members, a lower mudstone-dominated sequence, followed by two fining upwards sequences. Note: the intraformational mud-chip conglomerates are not included on the simplified log. Legends are depicted on page 17.

Middle member, and the succession gradually changes from sandstone dominated to mudstone dominated.

3.4.4.3 Upper Member

The Upper member of the Bråpiggen Formation is only exposed at Bråpiggen, where a 160m fining-upwards succession is exposed. The lower 120m are dominated by trough cross-bedded sandstone, which is characterised by a high epiclastic content. Thick (up to 18m) massive tuff units are also present. In the upper 40m of the exposed succession, the mudstone units gradually increase in abundance, and the final 10m of the succession is dominated by these fine-grained deposits.

As neither the upper or lower contacts of the Bråpiggen Formation are exposed, a minimum thickness of *ca.* 530m is proposed.

3.5 CORRELATIONS BETWEEN THE BORGMASSIVET AND AHLMANN-RYGGEN REGIONS

The proposed stratigraphic subdivisions outlined above give rise to a separate stratigraphy for the Borgmassivet and Ahlmannryggen regions. Nonetheless, broadly similar lithostratigraphic characteristics displayed by these formations suggests that successions in the two different regions may be correlated (Figure 3.10).

Similarities are displayed by the Pyramiden and Veten Formations, the Schumacherfjellet and Framryggen Formations and the Grunehogna and Högfonna Formations. No equivalent of the Bråpiggen Formation is found exposed in the Ahlmannryggen region.

Considering the similarities exhibited by the two regions, it is tempting to describe the successions through the use of a broad, unifying stratigraphy that combines exposures in both the Ahlmannryggen and Borgmassivet into the same set of formations. Nevertheless, the differences (albeit slight) in lithostratigraphy, thickness and palaeocurrent direction (considered in Section B) exhibited by successions in the Borgmassivet and Ahlmannryggen justifies the establishment of different stratigraphic subdivisions for the two regions.

This approach is also in agreement with the basic principles of lithostratigraphy (e.g. Hedberg, 1976), which indicate that successions lacking a visible physiographic link should be assigned different unit names, in spite of certain similarities.

The stratigraphic subdivisions outlined above are also in keeping with historical precedence, and many of the well-known formation names have been retained.

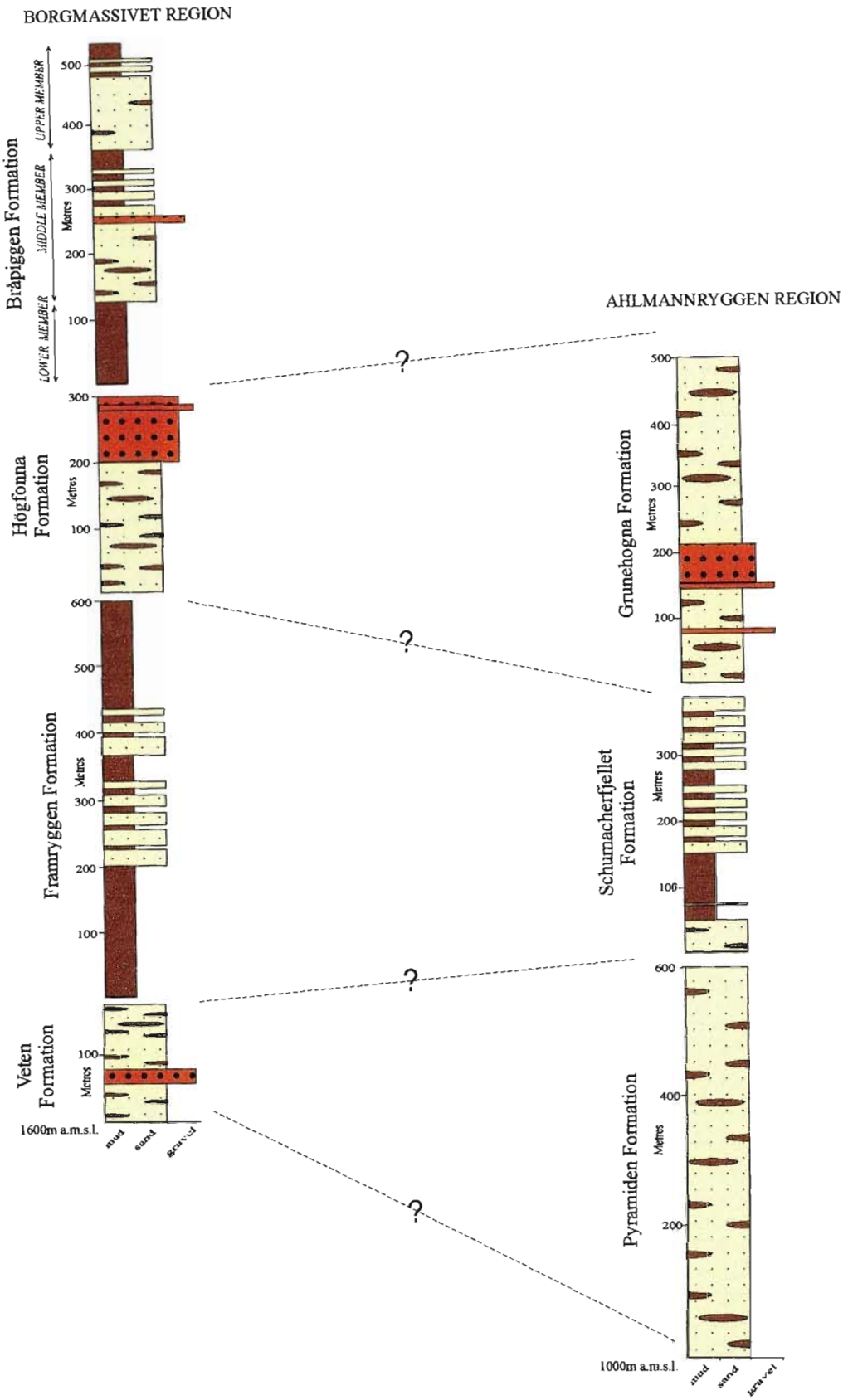

Figure 3.10: Stratigraphic subdivisions in the Borgmassivet and Ahlmannryggen regions can be correlated, based on broadly similar lithostratigraphic characteristics. However, slight differences between the two sequences and basic principles of lithostratigraphy justify the establishment of separate subdivisions for the two regions.

SECTION B

1-INTRODUCTION TO SEDIMENTOLOGY & LITHOFACIES CLASSIFICATION
2-SEDIMENTOLOGY OF FORMATIONS IN THE AHLMANNRYGGEN
3-SEDIMENTOLOGY OF FORMATIONS IN THE BORGMASSIVET
4-AHLMANNRYGGEN GROUP SEDIMENTARY BASIN MODEL

Overview:

Section B presents a description of the sedimentological characteristics of the Ahlmannryggen Group. A general introduction, including a description of the lithofacies classification system established during the course of this study, is followed by a detailed description of the characteristics of each formation, with exposures in the Ahlmannryggen and Borgmassivet regions being considered separately. A combination of vertical and lateral profile analysis is used to establish the nature of the depositional environments in each of these two regions. Observations from the two areas are then combined into an overall model summarising the sedimentological evolution of the Ahlmannryggen Group basin.

1. INTRODUCTION TO SEDIMENTOLOGY & LITHOFACIES CLASSIFICATION

1.1 INTRODUCTION

Exposures of the Ahlmannryggen Group provide an excellent opportunity to examine the characteristics of a Mesoproterozoic sedimentary deposit, and the use of vertical sections and lithofacies associations in combination with architectural element analysis has allowed for detailed investigation of depositional processes responsible for the development of the succession. A detailed approach was considered necessary in order to resolve the controversy surrounding the depositional setting of the Ahlmannryggen Group, as a number of contrasting environments have been proposed by previous researchers. Neethling (1970) described the depositional setting as mainly continental, varying initially from shallow water marine to subaerial at the time of closure. De Ridder (1970) envisaged a large, shallow flood-plain setting, with occasional episodes of transgression and regression. Aucamp (1972) favoured a deltaic environment. Ferreira (1986) considered the Ahlmannryggen Group to represent a regressive depositional cycle from marine to braided and meandering river environments, while Swanepoel (1988) recognised only meandering and braided fluvial environments.

According to Eriksson *et al.* (1998), the interpretation of the depositional environment of Precambrian sediments can be highly problematic, mainly due to a notable lack of fossil evidence and major differences in the depositional styles that are thought to have existed during pre-Devonian times, before stabilising terrestrial vegetation became abundant. The interpretation of sedimentary deposits traditionally relies on comparisons with classical sedimentary models, based on Phanerozoic occurrences and observations of modern processes and products. The application of such models to Precambrian deposits is a highly controversial issue (Eriksson *et al.*, 1998). Despite the numerous problematic factors involved, it has however been shown by a number of authors (e.g. Long, 1978; Roe and Hermansen, 1993; Hjellbakk, 1997 and Sonderholm and Tirsgaard, 1998) that the interpretation of ancient sedimentary successions can be successfully conducted, and provided there is careful examination of the depositional architecture, comparison with models developed from modern sedimentary systems may be a feasible approach.

In order to accurately ascertain the nature and distribution of lithofacies associations within the Ahlmannryggen Group, 24 separate vertical sedimentary logs were constructed from exposures in the Ahlmannryggen and Borgmassivet regions. The majority of these vertical sections were constructed during the initial reconnaissance stage of the project, when the aim was to cover as much of the study area as possible, and the quick and simple vertical profile method was considered the optimum approach. Difficulties in access, and a lack of continuous lateral exposures at many localities also favoured the use of the vertical profiling method.

As both the Ahlmannryggen and Borgmassivet regions have been investigated on numerous previous occasions, there was an abundance of pre-existing information. Where sedimentary logs had previously been constructed, these were used as reference guides in the field, and modified to accommodate new observations, as well as to reflect a revised lithofacies classification scheme. For exposures where no previous logs existed, detailed vertical profiles were constructed. The successions under investigation proved to contain an abundance of small-scale sedimentary structures, and bed thicknesses of less than 10cm are a common feature. Considering the impracticality of representing units of this scale on the graphic sedimentary logs, it was necessary to omit units thinner than 0.2m during the compilation of the logs. These thinner beds were however taken into consideration when determining the nature of the lithofacies associations present. The sedimentary logs are presented in Appendix 5, and have been annotated to reflect lithofacies type, palaeo-current direction and sample localities.

Eight separate cliff face sketches were constructed in order to facilitate architectural element analysis of the Ahlmannryggen Group. Attempts were made to obtain at least one lateral profile specific to each formation in the

Ahlmannryggen Group, however suitable cliff face exposures were found to be rare. In the case of the Pyramiden and Bråpiggen Formations, no suitable exposures were located, and determination of the depositional settings of these formations is based entirely on the analysis of vertical logs.

The following discussions (Sections B2 and 3) detail the sedimentological characteristics and depositional environment of each of the seven formations that have been defined for the Ahlmannryggen Group, before attempting to define an overall model for the deposition of the Ahlmannryggen Group (Section B4).

1.2 LITHOFACIES AND LITHOFACIES ASSOCIATIONS

1.2.1 Lithofacies

According to Miall (1990) the objective during basin analysis should be the development of a facies scheme that encompasses all the rock types present, but is kept as simple as possible. The lithofacies codes and descriptions used below are adapted from the lithofacies scheme outlined in Miall (1978). Each lithofacies code consists of two parts, a initial capital letter designating modal grain size (G: gravel, S: sand, F: fines, V: volcanicalstics) followed by a lower case letter/s chosen as a mnemonic of a distinctive feature of each lithofacies. The use of lithofacies codes/abbreviations is widely accepted, and a number of the codes defined below are in common usage. Nevertheless, each lithofacies described here and its interpretation is based on characteristics observed in the Ahlmannryggen Group.

The lithofacies types are summarised in Table 1.1, and outlined in detail in Appendix 4.

The Ahlmannryggen Group is a predominantly sandstone to fine-grained facies dominated succession, in which gravel facies comprise only 6% of the total succession. Four distinctive gravel lithofacies types were identified (Figure 1.1). These include massive gravel (Gm), flat lying gravel (Gfl), and stratified gravel lithofacies, the latter containing either planar (Gp) or trough (Gt) cross-stratification.

Sandstone lithofacies (Figure 1.1) are the dominant facies type in the Ahlmannryggen Group, forming approximately 65% of the observed succession. The characteristics of the sandstone lithofacies vary remarkably, and as a result, can be subdivided into 12 different facies types, including massive (Sm), horizontally laminated (Sh), high and low angle planar cross-stratified (Sph, Spl), trough cross-stratified (St), rippled ($Sr_{1,2}$), scour fill (Ss), ripple cross-laminated (Srl), flaser bedded (SFf) and wavy bedded (SFw) sandstone lithofacies. A separate code (Se) is assigned to basal sandstone deposits containing mudchip intraclasts. Although not strictly a facies, these deposits represent a recognisable 'state' within the sedimentary succession.

Fine-grained lithofacies (Figure 1.1) comprise 26% of the Ahlmannryggen Group succession. As is the case with the sandstone lithofacies, the characteristics of the fine-grained facies vary remarkably, and are assigned to 6 different lithofacies types. Facies types include massive mudstone (Fm), mudstone with desiccation cracks (Fd), mudstone with rain-drop impressions (Frd), horizontally laminated mudstone (Fh), ripple cross-laminated mudstone (Frl) and sandy mudstone with ripple casts ($Fr_{1,2}$).

Volcaniclastic lithofacies are relatively common in the Ahlmannryggen Group, but constitute only 3% of the total succession. Reworked volcaniclastic deposits (V) are more common than massive primary pyroclastic deposits (Vm), with examples of the former occurring virtually throughout the succession. The reworked volcaniclastic deposits display depositional sedimentary structures similar to those recorded in the sandstone units. Massive primary fallout deposits tend to be restricted to the upper formations of the Ahlmannryggen Group exposed in the Borgmassivet region.

Heavy mineral laminae and soft-sediment deformation are common in the Ahlmannryggen Group, but show no direct relation to a specific facies type (Figure 1.1). Heavy mineral laminae have been recorded from almost all the formations in the Ahlmannryggen Group. These are generally found in association with facies St, Sp, and Sh, and commonly occur as thin, concentrated layers along cross-bed foresets. The heavy mineral laminae reach a maximum thickness of 30mm, however thicknesses of approximately 3mm are the norm.

Table 1.1: Summary of the various lithofacies types recognised in the Ahlmannryggen Group. Detailed descriptions in Appendix 3.

LITHOFACIES	TEXTURE	CHARACTER AND STRATIFICATION	MODE OF FORMATION	CODE
Massive gravel	Matrix supported, matrix medium- to very coarse-grained, quartz dominated, clasts range from 10mm to 60mm, very poorly sorted, moderately well rounded.	No stratification and no imbrication in pebbles, erosional base, bed thickness less than 0.2m to 2.0m, may contain layers and lenses of clast supported gravel, mud/silt rip-up clasts.	Matrix supported, suggesting debris - flood deposition / debris flow deposits (Bridge, 1993), or a sediment gravity flow deposit (Miall, 1996).	*Gm1*
	Clast supported, matrix medium- to very coarse-grained, quartz dominated, clasts range from 5mm to 200mm, moderately to well sorted, sub-angular to well rounded.	May contain layers and lenses of matrix with scattered clasts and gravel stringers, clasts may be imbricate, erosional base, bed thickness maximum 2m, mud/silt rip up clasts.	Longitudinal bars, lag deposits, sieve deposits, deposition from migrating low height bedload sheets (Bridge, 1993). Deposition from low density bedload gravel sheets (Todd and Went, 1991).	*Gm2*
Flat lying gravel	Matrix supported, matrix medium- to coarse-grained, quartz dominated, clasts 10mm to 60mm, sub-angular to well rounded, poorly sorted.	Stratification is flat lying, no imbrication, bed thickness maximum 0.2m, mud/silt rip up clasts, may be normally graded or inversely graded.	Formed as part of longitudinal bars (Miall, 1993).	*Gfl*
Stratified gravel with planar cross-beds	Matrix to clast supported, matrix medium- to very coarse-grained, quartz dominated, clasts up to 80mm, sub angular to well rounded, poorly to moderately sorted.	Foresets dip from 15° to 35°, bed thickness varies from less than 0.2m to 1.5 m, erosional base, often normally graded, clasts may be imbricate, occasional lenses of matrix.	Deposited by the migration of large, gravelly bedforms with slip faces, under high flow regime conditions (Harms *et al.*, 1975 and Karpeta, 1993).	*Gp*
Stratified gravel with trough cross-beds	Varies from matrix to clast supported, matrix very coarse-grained, clasts up to 60mm, moderately to poorly sorted.	Trough cross-bed thickness maximum 1.5m, basal contact erosional, often normally grades, ± heavy mineral laminae.	Deposited by the migration of large, gravelly 3-D bedforms under high flow regime conditions (Karpeta, 1993), and as minor channel fills (Miall, 1988).	*Gt*
Massive sandstone	Fine- to very coarse-grained, ± clasts up to 60mm, (predominantly less than 10mm), moderately to well sorted.	No stratification, base erosional to gradational, occasional mud/silt rip-up clasts, tops transitional or erosional, ± Se, may contain scattered clasts.	Short lived mass flows dump sediments at a rate too fast for hydraulic sorting processes to work effectively (Smith 1986).	*Sm*
Horizontally laminated sandstone	Medium- to coarse-grained, occasional gravel stringers and scattered clasts, moderately well to poorly sorted.	Lamination up to 5^0, minor evidence of parting lineations on bedding plane surface, occasional mud/silt rip-up clasts, ± Se.	Deposited under unidirectional upper flow regime conditions (Moore, 1979 and Harms *et al*, 1975).	*Sh1*
	Medium- to fine-grained, moderately to well sorted.	Lamination up to 5^0, no evidence of parting lineations.	The absence of parting lineations and the relatively common upward transition into silt/mud dominated facies suggests deposition under lower flow regime conditions (Moore, 1979 and Harms *et al*, 1975). Formed by very low amplitude sand waves (Miall, 1977).	*Sh2*

LITHOFACIES	TEXTURE	CHARACTER AND STRATIFICATION	MODE OF FORMATION	CODE
Planar cross-stratified sandstone (high angle)	Fine- to coarse-grained, moderate sorting, ± scattered clasts up to 20mm.	Foreset thicknesses range from 0.10m to 1.5m, foreset dips between 16^0 and 35^0, erosional base, top transitional to erosional, ± Se and mud/silt rip-up clasts, may be normally graded and foreset thickness may decrease in scale vertically, ± heavy mineral	Attributed to the migration of straight crested (2-D) dunes (Bridge, 1993; Harms *et al.*, 1975) or transverse or slipfaced bars under low flow regime conditions (Smith 1972).	*Sph*
Planar cross-stratified sandstone (low angle)	Fine-to very coarse-grained, ± gravel stringers, ± scattered clasts up to 10mm, moderately sorted.	Foreset thicknesses range from 0.2m to 2.5m, foreset dips between 5^0 and 15^0, top erosional to transitional, ± Se and scattered mud/silt rip-up clasts, ± heavy mineral laminae.	Represent deposition on inclined surfaces of side, lateral or point bars (Todd and Went, 1991).	*Spl*
Trough cross-stratified sandstone	Fine- to very coarse-grained, moderately sorted, ± occasional scattered clasts up to 10mm.	Small to large scale cross-beds which may form cosets of several meters, thickness ranges from 0.05m to 2.0m, ± heavy mineral accumulation along foresets, erosional base, ± mud/silt rip-up clasts, ± Se, may be normally graded.	Formed by migrating sinuous crested (3-D) dunes under low to high flow conditions (Harms *et al.*, 1975).	*St*
Sandstone with ripples	Fine- to medium-grained, moderately to well sorted, ripples found as solitary trains, occasional as interference sets.	Ripple crests symmetrical and either straight or slightly sinuous, occasionally bifurcate. amplitude from 2mm to 10mm, wave length from 10mm to 80mm.	Wave ripples, formed in the lower part of lower flow regime (Allen, 1964).	*Sr1*
		Ripple crests asymmetrical and either straight or sinuous to linguoid, amplitude from 3mm to 6mm, wave length from 15mm to 33mm.	Current ripples. Formed during low flow regime conditions (Allen, 1964).	*Sr2*
Basal erosional sandstone deposit with mudchip intraclasts	Medium- to coarse-grained sandstone, with a generally well developed mudchip breccia, ± exotic gravel clasts.	Thin layer of massive sandstone overlies a generally well pronounced erosional/scoured basal surface. Contains a well developed mudchip breccia and occasionally exotic gravel clasts. Commonly overlain by either planar or trough cross-stratified sandstone.	Not strictly a facies, but a recognisable "state" within the sedimentation sequence. Formed through the scouring action of currents on underlying less competent units followed by rapid deposition of sandstone and mud/silt rip up clasts.	*Se*
Scour fill sandstone	Coarse-grained to pebbly sandstone, may contain clasts - sub-angular to rounded, matrix to clast supported.	No stratification, distinct basal erosional surface, width ranges from 0.5m to 10m, ± mud/silt rip-up clasts.	May be related to strong separation eddies or to local vortices developed around obstructions. The erosion of the scour hollow and its subsequent infilling do not represent simultaneous events. The larger scours may form at the confluence of two channels	*Ss*
Ripple cross-laminated sandstone	Very fine- to fine-grained, well sorted.	Small scale cross-stratification. May be present as climbing ripples, occasionally upper surface may show ripple forms.	Formed in the lower part of lower flow regime (Allen, 1964).	*Srl*

LITHOFACIES	TEXTURE	CHARACTER AND STRATIFICATION	MODE OF FORMATION	CODE
Flaser bedded sandstone - mudstone	Very fine- to fine-grained, moderately sorted.	Cross-bedded sandstone with numerous intercalated fine grained mud/silt flasers, flasers vary from wavy to bifurcated wavy.	Formed by the alternation of current or wave action and slack water (Rieneck and Wunderlich, 1968).	*SFf*
Wavy bedded sandstone - mudstone	Fine-grained sandstone and mudstone.	Interbedded sandstone and mudstone, wavy bedding, occasional minor soft sediment deformation. The mud layers overlie ripple crests and more or less fill the ripple troughs.	Formed due to alternating periods of current activity and quiet water (as for flaser bedding), however with greater periods of quiet water permitting increased mud build up (Rieneck and Wunderlich, 1968).	*SFw*
Massive mudstone	Mud/silt, well sorted.	No stratification, thickness ranges from a few cm's to 1.5 m, basal contacts non-erosional, top contacts often erosional. May form laterally extensive sheets or lenses.	Deposition during slack water of otherwise suspended fines (Reineck 1960).	*Fm*
Mudstone with desiccation cracks	Mud/silt, well sorted.	Desiccation cracks on upper bedding plane surfaces, often infilled with sandstone.	Shrinkage cracks form due to temporary subaerial exposure (Allen, 1984).	*Fd*
Mudstone with rain-drop impressions	Mud/silt, well sorted	Raindrop imprints on upper bedding plane surfaces.	Falling rain drops can leave marks on a temporarily exposed surface (Allen, 1984).	*Frd*
Horizontally laminated mudstone	Mud/silt, moderately sorted, very fine- to fine-grained sandstone laminae.	Mudstone with thin sandstone laminae, occasional soft sediment deformation, basal contact generally non-erosional, upper contact erosional to transitional.	Dominant sedimentary process was suspension fall out accompanied by the periodic input of current transported sands (Hjellbakk, 1997).	*Fh*
Ripple cross-laminated silty mudstone	Mud/silt, moderately sorted.	Small scale cross-stratification, lower contact non-erosional, upper contact erosional to transitional.	Migration of ripples during the lower part of the lower flow regime (Allen, 1964).	*Frl*
Mudstone (sandy) with ripples	Sandy mud/silt, moderately sorted.	Ripple crests symmetrical and either straight or slightly sinuous, occasionally bifurcate.	Wave ripples. Small scale ripples formed during the lower part of lower flow regime (Allen, 1964).	*Fr1*
		Ripple crests asymmetrical and either straight or sinuous.	Current ripples. Formed during low flow regime conditions (Allen, 1964).	*Fr2*
Massive volcaniclastic	Medium to coarse grained, lapilli and volcanic glass shards.	No stratification, basal contact non-erosional, may exhibit load structures, blankets pre-exiting topography, top transitional.	Represents air-fall accumulation with little or no subsequent reworking into either fluvial or eolian bedforms, explaining the absence of traction-produced sedimentary structures (Vicars and Breyer, 1981).	*Vm*
Reworked volcaniclastic	Shows a distinct volcaniclastic content, may include lapilli and volcanic glass shards.	Stratification characteristics described through the use of one or more of the previous lithofacies codes.	Volcaniclastic material reworked subaqueously by upper to lower flow regime currents.	*V*

Figure 1.1: Photographs depicting the field appearance of selected lithofacies types. For scale, the ice axe is 70cm in length. (a) Massive gravel-Gm_1, with brilliant red jasper pebbles (Friis-Baastadnuten). (b) Low-angle, planar cross-stratified sandstone-Spl (Ovebratten). (c) Trough cross-stratified sandstone-St, with mudchip rip-up clasts along base (Grunehogna). (d) Trough cross-stratified sandstone-St, with foresets highlighted by heavy mineral laminae (Högfonna). (e) Wavy bedded sandstone - mudstone laminae- SFw (Ruvungane). (f) Alternating massive mudstone-Fm and horizontally laminated mudstone-Fh layers (Nashornkalvane). (g) Mud-cracks- Fd (Ryvingen). (h) Sinuous, asymmetrical ripple crests in sandy mudstone- Fr_2 (Ryvingen). (i) Epidotised tuff- Vm (Bråpiggen). (j) Soft-sediment deformation of heavy mineral layers in trough cross-stratified sandstone at Högfonna.

Soft-sediment deformation is generally manifested as relatively small-scale structures confined to individual units or layer boundaries. The most commonly occurring deformation structures include recumbent folds, convolute laminations, load casts, dish structures and ball-and-pillow structures. Occasional flame structures, and flamed convolution and flamed load cast horizons, similar to types H and I of Brodzikowski and Haluszczak, (1987; Figure 7), are also present. Where present, the soft-sediment deformation tends to be pervasive, but internal laminae are generally retained, suggesting that liquefaction, rather than fluidisation, was the dominant deformation mechanism (Owen, 1987).

As described by Owen (1987), the development of soft-sediment deformation requires additional influencing factors other than the operation of a deformation mechanism (such as fluidisation). If deformation is to occur, a deviatoric stress/ driving force must also be present. Based on the classification system of Owen (1987; Figure 10), possible driving force systems responsible for the development of the deformation horizons within the Ahlmannryggen Group include gravitational body forces, gravitationally unstable density gradients and shear stresses.

An additional consideration is the nature of the external trigger agent responsible for initiating the deformation mechanism (Owen, 1987). Unfortunately, the nature of the triggering agent cannot be determined merely from examining the style of deformation. Instead, the trigger agent must be established from the sedimentological context of the soft-sediment deformation (Owen, 1987). Within the context of the Ahlmannryggen Group, possible trigger agents that must be considered include rapid sediment deposition, turbulent pressure fluctuations due to flow separation and tectonic agents such as earthquakes.

1.2.2 Lithofacies Associations

Within the scope of this investigation, the purpose of a lithofacies classification scheme is primarily to aid determination of the nature of the lithofacies associations present, which form a key part in the interpretation of the depositional environment of the Ahlmannryggen Group. Individual facies types examined in isolation will not provide much assistance in the determination of the environment of deposition of a given succession; they merely provide an indication of the physical process operational at the time of their formation (Selley, 1985). Instead, lithofacies need to be grouped into associations or assemblages, which are characteristic of specific depositional environments.

Two distinctly different methods of recording and analysing lithofacies associations/ assemblages exist, namely vertical sections and lateral profiles. Vertical sections represent a simple, rapid method of recording the details of an outcrop and are a useful tool during reconnaissance work (Miall, 1990). Nonetheless, over the past years, the use of vertical profiles has come in for much criticism and they are no longer regarded as the rigorously diagnostic interpretive tools that they were once considered to be (Miall, 1985). Sedimentologists have sought to progress beyond simple vertical profiles, and the use of lateral profiles and the concept of architectural element analysis has gained widespread popularity. However, despite the fact that the reliability and overall value of vertical sequence models is considered highly questionable, their continued use is ensured where one-dimensional data is all that is available, as is the case for borehole logs and widely spaced outcrops (Fielding, 1993).

One of the problems with the extensive use of vertical profiles is that the lateral variations common to depositional systems are not considered, and as such, certain characteristics particular to a given depositional environment may be omitted. The use of a coded lithofacies system may also lead to the omission of small details and applies a general interpretation to the successions under investigation (Bridge, 1993). The use of vertical sections and lithofacies associations has therefore been combined with architectural element analysis, allowing for detailed investigation of the sedimentological characteristics of the Ahlmannryggen Group, and facilitating determination of the depositional processes responsible for the development of the Ahlmannryggen Group. Detailed analysis of the eight cliff face exposures for which lateral profiles were constructed has resulted in the definition of eight distinct architectural elements for the Ahlmannryggen Group, the characteristics of which are summarised in Table 1.2.

Table 1.2: Architectural elements recognised in the Ahlmannryggen Group (adapted from Miall, 1996).

ELEMENT	SYMBOL	CHARACTERISTIC LITHOFACIES	DESCRIPTION & INTERPRETATION
Sandy Bedform	SB	St, Sph, Ss, Srl, Sr, Se	Lens or sheet-like geometry, often laterally extensive (10's - 100's m). 3rd- or 4th-order bounding surfaces are flat lying to concave up. Abundant 2nd- and 3rd-order internal scours and erosion surfaces. Reflects deposition in unconfined to weakly channelised braided streams (Miall and Gibling, 1978).
Delta Plain Fines	DF	Frl, Fh, SFw, SFf, Fm, Srl	Sheet-like geometry, laterally extensive (100's - 1000's m). 3rd- or 4th-order bounding surfaces, abundant 2nd-order internal surfaces. Reflects vertical aggradation in low energy interdistributory delta plain settings.
Fine-grained Channel Fill	FF(CH)	Fm, Fh, Frl	Lens or sheet-like geometry, often the basal 4th-order bounding surfaces are concave up. Internal 2nd-order surfaces common. Reflects deposition from suspension in abandoned channels (Miall, 1996).
Downstream-Accretion Macroform	DA	St, Sph, Spl, Srl, Se	Lens shape, with convex up 4th-order upper bounding surfaces, flat lying basal 3rd-order bounding surfaces. Abundant downstream dipping internal 2nd- and 3rd-order surfaces indicate downstream accretion. Refelects deposition in fluvial bar forms (Miall, 1994).
Lateral-Accretion Macroform	LA	Spl, Srl, Se	Wedge shape or sheet-like geometry with 4th-order bounding surfaces. Abundant internal 2nd- and 3rd-order surfaces orientated at right angles to the dominant palaeoflow direction indicate repeated episodes of lateral accretion. Reflects deposition in fluvial bar forms where the main channel flow is directed away from the river bank (Miall, 1994).
Laminated Sand Sheet	LS	Sh, Srl, St	Sheet-like geometry with laterally extensive 4th-order bounding surfaces. Reflects deposition under flash-flood conditions (Turnbridge, 1981).
Scour Hollow	HO	Ss, Sh, Gt, St	Scoop-shaped hollow with 2nd- or 3rd-order, concave up lower bounding surfaces. Steep margins and limited lateral extent favour interpretation as HO rather than CH. Forms at the confluence of two channels or downstream from large bars, causing deep scouring (Cowan, 1991).
Channel	CH	St, Sph, Sh	Lens shaped with a concave-up, 4th-order erosional basal surface and planar, laterally extensive upper 4th-order bounding surface. Channel margins are characterised by a shallow slope angle. Simple channel fill consists of deposits from migrating two and three-dimensional dunes. Reflects deposition in minor channels (Miall, 1996).

2. SEDIMENTOLOGY OF FORMATIONS IN THE AHLMANNRYGGEN REGION

2.1 INTRODUCTION

Three formations have been defined for exposures of the Ahlmannryggen Group occurring in the Ahlmannryggen region of the Grunehogna Province (this study). These include a lower Pyramiden Formation, a middle Schumacherfjellet Formation and an upper Grunehogna Formation (Figure 2.1). The following discussion details the sedimentological characteristics of each of these formations, based on a combination of vertical and lateral profile analysis, and attempts to place constraints on their depositional environments.

2.2 THE PYRAMIDEN FORMATION

The Pyramiden Formation is composed of lithofacies St, Sph, Spl, Sh_l, Sm, Frl, Fm, Se, Sr_2, Sr_l, SFw and Fd (shown in decreasing order of abundance). The presence of desiccation cracks (facies Fd) and the predominantly unidirectional palaeocurrents (Figure 2.1) support a continental rather than marine setting for the Pyramiden Formation.

2.2.1 Vertical profile analysis

Two lithofacies associations have been identified in the Pyramiden Formation, both indicative of a continental depositional setting. A detailed vertical section, taken from the base of the formation and highlighting common vertical bedform relationships, is shown in Figure 2.2.

2.2.1.1 Association 1

The predominant lithofacies association consists of 6 – 10m thick fining-up packages dominated by medium- to large-scale trough and planar cross-stratified sandstone facies. The base of each package is invariably marked by an erosive surface highlighted by mud/silt rip-up clasts of facies Se. This basal erosive layer is generally overlain by between 2 - 5m of St lithofacies followed by 3 - 5m of Sph lithofacies. The sequence is often capped by one or more of the fine-grained lithofacies. The St and Sph lithofacies display a common, strongly unimodal palaeocurrent direction, to the north-northeast (Figure 2.1).

This association is interpreted as a channel aggradation deposit. The basal Se lithofacies was formed through the initial scouring action of currents on underlying, less competent units, and represents channel initiation. The overlying St and Sph lithofacies accumulated during channel aggradation. Gradual waning of the current strength is suggested by the transition from trough cross-stratification to planar cross-stratification, accompanied by a decrease in grain size.

A continued decrease in current strength resulted in the formation and migration of small-scale ripple structures, and the deposition of an increasing quantity of fine-grained sediment (forming facies Sr, SFw and Frl). Exposed ripple crests are generally asymmetric in form, varying from straight crested to linguiod, and indicate a palaeoflow direction varying only slightly from the dominant north-northeast direction. Subordinate symmetrical wave ripples, orientated oblique to main flow direction, were also identified. Williams and Rust (1969) explain that wave ripples may form in a fluvial setting due to the regular pulsation of small lateral waves, generated at the stream margins, by the passage of channel flow around small bars.

Finally, mud deposits settled out of suspension after channel abandonment (facies Fm). Occasionally, the sequence culminated in exposure and desiccation, forming the mudcracks of facies Fd. These upper, shallow-water accretion and suspension fallout deposits are considered to have originally been more extensive, but were subjected to a high degree of reworking, as indicated by the widespread occurrence of mud/silt intraclasts.

2.2.1.2 Association 2

The second lithofacies association identified in the Pyramiden Formation is dominated by facies Spl. This association forms a minor portion of the overall sequence, and was only recorded on three occasions. Other lithofacies occurring in association include minor Srl, Frl and Fm lithofacies. This association typically directly overlies the St lithofacies of Association 1, and exhibits a similar palaeoflow direction.

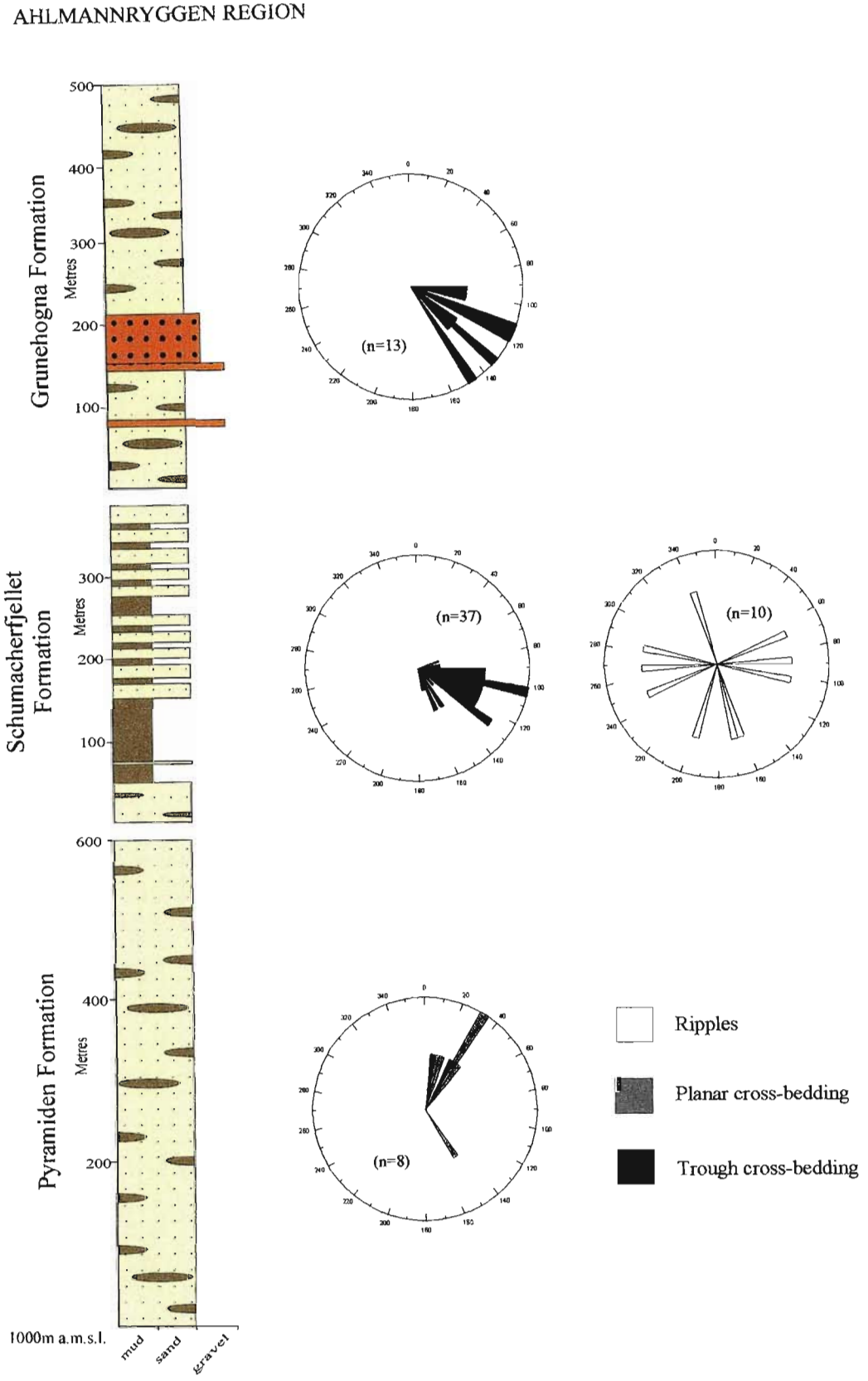

Figure 2.1: Simplified lithostratigraphy for exposures in the Ahlmannryggen region of the Grunehogna Province. Adjacent rose diagrams depict palaeocurrent orientations recorded in the three formations, from trough and planar cross-beds and ripple structures. Readings obtained from ripples are shown on a separate diagram for the sake of clarity.

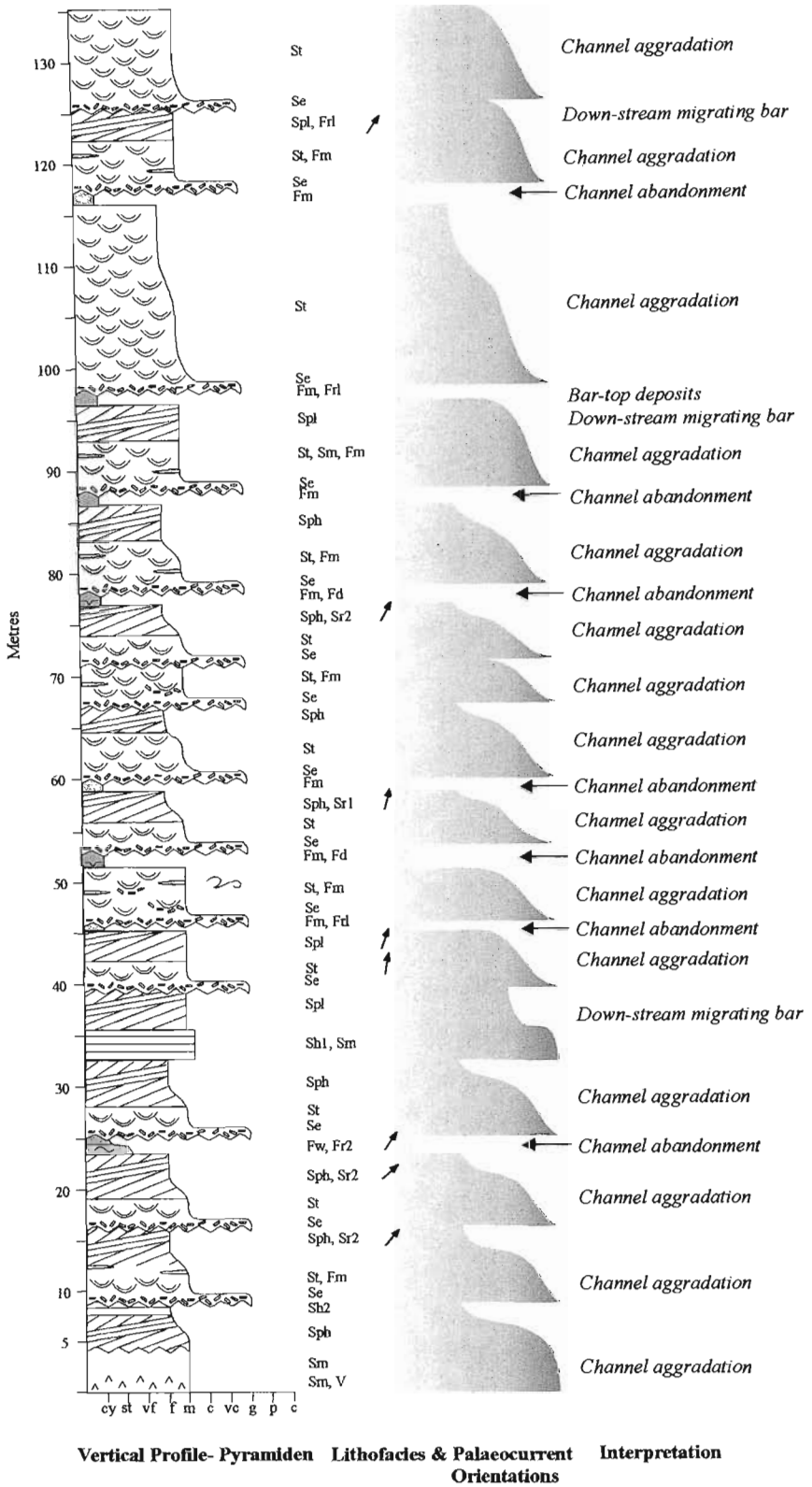

Figure 2.2: Detailed vertical section from the base of the Pyramiden Formation, highlighting common vertical bedform relationships. Lithofacies codes and palaeocurrent directions are marked beside the section. Interpretations of the vertical lithofacies associations are also indicated. Overall, the Pyramiden Formation is dominated by channel aggradation and down-stream migrating bar deposits formed in a braided fluvial system.

Association 2 is interpreted as the deposits of a downstream migrating bar, and closely resembles those described for modern braided streams (Collinson, 1970; Smith, 1970, 1971 and Williams, 1971). The overlying small-scale cross-lamination (facies Frl) resulted from ripples migrating across the bar top during low water stage, allowing continued progradation of the bar-front avalanche slope (Miall, 1977; Smith, 1971, 1972; Collinson, 1970). The thin, lens-shaped deposits of facies Fm represent drape deposits formed in pools of standing water, possibly associated with minor channels and scours cut into the bar surface. The rare occurrences of Association 2 are invariably overlain by deposits of Association 1, indicating renewed channel aggradation.

2.2.1.3 Other features of interest

Occasional occurrences of Sm and Sh_l lithofacies, in combination with either Association 1 or 2 are interpreted as the deposits of sporadic higher energy events.

2.2.1.4 Depositional environment

The repeated vertical stacking of Association 1 has led to the formation of a profile characterised by cyclic sedimentation/channel aggradation, occasionally interrupted by isolated bar deposits (Association 2). Combined with a lack of evidence for lateral accretion, and the dominance of sand sized sediment arranged in laterally continuous layers, this suggests a fluvial style similar to modern and Phanerozoic braided rivers/braidplains (e.g. Rust, 1972; Miall, 1977; Cant and Walker, 1978, Rust and Gibling, 1990; Miall, 1996; Jones *et al.*, 2001). The Pyramiden Formation displays a close similarity to Miall's (1977) Donjek Type braided river depostional profile, although it is finer grained, and lacks extensive gravel deposits. The profile also displays marked similarities to the South Saskatchewan braided river (Cant and Walker, 1978). The channel aggradation (Association 1) packages appear to thicken vertically, possibly associated with changing channel depths over time, related to low water and high water stages of the river system. Overall, the Pyramiden Formation is typically finer-grained than many other braided river examples, and lacks thick gravel deposits, suggesting a distal depositional setting. The dominance of finer-grained deposits may also be attributed to a low source elevation or low slope gradient (Rust, 1972).

2.2.2 Architectural element analysis

Unfortunately, no cliff-face exposures suitable for the construction of lateral profiles were available, and as such, determination of the depositional setting of the Pyramiden Formation is entirely dependent on vertical profile analysis.

2.3 THE SCHUMACHERFJELLET FORMATION

The Schumacherfjellet Formation is a fine-grained to sandy sequence composed of lithofacies St, Se, Ss, $Sr_{1\&2}$, Frl, Fm, Fd, Fh, $Fr_{1\&2}$, SFf, SFw, Sh_2, Sm, Spl, Sph and Srl. The presence of desiccation cracks (facies Fd) is regarded as indicative of a continental depositional setting, in which occasional subaerial exposure occurred. The sandstone lithofacies typically exhibit a well-constrained, unimodal palaeocurrent orientation to the east-southeast (Figure 2.1). Both the fine-grained and sandy units display an exceptionally high degree of lateral continuity, and may be followed for the full extent of an exposure (up to 2km in some localities).

2.3.1 Vertical profile analysis

Three dominant lithofacies associations have been identified in the Schumacherfjellet Formation. Selected detailed sections, highlighting common vertical bedform relationships in the Schumacherfjellet Formation, are shown in Figure 2.3.

2.3.1.1 Association 1

Association 1, which was recorded predominantly from the base of the Schumacherfjellet Formation, and at sporadic intervals higher up, is dominated by sandstone lithofacies, including facies St, Se, Ss and Sr_2, and contains subordinate fine-grained facies Frl, Fm and Fd. The erosive base of each assemblage is often highlighted by a thin layer of facies Se. The overlying St lithofacies form single or stacked cosets up to 15m thick. A predominantly unimodal palaeocurrent flow direction, towards the east-southeast, is invariably exhibited (Figure 2.1). Occasional scour-fill deposits (facies Ss) were recorded. A thin overlying layer of fine-grained lithofacies may be preserved, however these often appear to have been reworked or removed by a subsequent erosive event, as indicated by the abundance of mud/silt

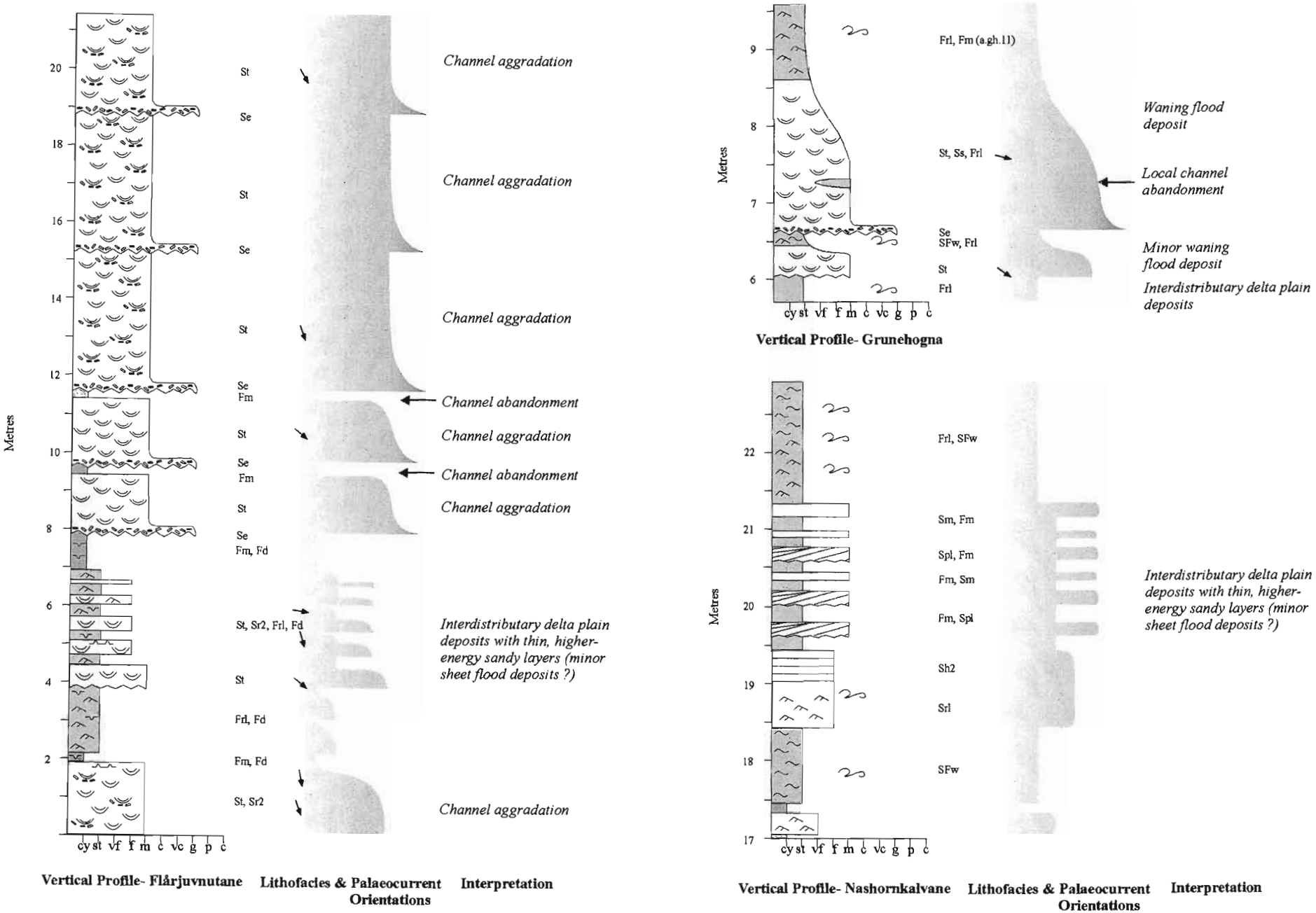

Figure 2.3: Selected vertical sections from the Schumacherfjellet Formation, highlighting common vertical bedform relationships. Lithofacies codes and palaeocurrent directions are marked beside each section. The Schumacherfjellet Formation is dominated by a combination of laterally extensive, distal fluvial channel deposits and interdistributory delta plain deposits. Graded units suggest that deposition from repeated waning flood events also occurred.

intraclasts in overlying units. All units exhibit a high degree of lateral continuity.

Association 1 is interpreted as a distal fluvial channel deposit. The basal erosive contact, highlighted by facies Se, represents the initial scouring action associated with channel initiation. The St lithofacies cosets reflect deposition by sandwaves in the channel complex, while the overlying fine-grained deposits accumulated as a result of low water accretion processes and suspension fallout. Periodic sub-areal exposure and desiccation resulted in the formation of facies Fd. The dominance of sandstone lithofacies over fine-grained lithofacies, lack of evidence for lateral accretion and the tightly clustered palaeocurrent directions are regarded as indicative of a braided fluvial origin (Rust, 1972; Miall, 1977). The notable lateral extent and lack of visible channel margins indicates deposition occurred in sheet-like, unconfined channels, flowing towards the east-southeast. A distal depositional setting is inferred from the overall fine-grained, sand-dominated nature of the channel fill sediment (gravel is absent) and the presence of occasional mud-dominated Association 2 layers.

2.3.1.2 Association 2

A fine-grained dominated lithofacies association, exhibiting a highly variable composition, is also readily identifiable in the Schumacherfjellet Formation. Laterally continuous layers of facies Frl, Fh, $Fr_{1\&2}$, Fm, Fd, SFf, SFw, Srl $Sr_{1\&2}$ and Sh_2, between 0.5 and 10m thick are occasionally interrupted by thin (generally < 1m thick) layers of sandstone lithofacies (including Sm, Spl, Sph and St) also exhibiting a high degree of lateral continuity.

Association 2 is interpreted as an interdistributary delta plain deposit. The dominance of fine-grained sediment characterised by desiccation cracks, ripple structures exhibiting a polymodal to bimodal dispersion, and tidal-type stratification (including flaser and wavy bedding) indicates deposition took place in a quiet water environment subjected to minor tidal influence and sporadic subaerial exposure. Such conditions are typical of interdistributory, delta plain environments (Collinson, 1968; Moore, 1979; MacNaughton *et al.*, 1997; Dreyer *et al.*, 1999). The occasional thin sandstone units found in association with these fine-grained deposits resulted from the introduction of coarser-grained sediment by higher energy currents, which periodically invaded the predominantly quiet water environment, possibly as a result of sheet floods.

2.3.1.3 Association 3

Lithofacies St, Srl, SFw, SFf, Ss, Se, Frl, and Fm form a common association in the mid- to upper-part of the Schumacherfjellet Formation. These different facies types all exhibit an exceptionally high degree of lateral persistence and are typically arranged in a normally graded, fining-upwards cycle. The base of the association is invariably erosional, but rarely marked by facies Se. The basal erosive surface is overlain by a variable thickness of St lithofacies (1-15m) which grades up into facies Srl, Frl, SFw, SFf and Fm (1-10m thick). Occasionally, scour-fill deposits (facies Ss) were also recorded in the lower, sandstone dominated portion of Association 3. The original thickness of the upper, fine-grained deposits is impossible to estimate, due to partial removal by subsequent erosive episodes.

Association 3 is interpreted as a fluvially dominated, waning flood deposit. The erosive base of the association reflects channel initiation, on top of which the normally graded, sandstone to fine-grained facies accumulated during waning flow conditions. The notable lack of lateral accretion deposits, and the high degree of lateral continuity exhibited by both the sandstone and fine-grained units, suggests deposition in a braided fluvial system (Rust 1972; Miall, 1977). A distal, possibly tidally influenced setting is inferred from the dominance of fine-grained and sandy lithofacies, the lack of gravel deposits, and the presence of poorly developed tidal-type stratification (facies SFw and SFf). The dominant palaeocurrent direction exhibited by the trough cross-stratification (towards the southeast to east-southeast-Figure 2.1) is in close agreement with that shown by the fluvially dominated Association 1 deposits. This, combined with a lack of tidal indicators in the higher energy, sandstone portions of the association, suggests that the dominant current activity was fluvial (as apposed to tidal) in origin. Possible tidal influence is only recorded in the fine-grained deposits, which formed when the fluvial effects are at their least.

2.3.1.4 Depositional environment

The intimate association of fine-grained, tidally influenced overbank deposits (Association 2) and fluvially dominated, channel deposits (Association 1 and 3) indicates that the Schumacherfjellet Formation was deposited in a distal, delta plain environment. The sequence shows marked similarities to published examples of fluvially dominated, delta plain sequences (e.g. Collinson, 1968; Moore, 1979; Dreyer *et al.*, 1999).

Conditions were initially characterised by deposition in laterally extensive, unconstrained fluvial channels, exhibiting many similarities to modern braided river systems (Rust, 1972; Miall, 1977). Repeated stacking of Association 1 created a vertical profile dominated in the lower part by channel aggradation. A distal setting, possibly affected by limited tidal influence, is indicated by occasional examples of Association 2. The paucity of upper flow regime horizontal stratification suggests discharge was continuous, rather than catastrophic (Sonderholm and Tirsgaard, 1998). This lower portion of the formation is regarded as reflecting deposition on the landward margin of a delta plain system, where distal, braided fluvial channels dominated, and tidal influence was restricted. A change in depositional conditions is reflected in the overlying 100m, where the vertical profile is characterised by thick deposits of Association 2. The depositional environment became dominated by the accumulation of fine-grained sediment in an interdistributary delta plain setting, influenced by limited tidal activity and subjected to repeated subaerial exposure. The remainder of the Schumacherfjellet Formation is characterised by repeatedly stacked Association 3 cycles, reflecting numerous, fluvially dominated flood events that blanketed the delta plain with repeated fining-upwards cycles, and which display marked similarities to Miall's (1996) model for sheetflood dominated, distal braided fluvial systems.

2.3.2 Architectural element analysis

Interpretation of vertical profiles can be complimented by recognising the type of lateral bedform variations recorded within the depositional system. An understanding of these lateral variations can be achieved by recognising and interpreting bounding surfaces and architectural elements within the system.

A single face sketch was constructed from a southeast-facing cliff near the base of Veslekletten (Figure 2.4). Unfortunately, this cliff face is completely inaccessible, and as a result, no detailed palaeocurrent analysis could be performed, reducing accuracy and detail of the analysis. On this, and all following sketches, 3rd- and higher order surfaces have been marked (Miall, 1988a,b). The un-numbered lines are all first and second order surfaces, except where individual cross-bed sets have been drawn in. Each architectural element that has been identified is numbered, in order of deposition. The two-letter code beside each element number refers to the element classification (see Table 1.2).

2.3.2.1 Sandy Bedforms

Six elements in profile 1 are interpreted as Sandy Bedforms. These elements are regarded as representing fields of individual bedforms that accumulated predominantly by vertical aggradation. Elements 1, 3, 5, 7, 9 and 11 are all characterised by deposits of small- to medium-scale three-dimensional dunes (facies St). The laterally extensive, generally 3rd- and 4th-order upper and lower bounding surfaces of each of these elements are characteristically flat lying, and lack the diagnostic upper convex-up bedding contact typical of lateral and downstream accretion units (Miall, 1996). Internally, the sheet-like elements often contain broad, shallow scours and erosion surfaces of 2nd- and 3rd-order.

These SB elements (Figure 2.4b) are characteristic of weakly channeled streams similar to braidplains (Williams, 1971; Miall, 1977). The flat basal surface commonly associated with these bedforms implies deposition from laterally unconfined to broadly channelised sheetflood deposits (Turnbridge, 1981). The concave up, internal erosion surfaces noted within some of these bedforms are likely to owe their origin to the scouring and filling of multiple low sinuousity channels / stage fluctuations. The SB elements show a marked similarity to the distal braidplain sheet sandstones described by Miall (1996).

2.3.2.2 Interdistributary delta plain elements

The five other elements identified in profile 1 are interpreted as fine-grained, interdistributary delta plain elements, and have been assigned the code DF. Elements 2, 4, 6, 8 and 10 are similar in some respects to element FF in Miall's (1996)

SW

NE

Figure 2.4 (a): Photomosaic from the middle of the Schumacherfjellet Formation, exposed at Veslekletten. Cliff is facing SE. An interpretation of this cliff face is presented in Figure 2.4(b).

Profile 1

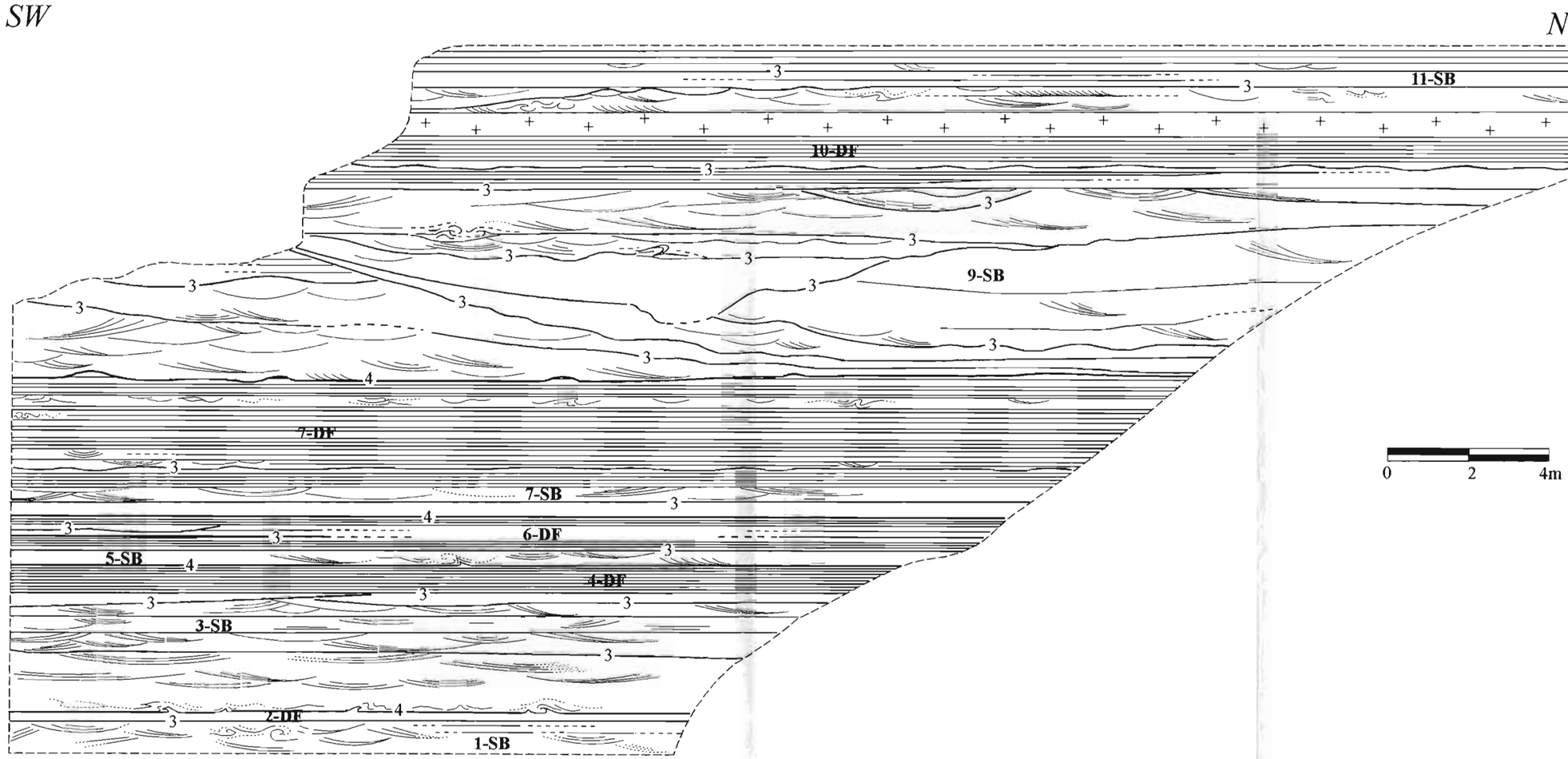

Figure 2.4(b): Field sketch from the Schumacherfjellet Formation, exposed at Veslekletten. The photo-mosaic of this face is depicted in Figure 4.4(a). Bounding surfaces are indicated by the appropriate hierarchical number, based on Miall's (1988) classification. A tentative element classification is indicated, using the two letter element code detailed in Table 1.2. According to both vertical and lateral facies variations, deposition of this formation took place in a braid delta plain setting. The sequence contains thin sandy units deposited in shallow, laterally extensive distal channels and thick fine-grained units which accumulated in quiet water, interdistributory regions.

classification, but were deposited in a tidally influence delta plain setting, rather than the fluvial flood plain environment in which element FF may be found. These DF elements are characterised by fine-grain dominated deposits (facies Frl, Fh, SFW, SFf and Fm) bound by flat, laterally extensive upper and lower 3rd- and 4th-order surfaces. Generally, these sheet-like units can be followed for the full extent of the exposure. Abundant 2nd-order internal bounding surfaces are easily identifiable. These elements are interpreted as vertical aggradation deposits that accumulated under low energy, tidally influenced conditions in a delta plain setting.

2.3.2.3 Environmental setting of the Schumacherfjellet Formation

Both the vertical profile analysis and the architectural element analysis of the Schumacherfjellet Formation suggests deposition took place in a distal, fluvially dominated, delta plain setting in which laterally extensive sheet-like architectural elements could accumulate. According to Miall (1996), distal braid-plain deposits may consist entirely of element SB. In this setting, sheets of sand developed in broad, virtually unconfined channels in which aggradation and progressive abandonment occurred, followed by the accumulation of fine-grained deposits subjected to minor tidal influence.

2.4 THE GRUNEHOGNA FORMATION

Lithofacies recognised within the Grunehogna Formation, in decreasing order of abundance, are: St, Gt, Se, Frl, Fh, Ss, Fm, Sr_2, Fr_2, SFw, Spl, Gm_1, Sm, Srl and Fd. As for the previous two formations, the presence of facies Fd and predominantly unimodal palaeocurrents (Figure 2.1) are regarded as indicative of a shallow water continental environment, subjected to occasional subaerial exposure.

2.4.1 Vertical profile analysis

Two dominant lithofacies associations have been identified in the Grunehogna Formation, both indicative of a continental depositional setting. Selected detailed sections, highlighting common vertical bedform relationships in the Grunehogna Formation, are shown in Figure 2.5.

2.4.1.1 Association 1

The dominant lithofacies association identified in the Grunehogna Formation consists primarily of St lithofacies, with subordinate Se, Srl, Frl, Sr_2, Fr_2, Fh and Fd lithofacies. This association accounts for approximately 80% of the exposed sequence. The base of Association 1 is generally marked by an erosive surface overlain by facies Se, which is in turn overlain by stacked cosets of medium- to large-scale trough cross-stratification (facies St). Thin, isolated lenses of Fh and Fm lithofacies occasionally occur within these cosets, and the sequence may be capped by minor Srl, Sr_2, Fr_2, Frl, SFw, Fh Fm and Fd lithofacies. Infilled scours (facies Ss) may also be present. On average, Association 1 attains a thickness of between 5 and 10m, and displays a strongly unimodal palaeocurrent direction, towards the southeast (Figure 2.1).

Association 1 is interpreted as a channel aggradation deposit. The basal erosive contact, highlighted by facies Se, represents the initial scouring action associated with channel initiation, while the numerous, stacked cosets of lithofacies St reflect deposition by sandwaves in the channel complex. The occasional scour-fill deposit (lithofacies Ss) may have formed in the deeper sections of the channels, possibly at channel confluences downstream of a mid-channel bar. The composition of the scour fill ranges from gravel to medium sand, suggesting development under both upper and lower flow regime conditions. The overlying finer-grained deposits, generally characterised by small scale cross-stratification and lamination, represent the products of low water accretion processes. Thin lenses of facies Fm owe their origin to the deposition of mud and silt from suspension, in standing bodies of water left in abandoned channels. Occasional exposure and desiccation of the fine-grained deposits led to the formation of facies Fd. The original thickness of the fine-grained deposits is impossible to estimate due to a high degree as reworking, as indicated by the abundance of mud/silt intraclasts.

2.4.1.2 Association 2

Lithofacies Gt, St, Gm_1, Se, Ss and Fm form a common association in the Grunehogna Formation, accounting for approximately 15% of the exposed sequence.

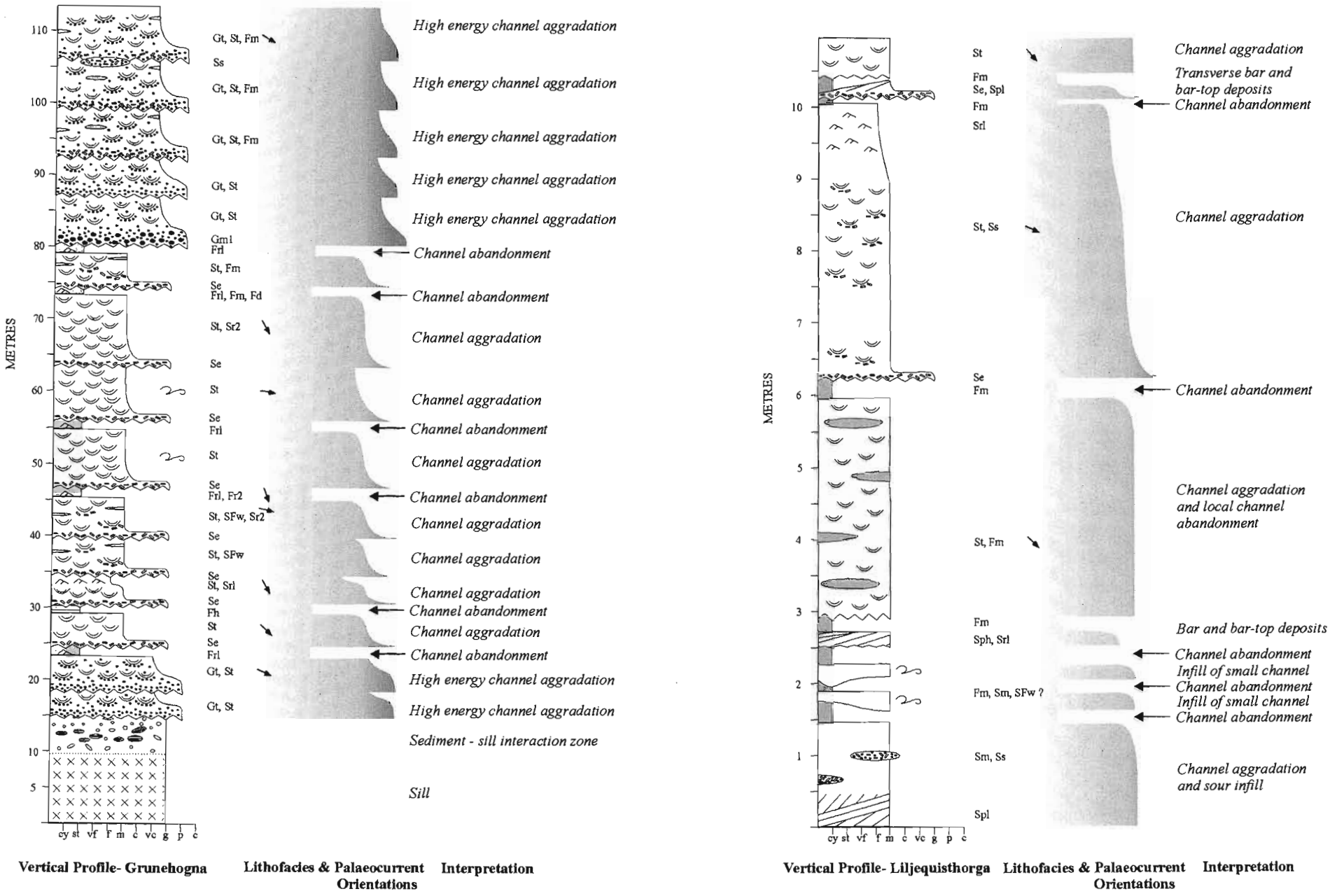

Figure 2.5: Selected detailed vertical sections from the Grunehogna Formation, highlighting common vertical bed form relationships. Lithofacies codes and palaeocurrent directions are marked beside each section. The Grunehogna Formation is dominated by channel aggradation deposits that accumulated under moderate to high energy conditions in a braided fluvial system.

This association shows similar characteristics to Association 1, but is coarser grained overall, and contains a high proportion of gravel deposits. A pronounced basal erosive contact may be marked by facies Se or more rarely, facies Gm_l. This is overlain by large-scale Gt lithofacies, which often pass vertically into large- to medium-scale St lithofacies with decreasing grainsize and a reduction in clast content. Scour-fill deposits (facies Ss) also occur in Association 2, and thin lenses of facies Fm are occasionally preserved.

Association 2 is also interpreted as reflecting channel aggradation, however relatively higher energy conditions are inferred from the coarse, gravel dominated nature of this association. The strongly unimodal, southeast palaeocurrent identified in Association 1 is also reflected in Association 2.

2.4.1.3 Other features of interest

The channel aggradation deposits that dominate the Grunehogna Formation are occasionally interrupted by isolated sets of planar cross-stratification (facies Spl) containing foresets orientated oblique to the dominant palaeoflow direction. These are interpreted as rare transverse bars that migrated across the channel system. Occasional massive sandstone units (facies Sm) may owe their origin to sporadic, higher-energy events from which sediment was rapidly deposited.

2.4.1.4 Depositional environment

The Grunehogna Formation is characterised by channel aggradation cycles dominated by sand and gravel deposits arranged in laterally continuous layers. Combined with a low palaeocurrent variability, this suggests deposition in a fluvial system similar to modern day braided rivers. Bedform orientations indicative of accretion oblique to the dominant palaecurrent flow direction were also identified, a feature common in many sandy braided fluvial systems (Cant and Walker, 1978), and which represent occasional bar deposits. The presence of gravel deposits (marked by Association 2) suggests periodic high-energy currents, however, upper flow regime horizontal lamination is conspicuously absent. According to Sonderholm and Tirsgaard (1998), this can be regarded as suggesting continuous rather than catastrophic discharge.

Unlike the Pyramiden Formation, deposits of the Grunehogna Formation lack a repetitive facies pattern. This is considered indicative of deposition in a fluvial system with minimal accommodation space and a consequently high degree of reworking (Sonderholm and Tirsgaard, 1998). This interpretation is supported by the limited nature of the fine-grained, shallow water accretionary deposits and the presence of abundant mud intraclasts. Overall, the Grunehogna Formation shows a marked similarity to the channel deposits of the modern South Saskatchewan braided river, as described by Cant and Walker (1978), with abundant trough cross-stratification and limited planar cross-stratified, transverse bar deposits. The sequence is also similar in many respects to Miall's (1977) Donjek Type profile, but does not exhibit the same degree of variability and lacks pronounced fining upwards cycles.

2.4.2 Architectural element analysis

Two face sketches were constructed in order to understand the lateral variability recorded in the Grunehogna Formation. The first sketch (profile 2, Figure 2.6a,b) was from a north-facing exposure located at the western limit of Grunehogna Peak 1390, and records the nature of the most common bedforms identified. The second sketch (profile 3, Figure 2.6c,d) was constructed from a south-facing exposure at the eastern limit of Göstapiggane, and is intended to reveal in greater detail the internal characteristics of the dominant bedform / architectural element type recorded in the Grunehogna Formation. Unfortunately, these cliff faces are largely inaccessible and as a result no detailed palaeocurrent analysis could be performed.

2.4.2.1 Sandy Bedforms

Eight elements in profile 2 are interpreted as Sandy Bedforms, and exhibit marked similarities to element SB in Miall's (1996) classification. These elements are regarded as representing fields of individual bedforms that accumulated predominantly by vertical aggradation. Elements 1-4, 6 and 8-10 are all characterised by deposits of three-dimensional dunes (facies St) which apparently exhibit a generally southeasterly palaeoflow direction. The laterally extensive 4^{th}-order upper and lower bounding surfaces of each of these elements are characteristically flat lying, and lack the diagnostic upper convex-up bedding contact typical of lateral and downstream accretion units (Miall, 1996). Internally, the eight

E

W

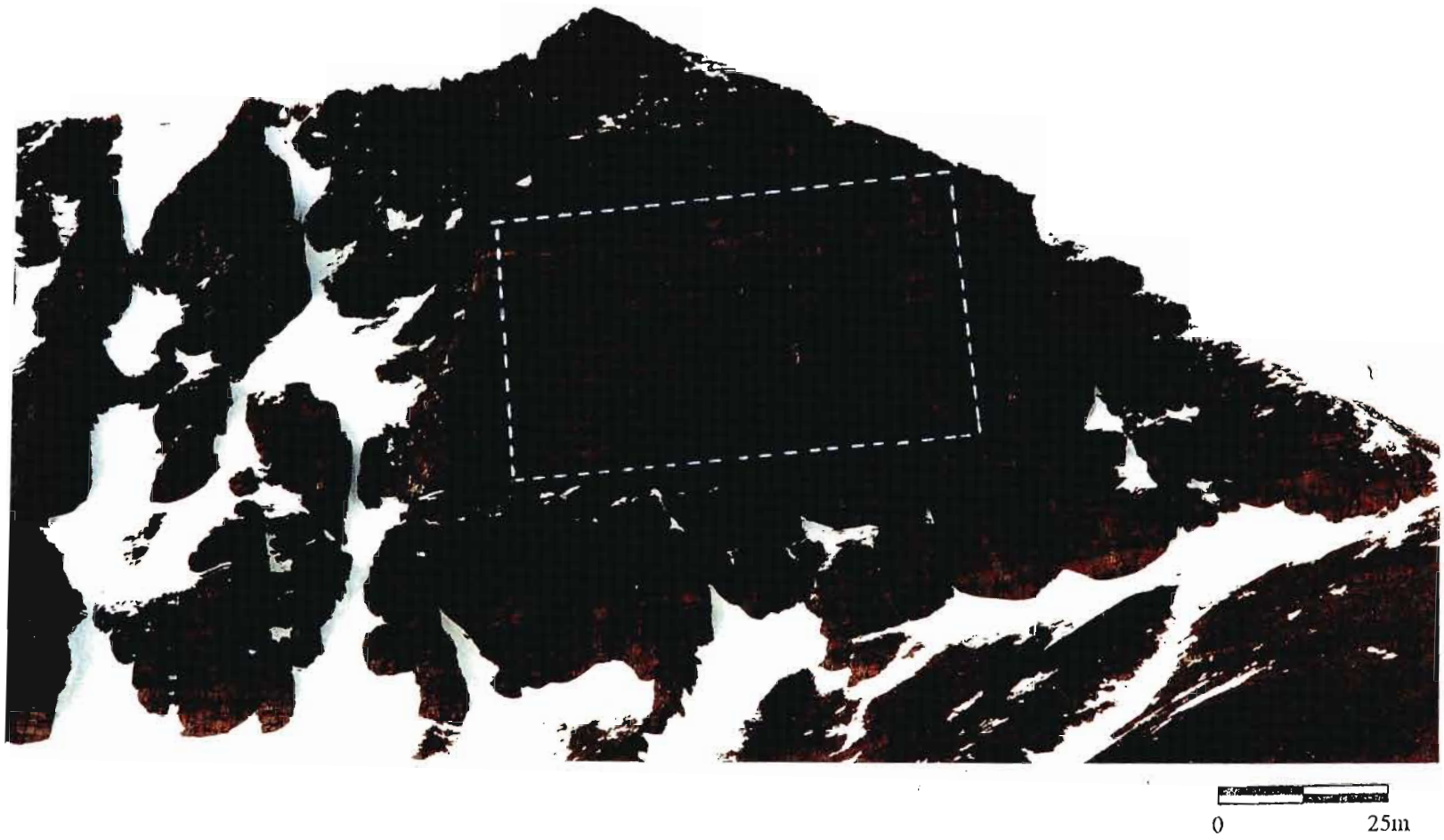

Figure 2.6 (a): Photograph from the base of the Grunehogna Formation, exposed at Grunehogna Peak 1390. The field sketch and interpretation of this face is shown in the following diagram, Figure 2.6(b). Cliff is facing N.

Profile 2

E *W*

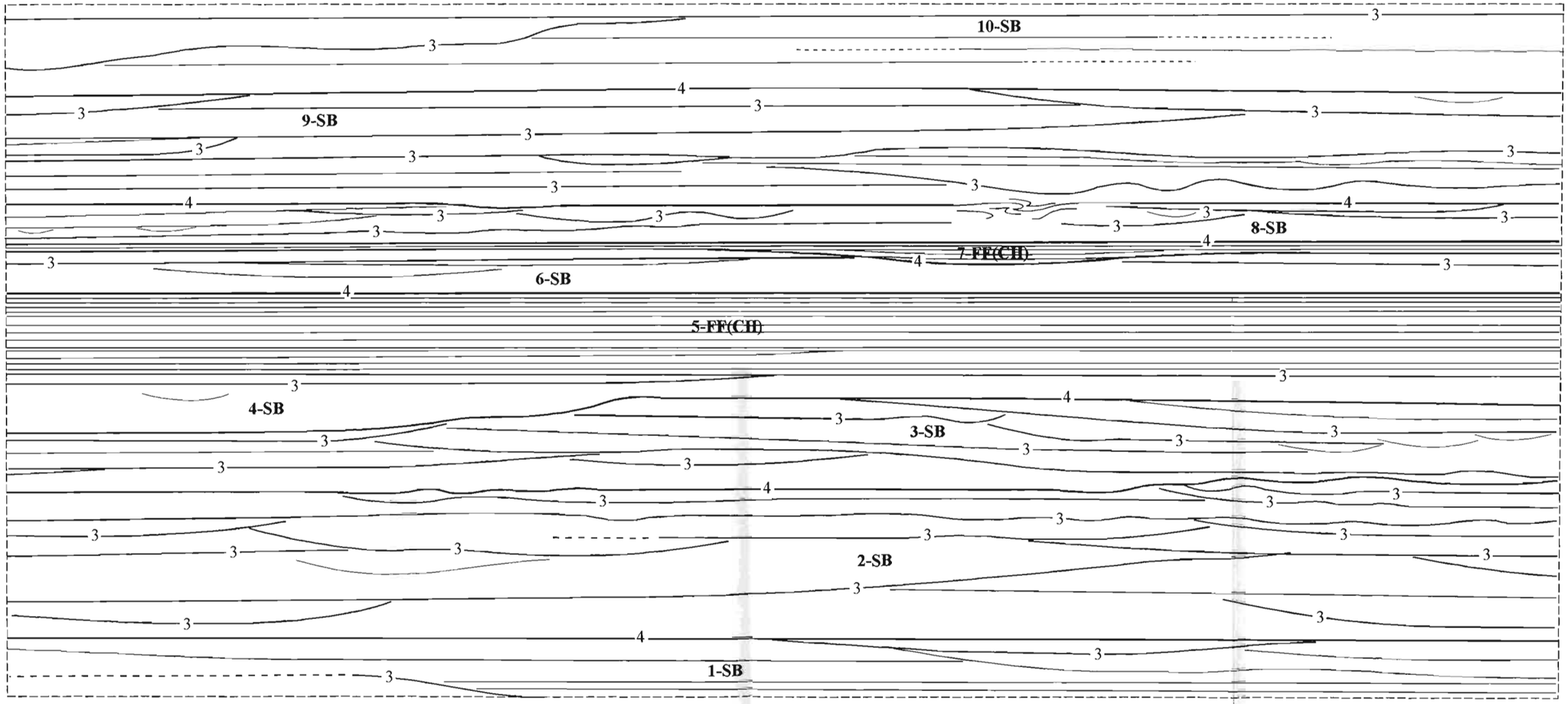

Figure 2.6(b): Field sketch from the Grunehogna Formation, exposed at Grunehogna. The photo-mosaic of this face is depicted on the previous page, 2.6(a). Bounding surfaces are indicated by the appropriate hierarchical number, based on Miall's (1988) classification. According to vertical and lateral facies variations, deposition of this formation took place in a braided fluvial setting. The sequence is dominated by sandy channel aggradation deposits.

W

E

0 1 2m

Figure 2.6(c): Photomosaic from the middle of the Grunehogna Formation, exposed at Göstapiggane. Cliff is facing S. The field sketch and interpretation of this cliff face section is shown in Figure 2.6(d).

Profile 3

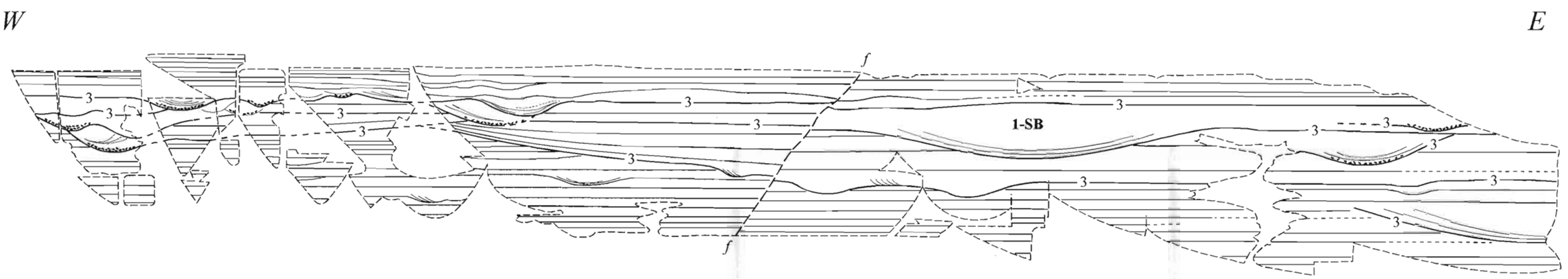

Figure 2.6(d): Field sketch from the Grunehogna Formation, exposed at Göstapiggane. The photo-mosaic of this face is depicted on the previous page, 2.6(c). Bounding surfaces are indicated by the appropriate hierarchical number, based on Miall's (1988) classification. According to both vertical and lateral facies variations, deposition of this formation took place in a braided fluvial setting. The sequence is dominated by sandy channel aggradation deposits containing numerous scour structures.

elements consist of lenses of medium- to large-scale trough cross-stratified sand 10's m wide, defined by broad, shallow scours and erosion surfaces of 2nd- and 3rd-order (Figure 4.6c,d).

These SB elements are characteristic of weakly channelised streams, similar to braidplains (Williams, 1971; Miall, 1996). The flat basal surface commonly associated with these bedforms implies deposition from laterally unconfined to broadly channelised sheetflood deposits (Turnbridge, 1981). The architecture and composition of these fluvial deposits show marked similarities to the channel-floor dune fields described by Miall (1996). The commonly occurring internal, concave up erosion surfaces were probably generated by the repeated scouring and filling of low sinuousity channels, associated with stage fluctuations.

2.4.2.2 Abandoned channel fill elements

The remaining two elements identified in profile 2 are interpreted as abandoned channel fill elements, similar in some respects to element FF(CH) in Miall's (1996) classification (Figure 2.6b). Elements 5 and 7 are characterised by fine grain dominated deposits, bound by laterally extensive 4th-order surfaces. Abundant 2nd-order internal bounding surfaces are easily identifiable, however, the marked 3rd-order erosive surfaces commonly recognised in the SB elements are absent. These elements are interpreted as vertical aggradation deposits that accumulated under low energy conditions in abandoned channels.

2.4.2.3 Environmental setting of the Grunehogna Formation

Both the vertical profile analysis and the architectural element analysis of the Grunehogna Formation indicate deposition took place in a sand to gravel bed-load dominated fluvial setting, similar to modern braided stream environments. The sequence is characterised by channel aggradation deposits and laterally extensive Sandy Bedform architectural elements. Channels were broad and poorly confined. This combined with apparently limited accommodation space, resulted in extensive reworking and only limited preservation of fine-grained, abandoned channel fill architectural elements.

3. SEDIMENTOLOGY OF FORMATIONS IN THE BORGMASSIVET REGION

3.1 INTRODUCTION

The following section presents the findings of an investigation into both the vertical and lateral variations recorded in the strata of the Ahlmannryggen Group encountered in the Borgmassivet region of the Grunehogna Province. Four formations have been defined during this study for exposures in the Borgmassivet region, namely the Veten, Framryggen, Högfonna and Bråpiggen Formations. The sedimentological characteristics of each of these four formations are considered separately, before being combined with observations from the Ahlmannryggen region in an overall model (Section B4).

3.2 THE VETEN FORMATION

The basal Veten Formation in the Borgmassivet region is dominated by a mixture of sand and gravel lithofacies. Lithofacies types identified include, in decreasing order of abundance, St, Spl, Se, Gt, Gm_l, Gm_2, Sph, Fm, Ss, Srl, Fh, SFw, Frl, Gfl, Sm, Sr_1 &2, $Fr_{1\&2}$, $Sh_{1\&2}$, Gp and Fd. A terrestrial depositional setting is suggested by the presence of desiccation cracks (facies Fd) and a strongly unimodal palaeocurrent direction (to the east-northeast) within the high-energy sandy lithofacies (Figure 3.1).

3.2.1 Vertical profile analysis

Exposures of the Veten Formation contain a wide variety of lithofacies types, and display a high degree of variability with regard to lithofacies associations. Three different associations have been identified, all indicative of a continental depositional setting. Selected detailed sections are shown in Figure 3.2.

3.2.1.1 Association 1

The dominant lithofacies association in the Veten Formation consists primarily of lithofacies St, Se, Ss and Fm. Other lithofacies types that may occur in this association include: $Sr_{1\&2}$, Srl, Frl, Fh, Sh_l, Sph and Gm_2. Typically, the base of the association is marked by a pronounced erosive surface, defined by facies Se. In some cases, a basal Sh_l or $Gm_{1/2}$ unit is present in place of facies Se. The overlying medium-scale St lithofacies generally form stacked cosets between 5 and 10m thick, but may reach 15m in rare cases, or may occur as single cosets. Occasional scour fill deposits (facies Ss) were noted. Lithofacies St may be succeeded by a variety of different lithofacies. On occasion, these are arranged into an overall fining-upwards sequence, which may include facies Sph, Srl, $Sr_{1\&2}$, Frl Fh and Fm. Alternatively, the St lithofacies may be draped by thin, often lens-shaped deposits of facies Fm. Facies St and Sph tend to display a unimodal palaeocurrent flow direction, towards the east-northeast, while the smaller scale structures exhibit a higher degree of variability.

Association 1 is interpreted as a channel aggradation deposit. The basal Se lithofacies was formed during the initial stages of channel development, and resulted from the scouring action of currents on underlying, less competent units. Occasionally, current strength may have increased, resulting in the formation of facies Sh_l, or the deposition of a thin gravel lag (facies Gm_2). The overlying St lithofacies cosets accumulated during channel aggradation. The vertical stacking of numerous cosets is taken to reflect deposition by sand waves in a relatively deep channel complex, while single cosets indicate a shallower depositional environment (Ashley, 1990). In some cases, a gradual waning of the current strength is indicated by a transition from trough cross-stratification to planar cross-stratification, accompanied by a decrease in grain-size. The overlying finer-grained / small-scale cross-stratified lithofacies represent the deposits of shallow water accretion processes. Alternatively, facies St may be draped by thin layers and lenses of facies Fm, which owe their origin to the deposition of mud from suspension, in standing bodies of water left in abandoned channels. Reworking of these fine-grained deposits accounts for the abundance of mudstone intraclasts in overlying units.

3.2.1.2 Association 2

Lithofacies Gfl, Gm_2, Gt and St form a common association in the Veten Formation. Subordinate Ss, Frl and Fm facies may also be present. These lithofacies are often arranged in fining-upwards cycles, which show a vertical transition from

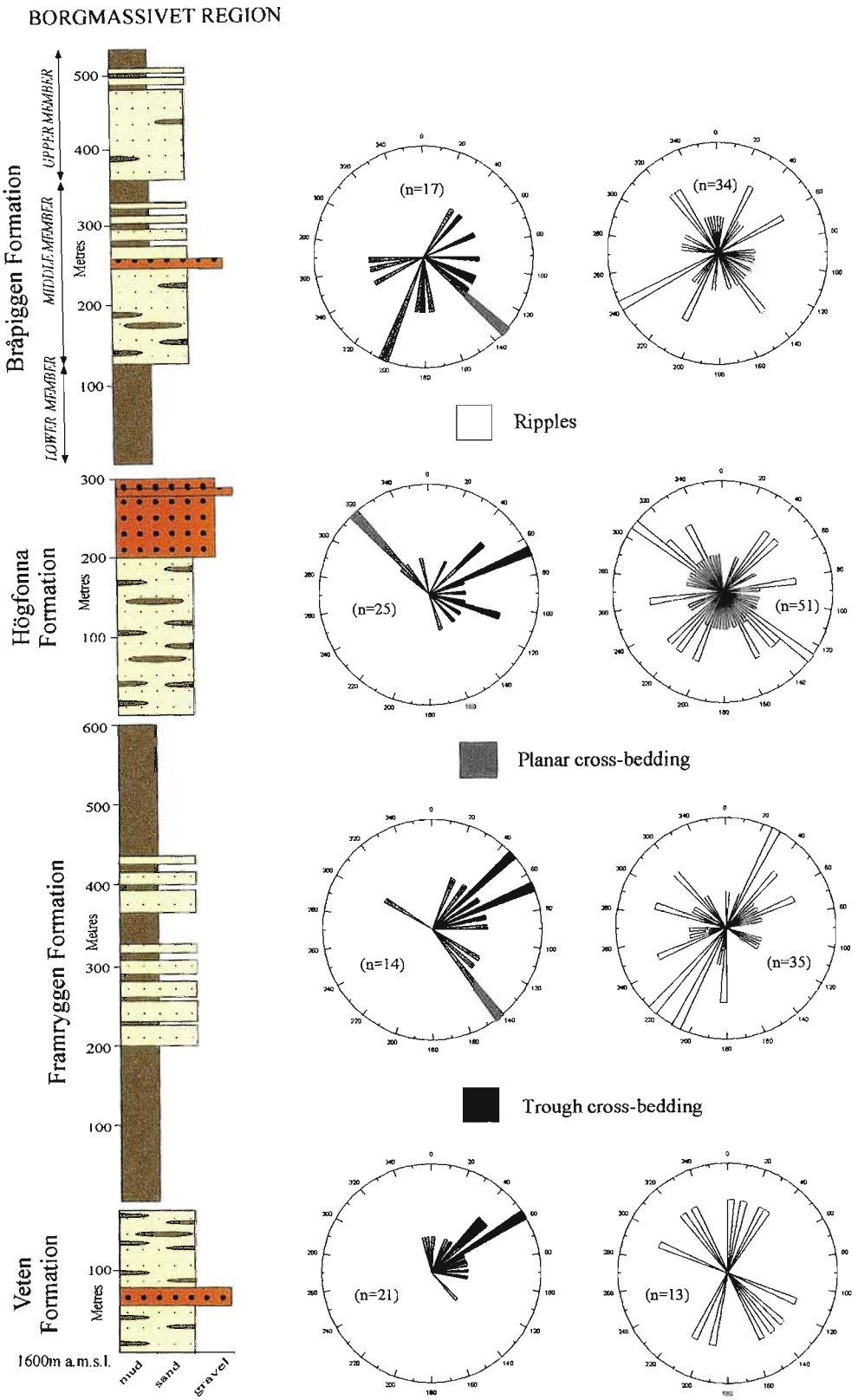

Figure 3.1: Simplified lithostratigraphy for the Borgmassivet region of the Grunehogna Province. The adjacent rose diagrams record palaeocurrent directions obtained from trough and planar cross-beds and ripple crest orientations- the latter depicted on separate diagrams for the sake of clarity.

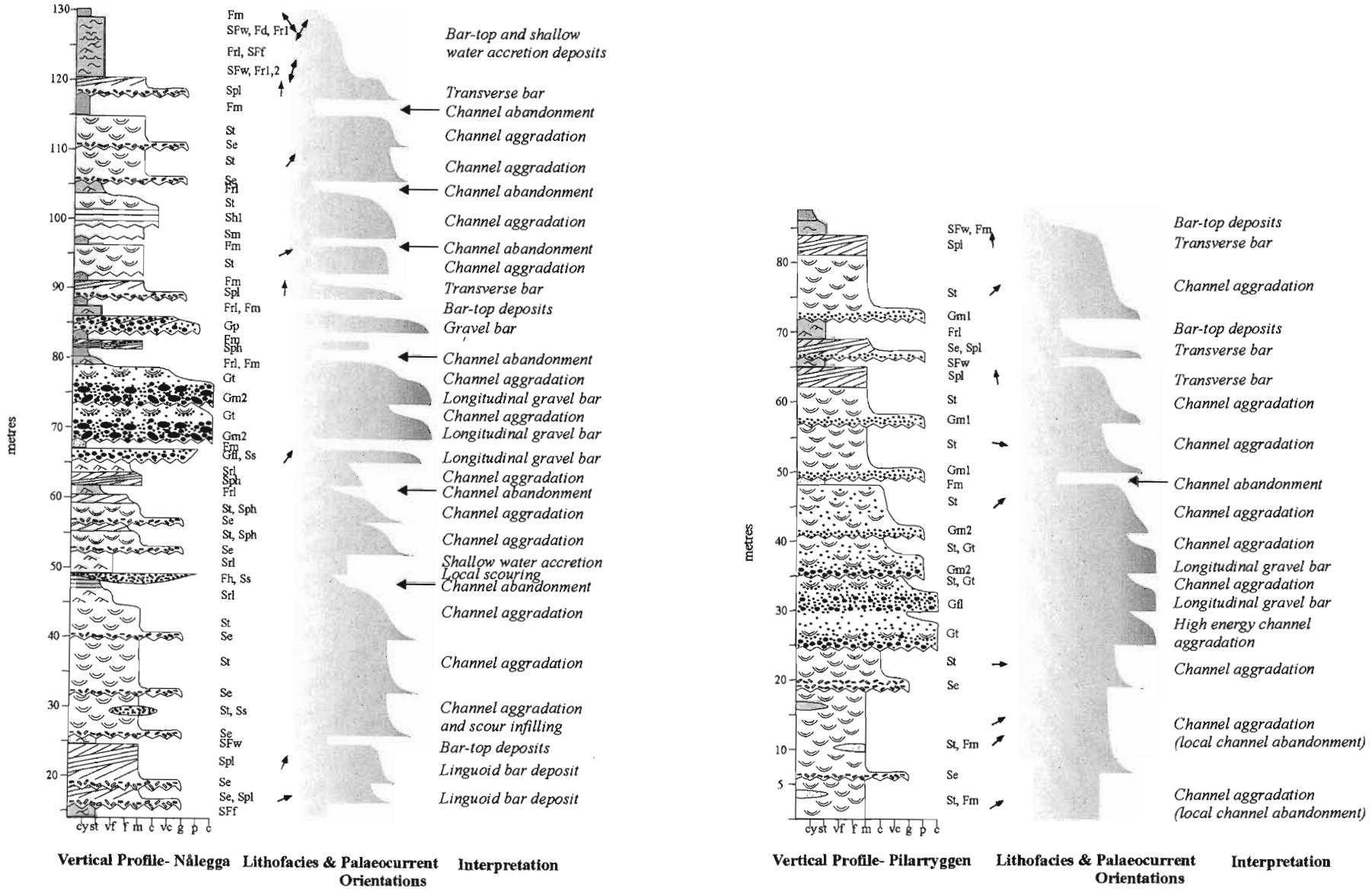

Figure 3.2: Selected detailed vertical sections from the Veten Formation. Lithofacies codes and palaeocurrent directions are marked beside each section. The Veten Formation is dominated by sandstone and gravel lithofacies that were deposited as a result of channel aggradation and the migration of gravel bars in a braided fluvial system. Occasional sandy transverse and linguoid bar deposits are also present, as are limited shallow water deposits.

gravel dominated to sandstone dominated facies. The base of the association may be marked by either facies Gfl or facies Gm_2. These lithofacies are erosively overlain by facies Gt, which may grade vertically into facies St. Facies Gfl is rarely found in isolation, but when it is, it is often overlain by a thin layer of Fm lithofacies.

The imbricated gravel deposits of facies Gfl and facies Gm_2 are interpreted to have formed from longitudinal bars. Longitudinal bars may be initiated during waning flow by bed-load deposition in mid-channel (Leopold and Wolman, 1957), or may evolve from diffuse gravel sheets formed during flooding events (Hein and Walker, 1977). Facies Gfl may show either an upward increase or decrease in clast size, depending on the mode of accretion. Clast accumulation in place tends to result in an upward fining trend, as the deposit builds to shallower water levels. However, these deposits also tend to migrate downstream, and in such cases, the upper, coarser deposits may migrate over the finer basal deposits (Miall, 1996). The occasional scour-fill deposit (facies Ss) found in association with facies Gfl may represent the infilling of scours formed by small channels cutting across the bar surface, during falling water stage (Collinson, 1970; Rust, 1972). The overlying Gt and St lithofacies represent channel aggradation deposits that accumulated during a subsequent high water stage, resulting in the submergence and reworking of the gravel bar deposits. Waning current flows caused a gradual decrease in bedform and grainsize, resulting in a transition from large-scale Gt facies to medium-scale St lithofacies. Occasionally, overlying fine-grained shallow water accretion deposits are preserved (facies Frl and Fm).

3.2.1.3 Association 3

A fine-grained dominated association, consisting of facies Fm, SFw, Frl, $Fr_{1\&2}$, Fh, Fd and subordinate Sm, Sh_2, Sph and Spl lithofacies, is recognised in the Veten Formation. Association 3 is characterised by repeated accumulations of 0.5 to 10m thick deposits of fine-grained lithofacies, interspersed with thin, laterally discontinuous, sandstone units.

The deposits of Association 3 are interpreted as reflecting sedimentation in overbank areas, where shallow water depth and low flow velocities result in the generation and migration of small scale bedforms and deposition of fine-grained sediment from suspension. Crevasse splays or sheet floods may have been responsible for the introduction of coarser-grained sediment, and deposition of sandstone lithofacies. Periodic exposure and desiccation led to the formation of Fd lithofacies.

3.2.1.4 Other features of interest

Isolated cosets of facies Spl and Gp represent bar deposits. According to Miall (1977), lithofacies Gp is generated by the migration of gravelly linguoid bars during high flow regime conditions. However, Williams (1971), Rust (1972) and Church (1983) suggest this lithofacies may alternatively represent gravelly transverse/diagonal bars. No one particular interpretation is favoured by this study. Occurrences of facies Spl, displaying foresets orientated either oblique or perpendicular to the dominant palaeoflow direction, are interpreted as the deposits of sandy transverse and linguoid bars.

3.2.1.5 Depositional environment

The Veten Formation is characterised by a vertical profile dominated by sand and gravel lithofacies associations, reflecting a variety of depositional processes typical of a braided fluvial system, and shows many similarities to descriptions of modern and Phanerozoic braided rivers (e.g. Miall, 1977, 1996; Barrett and Fitzgerald, 1985; Rust and Gibling, 1990; Jones *et al.*, 2001). Overall, the Veten Formation exhibits a high degree of variability, and a combination of bar, channel and overbank lithofacies associations are recognised. Bar types include gravelly longitudinal and possibly linguoid or transverse bars, and sandy linguoid and transverse bars. Channel deposits are predominantly sandy, and occasionally reflect waning flow conditions. The Veten Formation shows a marked similarity to Miall's (1977) Donjek Type profile, and is interpreted as reflecting deposition in a sand to gravel braided river system flowing towards the northeast. Reworking of finer-grained sediments is indicated by the abundance of mudstone intraclasts, however limited preservation of fine-grained overbank sequences (Association 3) has occurred, indicating reworking was not as extensive as is often reported for braided stream environments. A distal setting is therefore inferred, despite the presence of gravel deposits (e.g. Boothroyd and Ashley, 1975). This interpretation is also supported by the markedly

lower proportion of horizontal stratification in relation to planar cross-stratification (Rust, 1972).

3.2.2 Architectural element analysis

A single face sketch, from a south-southeast facing cliff at the base of Pilarryggen, was constructed in order to understand the lateral variability recorded in the Veten Formation (profile 4, Figure 3.3a,b). Unfortunately, difficulties in access limited the extent to which detailed palaeocurrent analysis could be performed. In addition, extensive soft sediment deformation (apparent in the upper, southwesterly portion of the profile) has interrupted the lateral continuity of certain units.

3.2.2.1 Sandy Bedforms

Six elements in profile 4 are interpreted as Sandy Bedforms (Figure 3.3b). Elements 1, 2, 4, 6, 8 and 10 are all characterised by deposits of three-dimensional dunes (facies St) which exhibit a generally northeasterly palaeoflow direction. The laterally extensive, generally 4th-order upper and lower bounding surfaces of each of these elements are characteristically flat lying to slightly concave up, and lack the diagnostic upper convex-up bedding contact typical of lateral and downstream accretion units. Internally, the five elements consist of lenses of medium-scale trough cross-stratified sand 10's m wide, defined by broad, shallow scours and erosion surfaces of 2nd- and 3rd-order.

These elements are regarded as representing fields of individual bedforms that accumulated predominantly by vertical aggradation. The SB elements are characteristic of weakly channelised streams, similar to braidplains (Williams, 1971; Miall, 1996). The flat basal surface commonly associated with these bedforms implies deposition from laterally unconfined to broadly channelised sheetflood deposits (Tunbridge, 1981). The architecture and composition of these fluvial deposits show marked similarities to the channel-floor dune fields described by Miall (1996). The commonly occurring internal, concave up erosion surfaces were probably generated by the repeated scouring and filling of low sinuousity channels, associated with stage fluctuations.

3.2.2.2 Downstream and lateral accretion macroforms

The limited nature of the palaeocurrent analysis and erosion of the tops of the bedforms, restricts the definite recognition of downstream accretion and lateral accretion elements. A single possible Lateral Accretion Macroform (LA) has been tentatively identified in profile 4 (Figure 3.3b). Element 3 is bounded by a flat lower 4th-order surface, and erosively overlain by element 4-SB. This subsequent erosive episode has resulted in removal and reworking of an unknown portion of the original element, and has limited preservation to a 13m long exposure located near the northeastern limit of the profile. Internally, element 3 consists of large-scale, gently dipping 2nd-order bounding surfaces orientated almost perpendicular to the dominant palaeoflow direction, suggesting successive increments of lateral growth. Lateral Accretion Macroforms such as element 3 form where the main flow of the channel is directed away from the river bank, and have often been recorded in braided stream deposits.

Lateral and downstream accretion deposits are the principle products of accretion within bar complexes of sandbed rivers, and are very common in braided sheet sandstones. As the bars are scaled to the size of the containing channel, their height is a rough guide to minimum channel depth (Miall, 1996). As such, a minimum depth of 2m can be estimated for the channels in which the Veten Formation was deposited.

3.2.2.3 Abandoned channel fill elements

The five other elements identified in profile 4 are interpreted as abandoned channel fill elements, similar in some respects to element FF(CH) in Miall's (1996) classification. Elements 5, 7, 9, 11 and 12 are characterised by predominantly fine-grained deposits (facies Frl, Fh and Fm), bound by flat to slightly concave up, laterally extensive lower 3rd- and 4th-order surfaces. Some of these elements (e.g. 11 and 12) appear to have been partially removed by subsequent erosive episodes, while intensive soft sediment deformation in certain parts of the profile prevents accurate interpretation of the original geometry of some elements. Abundant 2nd-order internal bounding surfaces are easily identifiable,

ENE

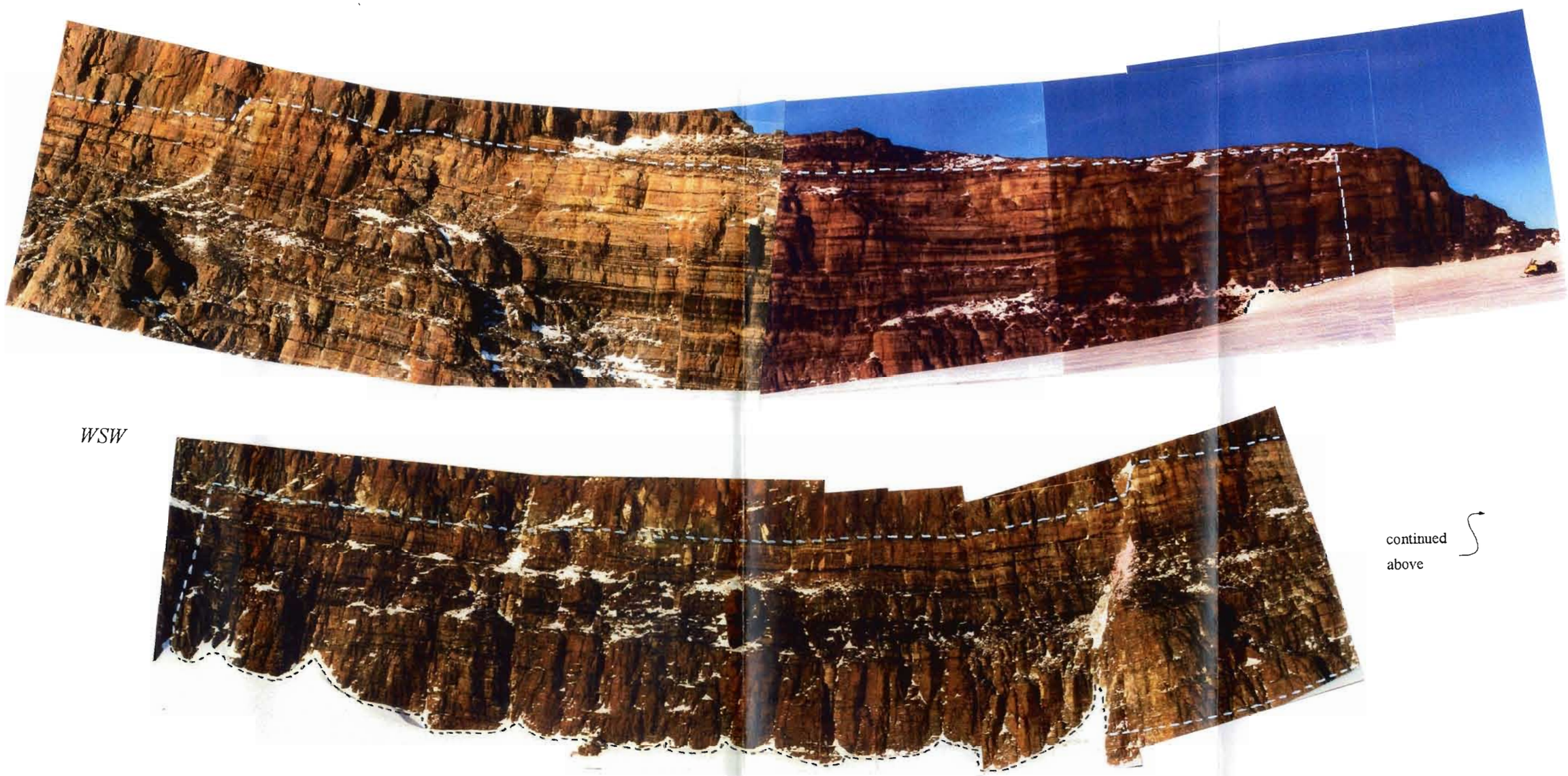

WSW

continued above

Figure 3.3(a): Photomosaic from the base of the Veten Formation, exposed at Pilarryggen. Cliff is facing SSE. The field sketch and interpretation of this cliff face is shown in Figure 3.3(b).

Profile 4

WSW *ENE*

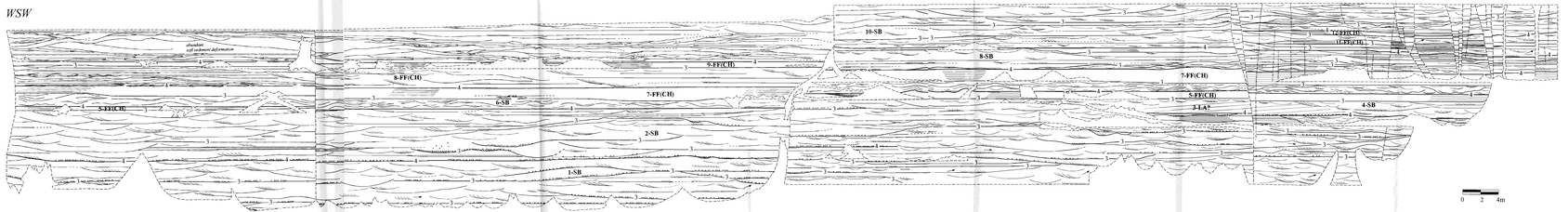

Figure 3.3(b): Field sketch from the base of the Veten Formation, exposed at Pilurryggen. The photo-mosaic of this face is depicted on the previous page, 3.3(a). Bounding surfaces are indicated by the appropriate hierarchical number, based on Miall's (1988) classification. A tentative element classification is indicated, using the two letter element code detailed in Table 1.2. Palaeocurrent flow directions are indicated with arrows orientated relative to the indicated compass directions. According to both vertical and lateral facies variations, deposition of this formation took place in a sand-dominated, low sinuosity fluvial setting characterised by channel aggradation deposit.

however, the marked 3rd-order erosive surfaces commonly recognised in the SB elements are absent. These elements are interpreted as vertical aggradation deposits that accumulated under low energy conditions in abandoned channels.

3.2.2.4 Environmental setting of the Veten Formation

Both the vertical profile analysis and the architectural element analysis of the Veten Formation indicate deposition occurred in a bed-load dominated, fluvial setting, similar to modern braided stream environments. The vertical sequence is characterised by channel aggradation deposits and gravely to sandy bar deposits. Laterally extensive Sandy Bedform elements, typical of braided stream environments, form the dominant architectural element types. Channels were broad and poorly confined; and combined with apparently limited accommodation space, this resulted in reworking of the fine-grained deposits, and only limited preservation of fine-grained, abandoned channel fill architectural elements.

3.3 THE FRAMRYGGEN FORMATION

The Framryggen Formation is a predominantly fine-grained sequence, composed of lithofacies Frl, SFw, Fm, St, Spl, Sph, Fh, SFf, $Fr_{1\&2}$, $Sr_{1\&2}$, Srl, Sm, Sh_2, Fd, Se, Ss, Gt, Gm_2, V and Frd, arranged in decreasing order of abundance. The presence of desiccation cracks and rain-drop imprints (facies Fd and Frd) is indicative of a continental depositional setting, in which periodic subaerial exposure occurred. Palaeocurrent orientations vary from unimodal, (towards the east-northeast) in the sandstone dominated sections, to polymodal and bimodal in the fine-grained dominated units (Figure 3.1). Both the fine-grained and sandy units display an exceptionally high degree of lateral continuity, and often persisted for the full extent of an exposure (up to 4km).

3.3.1 Vertical profile analysis

Two contrasting lithofacies associations were identified in the Framryggen Formation, including a sandstone dominated association and a fine-grain dominated association. Selected detailed sections, highlighting common vertical bedform relationships in the Framryggen Formation, are shown in Figure 3.4.

3.3.1.1 Association 1

A sandstone dominated lithofacies association, containing facies Se, St, Sph, Spl, Srl, Frl, Fh and Fm, is readily identifiable in the Framryggen Formation, and forms just under 25% of the exposed sequence. The base of the association is generally erosional, and sometimes marked by facies Se. The overlying medium-scaled St lithofacies occur predominantly as single cosets, which may grade into lithofacies Sph, followed by one or more of the fine-grained lithofacies. Both trough and planar cross-stratification tend to exhibit a stongly unimodal palaeocurrent orientation, towards the northeast to east-northeast (Figure 3.1). Alternatively, facies St may be erosively overlain by lithofacies Spl, containing foresets orientated oblique to the dominant palaeoflow direction. The Spl lithofacies are also generally overlain by one or more of the fine-grained facies.

Association 1 consists of a combination of channel aggradation and transverse bar deposits. The basal erosive surface reflects channel initiation, followed by deposition of facies St by sandwaves in the channel complex. Occasionally, gradual waning of the current strength resulted in a transition from trough cross-stratification to planar cross-stratification, accompanied by a decrease in grain size. The overlying fine-grained deposits are the result of shallow water accretion processes and channel abandonment. Alternatively, the trough cross-bedded channel deposits may be overlain by transverse bar deposits, containing planar cross-bed foresets orientated oblique to the dominant palaeoflow direction. Overlying, shallow-water, bar-top deposits may also be preserved.

3.3.1.2 Association 2

The second association recognised in the Framryggen Formation is dominated by fine-grained lithofacies, including Fm, Fh, Frl, SFw, SFf, $Fr_{1\&2}$, Srl Fd and Frd. Thin layers of subordinate sandstone facies are also present. Laterally continuous layers of fine-grained lithofacies, varying between 1 and 20m thick, are sporadically interrupted by thin (often <1m thick) layers of sandstone lithofacies (including facies Sm, Sh_2, Sph, Spl, St), which also exhibit a high degree of lateral continuity. Palaeocurrent orientations display a wide dispersion, and vary from bimodal to polymodal (Figure 3.1).

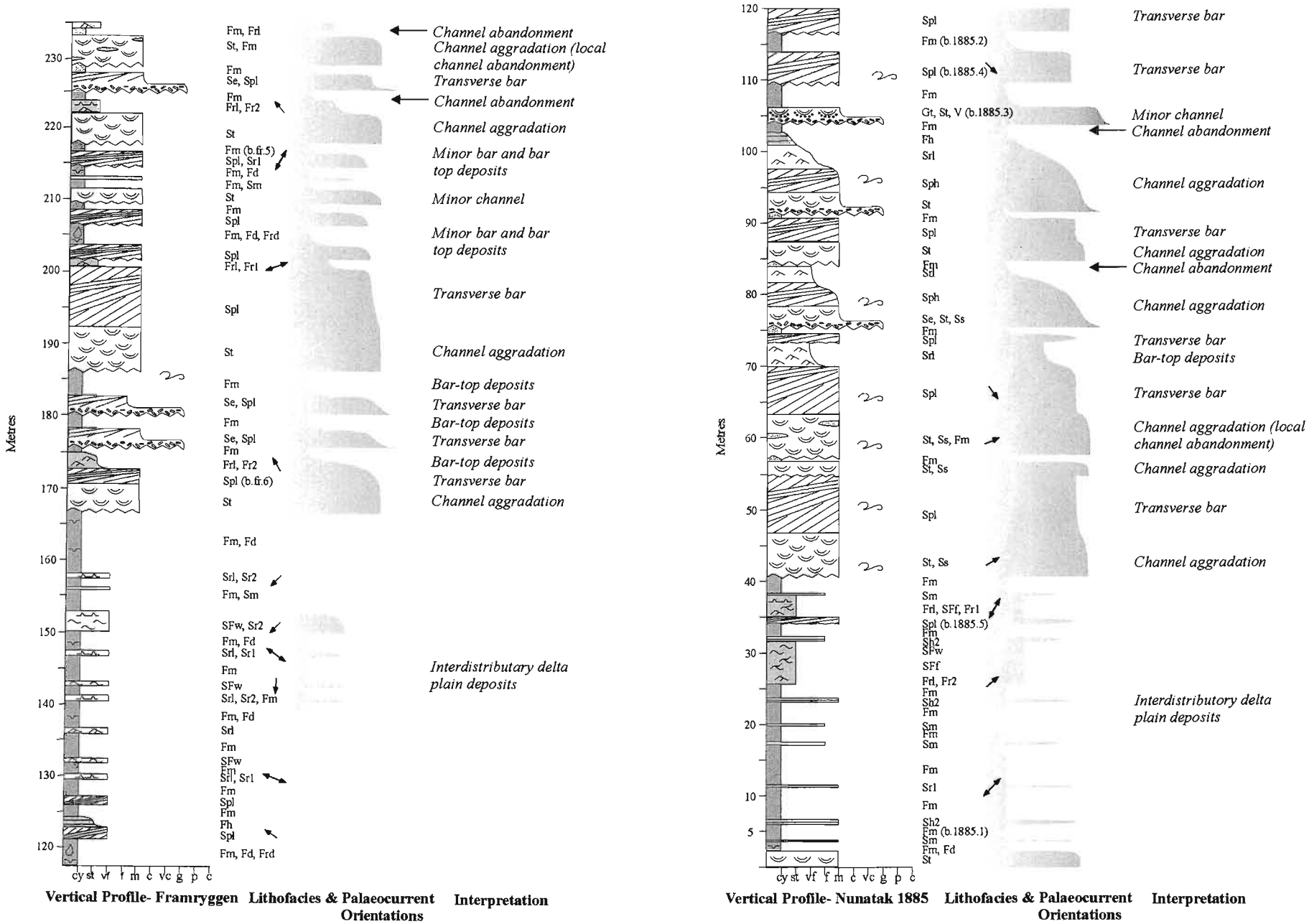

Figure 3.4: Selected detailed sections from the Framryggen Formation. Additional sections are included in Appendix 4. Lithofacies codes and palaeocurrent directions are marked beside each section. The Framryggen Formation was deposited in a distal setting, dominated by a braid delta plain on which thick interdistributory fine-grained facies accumulated. These alternate with laterally extensive/unconfined distributory channel and bar deposits.

Association 2 accounts for approximately 75% of the Framryggen Formation, and is interpreted as an interdistibutary delta plain deposit. The dominance of fine-grained sediment characterised by desiccation cracks, ripple structures exhibiting a bimodal to polymodal orientation, and tidal-type stratification (including flaser and wavy bedding) indicates deposition occurred in a distal, quiet water setting, subjected to limited tidal influence and sporadic subaerial exposure. Such conditions are typically encountered in interdistributary, delta plain environments (Collinson, 1968; MacNaughton *et al.*, 1997; Dreyer *et al.*, 1999).

3.3.1.3 Depositional environment

The combination of fine-grained, tidally influenced overbank deposits (Association 2) and fluvially dominated channel aggradation and bar deposits, indicates that the Framryggen Formation was deposited in a distal, delta plain setting. The sandstone dominated deposits of Association 1 show many similarities to the products of sheetflood distal braided rivers (e.g. Miall, 1996), and are interpreted as distal, fluvially dominated channels that spread across fine-grained, delta plain deposits. A lack of visible channel margins and high lateral persistence attests to the unconfined, sheet-like nature of the channel systems. The bulk of the Framryggen Formation was however deposited in the shallow water, low energy interdistibutary delta plain environment, where thick sequences of fine-grained sediment accumulated. Limited tidal influence and periodic subaerial exposure and desiccation is evident. Sheet floods were responsible for the periodic introduction of coarser-grained sediment, and the deposition of thin sandstone units.

3.3.2 Architectural element analysis

Two face sketches were constructed from exposures of the Framryggen Formation in order to facilitate architectural element analysis. Profile 5 (Figure 3.5a,b) was constructed from a generally northwest-facing exposure at Stridbukken, while profile 6 (Figure 3.5c,d) was taken from a south-facing exposure at Nunatak 1885. Unfortunately, these cliff faces are largely inaccessible, and as a result, only limited palaeocurrent analysis could be performed, reducing accuracy and detail of the analysis. Abundant soft sediment deformation also prevented determination of the internal structure of many elements.

3.3.2.1 Sandy Bedforms

Fourteen elements in profile 5 and seven elements in profile 6 are tentatively interpreted as Sandy Bedforms. These elements are all characterised by deposits of small- to medium-scale two- and three-dimensional dunes (facies St and Sph). The laterally extensive, generally 3rd- and 4th-order upper and lower bounding surfaces of each of these elements are characteristically flat lying, and lack the diagnostic upper convex-up bedding contact typical of lateral and downstream accretion units (Miall, 1996). The SB elements vary in thickness from under 0.5m to 2.0m. Internally, the thicker sheet-like elements may contain broad, shallow scours and erosion surfaces of 2nd- and 3rd-order.

These SB elements (Figure 3.5b,d) are regarded as representing fields of individual bedforms that accumulated predominantly by vertical aggradation and are characteristic of weakly channelled streams and braidplains (Williams, 1971; Miall, 1977). The flat basal surface commonly associated with these bedforms implies deposition from laterally unconfined to broadly channelised sheetflood deposits (Turnbridge, 1981). The concave up, internal erosion surfaces noted within some of these bedforms are likely to owe their origin to the scouring and filling of multiple low sinuousity channels / stage fluctuations. The SB elements show a marked similarity to the distal braidplain sheet sandstones described by Miall (1996).

3.3.2.2 Interdistributary delta plain elements

The remaining elements identified in profile 5, and three elements in profile 6 (elements 1, 3 and 5) are interpreted as fine-grained, inter-distributary delta plain elements, and have been assigned the code DF (Figures 3.5b,d). The DF elements in both profiles are characterised by fine-grain dominated deposits (facies Frl, Fh, SFW, SFf and Fm) bound by flat, laterally extensive upper and lower 3rd- and 4th-order surfaces. Generally, these sheet-like units can be followed for the full extent of the exposure. Abundant 2nd-order internal bounding surfaces are easily identifiable. These elements are interpreted as vertical aggradation deposits that accumulated under low energy, tidally influenced conditions in a delta plain setting.

3.3.2.3 Lateral accretion macroforms

A single possible Lateral Accretion Macroform (LA) has been tentatively identified in profile 6.

NE

Figure 3.5(a): Photomosaic from the base of the Framryggen Formation, exposed at Stridbukken. Cliff is facing NW. The field sketch and interpretation of this cliff face is shown in Figure 3.5(b).

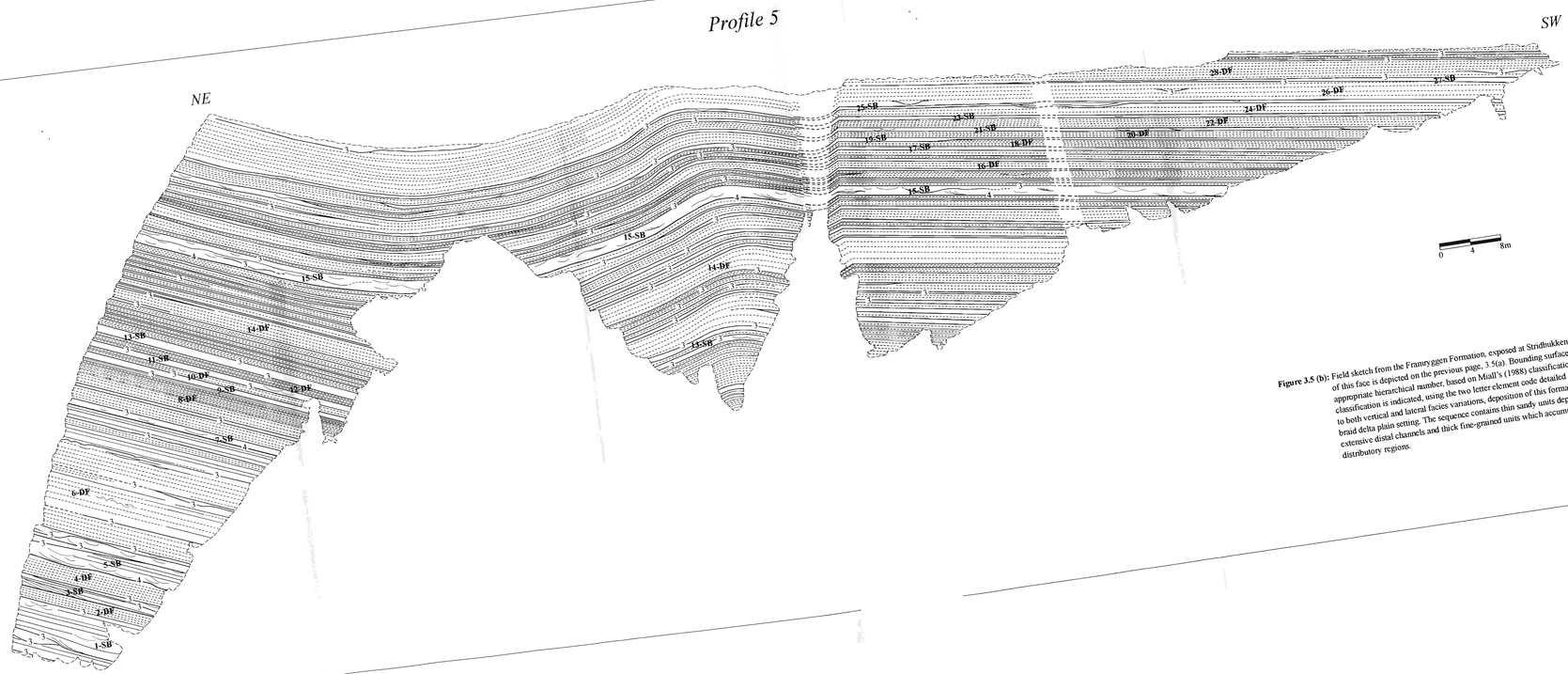

Figure 3.5 (b): Field sketch from the Framryggen Formation, exposed at Stridbakken. The photo-mosaic of this face is depicted on the previous page, 3.5(a). Bounding surfaces are indicated by the appropriate hierarchical number, based on Miall's (1988) classification. A tentative element classification is indicated, using the two letter element code detailed in Table 1.2. According to both vertical and lateral facies variations, deposition of this formation took place in a distal braid delta plain setting. The sequence contains thin sandy units deposited in shallow, laterally extensive distal channels and thick fine-grained units which accumulated in quiet water, inter-distributory regions.

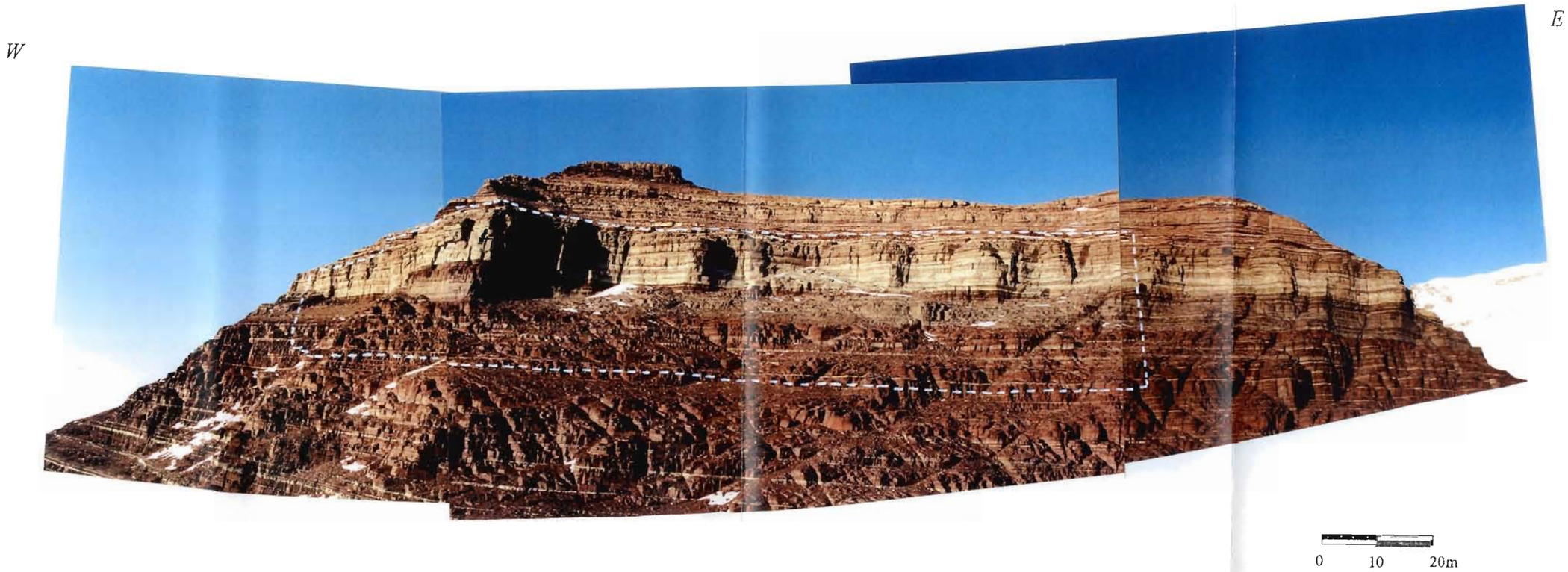

Figure 3.5(c): Photomosaic from the middle of the Framryggen Formation, exposed at Nunatak 1885. Cliff is facing S. The field sketch and interpretation of this cliff face is shown in Figure 3.5(d).

Profile 6

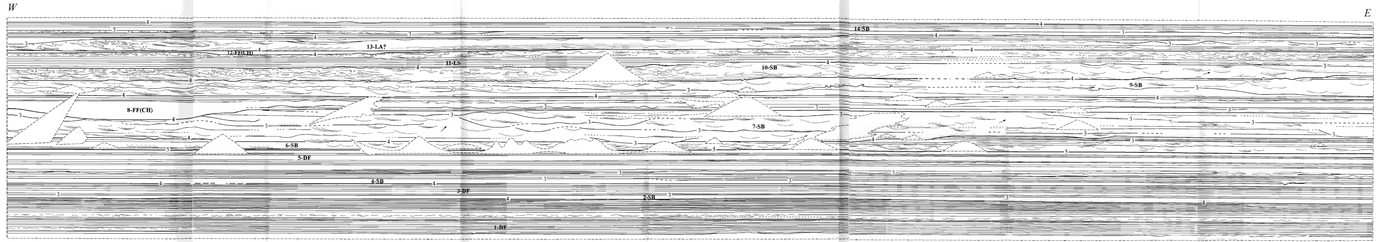

Figure 3.5 (d): Field sketch from the Fraenyggen Formation, exposed at Svanatak 1885. The photo-mosaic of this face is depicted on the previous page, 3.5(c). Bounding surfaces are indicated by the appropriate hierarchical number, based on Miall's (1988) classification. A tentative element classification is indicated, using the two letter element code detailed in Table 1.2. Palaeocurrent flow directions are indicated with arrows orientated relative to the indicated compass directions. According to both vertical and lateral facies variations, deposition of this formation took place in a distal, braid-delta plain setting. The sequence contains sandy units deposited in shallow, laterally extensive distal channels and fine-grained units which accumulated in quiet water, interdistributary regions.

Element 13 is bounded by a laterally extensive, 4th-order lower surface. The upper bounding surface is erosive in nature, and is related to the overlying SB element. This subsequent erosive episode has resulted in removal and reworking of an unknown portion of the original element, and has limited preservation of element 13 to a 45m long exposure near the top of the profile. Internally, element 13 consists of large-scale, gently dipping 2nd- and 3rd-order bounding surfaces orientated almost perpendicular to the dominant palaeoflow direction, suggesting successive increments of lateral growth. Lateral Accretion Macroforms such as element 13 form where the main flow of the channel is directed away from the river bank, and although typically characteristic of channel-confined river deposits (such as those of meandering river systems), they are also recorded from braided river deposits (Miall, 1996). From the preserved extent of element 13, a minimum depth of 1.2m can be estimated for the channels in which this portion of the Framryggen Formation was deposited.

3.3.2.4 Laminated sand sheets

Element 11 in profile 6 is tentatively designated a Laminated Sand Sheet (LS). This 2m thick architectural element rests on a laterally extensive 4th-order lower bounding surface, and can be followed across the entire length of the exposure (Figure 3.5d). The lower part of element 11 is characterised by facies Sh_l and contains abundant horizontal 2nd-order internal bounding surfaces, gradationally overlain by medium-scale trough cross-stratification (facies St). The overall sheet-like geometry of element 11 signifies deposition from an unconfined or broadly channelised sheet-flood.

Laminated Sand Sheets are commonly interpreted as the products of flash floods depositing sand under upper flow regime conditions (Miall, 1977; McKee *et al.*, 1967; Tunbridge, 1981). The overlying trough cross-stratification was probably deposited during waning flow conditions at the end of the flood event. However the paucity of element LS in the Framryggen Formation, and the Ahlmannryggen Group in general, suggests that high-energy, flash flood events were not a common occurrence.

3.3.2.5 Abandoned channel fill elements

Two FF(CH) elements have been identified in profile 6 (Figure 3.5d). Elements 8 and 12 are characterised by fine-grain dominated deposits (facies Frl, Fh and Fm), bound by laterally extensive, slightly concave up 3rd- and 4th-order surfaces. Abundant 2nd-order internal bounding surfaces are easily identifiable. These elements are interpreted as vertical aggradation deposits that accumulated under low energy conditions in an abandoned channel.

3.3.2.6 Environmental setting of the Framryggen Formation

Both the vertical profile analysis and the architectural element analysis of the Framryggen Formation suggests deposition took place in a distal, delta plain setting in which laterally extensive sheet-like architectural elements could accumulate. Evidence for both fluvial and tidal influence is present. Sheets of sand developed in broad, virtually unconfined channels in which aggradation and progressive abandonment occurred, followed by the accumulation of fine-grained deposits subjected to minor tidal influence.

3.4 THE HÖGFONNA FORMATION

A distinct coarsening upwards cycle is recognised in the Högfonna Formation. Sandy lithofacies dominate the lower portion, and grade upwards into a predominantly gravel lithofacies system. In decreasing order of abundance, the Högfonna Formation consists of lithofacies St, Sph, Se, Gt, Spl, Fh, Gm_2, Fm, Sm, Frl, Fd, $Fr_{1\&2}$, $Sr_{1\&2}$, Gm_1, Ss, V, SFw, Sh_l, and Frd. The dominance of sand and gravel lithofacies, displaying a predominantly unimodal palaeocurrent flow direction to the east-northeast (Figure 3.1), and the presence of facies Fd and Frd suggest deposition occurred in a continental setting.

3.4.1 Vertical profile analysis

Three lithofacies associations have been identified in the Högfonna Formation. Selected detailed sections highlighting common vertical bedform relationships, are shown in Figure 3.6. Additional sections are included in Appendix 4.

3.4.1.1 Association 1

A commonly occurring association in the Högfonna Formation comprises lithofacies St, Se, Sm, Fh, Fm, and minor $Sr_{1\&2}$, Ss, Fd and Frd. The base of Association 1 is invariably marked by a pronounced erosive contact, highlighted by

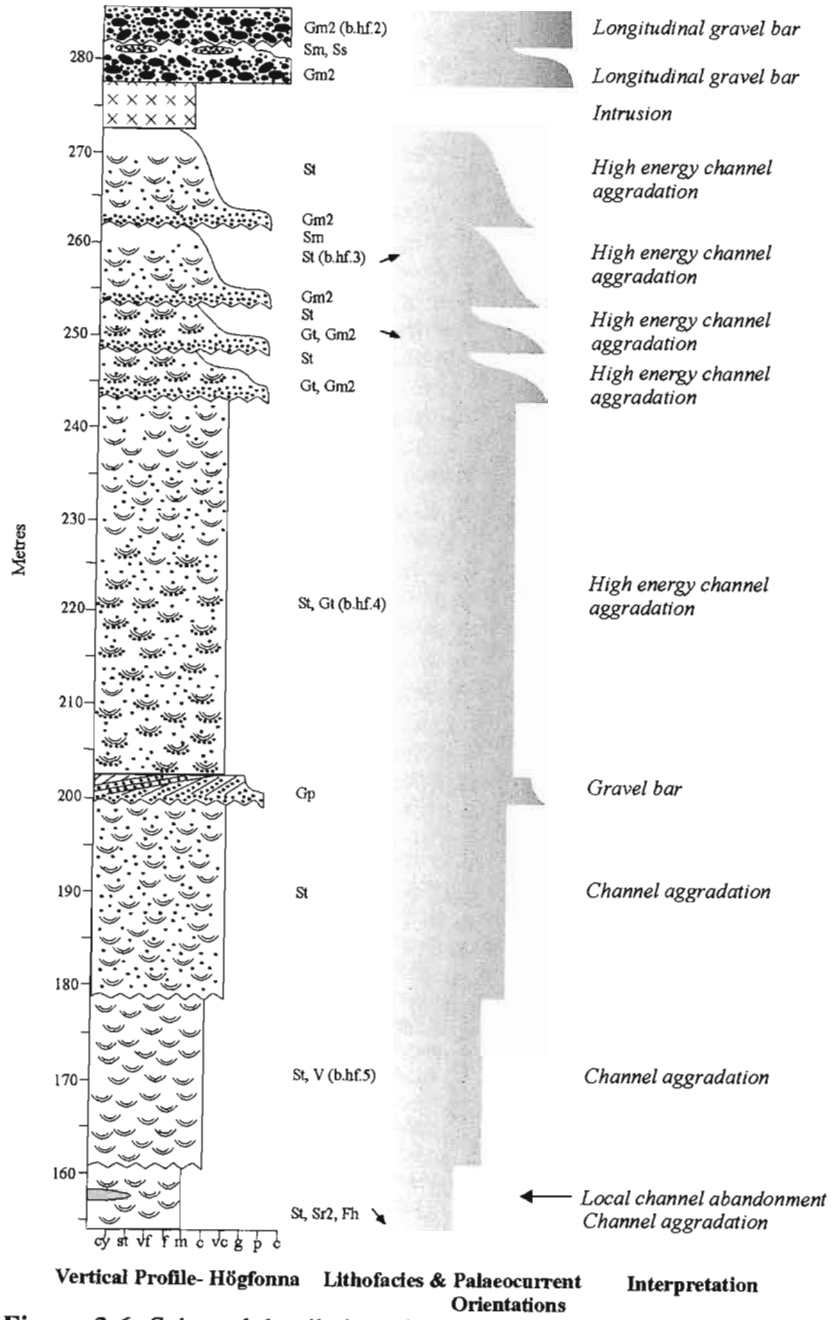

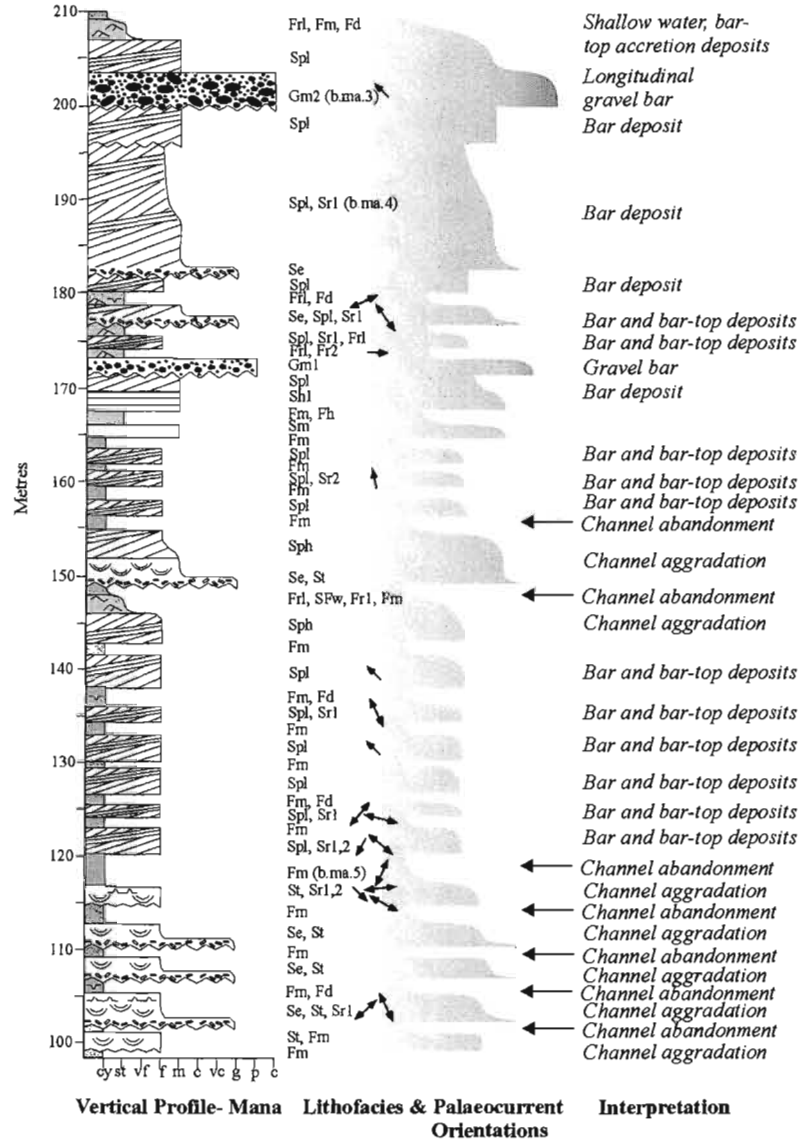

Figure 3.6: Selected detailed sections from the Högfonna Formation. Additional sections can be found in Appendix 4. Lithofacies codes and palaeocurrent directions are marked beside the sections. The Högfonna Formation is dominated by channel aggradation and bar deposits, arranged in an overall coarsening-upwards sequence. Deposition occurred in a sand to gravel dominated braided fluvial system.

facies Se. This is overlain by the dominant lithofacies of Association 1, facies St. The large- to small-scale trough cross-stratification of facies St may form repeatedly stacked cosets, resulting in units up to 15m thick, or may occur as single cosets, only a few metres thick. A dominant palaecurrent flow direction, towards the northeast to east is indicated (Figure 3.1). Infilled scours (facies Ss) may be present. A variable thickness of overlying, finer-grained deposits may be found in Association 1, including fine-grained massive sandstone (facies Sm), rippled sandstone (facies $Sr_{1\&2}$) and laminated to massive mudstone (facies Fh and Fm), which may display desiccation cracks or rain-drop imprints (facies Fd and Frd).

Association 1 is interpreted as a channel aggradation deposit. The basal erosive contact and Se lithofacies were formed through the initial scouring action of currents on underlying, less competent units, and represent channel initiation. The overlying St lithofacies accumulated during channel aggradation. Thick units, consisting of numerous stacked cosets, reflect deposition by sandwaves in deeper reaches of the channel complex, while single cosets imply a shallower depositional environment. Scour fill deposits (facies Ss) may have formed at the confluence of two flows, or in the lee of advancing dunes / sandwaves. The composition of the scour fill ranges from medium sand to gravel, suggesting development under both low and high flow regime conditions. The overlying finer-grained deposits represent the products of shallow water accretion processes. Thin, lenticular mud drapes (facies Fm) owe their origin to suspension settling in abandoned channels. Occasional subaerial exposure resulted in desiccation (facies Fd) or the preservation of rain-drop imprints (facies Frd). The original thickness of the fine-grained deposits is impossible to estimate due to a high degree of reworking, as indicated by the abundance of mudstone intraclasts.

3.4.1.2 Association 2

A gravel dominated association, consisting of lithofacies Gm_2, Gt, and St, is also readily identifiable in the Högfonna Formation. The erosive basal contact of the association is generally marked by a moderately to well developed gravel lag deposit (facies Gm_2), which is overlain by a fining upwards sequence grading from facies Gt to facies St. These medium- to large-scale trough cross-beds cosets may occur in isolation, or may be stacked, forming units varying from 5 to 40m thick.

This association is also interpreted as a channel aggradation deposit, but the dominance of gravel lithofacies indicate formation under markedly higher energy conditions than Association 1.

3.4.1.3 Association 3

Association 3 is dominated by planar cross-stratification (facies Sph or Spl) but also contains subordinate Se, Fm, SFw, Frl, $Fr_{1\&2}$, Fh and Fd lithofacies. The erosive base of Association 3, occasionally marked by facies Se, is overlain by a 2 to 15m thick, planar cross-stratified unit. The foresets may be orientated either oblique or perpendicular to the dominant palaeocurrent flow direction. The planar cross-bedded units are overlain by a variable thickness of fine-grained, small-scale cross-laminated lithofacies.

Association 3 is interpreted as the deposits of migrating slip-faced bars, under low flow regime conditions (Harms and Fahnestock, 1965 and Harms, 1975). Depending on their orientation relative to the dominant palaeoflow direction (determined from trough cross-stratified channel aggradation deposits) the planar cross-stratification of Association 3 may be regarded as originating from either linguoid or transverse sandy bars. The small-scale structures superimposed on the bar surface represent the deposits of shallow water accretionary processes (forming facies Frl, $Fr_{1\&2}$ and SFw). Migration of the bar-top ripples during low water stage would have allowed continued progradation of the bar-front avalanche slope (Miall, 1977; Smith, 1971, 1972; Collinson, 1970). Thin, lens-shaped deposits of facies Fm represent suspension fall-out deposits that formed in pools of standing water, possibly associated with minor channels or scours cut into the bar surface. Occasional subaerial exposure and desiccation of these fine-grained bar top deposits resulted in the formation of facies Fd.

3.4.1.4 Other features of interest

A single, isolated unit of Gp lithofacies was identified in the upper, gravel-dominated section of the Högfonna Formation. No one particular interpretation is favoured for this study, and a broad mode of formation, namely the migration of a gravelly bar under high flow regime conditions, is assigned to occurrences of this lithofacies. Occasionally, thick (up to 8m), isolated units of facies Gm_2 were encountered.

These deposits are interpreted as forming from rare longitudinal bars. The occasional scour-fill and massive sandstone deposit (facies Ss and Sm) found in association with facies Gm_2 may represent the infilling of scours formed by small channels cutting across the bar surface (Collinson, 1970).

3.4.1.5 Depositional environment

The sand and gravel dominated Högfonna Formation displays many similarities to modern braided rivers. Overall, the vertical profiles indicate a gradual coarsening upwards, from sandstone dominated at the base of the formation, to gravel dominated at the top. Comparison of sections from different outcrops reveals that the Högfonna Formation shows a high degree of lateral variability. Certain exposures (e.g. Högfonna and Raudberget) are characterised by a repeated vertical stacking of channel aggradation cycle deposits (Associations 1 and 2), interrupted by occasional bar deposits (Association 3 and rare Gm_2 and Gpl). These show a marked similarity to Miall's (1977) Donjek Type profile and parts of the modern South Saskatchewan River (Cant and Walker, 1978). More southerly exposures of the Högfonna Formation (e.g. Ovebratten, Kjellbergnuten, Vindegga and to a lesser extent, Mana) are dominated by the sandy bar deposits of Association 3, and compare more favourably with Miall's (1977) Platte Type profile. Exposures of the Högfonna Formation are therefore considered to preserve an apparent lateral transition from a relatively deep river system, characterised by thick channel accumulation deposits, to a shallower system dominated by linguoid and transverse bars. The absence of abundant longitudinal bar deposits suggest a distal setting; while the absence of fine-grained overbank deposits and the presence of abundant mud intraclasts, is indicative of a fluvial system characterised by little available accommodation space and a high degree of reworking.

3.4.2 Architectural element analysis

Two face sketches were constructed in order to understand the lateral variability recorded in the Högfonna Formation. The first sketch (profile 7, Figure 3.7a,b) was made from a northeast-facing exposure located near the base of Högfonna Peak 2130, while the second sketch (profile 8, Figure 3.7c,d) was constructed from a north-northwest-facing exposure near the northern limit of Högfonnaksla ridge at Högfonna. Unfortunately, difficulties in access limited the extent to which detailed palaeocurrent analysis could be performed.

3.4.2.1 Sandy Bedforms

Three elements in profile 7 and two elements in profile 8 are tentatively interpreted as Sandy Bedforms. Elements 1, 6, 10 (profile 7) and 1, 6 (profile 8) are all characterised by deposits of two and three-dimensional dunes (facies St and Sph) which exhibit a generally northeasterly palaeoflow direction. The laterally extensive, generally 4th-order upper and lower bounding surfaces of each of these elements are characteristically flat lying, and lack the diagnostic upper convex-up bedding contact typical of lateral and downstream accretion units (Miall, 1996). Internally, the five SB elements contain numerous 2nd and 3rd-order bounding surfaces, often occurring as broad, shallow scours and channel-shaped erosion surfaces.

Vertical stacking of these different lithofacies types within the same architectural element may be attributed to fluctuations and short-term changes in the flow regime. Fields of three-dimensional dunes (facies St) generally occupy the deeper reachers of active channels, while transverse bedforms and sandwaves (2-D dunes, facies Sph) commonly occur in the shallower areas (Miall, 1996). These elements represent fields of individual bedforms that accumulated predominantly by vertical aggradation, and are characteristic of weakly channelised streams, similar to braidplains (Williams, 1971; Miall, 1996). The flat basal surface associated with these bedforms implies deposition from laterally unconfined to broadly channelised sheetflood deposits (Turnbridge, 1981). The commonly occurring internal, concave up erosion surfaces were probably generated by the repeated scouring and filling of low sinuousity channels, associated with stage fluctuations.

3.4.2.2 Downstream accretion macroforms

The limited nature of detailed palaeocurrent analysis and erosion of the tops of the bedforms restricts the definite recognition of Downstream-Accretion Macroforms. Possible DA elements include elements 3, 5 and 8 in profile 7 and elements 3 and 5 in profile 8. The three possible DA elements recognised in profile 7 all exhibit a slightly convex up, 4th-order upper bounding surface, and rest on flat basal 3rd or 4th-order

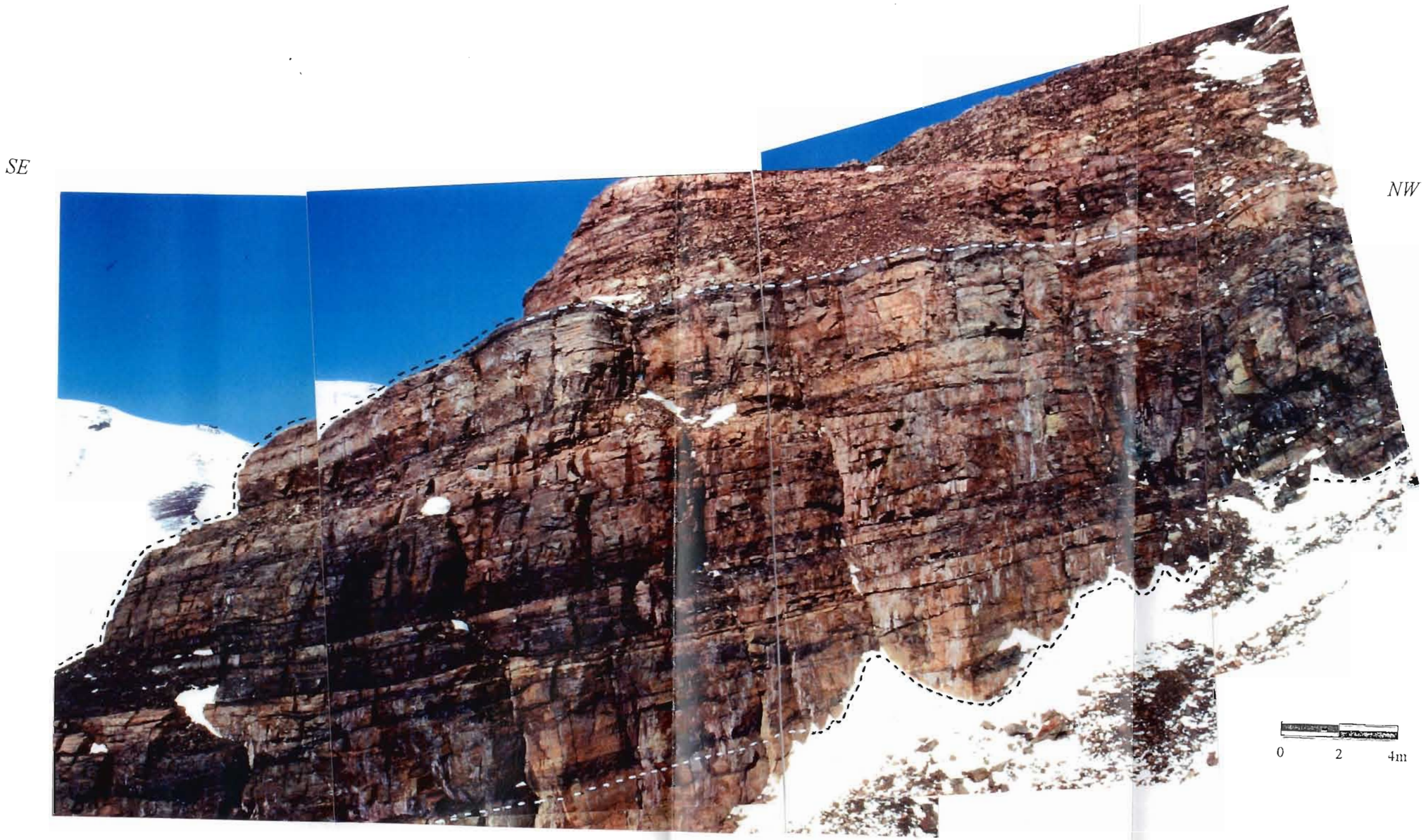

Figure 3.7 (a): Photomosaic from the base of the Högfonna Formation, exposed at Högfonna Peak 2130. Cliff is facing NE, and is approximately 20m high. The field sketch and interpretation of this face is shown in Figure 3.7(b).

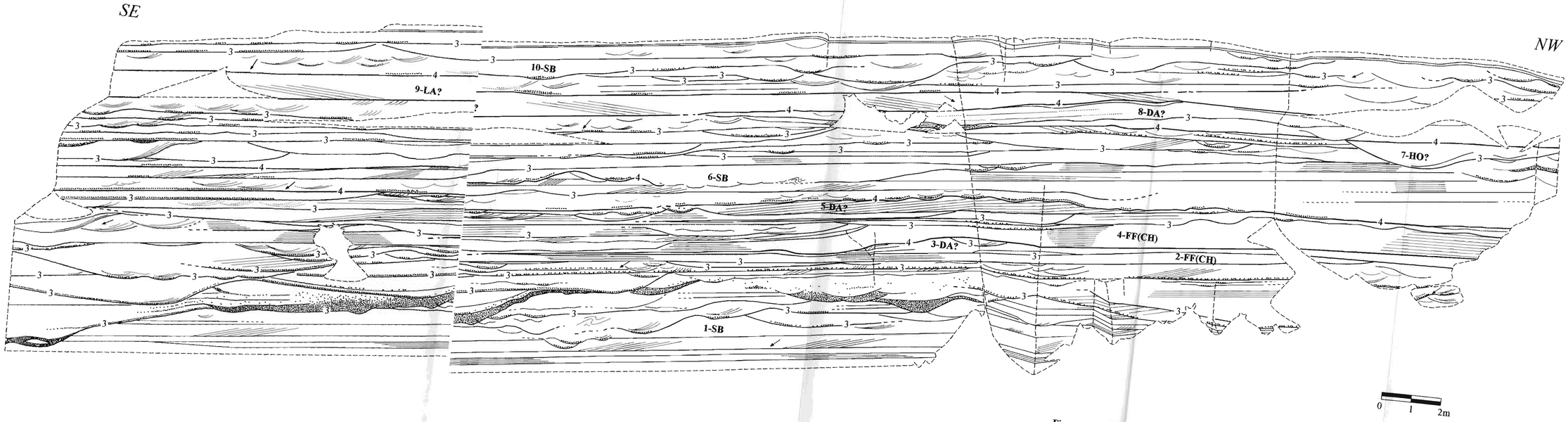

Figure 3.7(b): Field sketch from the base of the Högfonna Formation, exposed at Högfonna Peak 2130. The photomosaic of this face is depicted on the previous page, 3.7(a). Bounding surfaces are indicated by the appropriate hierarchical number, based on Miall's (1988) classification. A tentative element classification is indicated, using the two letter element code detailed in Table 1.2. Palaeocurrent flow directions are indicated with arrows orientated relative to the indicated compass directions. According to both vertical and lateral facies variations, deposition of this formation took place in a sand-dominated, low sinuosity fluvial setting characterised by channel aggradation deposits and sandy bar deposits.

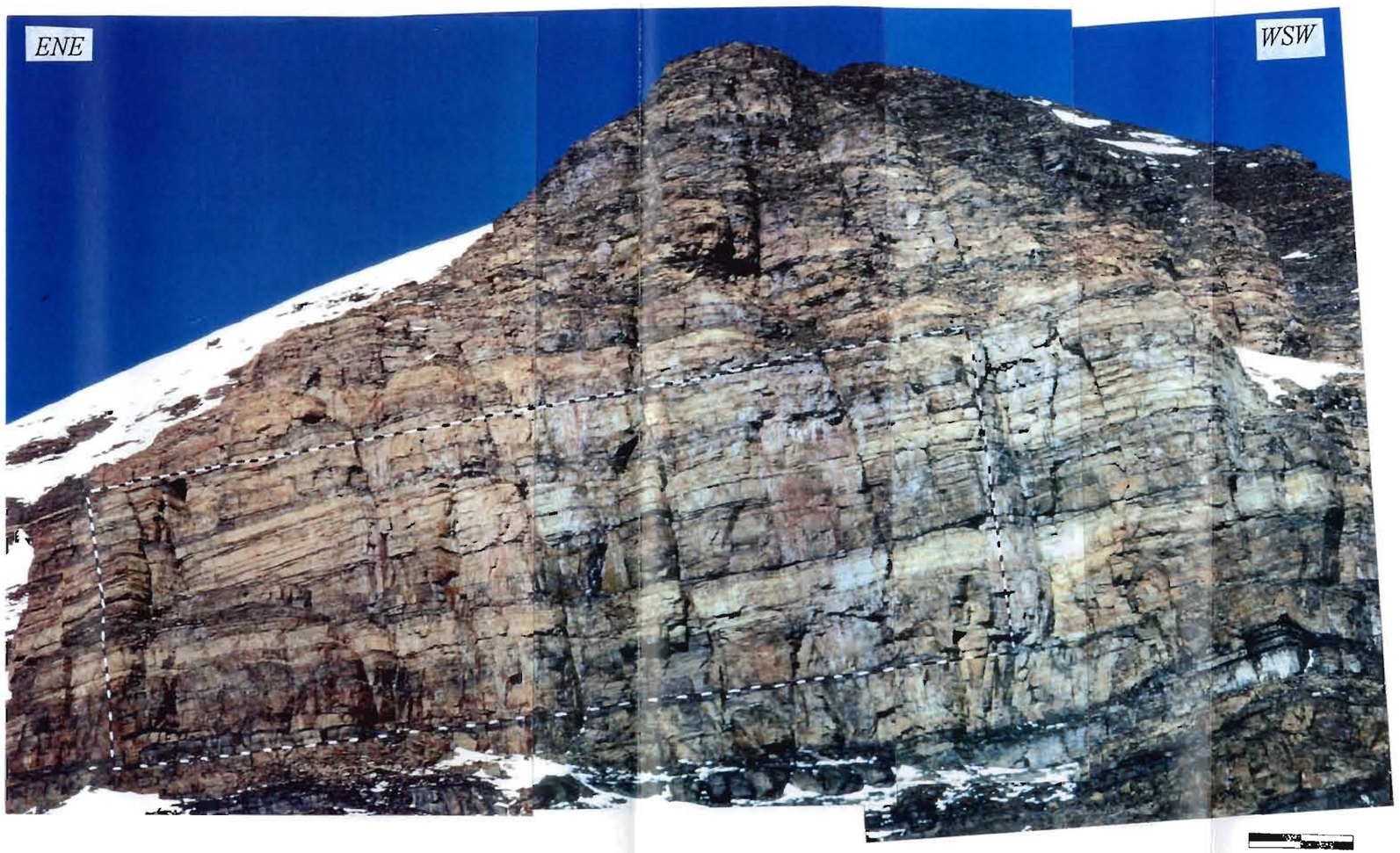

Figure 3.7 (c): Photo-mosaic from the middle of the Högfonna Formation, exposed on the nunatak of Högfonna. Cliff is facing NNW, and is approximately 28m high. The field sketch and interpretation of this face is shown in Figure 3.7(d).

Profile 8

ENE *WSW*

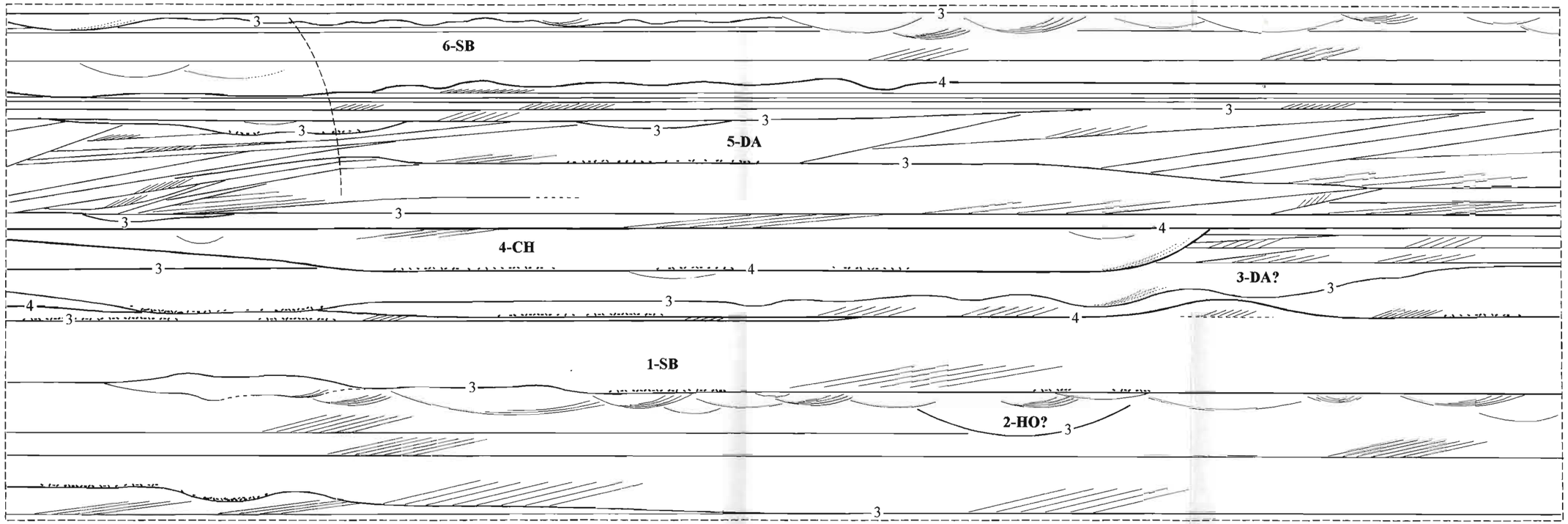

Figure 3.7(d): Field sketch from the Högfonna Formation, exposed at Högfonna. The photomosaic of this face is depicted on the previous page, 3.7(c). Bounding surfaces are indicated by the appropriate hierarchical number, based on Miall's (1988) classification. According to both vertical and lateral facies variations, deposition of this formation took place in a braided fluvial setting. The sequence is dominated by sandy bar and channel deposits.

lower bounding surfaces. Due to subsequent erosive episodes, the two possible DA elements tentatively identified in profile 8 lack the pronounced convex-up upper bounding surface considered characteristic of DA elements. However, on the basis of the internal arrangement of flow-regime bedforms and 2nd- and 3rd-order surfaces, these elements have been provisionally designated as downstream accreting macroforms.

Within each of the DA elements, cosets of downstream orientated flow-regime bedforms (facies Spl, Sph and St) and downstream dipping internal bounding surfaces (2nd and 3rd-order) can be identified. According to the limited palaeocurrent analysis, these planer and trough cross-stratified bedforms apparently advanced down the gently dipping slopes defined by the 2nd and 3rd-order surfaces, indicating the elements were formed by fields of 2-D and 3-D bedforms driving across and down fluvial bar forms (Allen, 1983; Hazeldine, 1983a,b; Miall, 1988a,b, 1996).

3.4.2.3 Lateral accretion macroforms

A single possible Lateral Accretion Macroform (LA) has been tentatively identified in profile 7 (Figure 3.7b). Element 9 is bounded by laterally extensive, 4th-order surfaces, resulting in an overall sheet-like geometry. The upper bounding surface is erosive in nature, and is related to the overlying SB element. The basal 4th-order bounding surface forms the upper bounding surface of elements 8-DA and 6-SB, and appears to be a surface of deposition rather than erosion. Internally, element 9 consists of large-scale, gently dipping 2nd- and 3rd-order bounding surfaces orientated almost perpendicular to the dominant palaeoflow direction, suggesting successive increments of lateral growth. Lateral Accretion Macroforms such as element 9 form where the main flow of the channel is directed away from the river bank, and have often been recorded in braided stream deposits (Miall, 1996).

As bar complexes with sandbed rivers are scaled to the size of the containing channel, their height is a rough guide to the minimum channel depth (Miall, 1996). As such, a minimum depth of between 1 and 4m can be estimated for the channels in which the Högfonna Formation was deposited.

3.4.2.4 Channel elements

A single Channel element (CH) has been identified in profile 8. Element 4 has been designated CH as the channel fill appears to be simple in nature, and cannot be further subdivided into components such as DA or LA elements. This minor channel exhibits a concave-up, 4th-order erosional basal surface, and a planar, laterally extensive upper, 4th-order bounding surface, related to the overlying DA element. The channel margins are characterised by a shallow slope angle, a characteristic expected in a sand-dominated system typified by low bank stability.

3.4.2.5 Hollow elements

Small-scale scours (element 7 in profile 7 and element 2 in profile 8), bounded by 2nd or 3rd order surfaces are tentatively designated Hollow elements (HO) (Figure 3.7b,d). The lack of extensive three-dimensional exposure prevents definite recognition, but the presence of gravel and sand sized-sediment confined within steep margins and exhibiting limited lateral extent supports this interpretation, rather than that of Channel element (CH). Hollow elements may form at the confluence of two channels or downstream from large bars, where current action causes deep scouring, forming trough-shaped three-dimensional hollows below the mean river level (Cowan, 1991).

3.4.2.6 Abandoned channel fill elements

The two remaining elements identified in profile 7 are interpreted as abandoned channel fill elements, FF(CH) (Figure 3.7b). Elements 2 and 4 are characterised by fine-grain dominated deposits (facies Frl, Fh and Fm), bound by laterally extensive 3rd- and 4th-order surfaces. Abundant 2nd-order internal bounding surfaces are easily identifiable, however, the marked 3rd-order erosive surfaces commonly recognised in the SB, DA and LA elements are absent. These elements are interpreted as vertical aggradation deposits that accumulated under low energy conditions in abandoned channels.

3.4.2.7 Environmental setting of the Högfonna Formation

Both the vertical profile analysis and the architectural element analysis of the Högfonna Formation indicate that deposition occurred in a sand to gravel bed-load dominated fluvial setting, similar to modern braided stream environments. The vertical sequence is characterised by channel aggradation deposits and sandy bar deposits.

Laterally extensive Sandy Bedform elements and commonly occurring Downstream Accretion macroforms, both typical of braided stream environments, form the dominant architectural element types. Channels were broad and poorly confined; and combined with apparently limited accommodation space, this resulted in extensive reworking of fine-grained deposits, and only limited preservation of fine-grained, abandoned channel fill architectural elements.

3.5 THE BRÅPIGGEN FORMATION

The Bråpiggen Formation is composed of lithofacies St, Spl, Sh_l, Se, Sph, Frl, SFw, SFf, Fh, Srl, Fm, Sm, Ss, Gm_l, Vm, V, Fd and Frd. The presence of desiccation cracks (facies Fd) and rain-drop imprints (facies Frd) is considered indicative of a continental depositional setting.

3.5.1 Vertical profile analysis

Four lithofacies associations have been identified in the Bråpiggen Formation. Selected detailed sections, highlighting common vertical bedform relationships, are shown in Figure 3.8.

3.5.1.1 Association 1

Association 1 is dominated by a variety of fine-grained lithofacies types, including Frl, SFw, SFf, Fh, Fm and Fd, which are arranged into laterally continuous layers, varying in thickness between 1 and 15m thick. These fine-grained deposits are commonly interrupted by thin (generally < 2m thick) sandstone lithofacies units (including facies Se, St, Sm, Spl, Sph). Palaeocurrent orientations display a high degree of variability (Figure 3.1).

Association 1 is interpreted as an interdistributary plain deposit. The predominance of fine-grained lithofacies types characterised by desiccation cracks and tidal-type stratification, and exhibiting a high palaeocurrent variability, indicates deposition occurred in a quiet water setting, under the influence of tidal fluctuations. The thin sandstone units resulted from the introduction of coarser-grained sediment by higher energy currents, which periodically invaded this quiet water environment. Whether these currents were fluvial or tidal in origin is difficult to determine, however, the lack of abundant re-activation surfaces, tidal stratification and mud drapes in the sandstone units suggests deposition from a fluvially dominated current, possibly associated with crevasse splays or migrating distributary channels.

3.5.1.2 Association 2

Association 2 is dominated by sandstone lithofacies St, Sph, Ss and Se, with subordinate fine-grained facies Frl, SFw, Fh, Fm, Fd also occurring. The base of the assemblage is invariably marked by an erosive contact, occasionally highlighted by facies Se. The overlying trough cross-stratified sandstone deposits (facies St) vary in thickness from under 2m to over 15m, within which scour-fill deposits may occur. The assemblage is often capped by one or more of the fine-grained lithofacies, generally forming lens shaped deposits.

Association 2 is interpreted as a channel aggradation deposit. The basal erosive surface, and overlying Se lithofacies were formed during channel aggradation, while the overlying trough and planar cross-stratification was deposited by migrating sandwaves in the channel complex.

The shallow water accretion deposits and mudstone lenses accumulated during channel abandonment, which varied from gradual to sudden/abrupt. Periodic subaerial exposure resulted in the formation of facies Fd. A predominant palaeocurrent direction towards the east-southeast is recorded (Figure 3.1).

3.5.1.3 Association 3

Association 3 is also dominated by sandstone lithofacies. The dominant lithofacies types include facies Sh_l and Spl, with minor Se, Frl, Fh and Fd lithofacies. The base of this association is generally erosional, and occasionally highlighted by the development of facies Se. This is often overlain by facies Sh_l which is in turn overlain by facies Spl, containing foresets orientated oblique to the dominant palaeoflow direction. The association is capped by thin units of fine-grained facies, occasionally preserving evidence for periodic subaerial exposure (facies Fd).

Association 3 is interpreted as a fluvial bar deposit. The angle of the bedforms suggests that the accretionary surfaces were orientated oblique to the dominant channel direction, and a transverse bar origin is envisaged. The finer-grained, bar top deposits represent the products of shallow water accretion processes. Migration of bar-top ripples, even under very low water

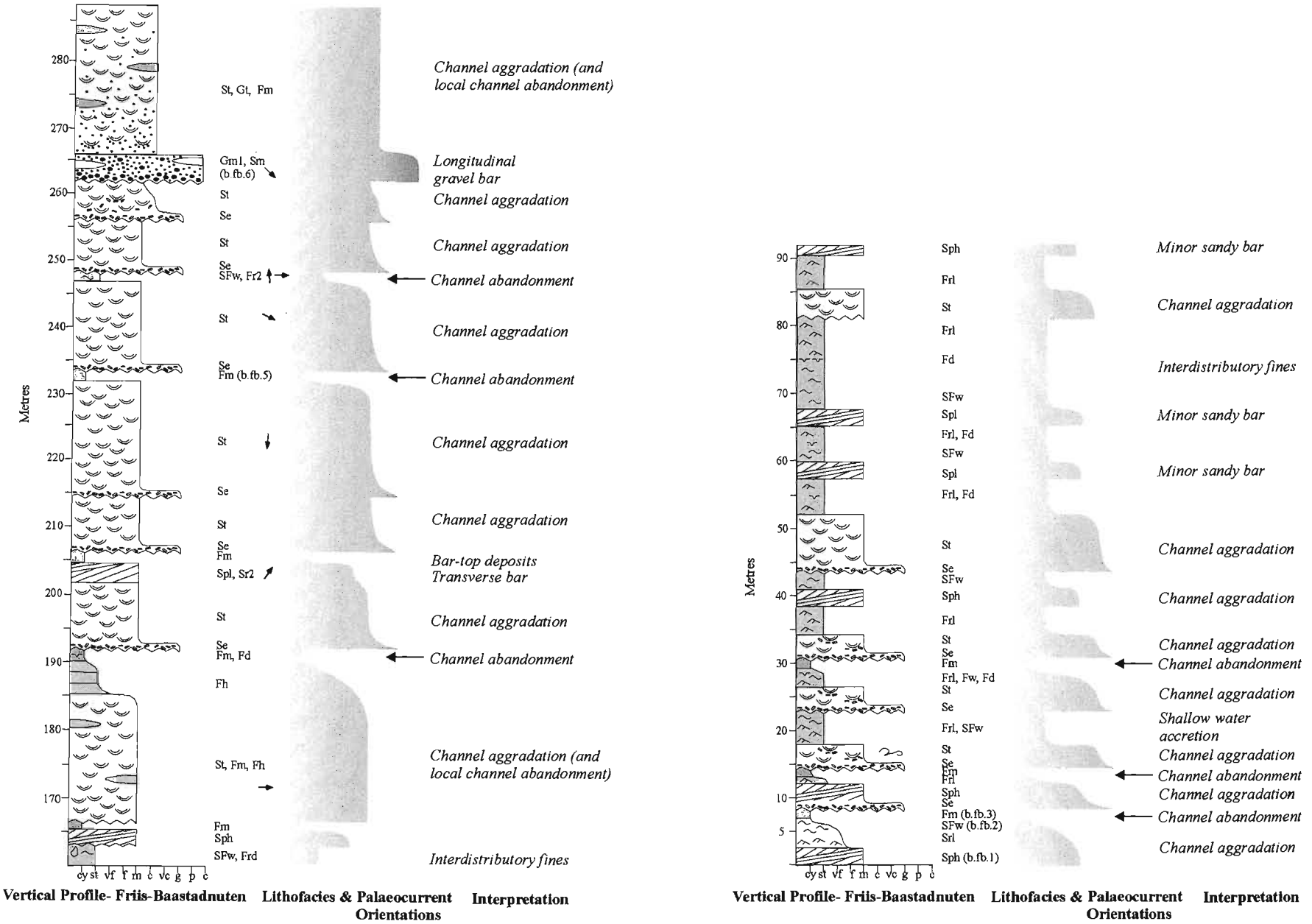

Figure 3.8: Selected detailed sections from the Bråpiggen Formation. Lithofacies codes and palaeocurrent directions are indicated beside each section. The Bråpiggen Formation exhibits a variety of vertical lithofacies associations, including channel aggradation deposits, fluvial bar deposits and fine-grained, interdistributory deposits. Periodic flood deposits and volcaniclastic layers are also present in some exposures (see Appendix 4 for additional sections depicting these lithofacies types).

conditions, would have allowed the continued progradation of the bar-front avalanche slopes (Miall, 1977; Smith, 1971, 1972).

3.5.1.4 Association 4

The final lithofacies association recognised in the Bråpiggen Formation is dominated by gravel facies Gm1, with minor sandstone and fine-grained lithofacies also occurring (Spl, Srl, Frl, Fm). A basal erosive contact is overlain by a thin (<1m thick) massive gravel unit, which may grade upwards into planar cross-stratified sandstone (facies Spl) and fine-grained facies Srl, Frl and Fm. Alternatively, lithofacies Gm_1 may be directly overlain by one or more of the fine-grained deposits.

This association is interpreted as the product of periodic higher-energy events, with the poorly sorted, matrix supported nature of the basal gravel layer suggesting a flood origin (e.g. Bridge, 1993). The flood events were possibly short-lived, and apparently lacked excessively high flow velocities, suggested by the thin nature of the gravel deposits, and small clast size. A rapid return to lower energy conditions is indicated by the presence of the overlying sandstone and fine-grained lithofacies. Where present, the bedform orientation of the planar cross-stratified sandstones suggests that down stream accretion was the dominant style of deposition.

3.5.1.5 Other features of interest

A single, 3m thick Gm_2 unit was recorded, and is interpreted as an isolated longitudinal bar deposit. The occasional scour-fill deposit (facies Ss) found in association with facies Gm_2 may represent the infilling of scours formed by small channels cutting across the bar surface, during falling water stage (Collinson, 1970; Williams and Rust, 1969).

3.5.1.6 Depositional environment

Vertical profiles from the Bråpiggen Formation display a high degree of variability. The Lower member is dominated by lithofacies Association 1, and accumulated in a distal, delta plain setting, influenced by both fluvial currents and tidal fluctuations. The overlying Middle and Upper members exhibit an overall fining upwards trend, and similar depositional environments are inferred for both. The presence of sandstone dominated units, arranged in laterally continuous layers, and containing a combination of channel and bar deposits, suggests a fluvial style similar to modern braided river systems (Rust, 1972; Miall, 1977). The Middle member exhibits both lateral and vertical variability. In the north (at Friis-Baastadnuten) the lower part of the Middle member is characterised by a repeated vertical stacking of channel aggradation deposits (Association 2) with minor longitudinal gravel bar deposits, resulting in a vertical sequence showing some similarity to Miall's (1977) Donjek Type profile. Further south, at Ryvingen, the Middle member is characterised by an abundance of planar cross-stratification (Associations 3 and 4), and is dominated by bar deposits, showing a greater similarity to Miall's (1977) Platte Type profile, indicating deposition probably occurred in a relatively shallow setting. Both the Middle and Upper members exhibits a gradual fining upwards trend, with the proportion of fine-grained lithofacies increasing vertically. Transition to more distal depositional conditions, characterised by deposition in a sheetflood, sand-bed river, is inferred. Both members are interpreted as distal deposits of a braided fluvial system that flowed towards the southeast, and cut across the fine-grained, interdistributary delta plain deposits of the Lower member.

3.5.2 Architectural element analysis

Unfortunately, no cliff face exposures suitable for the construction of face sketches and architectural element analysis were located, and as such, determination of the depositional setting of the Bråpiggen Formation is entirely dependent on vertical profile analysis.

4. DEPOSITIONAL MODEL FOR THE AHLMANNRYGGEN GROUP

4.1 INTRODUCTION

Exposures in the Ahlmannryggen and Borgmassivet regions exhibit many similarities, with the successions in both regions not only recording sedimentation in similar depositional settings, but also displaying comparable transitions between depositional environments (Figure 4.1). It is therefore proposed that the sequences from these two areas preserve a record of contemporaneous sedimentation in different portions of the same basin. The Pyramiden and Veten Formations, the Schumacherfjellet and Framryggen Formations and the Grunehogna and Högfonna Formations are considered lateral equivalents, with minor differences in sedimentology reflecting lateral variations in sedimentation style. There is no succession comparable to the Bråpiggen Formation preserved in the Ahlmannryggen region.

4.2 STAGE 1: FLUVIAL BRAIDPLAIN

The oldest exposed strata of the Ahlmannryggen Group, represented by the Pyramiden and Veten Formations, reflect deposition in a fluvial braidplain system that extended across both the Borgmassivet and Ahlmannryggen regions, and discharged towards the northeast (Figure 4.2a). This braidplain system is considered to have occupied the medial to distal reaches of the sedimentary basin, having likely arisen from the coalescence of proximal alluvial fans or braided rivers (Rust and Koster, 1984). A comparison of the two formations reveals lateral variations in sedimentation style, with the more proximal Veten Formation containing abundant gravelly channel and bar deposits, and the more distal Pyramiden Formation being characterised by predominantly sandy deposits.

In drawing comparisons with modern braided alluvium, it would be logical to initially propose fluvial systems such as the Platte River as an appropriate correlative for sandy Precambrian braid-plains. Its broad shallow tract (valley width is 10 to 18km in the lower reaches) and scarcity of fine sediment capable of forming confining banks (Smith, 1971) should approximate poorly-confined Precambrian braidplain conditions, which would have lacked stabilising terrestrial vegetation capable of creating confining channel banks. However, the Platte River sediments are dominated by sets of planar cross-stratification formed by the migration of linguoid bars in shallow water (Crowley, 1983). In contrast, the Veten and Pyramiden Formations contain abundant channel aggradation deposits dominated by trough cross-stratification and, in the case of the Pyramiden Formation, numerous fining-upwards successions resulting from channel migration. The South Saskatchewan and Donjek rivers therefore represent more favourable comparisons for the oldest formations in the Ahlmannryggen Group.

Compared with the Platte River, the deeper channels and abundant trough cross-strata of the South Saskatchewan and Donjek rivers can be understood as a response to valley confinement and the effect of stabilising vegetation (Williams and Rust, 1969; Smith, 1971; Rust and Gibling, 1990). Such influences were absent during the deposition of the Pyramiden and Veten Formations. Instead, active braid tracts were probably temporarily confined by banks of alluvium, stabilised by the presence of fine-grained sediment, but over time traversed the whole braidplain.

A marked absence of sheetflood deposits, such as those documented from the modern Bijou Creek (McKee *et al.*, 1967) and the Jurassic Kayenta Formation (Bromley, 1991; North and Taylor, 1996), and an abundance of channel aggradation and bar deposits, suggests perennial, rather than ephemeral, discharge dominated. The presence of sporadic desiccation horizons within this perennial system is attributed to episodes of sub-areal exposure following channel abandonment.

4.3 STAGE 2: BRAID DELTA PLAIN

The fluvial braidplain deposits of Stage 1 are overlain by the Framryggen Formation in the Borgmassivet region and the Schumacherfjellet Formation in the Ahlmannryggen region. These two formations record a change to distal, delta plain conditions in which sheet-like braid channels traversed a delta plain dominated by tidally influenced fine-grained deposits (Figure 4.2b).

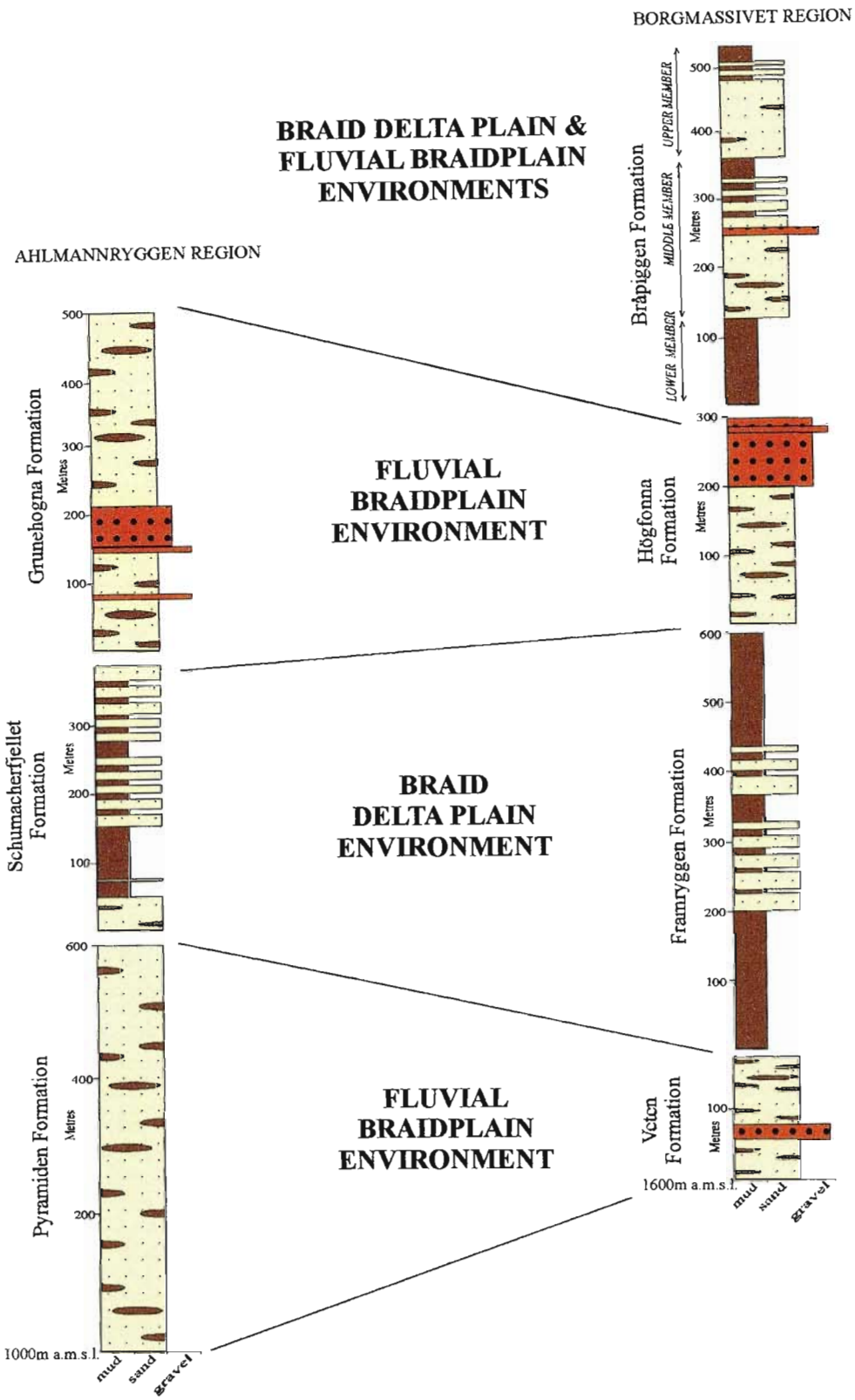

Figure 4.1: Sequences exposed in the Ahlmannryggen and Borgmassivet regions record sedimentation under the same range of depositional environments and are considered lateral equivalents within a single basin system.

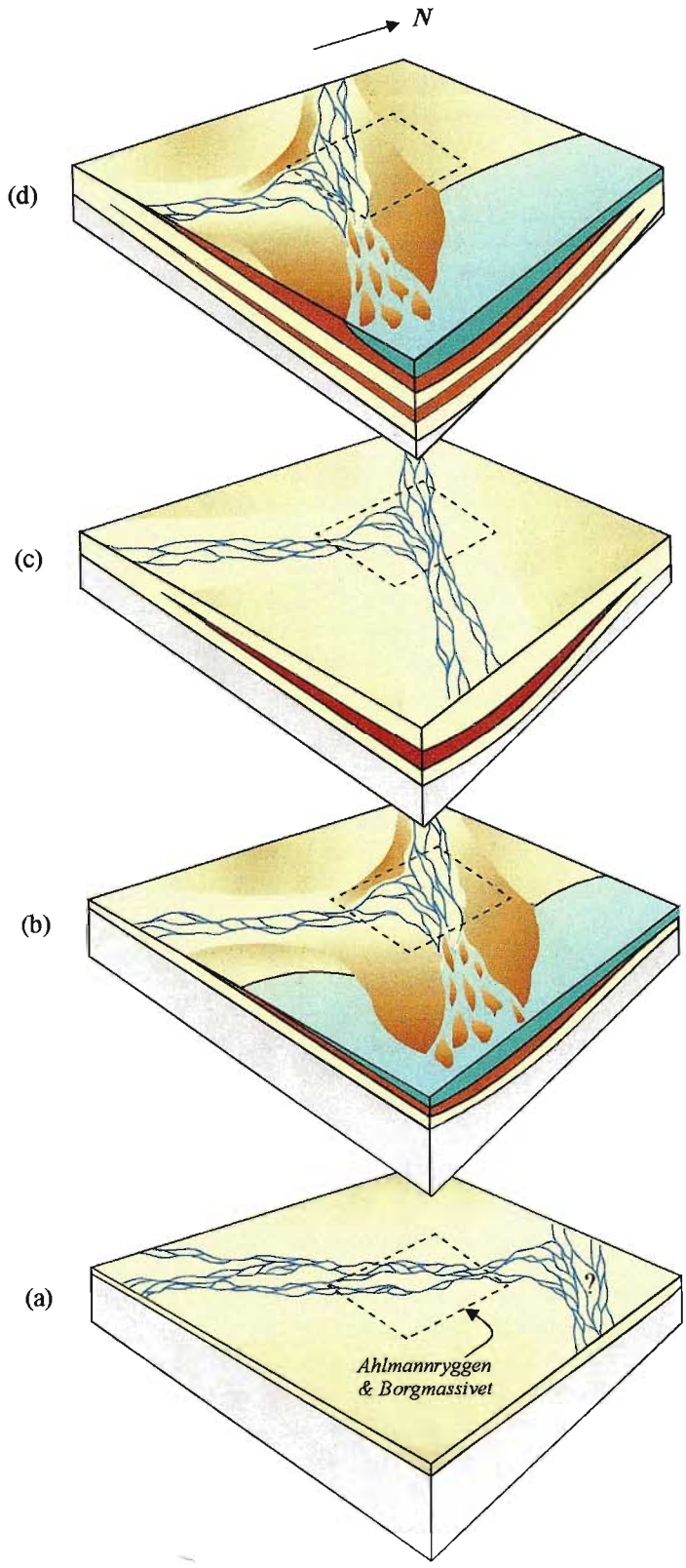

STAGE 4
Fluctuating environment characterised by short cycles of progradation of the fluvial braidplain across delta plain. Fluvial channels dominated by longitudinal drainage, discharging towards the southeast, suggesting further southward migration of the basin axis

STAGE 3
Re-establishment of a fluvial braid-plain in which the transverse and longitudinal drainage systems of the braid delta plain are maintained.

STAGE 2
Braid delta plain with both transverse and longitudinal drainage patterns, suggesting southerly migration of the basin axis.

STAGE 1
Fluvial braidplain dominated by transverse drainage towards the northeast.

Figure 4.2: Cartoon diagrams depicting changes in the sedimentary environments within the Ahlmannryggen and Borgmassivet regions of the Grunehogna Province, during the evolution of the Ahlmannryggen Group basin. The environment fluctuated between fluvial braidplain and braid delta plain settings, with changes in palaeocurrent orientations suggesting a gradual southwards migration of the basin axis over time.

In both regions, tidal indicators are restricted to the low-energy, fine-grained units, while the high-energy channel deposits display well-constrained unimodal palaeocurrent orientations, and are inferred as having been fluvially dominated. Within the Borgmassivet region, the northeasterly-orientated transverse drainage system of Stage 1 was maintained across the delta plain, but to the north, a longitudinal drainage system flowing towards the southeast dominated. This marked change in the drainage pattern is attributed to a southerly shift in the basin axis, and it is possible to speculate that during Stage 1 the longitudinal drainage network had been positioned to the north of the Ahlmannryggen region.

The channel deposits in the Ahlmannryggen region are dominated by trough cross-stratification and normally graded, fining-upwards cycles, suggesting continuous, rather than catastrophic, discharge (Sonderholm and Trisgaard, 1998). Current flow in the longitudinal drainage network was therefore more consistent than discharge through the transverse system, as the Framryggen Formation preserves evidence of occasional flash-flood events in the form of horizontal stratification and Laminated Sand Sheets. In both drainage systems, channel depths were sufficient for the migration of in-channel dunes and the development of abundant trough cross-stratification, but few channel margins are observed. It is unlikely that the fluvial discharge extended simultaneously and unbroken over the entire delta plain. Instead, channel depth may have been maintained though the formation of temporary confining banks stabilised by the abundant fine-grained sediment, and reworked as the channels migrated across the delta plain over time.

It is difficult to determine whether the delta system debouched into a lacustrine or marine environment, however the presence of limited tidal type stratification and an absence of typical lacustrine deposits suggests the latter scenario is the most feasible. Tidal fluctuations are also likely to have been responsible for the repeated episodes of sub-areal exposure recorded by the numerous desiccation horizons in both the Framryggen and Schumacherfjellet Formations.

4.4 STAGE 3: FLUVIAL BRAIDPLAIN RE-ESTABLISHED

A return to fluvial braidplain conditions is recorded in the Grunehogna and Högfonna Formations (Figure 4.2c). In both the Borgmassivet and Ahlmannryggen regions, the braidplain was characterised by high-energy, sand-gravel bed-load dominated channels in which abundant trough cross-stratified deposits accumulated, similar to the modern Donjek and South Saskatchewan rivers. Occasional sand/gravel bars and minor fine-grained deposits are preserved, but these are scarce as accommodation space was apparently limited, resulting in a high degree of reworking. Some lateral variability in the sedimentation style is evident in the Borgmassivet region (Högfonna Formation), with more southerly/proximal exposures being dominated by shallow-water sandy bar deposits, comparing favourably with the modern Platte River (Crowley, 1983).

The transverse and longitudinal drainage patterns of the underlying delta plain succession were maintained in the Stage 3 fluvial braidplain. Palaeocurrents within the Borgmassivet region flowed towards the east-northeast, while the longitudinal drainage system in the Ahlmann-ryggen region maintained its southeasterly palaeoflow direction. The predominance of trough cross-stratification and the lack of horizontally stratified sheetflood deposits indicates that the perennial discharge recorded in the underlying successions was sustained during Stage 3.

Despite the high degree of reworking within the braidplain environment, isolated pyroclastic units have been preserved. Underlying successions contain limited reworked volcaniclastic material, but massive tuffaceous units are recorded for the first time in the Högfonna Formation, suggesting increased volcanic input.

4.5 STAGE 4: ALTERNATING BRAID DELTA PLAIN AND FLUVIAL BRAID-PLAIN

The youngest preserved deposits of the Ahlmannryggen Group are restricted to the southern Borgmassivet, where they form the Bråpiggen Formation. This succession records a change to a more distal setting in which the

conditions fluctuating between braid delta plain and fluvial braidplain environments (Figure 4.1, 4.2d). Palaeocurrent orientations indicate that a southeasterly-flowing drainage pattern dominated the fluvial braidplains, while tidal fluctuations influenced the fine-grained delta plain deposits. It is possible that a further southward migration of the basin axis was responsible for shifting the longitudinal drainage system from the Ahlmannryggen region to the vicinity of the Borgmassivet, but the limited extent of the Bråpiggen Formation exposures precludes anything but speculation on this point.

Within the Ahlmannryggen Group, Stage 4 exhibits the highest degree of variability with regard to sedimentation style. Environments not only fluctuated rapidly between delta plain and fluvial braidplain settings, but lateral variations in fluvial style, similar to those recorded in the underlying Högfonna Formation, are also present. In addition, pyroclastic input increased during Stage 4, resulting in the formation of abundant reworked volcaniclastic deposits and the deposition of thick tuffaceous units. This introduction of large volumes of volcanic ash could be partly responsible for the rapid fluctuations in sedimentation style, as this may have resulted in a periodic oversupply of detritus and intermittent progradation of the fluvial braidplain over underlying delta plain deposits.

4.6 BASIN EVOLUTION MODEL

An overall basin evolution model, integrating the lithostratigraphic, sedimentological, geochemical and geochronological aspects of the study, is presented in Section D1.

SECTION C

1-PETROGRAPHIC & GEOCHEMICAL EVIDENCE FOR PROVENANCE & TECTONIC SETTING
2-AGE OF THE AHLMANNRYGGEN GROUP & SOURCE TERRAINS
3-STRUCTURAL DEFORMATION IN THE AHLMANNRYGGEN & BORGMASSIVET

Overview:

To further constrain the geological evolution of the Ahlmannryggen Group sedimentary basin, investigations into the petrographic, geochemical, geochronological and structural characteristics of this sequence were conducted. Consideration of these aspects is necessary in order to establish the nature of the source terrains supplying detritus to the basin, to constrain the timing of deposition and tectonic setting of the basin, as well as to determine the nature and age of deformation affecting the region. Each of these factors are considered in detail in this section and, combined with the findings of the sedimentological investigation, form the basis of the basin evolution model presented in Section D.

1. PETROGRAPHIC & GEOCHEMICAL EVIDENCE FOR PROVENANCE AND TECTONIC SETTING

1.1 INTRODUCTION

Provenance and tectonic setting determinations for sedimentary successions can be performed using a variety of techniques, relying on petrographic, geochemical or isotopic analysis. Provenance studies initially relied primarily on petrographic techniques (Blatt, 1967; Dickinson, 1970, 1985; Ingersoll *et al.*, 1984). However, in recent years, whole rock and mineral geochemical and isotopic techniques have been increasingly used (e.g. Roser and Korsch, 1988; McLennan *et al.*, 1993; Roser *et al.*, 1996). These studies have shown that the integration of petrological, geochemical and isotopic techniques provides an opportunity to understand the interrelationships between factors controlling provenance, and reduces the chances of misinterpretation of complex data (Roser and Korsch, 1986, 1988; Cox and Lowe, 1996; Johnsson and Basu, 1993). This integrated approach also assists in refining the tectonic configuration of a sedimentary succession (e.g. Cox and Lowe, 1996) and forms a crucial step towards understanding the nature of a sedimentary basin. This section presents an integrated analysis of petrological, geochemical and isotopic data from the Ahlmannryggen Group, in order to determine its provenance and tectonic setting.

1.2 PETROGRAPHIC ANALYSIS

1.2.1 Sandstone

Sandstone lithofacies formed the main focus of the petrographic investigation. A total of 35 representative thin sections were examined, of which 26 were selected for modal analysis (Table 1.1) according to the Gazzi-Dickinson method of point counting (Dickinson, 1970; Dickinson and Suczek, 1979; Ingersoll *et al.*, 1984). The 9 thin sections not point counted were considered too highly altered, as a result of pervasive low-grade metamorphism, to provide reliable data.

Within the Ahlmannryggen Group, the sandstone composition is variable, but no systematic changes were identified. As such, the petrographic data for the Ahlmannryggen Group sandstones is considered as a whole, rather than in the context of individual formations.

1.2.1.1 Detrital Minerals

Monocrystalline quartz (Qm) is a common detrital mineral in the samples and is often the principle framework grain type. Both straight and undulose extinction are common, and while clear grains predominate, cloudy varieties of possible quartz vein origin are also present. Quartz overgrowths in optical continuity with the detrital grains are a common feature, often obscuring the original grain shapes (e.g. Figure 1.1a). Partial preservation of ferruginous coatings on some detrital grains suggests these were predominantly sub-rounded to angular.

Polycrystalline quartz grains (Qp) are recorded in relatively low abundance in all but four of the thin sections studied. These composite grains are characterised by a varying number of quartz sub-grains which may exhibit either straight or undulose extinction (e.g. Figure 1.1b). Two varieties of Qp grains are recognised, those with few sub-grains which tend to exhibit straight contacts, and those with multiple sub-grains typically displaying sutured contacts. The former are possibly of plutonic origin, while the latter imply a metamorphic source (Basu *et al.*, 1975).

Of the many varieties of lithic grains identified in the samples (Lc, Ls, Lm, Lv), only chert (Lc) and volcanic (Lv) lithic grains occur to any notable extent. The chert grains vary from fine- to medium-grained and are generally clear, although jasper varieties stained red by abundant ferruginous material and silty chert grains are also present. Volcanic lithic grains include rhyolitic fragments, grains of welded pumice and devitrified glass shards (Figure 1.1e). A number of samples apparently lack a volcanic component, however most of the samples contain abundant highly altered grains (PMg), which have been entirely replaced by secondary minerals, termed pseudomatrix for the purpose of this study (e.g. Figure 1.1g). Although all traces of the original composition of these grains have been removed, remnant textures (including devitrification, microlitic and welded pumice textures) are often preserved, suggesting a volcanic origin. A minor component of

Table 1.1: Modal analyses (Gazzi-Dickinson point counting method) and re-calculated data for the Ahlmannryggen Group sandstone samples.

		Detrital Grains									Alteration Components			QFL Parameters		
Sample	Formation	Qm	Qp	F	Lc	Ls	Lm	Lv	D	M	PMg	PMm	Ca	Q	F	L
A.PM.6	Pyramiden	45.0	1.4	11.0	1.4	0.0	0.0	0.4	0.4	0.0	13.2	27.2	0.0	64.1	15.2	20.7
A.GH.6	Schumacherfjellet	26.4	11.6	3.8	8.8	0.4	0.0	3.8	1.2	0.0	17.2	26.2	0.6	52.8	5.3	41.9
A.GH.7	Grunehogna	39.4	14.6	9.8	1.2	0.0	0.0	0.0	7.8	0.0	2.6	24.6	0.0	79.9	14.5	5.6
A.JE.1	Grunehogna	38.2	0.0	18.2	0.8	0.0	0.0	0.2	1.8	0.2	20.2	15.0	5.4	49.2	23.5	27.3
A.JE.3	Grunehogna	27.4	1.4	18.6	3.8	0.0	0.0	4.4	0.8	0.4	22.8	16.8	3.6	36.7	23.7	39.5
A.JE.5	Grunehogna	61.8	1.8	21.2	2.2	0.0	0.0	0.0	0.2	0.2	0.0	9.8	2.8	73.1	24.4	2.5
B.NL.1	Veten	51.4	17.0	4.0	14.2	0.0	0.8	0.0	0.6	0.0	2.8	9.2	0.0	75.8	4.4	19.7
B.NL.7	Veten	42.2	2.6	22.0	1.6	0.0	0.0	1.4	3.2	0.0	12.2	13.8	1.0	54.6	26.8	18.5
B.SO.4	Veten	9.6	2.8	27.0	4.0	0.0	0.0	8.0	6.0	0.0	18.6	24.0	0.0	17.7	38.6	43.7
B.PR.1	Veten	16.2	3.0	29.2	1.0	0.0	0.0	13.4	1.4	0.0	23.6	9.6	2.6	22.2	33.8	44.0
B.ST.3	Framryggen	39.5	3.0	0.4	1.6	0.0	0.0	0.0	3.6	0.0	0.0	51.5	0.4	95.5	0.9	3.6
B.VE.3	Framryggen	14.8	6.4	27.2	3.2	0.0	0.0	7.4	1.4	0.0	20.0	18.8	0.8	26.8	34.4	38.7
B.FR.3	Framryggen	64.4	0.8	23.2	1.0	0.0	0.0	0.0	0.4	0.0	3.6	6.6	0.0	70.1	24.9	4.9
B.FR.6	Framryggen	24.8	4.4	25.0	1.1	0.0	0.3	8.4	4.5	0.0	13.7	16.8	1.0	37.6	32.2	30.2
B.1885.3	Framryggen	14.4	3.8	22.2	3.7	0.3	0.3	11.5	3.7	0.6	16.7	22.8	0.0	25.0	30.5	44.6
B.MA.1	Högfonna	48.5	7.2	16.2	4.0	0.0	0.3	7.0	1.2	0.0	12.2	3.4	0.0	58.4	17.0	24.6
B.OB.5	Högfonna	36.0	2.5	20.9	1.7	0.0	0.0	0.0	0.4	0.0	16.1	22.4	0.0	49.9	27.1	23.1
B.OB.7	Högfonna	40.4	0.0	22.6	0.3	0.0	0.0	0.0	0.4	0.0	13.9	22.4	0.0	52.3	29.3	18.4
B.RB.1	Högfonna	52.2	4.5	9.9	1.6	0.0	0.0	7.9	2.7	0.0	13.2	8.0	0.0	63.5	11.1	25.4
B.Hh.1	Högfonna	18.6	4.4	14.5	3.9	0.0	0.3	12.3	1.2	0.0	25.6	15.4	3.8	28.9	18.2	52.9
B.Hh.3	Högfonna	16.7	5.5	7.4	10.2	5.0	1.1	23.5	3.2	0.0	13.8	10.1	3.5	26.7	8.9	64.4
B.Hh.4	Högfonna	13.4	6.3	7.8	6.0	3.3	1.0	21.1	5.0	0.4	20.8	6.8	8.1	24.7	9.8	65.5
B.HF.101	Högfonna	43.9	0.0	4.1	1.4	0.0	0.0	0.0	2.1	0.0	0.0	48.5	0.0	88.9	8.3	2.8
B.HF.103	Högfonna	40.0	0.5	1.6	2.0	0.0	0.0	0.0	0.0	0.0	20.9	35.0	0.0	62.3	2.5	35.2
B.RY.1	Bråpiggen	29.8	3.8	14.7	2.5	0.0	0.5	0.6	0.4	0.0	18.7	29.0	0.0	47.6	20.8	31.6
B.RY.2	Bråpiggen	38.9	0.0	10.6	0.8	1.2	0.0	0.5	2.2	0.0	5.8	40.0	0.0	67.3	18.3	14.4

Re-calculated QFL parameters
Q = Qm + Qp
F = Plag + K-feld
L = Lc + Ls + Lm + Lv + PMg

Qm- monocrystalline quartz
Qp- polycrystalline quartz
F- feldspar
Lc- lithics, chert
Ls- lithics, sedimentary
Lm- lithics, metamorphic
Lv- lithics, volcanic
D- heavy minerals
M- micas
PMg - pseudomatrix, grains
PMm- pseudomatrix, groundmass
Ca- calcite

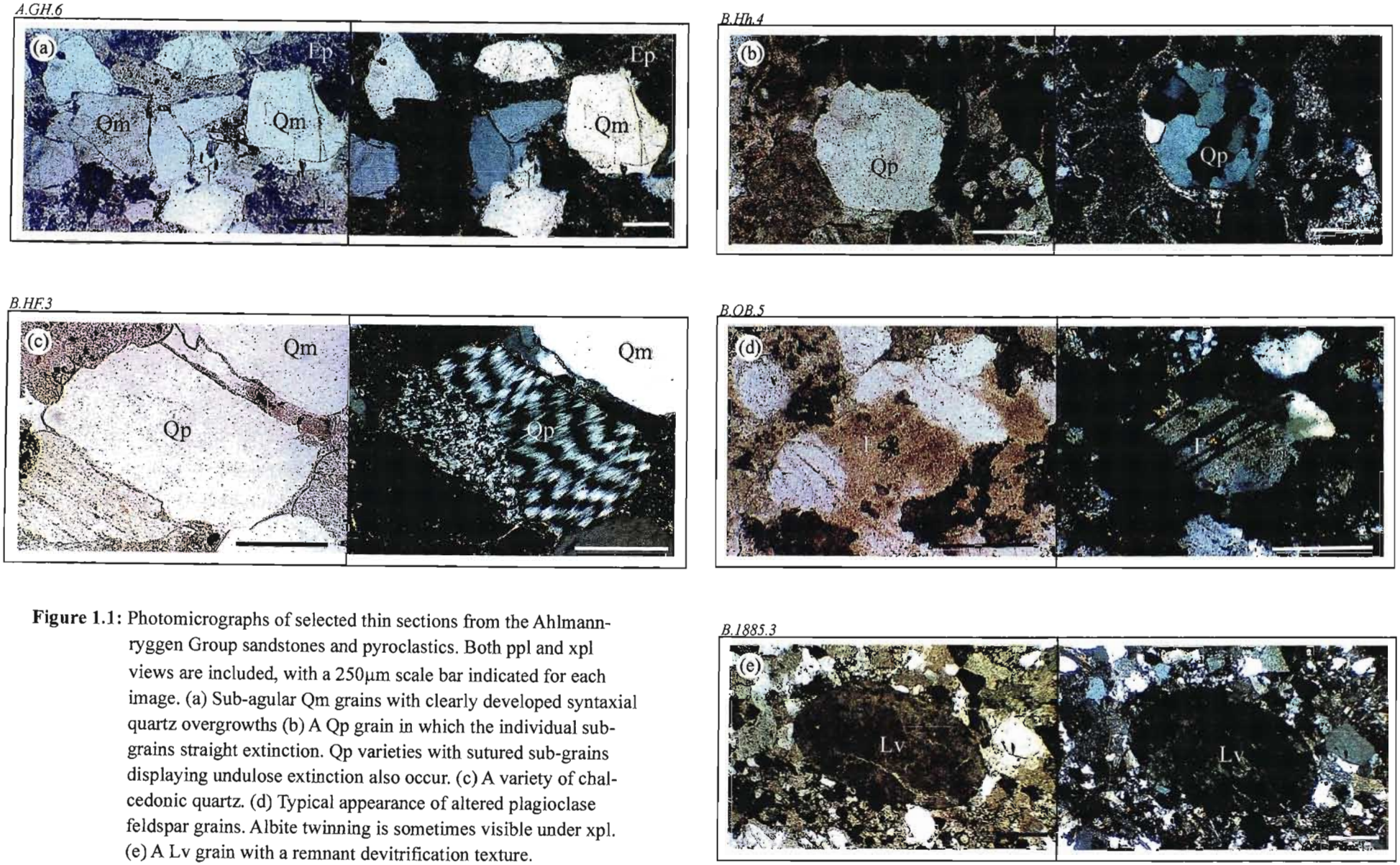

Figure 1.1: Photomicrographs of selected thin sections from the Ahlmann-ryggen Group sandstones and pyroclastics. Both ppl and xpl views are included, with a 250μm scale bar indicated for each image. (a) Sub-agular Qm grains with clearly developed syntaxial quartz overgrowths (b) A Qp grain in which the individual sub-grains straight extinction. Qp varieties with sutured sub-grains displaying undulose extinction also occur. (c) A variety of chal-cedonic quartz. (d) Typical appearance of altered plagioclase feldspar grains. Albite twinning is sometimes visible under xpl. (e) A Lv grain with a remnant devitrification texture.

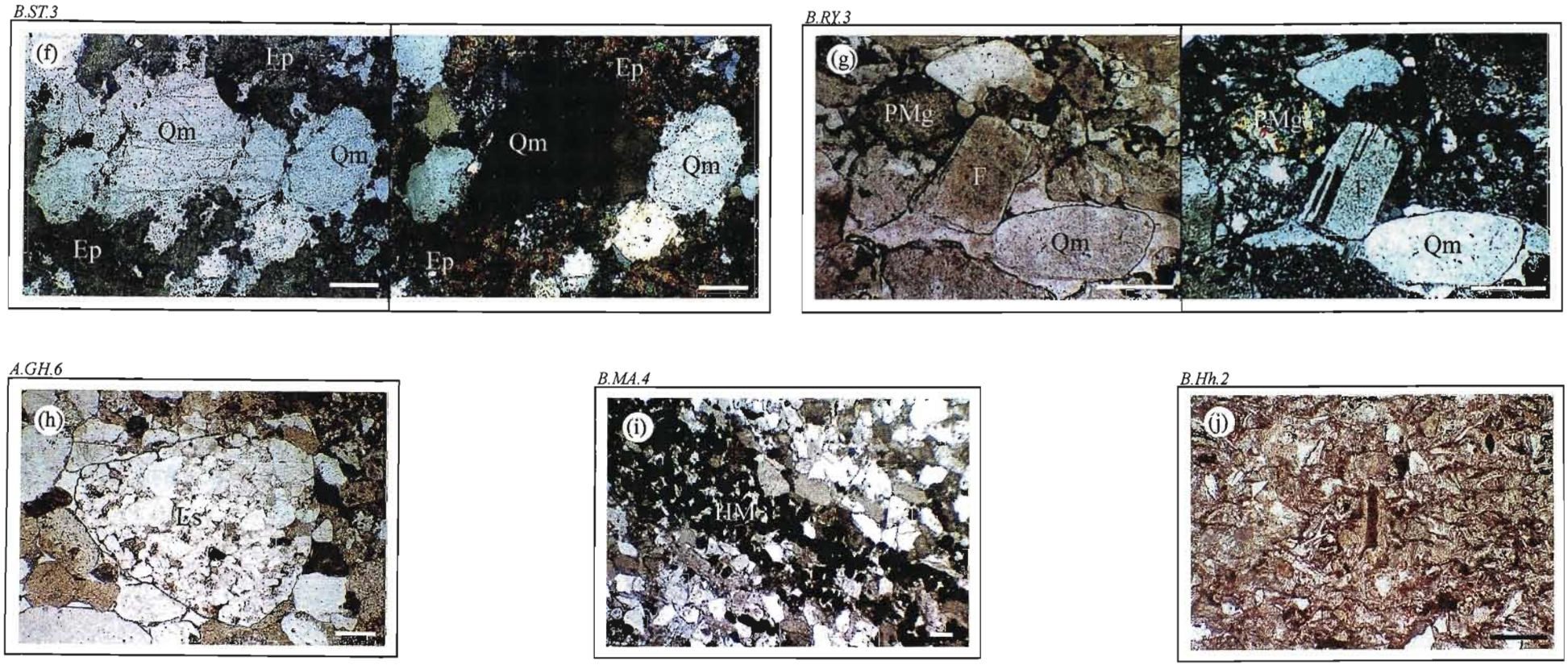

Figure 1.1: ...continued. (f) Photomicrograph showing extensive epidotisation, forming pseudomatrix. (g) Selection of commonly occurring detrital grains, including monocrystalline quartz and feldspar grains. A completely altered grain of unknown original composition (PMg) is also present. Despite the extensive alteration, the original detrital grain boundary is preserved. (h) A fine-grained sandstone sedimentary lithic (Ls) grain in which the individual sub-grains are visible under ppl due to the presence of remnant grain coatings. (i) In some samples detrital heavy mineral grains have been hydraulically fractionated to form thin laminae. (j) A vitric tuff under ppl, in which individual glass shards are clearly visible.

sedimentary lithics (Ls) is present in five of the samples (e.g. Figure 1.1h). These include fine-grained quartzite fragments and angular mudstone flakes, the latter representing rip-up clasts of intraformational origin. A metamorphic lithic component (Lm), consisting of stretched/ sheared metamorphic quartz and schistose metamorphic quartz grains, is also recognised in a number of samples.

Feldspar grains (F) are a common framework constituent (Figure 1.1d). The grains are often highly altered, and typically reduced to patches of cloudy alteration products due to extensive sericitisation and chloritisation, often prohibiting discrimination of the feldspar composition. A few feldspars exhibit remnant albite, microcline and Carlsbad twinning, indicating the presence of both plagioclase and K-feldspar varieties. Subordinate fresh, Ab-rich plagioclase is present in some samples, possibly of volcanic origin. This interpretation is supported by an association with volcanic lithic fragments. Overall, the feldspar grains tend to exhibit angular to sub-angular morphologies, indicating that the Ahlmannryggen Group sandstones are both texturally and mineralogically relatively immature.

Other minor detrital components occurring in the sandstones include occasional flakes of detrital muscovite (M) and heavy minerals (D). The micas are often characterised by iron oxide staining along the cleavages, and are typically distorted around adjacent detrital grains as a result of compaction. The heavy mineral fraction includes haematite, magnetite, ilmenite, zircon, rutile, apatite and rare pyrite grains, and is occasionally concentration along thin laminae (e.g. Figure 1.1i).

1.2.1.2 Secondary Minerals

All samples contain abundant alteration products, including sericite, chlorite, zoisite, epidote, actinolite, calcite and microcrystalline silica, which are collectively classified as 'pseudomatrix' (Figure 1.1f). These secondary minerals completely pseudomorph many of the original detrital grains (classified as PMg) and also occur as abundant interstitial 'matrix' (classified as PMm). Typically, current deposited sandstones such as those of the Ahlmannryggen Group will contain minimal primary detrital matrix (Pittman, 1979). The abundant pseudomatrix (which can constitute up to 52% of a sample) therefore cannot simply be attributed to the alteration of original interstitial material, but must have formed by *in situ* breakdown of unstable detrital mineral grains and rock fragments (Cummins, 1962). An abundance of pseudomatrix adversely affects provenance and tectonic discrimination schemes based on petrographic data, as these tend to be critically sensitive to unstable components such as feldpsars and lithics (Ingersoll, 1978; Dickinson and Suczek, 1979; Sutter *et al.*, 1981; Ingersoll *et al.*, 1984; Dickinson, 1985; Suttner and Basu, 1985; Harwood, 1988). Preferential removal of these phases results in a shift towards more mature, quartz-rich compositions, and incorrect interpretation of provenance and tectonic setting (Cox and Lowe, 1996). As such, the petrographic data is not used in isolation for tectonic discrimination, but is integrated with the results of the geochemical analysis, according to the methods of Cox and Lowe (1996), in an attempt to re-establish the original composition of the sediment. Nevertheless, the petrographic results are considered sufficient for a preliminary assessment of possible source terrains, which will be supplemented with the results of the geochemical investigations.

1.2.2 Mudstone

The fine-grained lithofacies consist of silt-sized fragments of quartz and feldspar in a strongly epidotised and chloritised matrix in which finely divided, black ferruginous material is disseminated. Abundant secondary actinolite is also present in most samples. The quartz grains are angular to sub-rounded, and in places form an interlocking mosaic texture. Syntaxial quartz overgrowths are a common feature. The feldspar grains are typically highly altered due to intense sericitisation and epidotisation, which in most cases prevents identification.

1.2.3 Pyroclastics

Volcanic airfall deposits introduced a large proportion of pyroclastic material into the Ahlmannryggen Group basin, which was extensively reworked in the sedimentary environment (as evidenced by the abundance of rounded volcanic lithic grains in the sandstone samples). Nevertheless, some of the thicker pyroclastic layers towards the top of the sequence appear to be primary airfall deposits. These primary pyroclastic deposits are predominantly highly altered acidic tuffs containing varying proportions of vitric and

crystal particles and often exhibiting laminated and welded textures (Figure 1.1j). A variety of lapilli-tuff, characterised by spherical to ovoid accretionary lapilli, was also identified. These pyroclastic units have been extensively altered, and the ash groundmass is commonly reduced to a microcrystalline aggregate of silica and flaky minerals in which granular epidote is often distributed, while the angular glass shards have been devitrified and the feldspar crystals subjected to saussuritisation.

1.2.4 Provenance Implications

The framework grain point-count data (Table 1.1) suggest dominance of magmatic and sedimentary source terrains relative to metamorphic source rocks, due to the high feldspar concentrations and the ubiquitous presence of chert. This observation is supported by the low concentration of metamorphic lithics.

Petrographic data indicate that contributions from two distinct magmatic terrains are represented. These include a felsic plutonic source, from which the K-feldspars were derived, and a contemporaneously active volcanic terrain, characterised by explosive acid volcanism, from which the volcanic fraction was sourced. Unlike the plutonic component, which does not exhibit any marked stratigraphic or geographic variations, the volcanic fraction is typically better represented in the more southerly exposures of the Borgmassivet region, suggesting this area was more proximal to the volcanic source. An increase in the abundance of primary airfall deposits towards the top of the sequence suggests an increase in the volcanic activity of this terrain towards the closing stages of deposition.

The sedimentary source terrain evidently consisted of a combination of quartzites and chert/jasper chemical precipitates, suggesting a banded ironstone association. Detritus sourced from this terrain is represented in all samples and evidently lacked geographic restrictions, suggesting the banded ironstone terrain formed an extensive pre-existing cover sequence.

Metamorphic lithic grains are restricted to sandstones deposited in the transverse drainage systems of the Borgmassivet. This suggests a localised metamorphic terrain was situated to the south/southwest of the Ahlmannryggen Group basin.

Within the context of WDML, a potential plutonic magmatic source is represented by the Annandagstoppane basement granites, while the magmatic arc system of the Maudheim Province, which docked against the southern margin of the Grunehogna Province during the Meso-proterozoic (Grantham *et al.*, 1995; Groenewald *et al.*, 1995; Jacobs *et al.*, 1996), represents a likely source of the pyroclastics. Uplifted orogenic regions of the latter may have supplied the metamorphic component. The sedimentary source terrain is either no longer preserved, or is obscured by the extensive ice cover, but was likely part of an older, possibly early Proterozoic, stable continental cover sequence similar to that of the Transvaal Basin of South Africa or the Hammersley Basin of Western Australia.

1.3 GEOCHEMICAL ANALYSIS

Twenty-six sandstone, nineteen mudstone and five pyroclastic samples were analysed by a combination of XRF and ICP-MS methods (Appendix 1). The resulting geochemical data and correlation matrixes are included in Appendix 6.

1.3.1 Sandstone

The sandstone samples selected for major and trace element analysis consisted of the same representative suite of samples for which detailed petrographic investigations had been conducted. This sample suite was specifically selected in order to permit integration of the data sets. Eight of the sandstone samples within the suite contain elevated heavy mineral contents, due to the presence of thin heavy mineral laminae. These samples are highlighted in all plots and tables and are treated with caution.

Variations in the major element geochemistry of the studied samples are shown on Harker diagrams (Figure 1.2). The sedimentary rocks of the Ahlmannryggen Group have a relatively wide range of SiO_2 content (62-89%), and for all samples there are variable degrees of negative correlation for SiO_2 versus Al_2O_3 ($r = -0.8$), Fe_2O_3 ($r = -0.7$), MgO ($r = -0.6$) and TiO_2 ($r = -0.5$); however K_2O, CaO, Na_2O and MnO yield scatter. No systematic variations through the Ahlmannryggen Group sequence were identified from either the major or the trace element data.

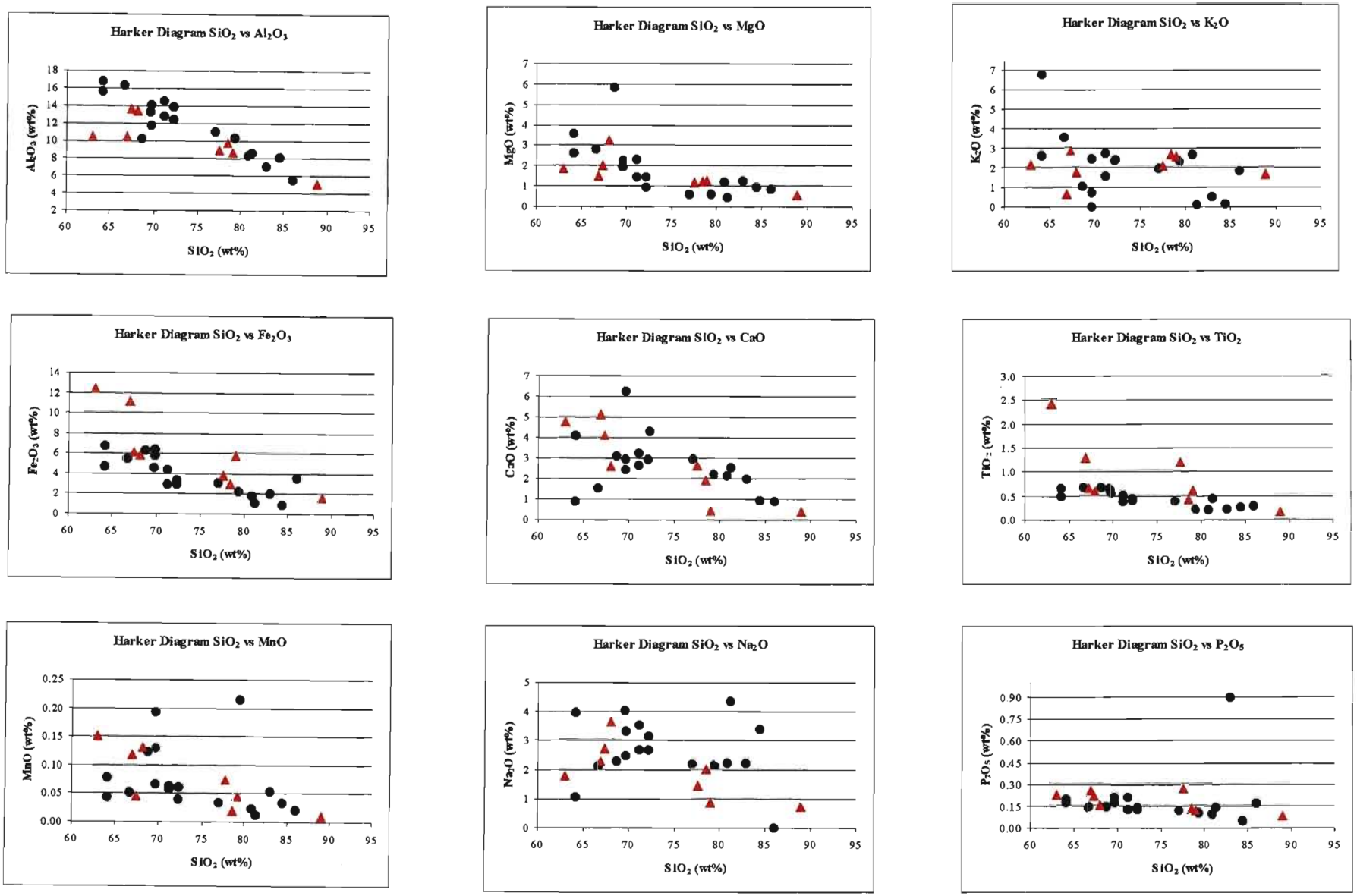

Figure 1.2: Harker variation diagrams for the Ahlmannryggen Group sandstones. No systematic variations through the Ahlmannryggen Group sequence were identified from the major element data, and as such no formation subdivisions have been included. (Black dots- sandstones; red triangles- heavy mineral enriched sandstones)

According to both major and trace element abundances, the majority of the Ahlmannryggen Group sandstones are geochemically classified as greywackes, although some samples fall within the arenite and arkose fields, based on plots from Pettijohn *et al.* (1972) (modified by Herron, 1988); Herron, (1988) and Blatt *et al.* (1980) (Figure 1.3a-c). Caution must be exercised in interpreting chemical classifications such as these, as classification systems tend to rely on large ion lithophile elements (such as K and Na) which may be mobilised during alteration. Nevertheless, there is some agreement between the results of the different classification schemes, encouraging confidence in the results.

1.3.2 Mudstone

Major and trace element abundances in the Ahlmannryggen Group mudstones are similar to published examples of average post-Archaean shales (Table 1.2), suggesting evolved crustal sources predominated in the source terrains. This observation is supported by a comparison of average rare earth element (REE) concentrations, which reveals that the Ahlmannryggen Group sediments exhibit a pattern closely resembling those for post-Archaean shales sourced from evolved magmatic provenances (Figure 1.3d).

1.3.3 Pyroclastics

Major and trace element abundances were determined for samples from five distinct pyroclastic units exposed in the Borgmassivet region. These samples fall within the rhyolite and dacite fields defined on Le Maitre *et al.*'s (1989) total alkali versus silica (TAS) diagram, supporting earlier interpretations, based on petrographic analysis, that these pyroclastic deposits were formed as a result of acidic volcanism (Figure 1.4).

1.3.4 Provenance Implications

Although the chemical composition of sedimentary rocks is a function of the complex interplay of such variables as weathering, sorting, diagenesis and metamorphism, the nature of the source rock is generally considered the most important attribute governing the diversity of composition of clastic sedimentary rocks (McLennan, 1989; McLennan *et al.*, 1993).

Condie *et al.* (1991) regard elevated Cr and Ni sediment concentrations as indicative of a mafic source rock influence. They consider Cr values below 152ppm and Ni values below 38ppm to be relatively 'low', and recognisably different from the Cr and Ni values of most Archaean greywackes (Taylor and McLennan, 1985; Wronkiewicz and Condie, 1989). They cite these low values as evidence for a dominantly felsic granitoid source terrain, and the presence of negligible mafic/ ultramafic weathering products. The Cr values within the Ahlmannryggen Group sandstones average 49ppm (varying from 5-95ppm), while the Ni concentrations average 42ppm (varying from 2-249ppm). These values imply a close affinity with a felsic-dominated provenance, although occasional elevated Ni concentrations indicate that minor mafic/ ultramafic sources cannot be ruled out. Further support for a felsic-dominated provenance is provided by the Cr/Th and K/Rb ratios. Condie *et al.* (1991) consider Cr/Th ratios below or equal to 75 as indicative of a provenance dominated by felsic terrains. The Ahlmannryggen Group sandstones exhibit a Cr/Th ratio varying between 0.5 and 11, indicating an overwhelming predominance of felsic source rocks. These results are supported by a plot of K_2O versus Rb, in which the Ahlmannryggen Group sandstone samples predominantly fall within the intermediate to acidic field (Figure 1.5). A plot of Ti versus Ni can separate immature sediments, derived from magmatic sources, from more mature sediments (after Floyd *et al.*, 1989; Figure 1.6). The Ahlmannryggen Group sandstone samples plot in both these fields, suggesting multiple source terrains supplied detritus to the basin. In terms of an Al_2O_3 - $CaO+Na_2O+K_2O$ - Fe_2O_3+MgO ternary diagram (Figure 1.7), the composition of the Ahlmannryggen Group rocks overlaps that of the intermediate to acid igneous lithologies of the Maudheim Province and Annandagstoppane granites, while a strong trend towards an average banded ironstone field is also exhibited.

Both the geochemical and petrographic studies imply derivation from mixed sources. The contributing terrains apparently consisted of a mix of stable cratonic provenances and tectonically active regions. The former comprised basement granites and a sedimentary cover sequence dominated by a banded ironstone association, while the latter consisted of uplifted and volcanically active portions of an accreting volcanic arc terrain. Of these multiple source terrains recognised for the Ahlmannryggen Group, the orogenic Maudheim Province and

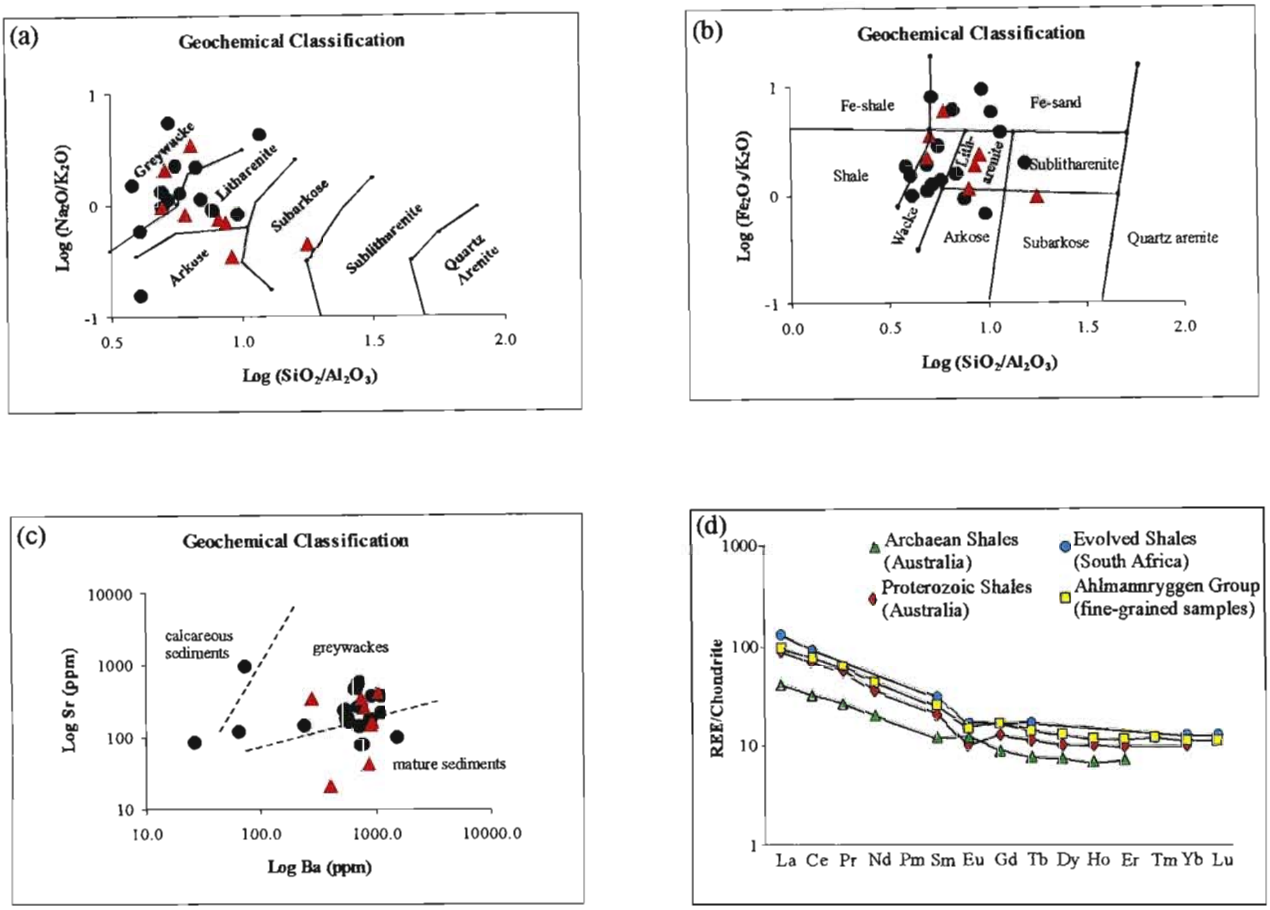

Figure 1.3: (a-c) Geochemical classification of the Ahlmannryggen Group sandstone samples, based on major and trace element ratios. Discrimination boundaries after (a) Pettijon *et al.* (1972), with the boundaries redrawn by Herron (1988); (b) Herron (1988) and (c) Blatt *et al.* (1980). Black dots- sandstones; red triangles- heavy mineral enriched sandstones. (d) The Ahlmannryggen Group fine-grained rocks exhibit a REE pattern similar to that of Proterozoic shales from Australia and evolved shales from South Africa and, like most post-Archaean shales, are characterised by LREE enrichment, a flat HREE pattern and a significant negative Eu-anomaly.

Table 1.2: Comparison of geochemical characteristics of the fine-grained Ahlmannryggen Group samples with a selection of average post-Archean shales.

	NASC[1]	ES[2]	Proterozoic Shales (Australia)[3]	Evolved Shales (South Africa)[4]	Ahlmannryggen Group
SiO_2	64.8	-	64.10	59.48	64.65
TiO_2	0.78	-	0.63	0.77	0.75
Al_2O_3	16.9	-	14.21	20.14	16.27
Fe_2O_3	6.33	-	5.53	9.39	7.58
MnO	0.06	-	0.10	0.06	0.07
MgO	2.85	-	2.63	1.96	3.12
CaO	3.56	-	1.85	0.52	1.24
Na_2O	1.15	-	1.21	0.93	1.29
K_2O	3.99	-	3.91	2.62	4.40
P_2O_5	0.11	-	0.13	0.14	0.16
Nb	13	-	-	15.33	14.46
Y	35	31.8	19.50	32.33	28.42
Rb	125	-	-	134	170.36
Zr	200	-	-	184.67	203.13
Sr	142	-	-	98.67	195.66
U	2.7	-	3.10	5.7	3.44
Th	12	-	12.84	19.33	11.73
Zn	-	-	-	-	59.56
Cu	-	-	-	-	29.75
Ni	58	-	-	71	82.30
Cr	125	-	-	151.67	68.63
V	130	-	-	164.67	53.76
La	31	41.1	31.9	47	34.33
Pb	-	-	-	25	12.62
Ga	-	-	-	-	3.66
Co	26	-	-	22.67	29.96
Ce	67	81.3	65.4	87.67	74.00
Nd	30.4	40.1	24.6	-	30.41
As	-	-	-	-	5.91
Ba	656	-	296.9	602	911.25
Sc	15	-	-	21.67	15.65
Cs	5.2	-	14.56	10.07	7.85
Pr	7.9	10.4	7.42	-	8.21
Sm	5.6	7.3	4.65	6.83	5.67
Eu	1.2	1.52	0.86	1.4	1.28
Gd	5.2	6.03	3.8	-	5.08
Tb	0.85	1.05	0.64	0.96	0.80
Dy	5.54	-	3.72	-	4.8
Ho	1.04	1.2	0.83	-	0.97
Er	3.28	3.55	2.38	-	2.79
Tm	0.5	0.56	-	-	0.42
Yb	3.1	3.29	2.37	3.03	2.74
Lu	0.46	0.58	-	0.46	0.42
Hf	6.3	-	3.83	5.5	4.59
Ta	1.1	-	-	1.37	1.13

[1] Gromet *et al*., 1984

[2] Haskin and Haskin, 1966

[3] Nance and Taylor, 1976 (Mnt Isa Group and Amadeus Basin)

[4] Wronkiewicz and Condie, 1990 (Ventersdorp and Transvaal Supergroups)

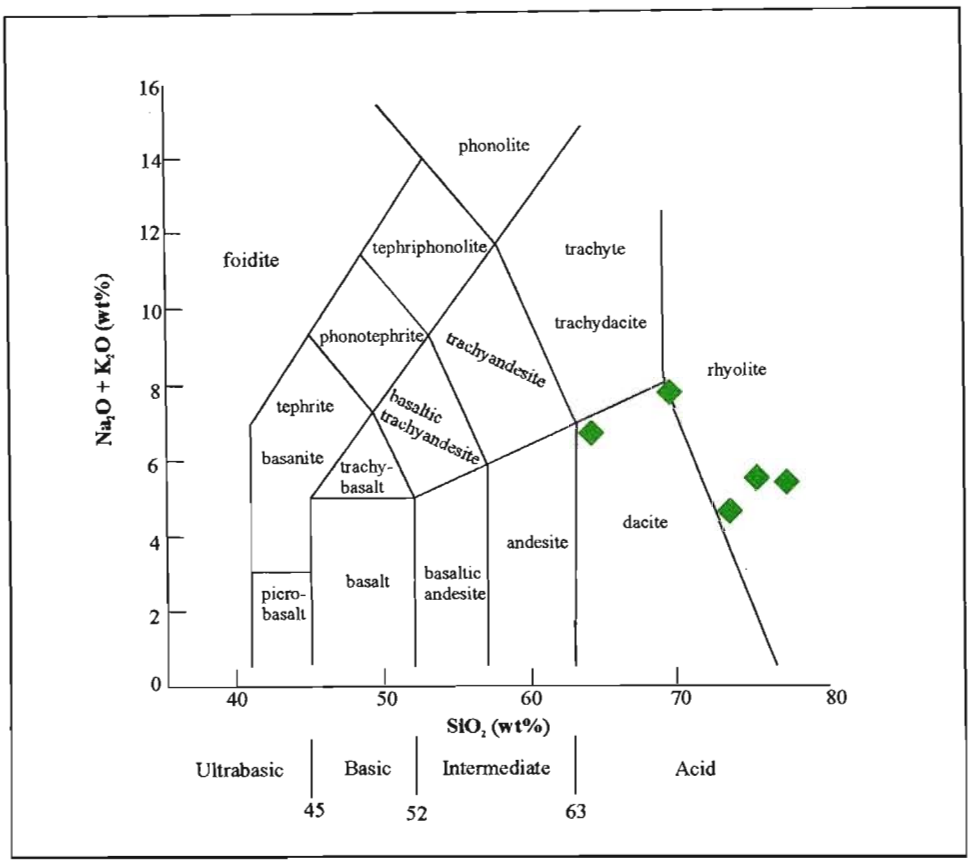

Figure 1.4: The geochemical classification of the pyroclastic samples using the total alkalis versus silica (TAS) diagram of Le Maitre *et al.* (1989) supports earlier interpretations based on petrographic analysis that the pyroclastic units are predominantly acidic in composition. These units are considered to have been formed as airfall deposits in response to explosive volcanism within an adjacent contemporaneously active arc system, now represented by the high-grade Maudheim Province.

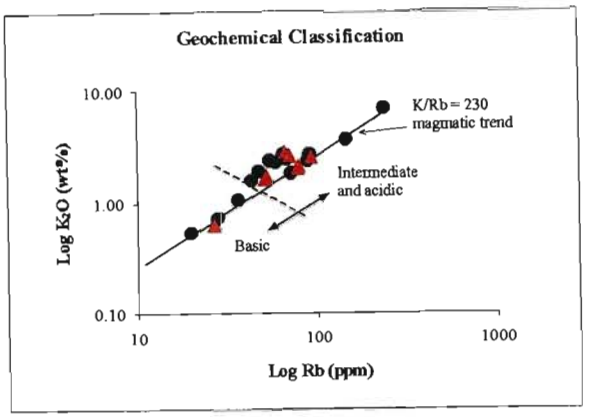

Figure 1.5: The log K_2O vs log Rb plot (after Caby *et al.*, 1977) of the Ahlmannryggen Group sandstone samples suggests that the provenance was dominated by intermediate to acidic source terrains, however a minor basic source cannot be ruled out. Black dots-sandstones; red triangles-heavy mineral enriched sandstones.

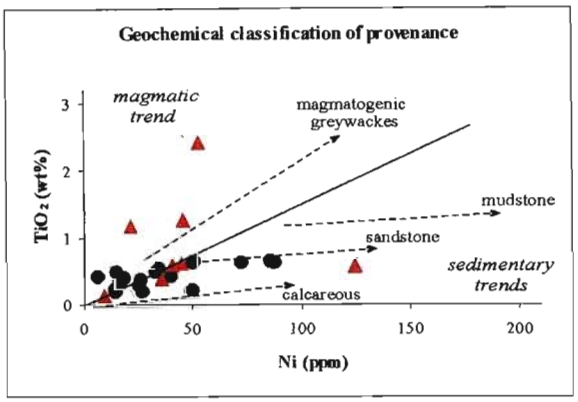

Figure 1.6: A TiO_2 vs Ni plot (after Floyd *et al.*, 1989) distinguishes between immature sediments derived from magmatic/magmatogenic sources, and mature sediments. The Ahlmannryggen Group sandstones exhibit trends within both fields, suggesting a number of different source terrains supplied detritus to the sedimentary basin. Black dots- sandstones; red triangles- heavy mineral enriched sandstones.

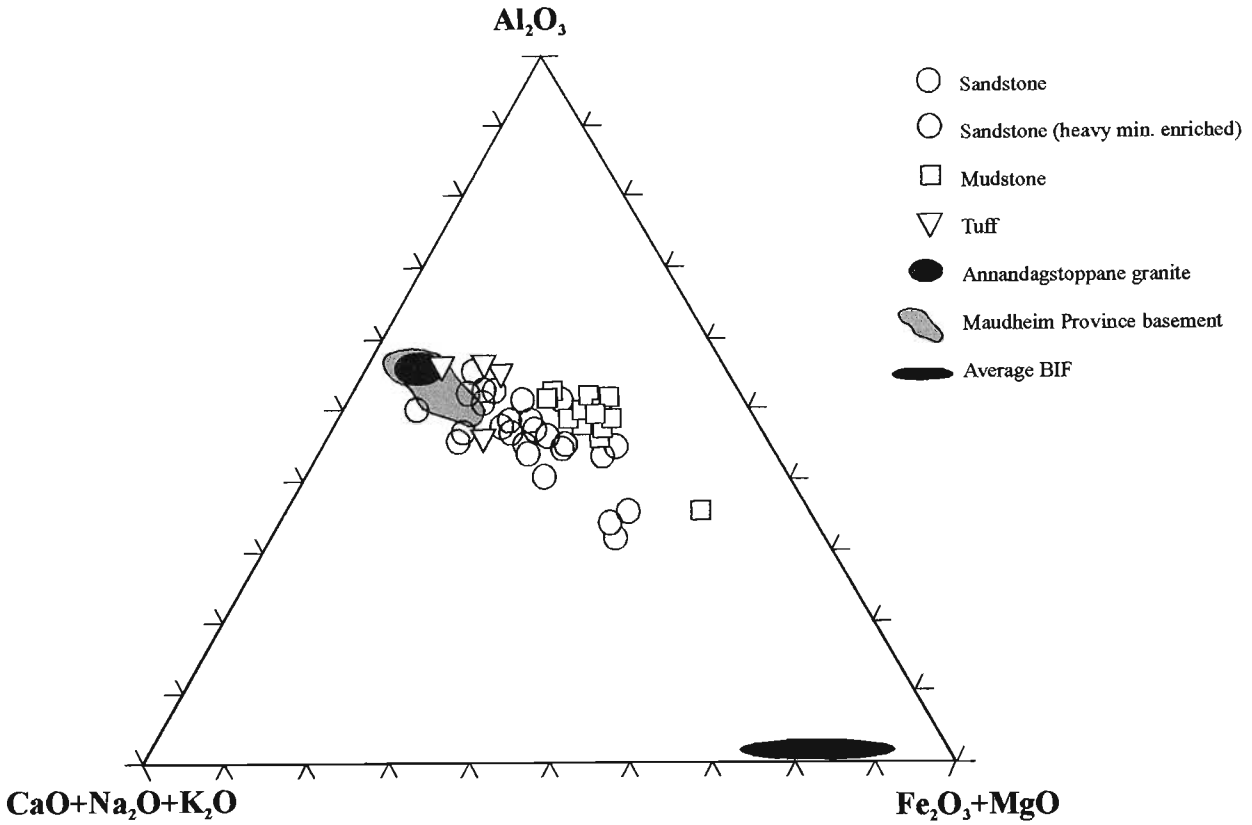

Figure 1.7: Al_2O_3 - $CaO+Na_2O+K_2O$ - Fe_2O_3+MgO ternary diagram for the Ahlmannryggen Group rocks. Fields for the Annandagstoppane basement granites (Krynauw, 2001, pers. comm.[1]), Maudheim Province basement lithologies (Grantham, 1992; Groenewald, 1995) and average banded iron-formations (Beukes and Klein, 1990) are also plotted. The Ahlmannryggen Group samples show a close affinity to local basement lithologies, indicating that these represent likely source terrains. The distinct trend towards the banded iron-formation field supports earlier interpretations, based on petrographic observations, that a banded ironstone association also supplied detritus to the basin.

[1]Dr J. Krynauw, 96 Mowbray Rd, Greenside, 2193, South Africa

Annandagstoppane basement granites represent currently exposed/preserved equivalents.

1.4 TECTONIC SETTING

"The birth and development of a sedimentary basin requires a theory which embraces uplift of the source area and subsidence to form the basin... [and the resulting]... pattern of erosion and sedimentation on the earth's surface and the nature of the basin is related to the plate tectonic setting of the region" (Bhatia, 1981).

Significant progress has been made in recent years, relating the geochemistry and petrography of sedimentary rocks to their tectonic setting (e.g. Crook, 1974; Dickinson and Suczek, 1979; Bhatia, 1981; Dickinson *et al.*, 1983; Bhatia, 1983; Bhatia and Crook, 1986; Roser and Korsch, 1986, 1988; Cox and Lowe, 1995; Cox and Lowe, 1996; Roser *et al.*, 1996). This section combines petrographic and geochemical data from the Ahlmannryggen Group with published tectonic discrimination schemes in order to elucidate the tectonic setting of the Ahlmannryggen Group sedimentary basin at the time of deposition.

1.4.1 Geochemical Discrimination

Bhatia (1983) followed a simplified plate tectonic classification of continental margins and oceanic basins based on the nature of the crust, and recognised four different tectonic settings from variations in sediment geochemistry:

- oceanic island arc,
- continental island arc,
- active continental margin and,
- passive margins

The Ahlmannryggen Group sandstones often show a wide scatter when plotted on Bhatia's (1983) discrimination diagrams (Figure 1.8a-d). Samples plot within all four tectonic fields defined by Bhatia, however most points concentrate within the continental island arc, the active continental margin and, to a lesser extent, the passive margin fields. Rare points falling within the oceanic island arc field generally correspond to heavy mineral enriched samples. Plots involving Al_2O_3/SiO_2, TiO_2 and $Al_2O_3/(CaO+Na_2O)$ appear to be the most consistent at classifying the Ahlmannryggen Group sandstones. Unfortunately the K_2O/Na_2O vs Fe_2O_3+MgO scheme is not effective at discriminating tectonic setting as the samples exhibit a highly variable K_2O/Na_2O ratio and generally plot as outliers. This may indicate chemical mobility of elements Na and K.

Roser and Korsch (1986) established a tectonic discrimination scheme for sandstone-mudstone suites using SiO_2 content and K_2O/Na_2O ratios. Three broad categories are recognised in this scheme:

- passive continental margin,
- active continental margins and,
- oceanic island arc

The application of Roser and Korsch's (1986) discrimination scheme to the Ahlmannryggen Group samples is undertaken with caution due to the possible chemical mobility of elements K and Na. The sandstone samples are predominantly confined to the active continental margin field, with outliers extending into the passive margin field (Figure 1.8e). Fine-grained samples exhibit an elevated K_2O/Na_2O ratio relative to the sandstone samples, and trend across both the passive margin and active continental margin fields.

Trace element characteristics were used by Bhatia and Crook (1986) in order to establish a tectonic setting discrimination scheme for greywackes, recognising the same four tectonic settings as Bhatia (1983). They record a systematic increase in the light rare earth elements (La, Ce, Nd), Th, Nb and the Ba/Sr, Rb/Sr, La/Y and Ni/Co ratios and a decrease in V, Sc, and the Ba/Rb, K/Th and K/U ratios in greywackes from oceanic island arc to continental island arc to active continental margin to passive margin settings.

Samples plot within all fields defined on the La-Th-Sc ternary discrimination diagram, with the greatest concentration occurring within the continental island arc field (Figure 1.8f). A wide scatter is also exhibited on the Th versus La discrimination diagram, with samples again plotting in all fields, however the majority of samples cluster near the continental island arc field (Figure 1.8g). The Th-Sc-Zr/10 ternary diagram appears to be the most effective trace element based discrimination scheme. Almost all samples fall within the defined fields, with tight clusters being recorded in the continental island

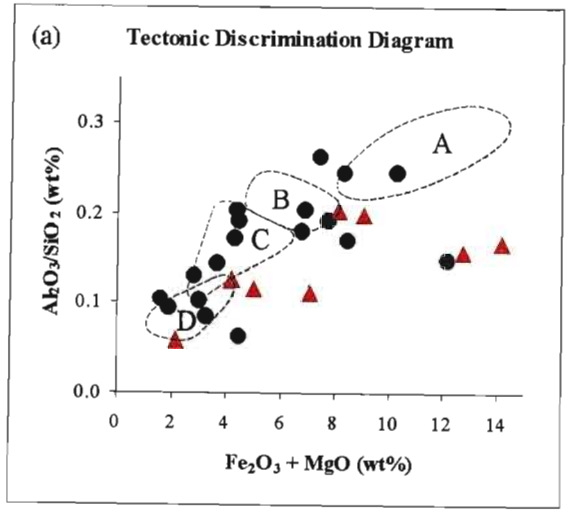
(a) Tectonic Discrimination Diagram
Al2O3/SiO2 (wt%)
Fe2O3 + MgO (wt%)
A
B
C
D

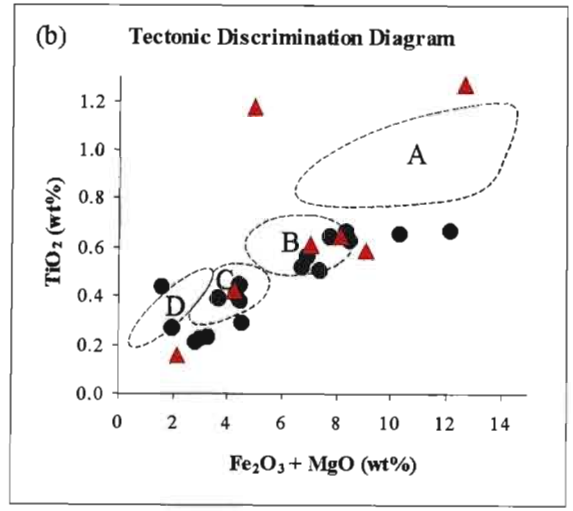
(b) Tectonic Discrimination Diagram
TiO2 (wt%)
Fe2O3 + MgO (wt%)
A
B
C
D

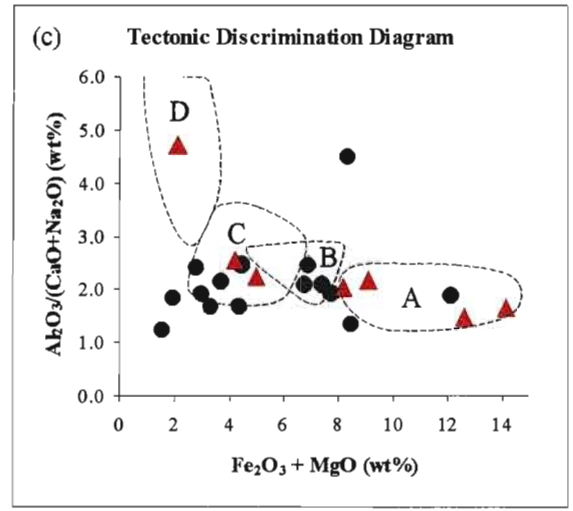
(c) Tectonic Discrimination Diagram
Al2O3/(CaO+Na2O) (wt%)
Fe2O3 + MgO (wt%)
A
B
C
D

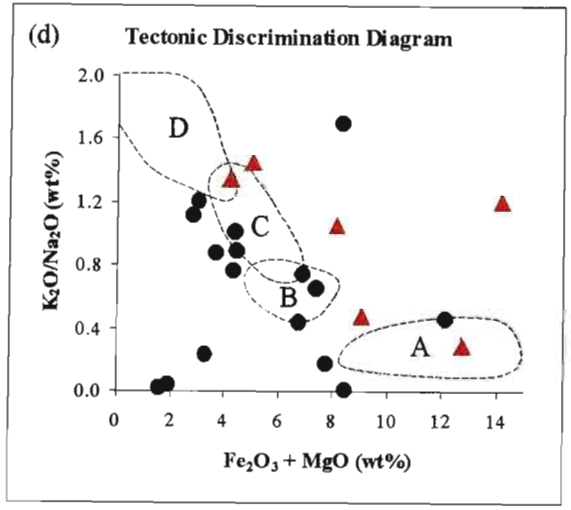
(d) Tectonic Discrimination Diagram
K2O/Na2O (wt%)
Fe2O3 + MgO (wt%)
A
B
C
D

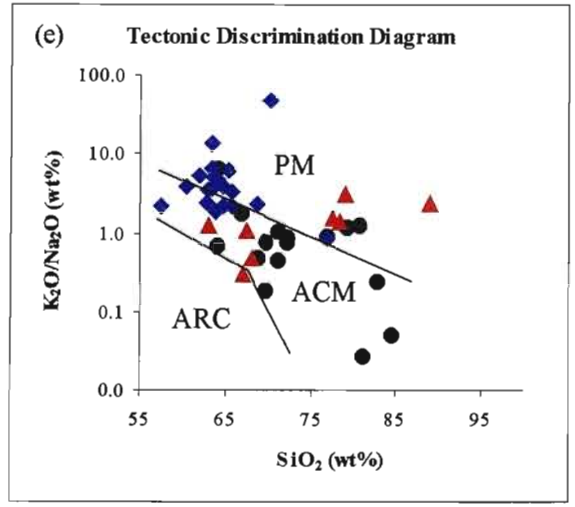
(e) Tectonic Discrimination Diagram
K2O/Na2O (wt%)
SiO2 (wt%)
PM
ACM
ARC

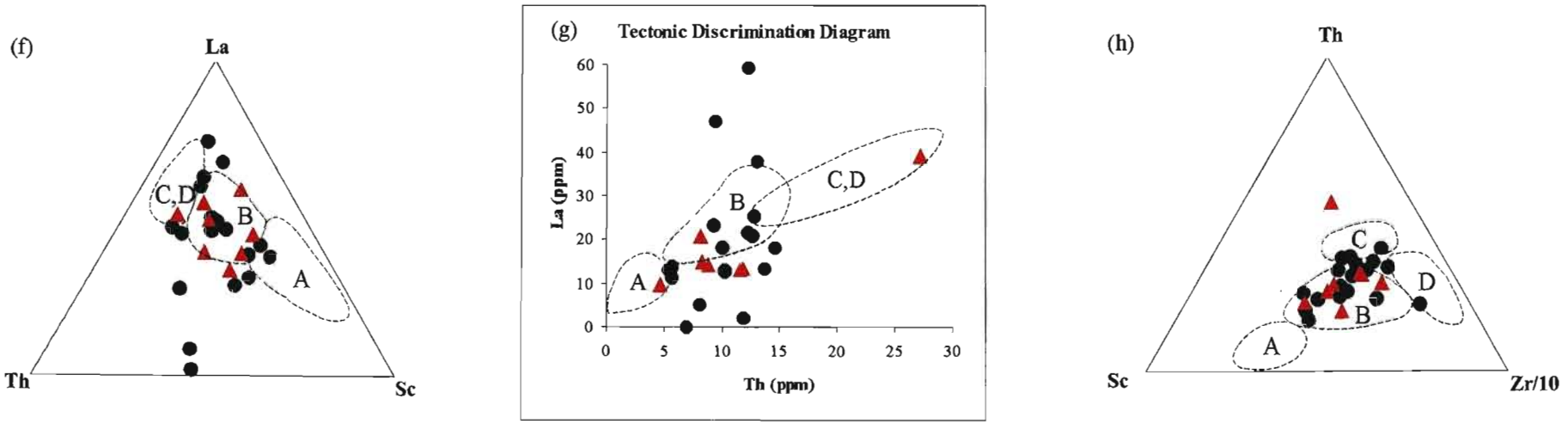

Figure 1.8: (a-d) Major element tectonic discrimination for the Ahlmannryggen Group using tectonic fields from Bhatia (1983). A=oceanic island arc, B=continental island arc, C=active continental margin, D=passive margin. Sandstone samples exhibit some scatter on these diagram, however continental island arc, active continental margin, and to a lesser extent, passive margin geochemical signature appear to dominate. (e) Tectonic discrimination using fields from Roser and Korsch (1986). PM=passive margin, ACM=active continental margin, ARC=oceanic island arc. Samples predominantly plot within the active continental margin field, but also extend into the passive margin field. Results must be interpreted with caution due to the apparent mobility of elements K and Na. (f-h) Trace element tectonic discrimination based on tectonic fields defined by Bhatia and Crook (1986). Field names as for the major element diagrams. Continental island arc and active continental margin geochemical signatures again dominate. (Symbols: solid black dot- sandstone, solid red triangle- heavy mineral enriched sandstone, solid blue diamond- fine grained sample.)

arc and active continental margin fields (Figure 1.8h). Two outliers plot on the boundary with the passive margin field, and a single heavy mineral enriched sample falls outside all defined fields.

Chemical discrimination of the Ahlmannryggen Group sedimentary rocks indicates a predominance of continental island arc and active continental margin signatures, although similarities to passive margin settings are also exhibited. These results are supported by the findings of an integrated petrographic-geochemical approach, outlined below.

1.4.2 Integrated Petrographic/Geochemical Discrimination

Many studies concerned with determining the provenance and tectonic setting of sandstone suites depend on modal analysis of framework grains, but rarely take into consideration the break-down products of unstable mineral grains and lithics (collectively termed pseudomatrix). Cox and Lowe (1996) demonstrate that when the proportion of pseudomatrix exceeds 10%, standard petrographic analysis can lead to incorrect provenance and tectonic setting interpretation. They therefore propose an integrated approach, combining both petrographic and geochemical data in order to construct normative compositions that approximate the original framework grain compositions. As the proportion of pseudomatrix in the Ahlmannryggen Group sandstones regularly exceeds 10% (occasionally reaching ~50%), it was considered unreliable to use petrographic data in isolation for tectonic discrimination, and the integrated approach of Cox and Lowe (1996) was adopted. A brief summary of the method used during the calculation of normative sandstone compositions is provided in Appendix 7, and described in detail by Cox and Lowe (1996).

The re-calculated, normative QtF*L* and QmF*Lt* modes for the Ahlmannryggen Group sandstone samples where incorporated with the tectonic discrimination schemes of Dickinson and Suczek (1979), Dickinson *et al.* (1983) and Dickinson (1985) (Figure 1.9). The majority of the samples fall within the Dissected and Transitional Arc fields, however Transitional Continental, Basement Uplift and Recycled signatures are also present on both the QtF*L* and QmF*Lt* plots. These results are in close agreement with discrimination schemes based wholly on geochemical data, again indicating that both older continental sources and tectonically active, arc dominated terrains supplied detritus to the Ahlmannryggen Group basin.

1.4.3 Isotopic Discrimination

When used in combination with other analytical methods and compared to possible source terrains, isotopic methods may provide some of the most accurate data for constraining the provenance and tectonic setting of a sedimentary succession (McLennan *et al.*, 1993). This aspect of the provenance/tectonic setting study is enhanced by the availability of published Sm/Nd and Rb/Sr isotopic data for the Ahlmannryggen Group.

1.4.3.1 Review of Rb-Sr and Sm-Nd Data

Moyes *et al.* (1995a) performed isotopic analysis of 11 samples from the Ahlmannryggen Group. A summary of the resulting Rb-Sr and Sm-Nd data is given in Table 1.3, along with the results of calculations performed as part of this study.

According to Moyes *et al.* (1995a), the samples scatter (MSWD=27) about a line equivalent to an age of 1085 ±27Ma, with an initial $^{87}Sr/^{86}Sr$ (R_o) = 0.70910 ($\varepsilon Sr = 81$). Given the statistical scatter evident in the MSWD value, they urge caution in the geological interpretation of this radiometric date, which may indicate that the samples do not form a homogeneous suite. The interpretation of isotopic data from sedimentary rocks requires caution as isotopic homogenisation is not guaranteed at the time of deposition, and may result from later processes (e.g. diagenesis, metamorphism).

The Sr T_{CHUR} model age averages 1129Ma, and is regarded as important as it approaches the radiometric dates defined by both the Rb-Sr and Sm-Nd data. McCulloch and Wasserberg (1978) demonstrated that in sediments, the Nd T_{CHUR} age is commonly much older than the Sr T_{CHUR} age, and concluded that the latter approaches the time of deposition or diagenesis of a sediment. Moyes *et al.* (1995a) therefore regard the Sr T_{CHUR} average age of 1129Ma as indicative of the depositional age of the Ahlmannryggen Group. The ~1080Ma average of the Rb-Sr and Sm-Nd dates is interpreted as an approximation of a consolidation or lithification age.

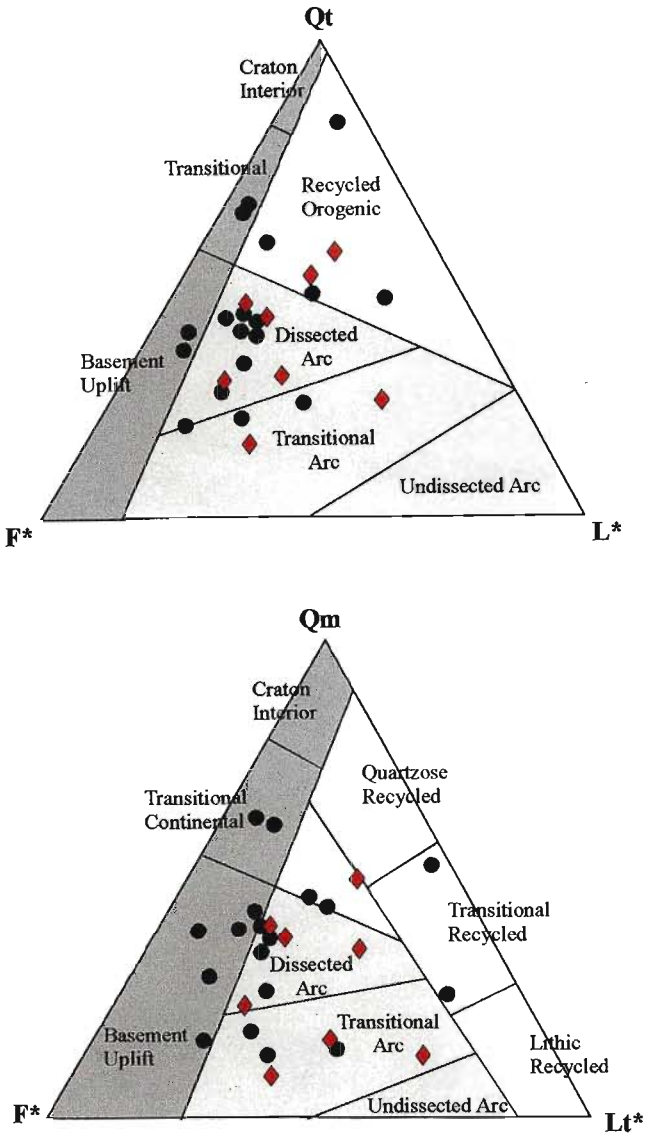

Figure 1.9: Calculated normative QtF*L* and QmF*Lt* plots for the Ahlmannryggen Group sandstone samples, after the methods of Cox and Lowe (1996) - see Appendix 7. The compositional field names and boundaries are after Dickinson (1985). A strong Transitional to Dissected Arc signature is present, however samples also plot within the Transitional Continental, Basement Uplift and Recycled fields. These results suggest that in addition to the dominant arc source terrain, detritus entering the Ahlmann-ryggen Group basin was also sourced from older continental terrains. This is in agreement with the results of the geochemical tectonic setting and provenance discrimination schemes, which also suggest the presence of multiple source terrains, including both stable continental provenances and tectonically active, volcanic arc sources. Black dots- sandstones, red triangles- heavy mineral enriched sandstones.

Table 1.3: Rb-Sr and Sm-Nd isotopic data from the Ahlmannryggen Group (from Moyes *et al*., 1995) along with εNd and *f* Sm/Nd values calculated as part of this study.

Sample	Rb	Sr	$^{87}Rb/^{86}Sr$	$^{87}Sr/^{86}Sr$	σ±2	Sm	Nd	$^{147}Sm/^{144}Nd$	$^{143}Nd/^{144}/Nd$	σ±2	εNd	*f* Sm/Nd
GS1/86	58	7.5	23.3	1.05752	2	7.69	35.1	0.133	0.51184	1	-6.37	-0.32
GS2/86	170.6	10.1	52.6	1.51095	4	5.63	28	0.121	0.51173	1	-6.78	-0.38
GS3/86	103.5	13	23.9	1.06528	2	5.7	31	0.111	0.51164	1	-7.09	-0.44
GS4/86	77.2	48.8	4.61	0.78956	1	5.88	31.7	0.112	0.51166	1	-6.84	-0.43
GS5/86	187.6	10.4	56.6	1.57505	2	9.01	48.2	0.113	0.51165	1	-7.18	-0.43
GS6/86	147.4	27.3	16	0.95767	1	4.1	20.5	0.121	0.51176	1	-6.19	-0.38
GS7/86	82.7	89	2.7	0.74947	2	6.64	36.2	0.111	0.51164	1	-7.09	-0.44
GS8/96	124.6	34.8	10.5	0.86803	2	4.74	24.4	0.117	0.51171	1	-6.59	-0.41
GS9/86	116	34.9	10	0.86061	3	4.62	23.7	0.118	0.51174	1	-6.15	-0.40
GS10/86	128.4	63	5.96	0.80650	4	5.19	26.4	0.119	0.51169	1	-7.27	-0.40
G43b/82	67.1	439.9	0.44	0.71582	1	11.6	63.7	0.110	0.51171	2	-5.57	-0.44

Rb-Sr Results

MSWD: 27
Age: 1085 ±27 Ma
R_o: 0.70909 ±45
ε: 81
Ave T_{CHUR}: 1129
Ave T_{dm} : 1136

Sm-Nd Results

MSWD: 1.4
Age: 1180 ±367 Ma
R_o: 0.51080 ±14
ε: -6.3
Ave T_{CHUR}: 1808
Ave T_{dm} : 2171

The significantly older Nd T_{CHUR} age of ~1808Ma is regarded as being indicative of the average age of the crust from which the sediments were sourced (assuming a bulk earth composition). However, if the crust was derived from depleted sources, the Nd T_{dm} age of ~2171Ma may be a closer approximation of the time of crust formation (Moyes *et al.*, 1995a).

1.4.3.2 Provenance/Tectonic Setting Implications

As outlined by McLennan *et al.* (1993), the influence of the isotopic and bulk composition of a provenance terrain can be summarised on a diagram of εNd versus Th/Sc. The εNd value represents deviations of the $^{143}Nd/^{144}Nd$ ratio, in parts per 10^4, from average chondritic meteorites-representative of the bulk earth, while the Th/Sc ratio is a convenient and sensitive index of bulk composition (Taylor and McLennan, 1985). Th is a relatively incompatible element in most igneous processes, whereas Sc behaves compatibly, and both appear to be transported in the terrigenous component during sedimentary processes. The plot in Figure 1.10 includes samples from the Ahlmannryggen Group (from Moyes *et al.*, 1995a), and published modern turbidite samples (McLennan *et al.*, 1993) from trailing edge, active margin and Andean Foreland settings. As no Th/Sc ratios were published for the samples analysed by Moyes *et al.* (1995a), values were obtained by averaging abundances from samples of similar lithologies and stratigraphic positions.

The main features of such a diagram are highlighted by McLennan *et al.* (1993): Samples from active margin settings tend to exhibit higher εNd values (reflecting young provenance components) and highly variable and commonly low Th/Sc ratios (reflecting heterogeneous and generally less differentiated provenance). In contrast, samples from trailing edge settings, sourced predominantly from older provenances, generally have lower εNd values and very uniform Th/Sc ratios of about 1.0, the value of the upper crust (Taylor and McLennan, 1985). The extension of the Andean Foreland samples (interpreted to be derived from Palaeozoic to Mesozoic upper crust) towards higher Th/Sc values is likely related to heavy mineral enrichments (McLennan *et al.*, 1993).

McLennan *et al.* (1993) also outlined a comparable approach using only Nd-isotopic data – an $f^{Sm/Nd}$ versus εNd diagram. The value $f^{Sm/Nd}$ represents the fractional deviation of the $^{147}Sm/^{144}Nd$ ratio from that in chondritic meteorites ($f^{Sm/Nd} = [^{147}Sm/^{144}Nd]_{sample}/[^{146}Sm/^{144}Nd]_{chondrite} - 1$). Since REE patterns tend to become more LREE enriched (i.e. lower Sm/Nd ratios) during igneous differentiation processes, $f^{Sm/Nd}$ monitors the general extent of differentiation, although in a far less sensitive manner than the Th/Sc ratio. Figure 1.11 contains a plot of $f^{Sm/Nd}$ versus εNd for the Ahlmannryggen Group samples (based on data from Moyes *et al.*, 1995a) as well as modern turbidites from both trailing edge and active margin settings, and Andean Foreland samples (McLennan *et al.*, 1993).

On both these plots, the Ahlmannryggen Group samples tend to cluster between the arc and old upper crust fields, but appear to be more closely associated with the latter. This supports earlier interpretations, based on petrological and geochemical data, that the Ahlmannryggen Group was sourced from a mix of tectonic terrains, consisting of both upper crustal and arc sources.

1.5 CONCLUSION

The Ahlmannryggen Group sedimentary rocks were evidently derived from a combination of provenance terrains. Cratonic sources included granitic basement exposures (the Annandagstoppane granites) supplemented by recycled sediment - a combination responsible for the active continental to passive margin tectonic signatures observed. An actively colliding magmatic arc system (represented by the Maudheim Province) supplied volcaniclastic and, to a lesser extent, metamorphic input - imparting an additional, continental island arc, tectonic signature.

This combination of tectonic signatures suggests the Ahlmannryggen Group sedimentary rocks were deposited in a foreland basin that developed along the edge of the Grunehogna Province and received input from both the stable craton and the accreting island arc terrain. Similar mixed cratonic and volcanic arc/fold-belt sources have been documented from a number of foreland basins (e.g. Meckel, 1967; Jones, 1972; Graham

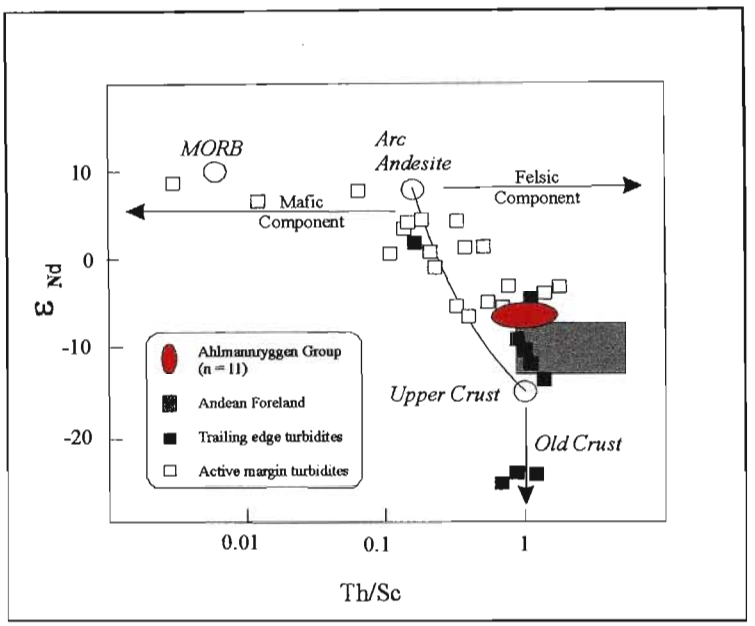

Figure 1.10: Plot of εNd vs Th/Sc ratio for the Ahlmannryggen Group and published examples from trailing edge and active continental settings as well as Andean Foreland settings (McLennan *et al.*, 1993). McLennan *et al.* (1993) indicate that the Nd isotopic composition is strongly controlled by the mean provenance age, while the Th/Sc ratio is sensitive to the bulk composition of the provenance. The Ahlmannryggen Group plots between the Arc Andesite and Upper Crust fields, suggesting detritus was sourced from both old continental crust and tectonically active terrains.

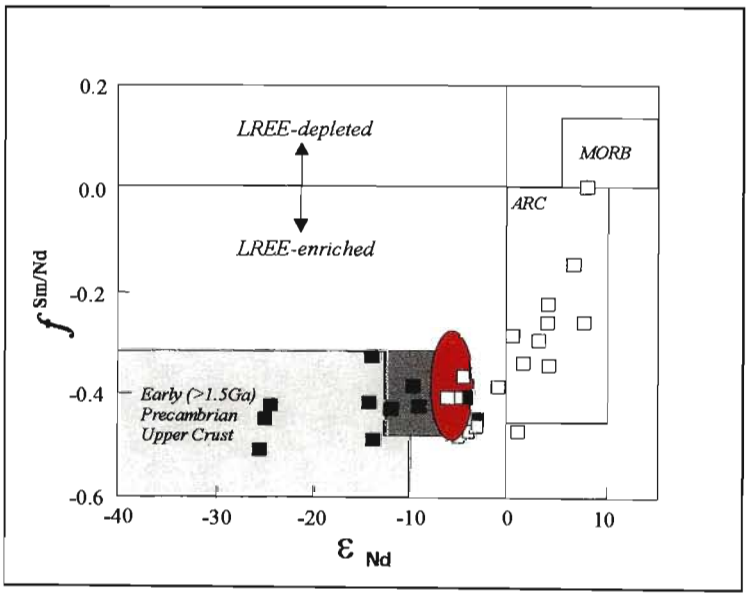

Figure 1.11: A plot of *f* Sm/Nd vs εNd for the Ahlmannryggen Group, turbidites from trailing edge and active margin settings and Andean Foreland samples (McLennan *et al.*, 1993). The Ahlmannryggen Group samples again fall between the Arc and Upper Crust fields, suggesting a mix of different provenance terrains. (Symbols as for Figure 1.10.)

et al., 1976; Heller *et al.*, 1988; Lopez Gamundi *et al.*, 1990; Baker *et al.*, 1993; Cowan, 1993; Colquhoun *et al.*, 1999). The nature and tectonic evolution of the basin are considered in greater detail in Section D:1 – Basin Evolution, where sedimentological, provenance and geo-chronological data are combined in a comprehensive model.

2. AGE OF THE AHLMANNRYGGEN GROUP & SOURCE TERRAINS

2.1 MINERAL ISOTOPE CHEMISTRY

In order to constrain the age of the Ahlmannryggen Group, two volcaniclastic layers were sampled specifically for zircon separation. These volcaniclastic units originated as air-fall deposits from a contemporaneously active volcanic terrain, and represent an opportunity to accurately constrain the maximum age of the Ahlmannryggen Group.

The first sample (B.VE.1) was taken from a fine-grained, light green coloured, pyroclastic horizon in the Framryggen Formation, exposed at Veten Nunatak. The sample has been strongly epidotised, and microscopically consists of an interlocking mosaic of silica and epidote, with the epidote occasionally occurring as distinctly rectangular patches (possibly representing altered feldspar or lithic fragments). Abundant devitrified, shard-like volcanic glass fragments suggest a volcanic origin. The second sample was taken from a welded tuff in the Bråpiggen Formation, exposed at Bråpiggen Nunatak. This prominent light green coloured unit consists of inclusions of crystals and rock fragments disseminated in a groundmass of glass shards and volcanic ash, which has been heavily epidotised.

Small euhedral zircon grains occur within both samples, and were extracted for radiogenic isotope analysis. The euhedral nature of these zircon grains is interpreted as reflecting a magmatic origin, while the small size is attributed to the effects of air-borne transport. The crystallisation age of the zircons is regarded as representing a close approximation of when sedimentation was occurring in the Ahlmannryggen basin.

U-Pb isotopic analysis was performed on four zircon grains from each sample by Prof. Frimmel at the University of Cape Town, Department of Geological Sciences, using conventional zircon dissolution techniques. Unfortunately, the small size of the zircons (they are at the limit of what is possible in single grain dating) has led to relatively large errors in the age data (Table 2.1; Figure 2.1a,b). The zircons analysed are all very close to concordant, inspiring confidence in the geological relevance of the ages, but unfortunately this does not provide for small errors on the isochron ages. The ages obtained from both samples are indistinguishable at 1130Ma and 1131Ma, with a 2σ error of ~7 Ma for both.

These results are in close agreement with those of Moyes and Harris (1996), who determined a 1136 ±2Ma age (based on ^{207}Pb-^{206}Pb evaporative zircon data) for volcaniclastics in the Bråpiggen Formation. Considering that the tuffaceous units show very little evidence of reworking, these results are interpreted as closely approximating the depositional age of the Ahlmannryggen Group. A *ca.* 1130Ma maximum age for the Ahlmannryggen Group is also supported by the ~1129 Ma depositional age proposed by Moyes *et al.* (1995a), based on Sr T_{CHUR} model data.

2.2 DETRITAL ZIRCON SHRIMP ANALYSIS

To further understand the provenance of the Ahlmannryggen Group, U/Pb Sensitive High Resolution Ion MicroProbe (SHRIMP) analysis of detrital zircons was undertaken. Zircon is an abundant trace mineral, predominantly formed in felsic-intermediate igneous rocks and high-grade metamorphic terrains, and its presence in sediments reflects the presence of such rocks in their ultimate source (Morton *et al.*, 1996). However, the well documented 'endurance' of zircon also means that older geological events, possible with no direct contribution to the sediment under investigation, may also be recorded in a sample (Sircombe, 1999). Measurement of zircon ages has been rendered simple and fast with the advent of the SHRIMP at the Australian National University. This method was applied to measure the ages of detrital zircon grains in the Ahlmannryggen Group. The zircon age spectra provide direct information about the origin of these sediments, and allow choice between the possible interpretations made during earlier petrographic and geochemical provenance studies.

The three samples selected for zircon extraction all consisted of medium-grained, moderately

Table 2.1: U-Pb isotopic data for single zircon grains from volcaniclastic layers in the Ahlmannryggen Group.

Sample	Wt (mg)	Conc. (ppm)			Atomic Ratios									Age (Ma)[c]			
		U	Th	Pb	$^{206}Pb/^{204}Pb$[a]	$^{206}Pb/^{238}U$[b]	2σ (%)	$^{207}Pb/^{235}U$[b]	2σ (%)	$^{207}Pb/^{206}Pb$[b]	2σ (%)	$^{208}Pb/^{232}Th$[b]	2σ (%)	$^{206}Pb/^{238}U$	$^{207}Pb/^{235}U$	$^{207}Pb/^{206}Pb$	$^{208}Pb/^{232}Th$
B.VE.1																	
#1	0.0013	104.3	102.1	23.39	223.5	0.18221	2.06	1.929	2.4	0.07678	1.13	0.02697	2.93	1079	1091	1115±23	538
#2	0.0016	114.6	56.3	38.21	99.71	0.19459	1.27	2.0829	1.57	0.07764	0.67	0.0616	2.39	1146	1143	1138±13	1209
#3	0.0007	99.7	52.7	25.67	108.76	0.17257	3.94	1.8284	4.16	0.07684	1.12	0.05362	6.05	1026	1056	1117±22	1056
#4	0.0015	106.1	46	22.69	382.54	0.19219	1.72	2.0482	1.78	0.07729	0.35	0.0572	2.97	1133	1132	1129±7	1124
B.BP.3																	
#1	0.0017	115.8	63.3	25.76	365.64	0.19024	1.43	2.0217	1.56	0.07707	0.56	0.05724	2.12	1123	1123	1123±11	1125
#2	0.0013	161.3	68	33.48	568.27	0.19302	1.33	2.0662	1.39	0.07764	0.37	0.0567	2.36	1138	1138	1138±7	1115
#3	0.0012	236.6	103	49.24	642.43	0.19267	1	2.0591	1.07	0.07751	0.34	0.05437	1.74	1136	1135	1134±7	1070
#4	0.0024	142.8	67.1	30.19	853.62	0.19594	0.85	2.0937	0.92	0.0775	0.31	0.05778	1.37	1154	1147	1134±6	1135

Decay constants: 238U = 1.55125 x10-10 yr-1; 235U = 9.8485 x10-10 yr-1; 232Th = 4.9475 x10-11 yr-1; 238U/235U = 137.88.

[a]Corrected for spike and fractionation only.

[b]Corrected for 3pg of blank Pb.

[c]Age errors are given at 95% confidence level.

Common Pb is assumed to have a Stacey and Kramers (1975) 1130 Ma model isotopic composition.

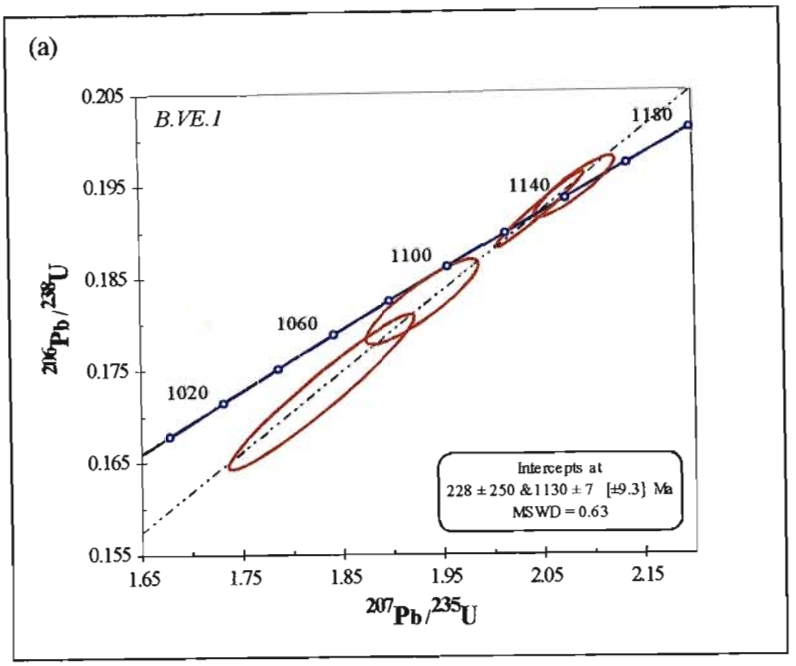

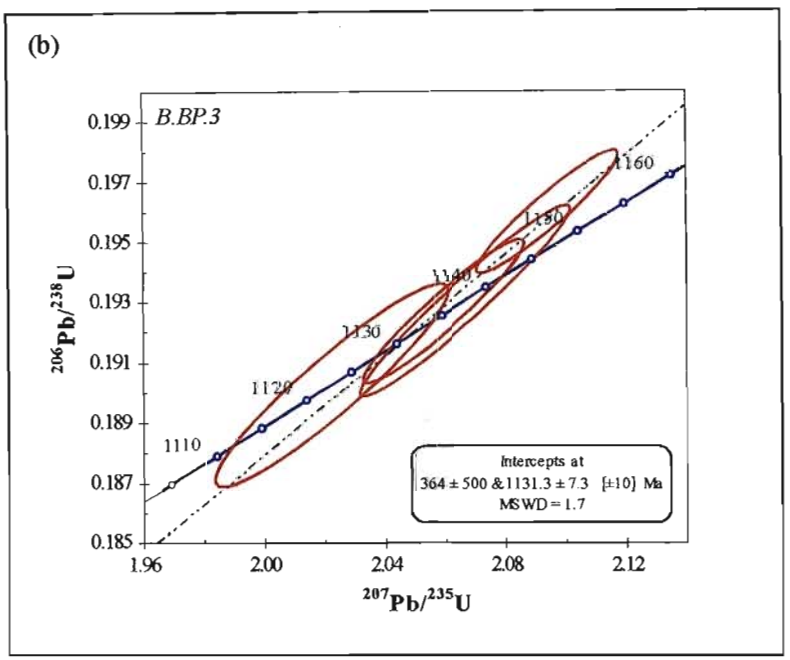

Figure 2.1: $^{206}Pb/^{238}U$ versus $^{207}Pb/^{235}U$ concordia diagrams based on conventional zircon dissolution analysis of zircon grains from two pyroclastic layers in the Ahlmannryggen Group. The results are all close to concordant, inspiring confidence in the data, however the small grain size has resulted in relatively large errors. The ages obtained from both samples are indistinguishable at ~1130Ma and 1131 Ma.

sorted sandstone with distinct heavy mineral laminae. These samples were chosen in order to obtain data sets representative of the dominant transverse and longitudinal drainage systems recorded in the Ahlmannryggen Group, in order to aid the placement of geographic constrains on source terrain distribution. Sample A.GH.5 was taken from the Grunehogna Formation in the Ahlmannryggen region, which is dominated by a well constrained, unidirectional palaeocurrent to the southeast. Samples B.HF.6 and B.MA.4 were obtained from similar stratigraphic positions in the Borgmassivet region, and are representative of the Högfonna Formation, which records dominantly east-northeasterly palaeocurrent orientations.

Following normal extraction procedures, zircon grains were mounted in epoxy, polished until approximately sectioned in half, photographed, cleaned and gold coated for maximum surface conductivity. Chips of standard zircon AS3 and SL13 were mounted near the samples. To maximise the data production rate, the number of mass scans per analysis was reduced to four, from the more typical six to seven. While this sacrifices some precision, the age uncertainties remain sufficiently small (typically ±20 Ma (2σ) depending on U content and common Pb corrections) for correlation with potential source terrains.

Identification of sediment source terrains from detrital zircon ages depends on probability and sampling statistics. It is essential that a statistically meaningful quantity of data is obtained, so there is a reasonable chance that all terrain components appear in the detrital age spectrum (Morton *et al.*, 1996). The approach also requires elimination of operator choice, which can introduce bias when selecting grain for dating; analysis must be random for the population to be representative. Both these requirements are readily met by the SHRIMP technique. Analysis by this method is rapid, and a data acquisition rate of approximately 80 analyses per 24 hr was employed, making a large data set available in a short time. Random sampling was achieved by mounting a randomly selected population of zircons from each sample on an epoxy mount in straight lines. Probing began at one end of the line and proceeded on every grain, eliminating subjective operator choice, until 'sufficient' grains were dated. Operator intervention was limited to selecting the optically most pristine part of each grain to optimise the acquisition of reliable concordant ages from grains which are partially altered or have inclusions. The test of statistical sufficiency is the probability of completely missing an important provenance component in the sediment (Dodson *et al.*, 1988). If a 95% confidence level is accepted, then dating only 10 grains can leave a component as important as a quarter of the sample undetected. Dating 50 grains reducing the importance of any undetected component to less than 6% of the sample spectrum (Morton *et al.*, 1996). A minimum of 50 analyses were therefore conducted on each sample.

The resulting radiogenic zircon compositions are recorded on Wetherill U-Pb concordia diagrams, and as cumulative probability and histogram plots. The concordia diagrams assist interpretation of the original age of each zircon by showing whether grains have closed isotopic systems (in which case calculated ages are reliable), or have leaked Pb since crystallisation (in which case ages are model dependent and are less reliable). The mixture modelling technique of Sambridge and Compston (1994) was used to identify distinct age population groupings in each sample.

2.2.1 Sample A.GH.5

Zircons are moderately abundant in sample A.GH.5, and display considerable variation in colour and transparency, from clear and colourless to pale pink or brown and semi-opaque. Some of the grains exhibit broken edges and are fractured, probably due to pre-analytical sample preparation. The intact zircon grains all tend to be relatively small in size, and average less than 300μm in length. Dark inclusions of variable size and form are common. The zircon crystals vary from euhedral with sharp pyramidal terminations to well rounded and almost spherical with frosted and pitted surfaces caused by abrasion during depositional processes (Figure 2.2a). The euhedral grains invariably display well-developed magmatic compositional zoning, both in transmitted light and with cathodoluminescence (CL) imaging. Magmatic zoning can be distinguished in the vast majority of grains, however CL imaging also reveals complex internal structures and overgrowths in a few grains (e.g. grain 27, Figure 2.2a), which may contain prominent irregular dark patches and embayments truncating magmatic zoning, suggesting a metamorphic origin.

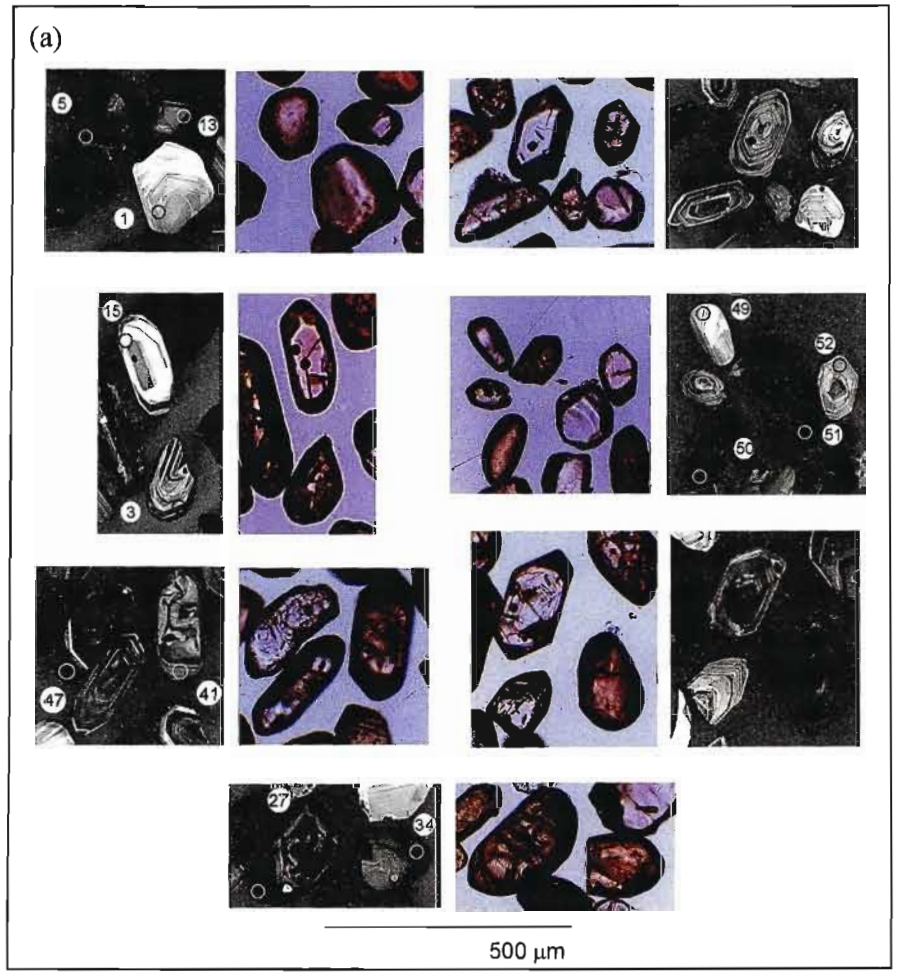

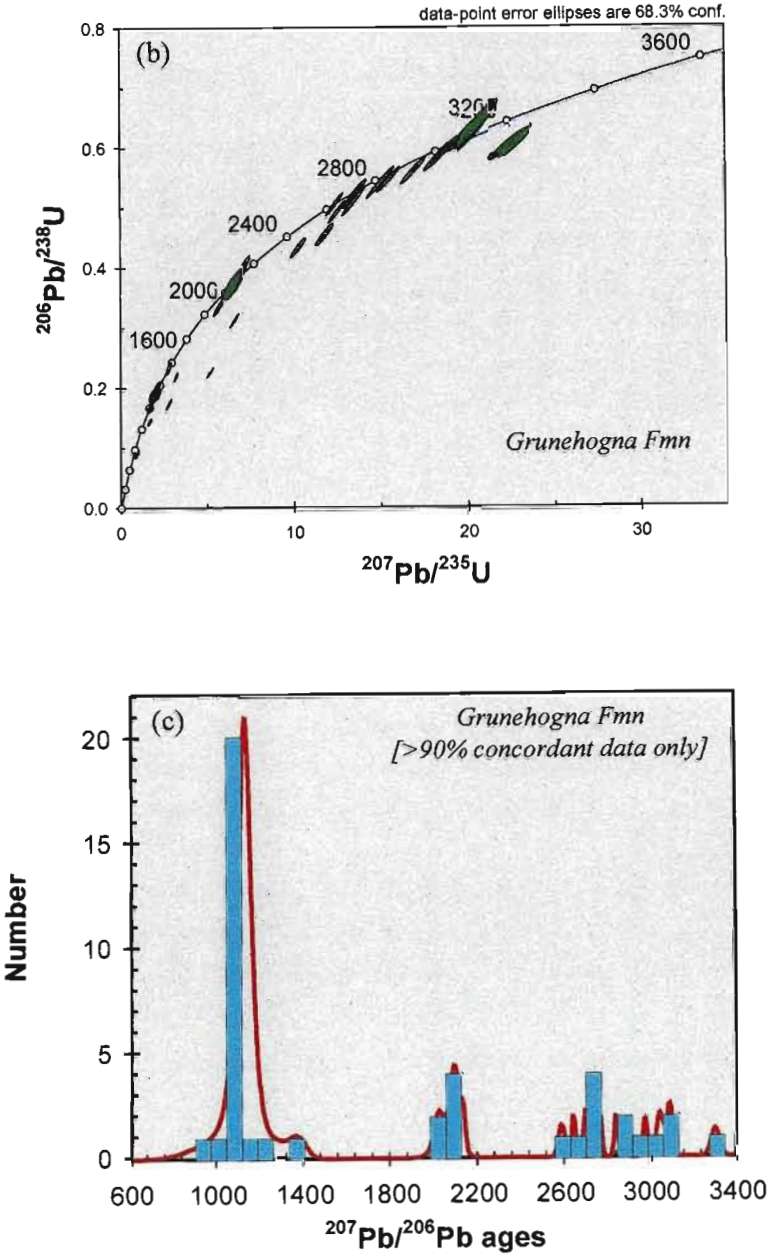

Figure 2.2: (a) Cathodoluminescence and transmitted light images of zircons from A.GH.5. (b) U-Pb concordia plot of all data. (c) Cumulative probability and histrogram plot of data which are more than 90% concordant. Three distinct age populations are present.

Often magmatic and metamorphic zircons can be discriminated using visual criteria (e.g. grain morphologies, identification of core-overgrowth relationships, presence or absence of compositional zoning, resorption etc.), however the U and Th contents of analysed grains can also be diagnostic of a metamorphic origin. Several recent investigations in granulite terrains have noted that high-grade metamorphic zircons and zircon overgrowths are generally characterised by high U contents and low Th/U ratios, and this distinctive chemistry can be used to characterise zircons in the absence of other distinguishing criteria (Williams and Claesson, 1987; Kröner and Williams, 1993; Williams *et al.*, 1996). In addition to the presence of the dark embayments, grain 27 (Figure 2.2a) also exhibits a relatively high U content (> 1200ppm) and a low Th/U ratio (0.04), suggesting that an original magmatic zircon crystal was exposed to high-grade metamorphic conditions. Analysis of the metamorphic embayments in grain 27 yields an apparent $^{207}Pb/^{206}Pb$ age of 1776 ±18Ma, however this age is only 72% concordant, which tends to suggest that it is unreliable as the grain is likely to have experienced Pb-loss and should not be used to precisely constrain the age of the metamorphic event. A second grain (no. 9) exhibiting metamorphic characteristics, including dark embayments, a high U content (739 ppm) and a low Th/U ratio (0.02), provides a $^{207}Pb/^{206}Pb$ age of 2645 ±9Ma. This age is 99% concordant, and can therefore be regarded as geologically significant and indicative of a late Archaean metamorphic episode.

Most of the zircon compositions adhere relatively closely to concordia (Appendix 8, Figure 2.2b), but there is significant Pb-loss in some grains, and more rarely, U-gain. In order to minimise the uncertainty regarding discordant data, a histogram plot of data greater than 90% concordant has been created (Figure 2.2c). Any Pb-leakage will not significantly cloud the age interpretation from these data, and this approach effectively reduces the scatter about populations without altering any of the major age groupings.

It is clear from zircon age histogram data (Figure 2.2c), that three distinct age groupings are present within sample A.GH.5. A Meso-proterozoic grouping forms the dominant age population at 1139 ±11Ma (2σ); zircons falling within this grouping are invariably colourless and preserve fragile euhedral shapes and all exhibit prominent magmatic zonation. A second, subordinate Proterozoic population groups around 2105 ±13Ma; zircons within this age population vary from strongly luminescent (low U, e.g. grains 1 and 49) to dark (high U, e.g. grain 5) in the CL images, sometimes exhibit poorly defined magmatic zonation and are invariably well-rounded. A spread of Archaean ages is also present, extending from ~2600Ma to ~3300Ma. The zircons falling within this age spectrum are all characteristically well rounded, abraded and pitted, and tend to appear pale pink to brown and semi opaque under transmitted light. Both strongly luminescent (e.g. grain 15) and poorly luminescent (e.g. grains 34 and 50) varieties are present, and two separate sub-populations can be tentatively identified. Late Archaean zircons (~2600Ma) often exhibit dark embayments with relatively high U contents and low Th/U, and are possibly of metamorphic origin. Older grains (>2700Ma) tend to contain poorly developed/preserved magmatic zonation and are interpreted as magmatic in origin.

The zircons within sample A.GH.5 provide a record of three distinct magmatic episodes, at ~1139Ma, at ~2105Ma and from ~2700Ma to ~3300Ma. Only the youngest event is interpreted as a primary source for the Ahlmannryggen basin, as the older grains all exhibit a high degree of rounding and pitted/abraded surfaces, suggesting prolonged transport and possibly sedimentary recycling through any number of intermediate repositories. The ~1139Ma population consists exclusively of small euhedral crystals with well preserved pyramidal terminations, indicating a low degree of reworking, and is interpreted as originating from contemporaneous volcanic input. These zircons also form the dominant population in the pyroclastic horizons (where they were used for conventional dating as described earlier), supporting the interpretation of a volcanic origin. A possible metamorphic episode, at ~2600Ma, is also recorded in sample A.GH.5. A second, younger metamorphic event may have occurred sometime later, at ~1770Ma, however the discordant nature of this age renders it unreliable.

2.2.2 Sample B.HF.6

This sample yielded abundant zircons varying in colour and transparency from translucent, through pale pink to turbid brown. The zircons tend to be relatively small in size, and average less than 200μm in length. Slightly elongate,

euhedral grains with well developed crystal faces (and often containing dark inclusions) dominate in sample B.HF.6, although well-rounded, pitted and abraded grains also occur (Figure 2.3a). As seen in sample A.GH.5, some of the grains exhibit broken edges and are fractured, probably due to pre-analytical sample preparation. CL imaging reveals magmatic zoning is ubiquitous, although it is best developed and most distinctive in the euhedral crystals (Figure 2.3a). Unlike in sample A.GH.5, no metamorphic overgrowths/ alterations were conclusively identified in sample B.HF.6.

Sixty grains from sample B.HF.6 were analysed by SHRIMP, and these data are recorded in Appendix 8. Most of the zircon compositions adhere relatively closely to concordia (Figure 2.3b), but there is significant Pb-loss in some grains, and some exhibit U-gain. In order to minimise the uncertainty regarding discordant data, a histogram plot of data greater than 90% concordant has been created (Figure 2.3c).

Four separate zircon age populations can be recognised in sample B.HF.6 through a combination of mixture modelling techniques and graphical representations. The dominant population once again groups around a Mesoproterozoic age, for which a $^{206}Pb/^{207}Pb$ age of 1129 ±9Ma can be calculated. Zircons falling within this age spectrum are invariably euhedral, exhibit well developed zonation and show very little evidence of reworking (e.g. grain 5, Figure 2.3a). As in the previous sample, this population is again interpreted as originating directly from a contemporaneously active volcanic source terrain. Minor populations also occur at ~1600Ma and ~2000Ma, while a spread of Proterozoic to late Archaean ages extends from 2400Ma to 2900Ma. The older zircons are typically rounded to well rounded (sometimes almost spherical) and commonly exhibit pitted and abraded surfaces (e.g. grain 1, Figure 2.3), indicative of sedimentary transport and suggesting possibly recycling through one or more intermediate repositories.

Sample B.HF.6 therefore records four separate magmatic episodes, three of which (at ~1130Ma, ~2000Ma and ~2400Ma-2900Ma) are also recorded in sample A.GH.5. The minor grouping at ~1600Ma suggest the existence of a fourth magmatic episode, which was not identified in the previous sample.

2.2.3 Sample B.MA.4

Zircons in sample B.MA.4 vary from translucent grains, which preserve fragile euhedral shapes, to turbid brown and semi opaque grains with abraded and pitted surfaces (Figure 2.4a). Grain size is typically restricted to a length of 300μm or less and dark inclusions of variable size and form are common. CL imaging reveals that striking concentric zonation (typical of magmatic zircons) dominates, however cross-cutting zones and overgrowths of structureless zircon (probably of metamorphic origin) are also present in some grains (Figure 2.4a). Rare, very narrow (<30μm), strongly luminescent (very low U) metamorphic growth rims are also revealed by CL imaging.

Fifty-two grains from sample B.MA.4 were analysed by SHRIMP, and these data are recorded in Appendix 8. Most of the zircon compositions adhere relatively closely to concordia (Figure 2.4b), but there is significant Pb-loss and in some grains, and more rarely, U-gain. Figure 2.4c contains a histogram plot of data greater than 90% concordant. Five potential $^{207}Pb/^{206}Pb$ zircon age populations are recognised in sample B.MA.4. The majority of the analyses combine to give a mean $^{207}Pb/^{206}Pb$ age of 1137±10Ma, with smaller subsets of the data indicating possible older populations with ages of ~1335Ma, ~1700Ma, ~2100Ma, ~2400Ma to 2700-2800Ma. As in the previous samples, the dominant Mesoproterozoic group is characterised by euhedral zircon crystals with distinct magmatic zonation and lacking evidence of prolonged sedimentary transport (e.g. grain 40, Figure 2.4a). The older populations all exhibit evidence of sedimentary reworking, varying from a slight rounding of the crystal faces, to pronounced rounding of almost spherical grains with pitted and abraded surfaces (Figure 2.4a).

The 1335±15Ma group is characterised by moderately rounded zircon grains in which the magmatic zoning is truncated by prominent irregular dark overgrowths and embayments, suggesting metamorphic alteration of original magmatic crystals (e.g. grain 1, Figure 2.4a). Further evidence for a metamorphic origin of the dark overgrowths is provided by the high U content (occasionally as high as 1731ppm) and low Th/U ratios (as low as 0.06) exhibited by this zircon phase (Williams and Claesson, 1987; Kröner and Williams, 1993; Williams *et al.*, 1996).

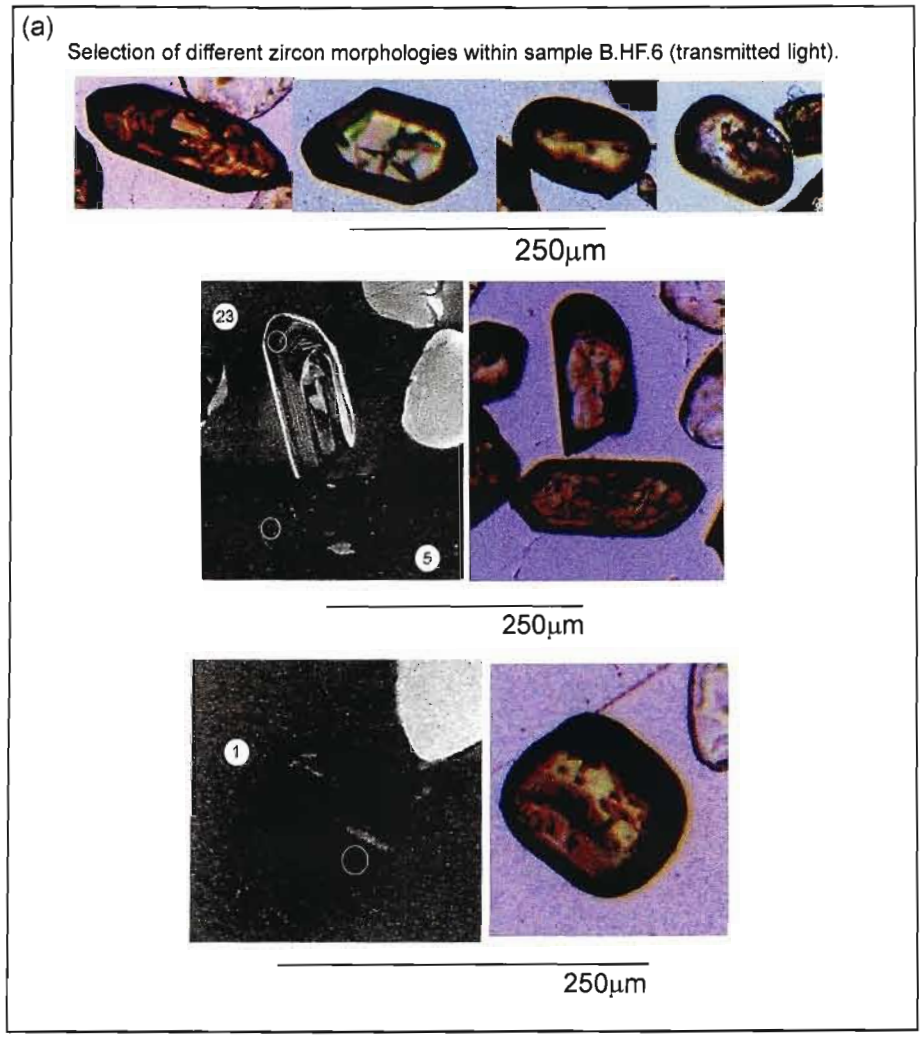

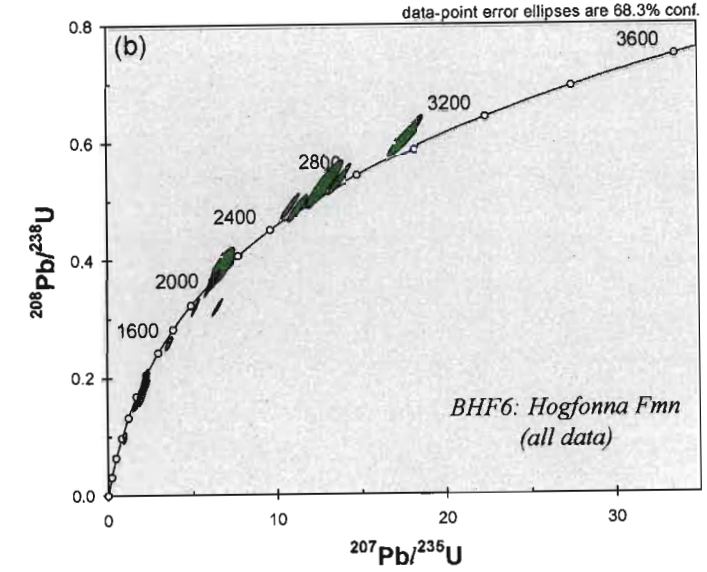

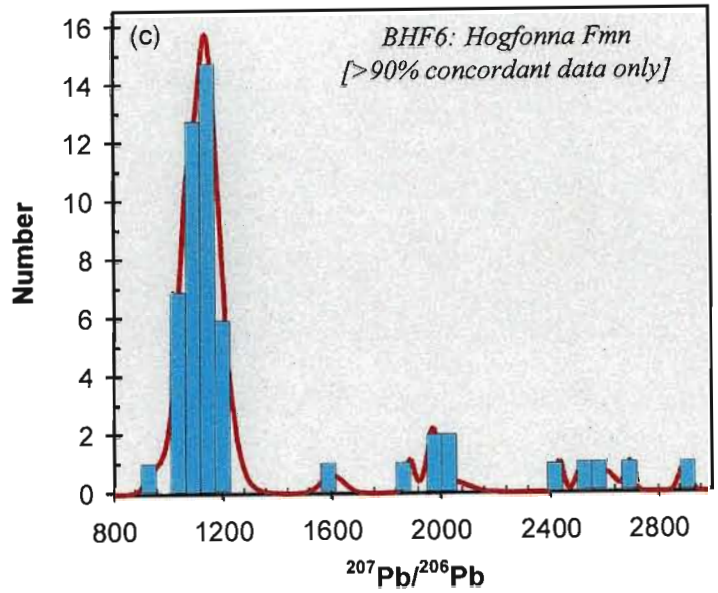

Figure 2.3: (a) Cathodoluminescence and transmitted light images of zircons from B.HF.6. (b) U-Pb concordia plot of all data. (c) Cumulative probability and histogram plot of data which are more than 90% concordant.

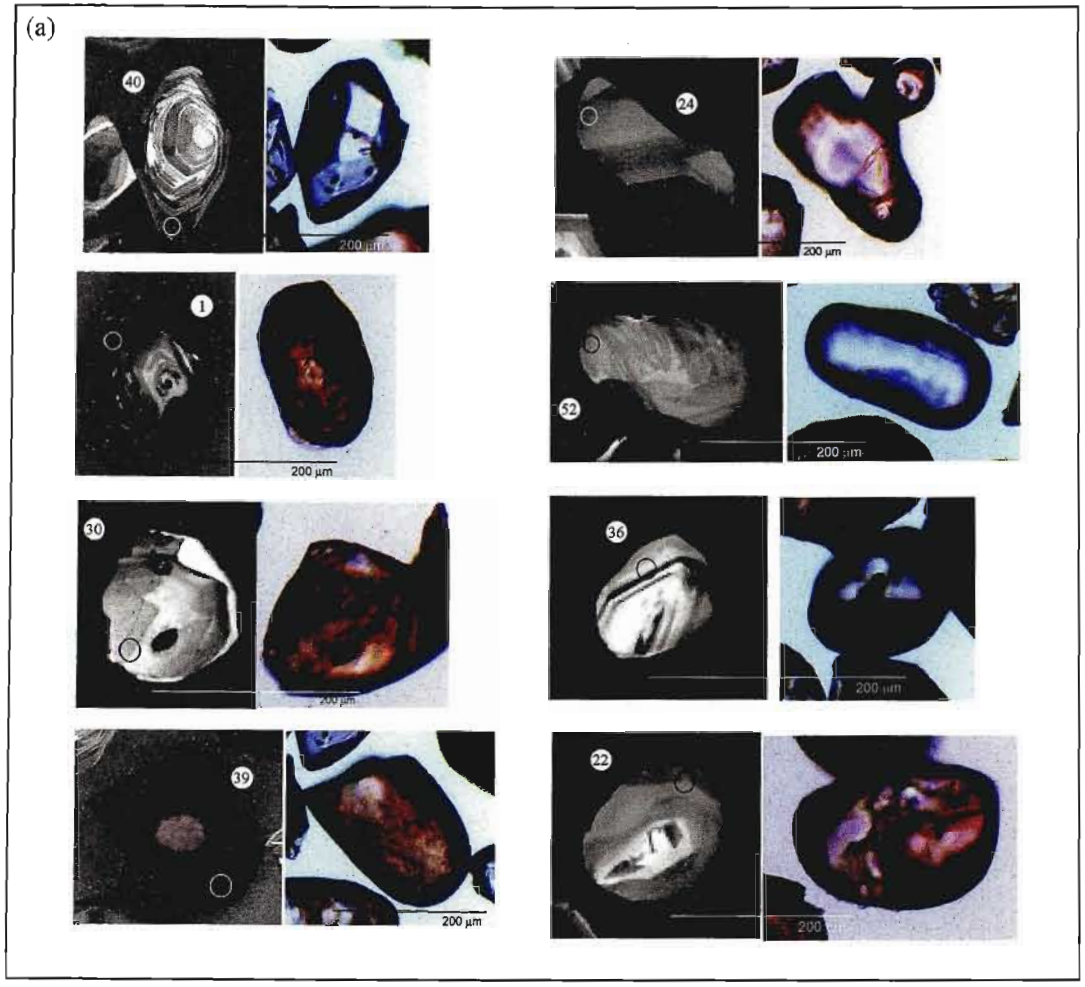

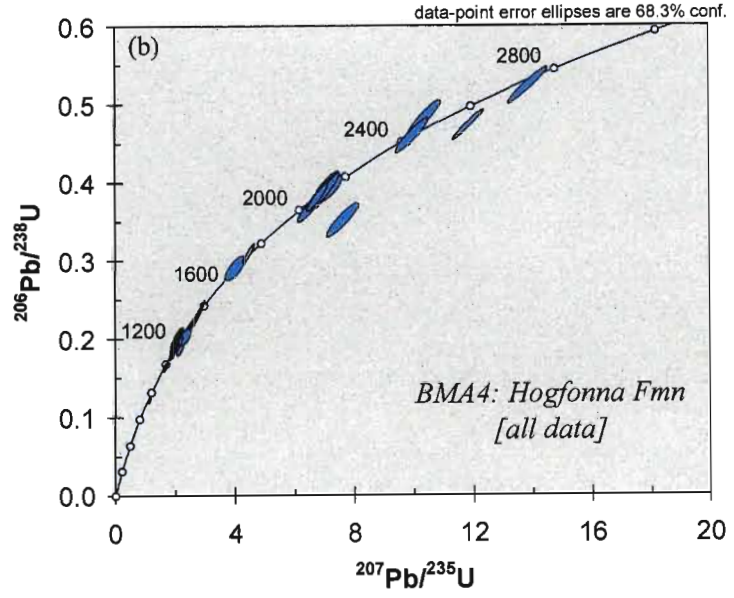

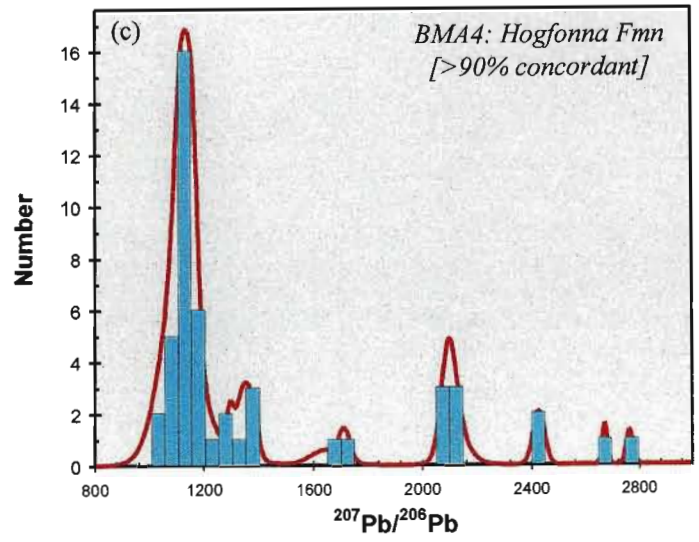

Figure 2.4: (a) Cathodoluminescence and transmitted light images of zircons from B.MA.4. (b) U-Pb concordia plot of all data. (c) Cumulative probability and histogram plot of data which are more than 90% concordant.

The minor grouping around ~1700Ma consists of small rounded zircon grains and fragments exhibiting magmatic zonation. These zircons may be strongly luminescent (low U) and typically preserve a very narrow (<30μm), strongly luminescent (very low U) metamorphic growth rim (e.g. grain 30, Figure 2.4a). These rims most likely reflect new growth or re-crystallisation of low-U metamorphic zircon, however their restricted occurrence within very narrow domains precludes reliable age dating for this phase.

A prominent grouping around ~2100Ma consists entirely of rounded to well rounded grains, often with slightly pitted surfaces, and prominent magmatic zonation (e.g. grains 24 and 52, Figure 2.4a). A scattering of zircon ages falling within the early Proterozoic and late Archaean has resulted in a number of small peaks on the histogram plot (Figure 2.4c) between 2400Ma and 2800Ma. The ~2400Ma age zircons generally consist of moderately to strongly luminescent, well rounded and magmatically zoned crystals (e.g. grains 22 and 36, Figure 2.4a). The older Archaean zircons are very well rounded and occasionally fractured (possibly during sample preparation procedures), but tend to be turbid brown and semi-opaque, inhibiting identification of the internal structure (e.g. grain 39, Figure 2.4a). This suggests that these zircons have suffered a significant degree of radiation damage to the crystal substructure, due to high U concentrations (>600ppm in grain 39). The lack of concentric zonation and elevated U content suggests that these grains may be metamorphic in origin, however the low Th/U ratios typically encountered in high-grade metamorphic zircons, are notably absent. The origin of the older Archaean zircons therefore remains obscure.

Sample B.MA.4 records four magmatic episodes (at ~1137Ma, ~1770Ma, ~2100Ma and 2400Ma-2800Ma), which are also represented in samples A.GH.5 and/or B.HF.6. A previously unidentified metamorphic event, at ~1335Ma is also recorded.

2.2.4 Interpretation of U/Pb SHRIMP Analyses

The U/Pb zircon ages provide important constraints on both the depositional age and the provenance of the Ahlmannryggen Group. The detrital ages recorded in the three samples are presumed to date the crystallisation of felsic igneous rocks and high-grade metamorphic events in the source area, but caution must be exercised as the well rounded and pitted nature of many of the zircon grains is suggestive of sedimentary recycling through intermediate repositories.

2.2.4.1 Depositional Age

The youngest zircon age grouping constrains the maximum depositional age of both the Grunehogna and Högfonna Formations. These groupings are virtually indistinguishable at 1139±11Ma (A.GH.5), 1137±10Ma (B.MA.4) and 1129±9Ma (B.HF.6). The zircon grains falling within this ~1135Ma age spectrum are invariably euhedral with pronounced magmatic zonation, and show no evidence for prolonged sedimentary reworking. These zircon grains are interpreted as originating from direct volcanic input, and are considered to approximate the depositional age of the Grunehogna and Högfonna Formations. This interpretation is supported by the results of the conventional zircon dissolution analysis, which indicates an age of 1130±7Ma for associated volcaniclastic units.

2.2.4.2 Provenance Constraints

Of the seven detrital zircon suites identified in the Ahlmannryggen Group samples, only two can be related to possible source regions presently exposed in WDML:

- the dominant ~1135Ma population closely matches ages determined for arc-related magmatic activity in the adjacent Maudheim Province (~1130Ma) (Arndt *et al.*, 1991; Harris *et al.*, 1995a, 1995b; Jacobs *et al.*, 1996; Jackson, 1997; Jackson and Armstrong, 1997).
- the Archaean grouping of 2700-3300Ma approximates the 2945-3115Ma age of the Annandagstoppane basement granites (Barton *et al.*, 1987).

The five other provenance terrains identified from the detrital zircon age groupings are either no longer preserved, or are obscured by the ice cover. It is therefore necessary to look further afield for possible correlatives. For this purpose, comparisons can be drawn with other Archaean provinces. Given that some researchers consider the Grunehogna Province to have originally been an extension of the Kaapvaal Craton of South Africa prior to Gondwana fragmentation (e.g. Krynauw *et al.*, 1991; Groenewald *et al.*, 1995),

this was considered an appropriate choice. Correlatives to all five 'missing' provenances can be found within the Kaapvaal Craton region:

- the 2400-2900Ma suite of magmatic zircons is comparative in age to the extensive granitic intrusions of the Barberton Mountain Land region and post-Pongola Supergroup intrusions such as the Usushwana Complex (Visser, 1998)
- the minor ~2645Ma metamorphic component corresponds to ~2652Ma metamorphism recorded in the Goudplaats Gneiss (Brandl, 1983), also of the Barberton Mountain Land region.
- the 2000-2100Ma magmatic zircon population approximates the age of the extensive ~2.0Ga Bushveld Igneous Complex (Walraven *et al.*, 1990; Visser, 1998).
- the ~1600-1700Ma spread of magmatic zircon ages corresponds to ~1650Ma intrusive events recorded in the Bushmanland Subprovince of the Namaqua Metamorphic Province (Reid *et al.*, 1987).
- finally, the ~1335Ma metamorphic zircon population corresponds in age to the emplacement of numerous alkali complexes, such as the ~1310Ma Spitskop and Pilanesberg complexes (Visser, 1998).

Based on these zircon age populations, and conventional provenance information presented earlier, it is possible to infer that a cratonic sequence similar to that of the Kaapvaal Craton is present beneath the ice sheets of the Grunehogna Province. This sequence evidently includes Archaean basement granites, Proterozoic intrusive complexes and metamorphic terrains and at least two sedimentary cover sequences (including a banded ironstone association and the Ahlmannryggen Group sequence).

3. STRUCTURAL DEFORMATION IN THE AHLMANNRYGGEN & BORGMASSIVET

3.1 INTRODUCTION

Understanding the post-depositional deformation affecting the Ritscherflya Supergroup provides unique insight into the Palaeozoic tectonic evolution of the Grunehogna Province, and reveals its significance within the regional geological framework of WDML. Compared to the adjacent high-grade metamorphic Maudheim Province, which has been subjected to a number of superimposed deformation events (Groenewald *et al.*, 1995; Grantham *et al.*, 1995), the deformation affecting the Grunehogna Province is apparently mild, and the region is often considered relatively undisturbed or undeformed (e.g. De Ridder, 1970; Grantham and Hunter, 1991; Krynauw, 1996; Moyes *et al.*, 1993). However, investigations of the Ritscherflya Supergroup exposed in the Borgmassivet and Ahlmannryggen regions has revealed that the Grunehogna Province has in fact been subjected to both ductile and brittle deformation.

An often-noted characteristic of the Grunehogna Province is a complete lack of exposed large-scale brittle-deformation structures. Brittle-deformation identified in outcrop tends to consist of small-scale features and visible faults show inconsistent displacements of only a few metres or at the most, a few tens of metres. These small-scale structures are regarded as inadequate when attempting to account for the major offsets that apparently exist between some exposures (Figure 3.1). Due to these offsets, researchers have traditionally inferred the existence of large-scale faults along the distinctive glaciers cross-cutting the area, without providing any further supporting evidence (e.g. Neethling, 1970; De Ridder, 1970; Ferreira, 1986; Wolmarans and Kent, 1982). The lack of an appropriate stratigraphy has in the past complicated the correlation of units across these inferred faults, and attempts to determine offsets and styles of faulting have been highly problematic. Nevertheless, these inferred faults are generally regarded as resulting from the development of grabens during extensional block faulting (de Ridder, 1970; Ferreira, 1986; Swanepoel, 1988; Wolmarans and Kent, 1982; Krynauw *et al.*, 1991). However, there have been no previous attempts to analyse the brittle structures in the rocks in order to justify such an interpretation.

One of the major problems encountered in the Borgmassivet and Ahlmannryggen is the localised juxtapositioning of sedimentary rocks of the Ahlmannryggen Group with volcaniclastic rocks of the overlying Jutulstraumen Group, which had led researchers to propose models incorporating contemporaneous volcanicity and sedimentation (e.g. Wolmarans and Kent, 1982; Watters *et al.*, 1991). It is, however, considered highly unlikely that thick sequences of volcaniclastics could have accumulated as isolated patches in the large-scale fluvial braidplain/braid delta plain complex in which the Ahlmannryggen Group sediments were deposited. In addition, the volcaniclastic outcrops are bound on all sides by glaciers, across which the sills of the Borgmassivet Suite cannot be correlated. It is therefore proposed that the juxtapositioning of these sequences is a direct effect of structural deformation in the region, rather than the formation of isolated volcaniclastic airfall deposits.

In order to constrain the nature of the deformation affecting the Grunehogna Province cover rocks, a detailed examination of the regional fracture pattern exposed in the Borgmassivet and Ahlmannryggen areas was undertaken. Fracture patterns within the Ahlmannryggen Group sediments, Jutulstraumen Group volcaniclastics, Borgmassivet Suite sills and Jurassic dykes were established. This relatively straightforward approach has revealed a complex structural history, and although no precise chronological constraints are placed on the timing of the deformation events, comparisons can be made with well-documented tectonic episodes recorded in adjacent regions, and preliminary conclusions are drawn regarding the most likely timing of the deformation.

The description and interpretation of the Ahlmannryggen Group deformational history draws on Map 1 (rear pocket) which summarises key structural features exposed in the Ahlmannryggen and Borgmassivet regions. Note, all bedding, cleavage, fracture and fault

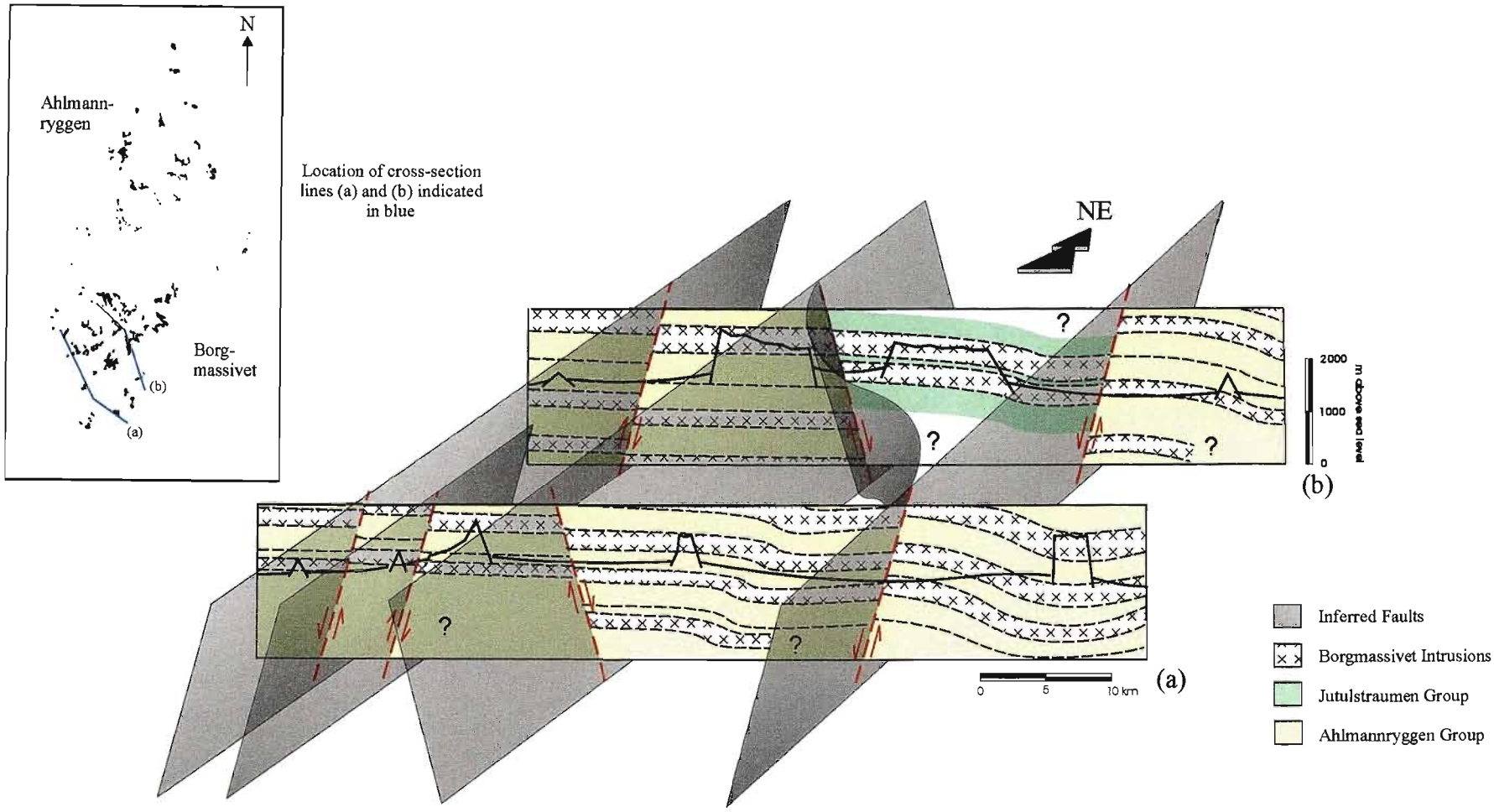

Figure 3.1: Large-scale brittle deformation structures are not exposed in the Grunehogna Province cover rocks, however their existence is inferred along the glaciers cross-cutting the region in order to explain the apparent offset that exists between some groups of nunataks. Previously, a lack of an appropriate stratigraphy for the Ritscherflya Supergroup prevented the determination of the nature and amount of offset across these inferred faults, and most researchers regarded the deformation in the Borgmassivet and Ahlmannryggen regions to be a result of extensional block faulting (e.g. de Ridder, 1970; Ferreira, 1986; Swanepoel, 1988). Detailed analysis of the folding and regional fracture pattern was performed in an attempt to better constrain the nature of the deformation.

orientations are described with reference to strike direction and dip value.

3.2 ANALYSIS

The Grunehogna Province cover rocks are gently folded and intensely fractured, and exhibit a complex regional fracture pattern. However, based on infill characteristics, cross-cutting trends and offset relationships, two distinct generations of fractures can be discriminated. The oldest generation is apparently associated with the folds, while the younger generation cross-cuts and clearly post-dating the folding event. The deformation episodes responsible for the formation of these two fracture generations are designated D_1 and D_2 respectively. Late stage re-activation of many of the fracture sets is attributed to a third event (D_3), which was characterised by extension and normal faulting.

3.2.1 D_1 Event

The earliest deformation recorded in the Grunehogna Province cover rocks is limited to the south-east Borgmassivet, and involved the development of gentle folding and the formation of two separate fracture sets.

3.2.1.1 Folds

Folding of the strata of the Ahlmannryggen and Jutulstraumen Groups, as well as the sills of the Borgmassivet Suite, is recorded in the south-east Borgmassivet, adjacent to the Pencksökket glacier. The extent of the folding is limited to the Huldreslottet-Möteplassen and Skoddemedet-Jokulskarvet ranges, where two synformal structures are exposed (Figure 3.2a, 3.3). Abundant sedimentary way-up indicators clearly indicate an inward younging direction, validating the use of the term 'syncline'.

According to the classification system established by Fleuty (1964), the two synclines can be described as open to gentle, subhorizontal and steeply inclined. They fall between Huddleston's (1973) 1D and 2D classes, based on visual harmonic analysis, and exhibit a wavelength of approximately 15km. The southern syncline is more completely exposed and more accessible than the northern syncline and the nature of the folding in this region is somewhat better constrained. Within the northern syncline, only the north-western limb is preserved to any extent, and access is tricky at the best of times. The northern syncline is also apparently interrupted by faulting, complicating interpretation somewhat. The anticline one would expect to encounter linking the two is entirely absent, and the area between the two mountain ranges is instead occupied by the 8km wide Frostlendet glacier.

The fold forming the southern syncline is characterised by an arcuate axial trace, varying in its trend from east-northeast to north-east. The syncline exhibits a slightly asymmetrical form, with a more steeply dipping north-western limb (up to 56° locally) and a shallowly dipping south-eastern limb (22° or less). The syncline consistently displays a plunge angle of 6°, varying in direction from 258° to 228°. The orientation of the axial plane also exhibits variations along the length of the fold, with the strike direction changing from 236° in the north, to 220° in the south (although the dip remains constant at ~50°). The northern syncline is characterised by a poorly constrained 04°/210° plunging fold axis, which also apparently varies in orientation along its length. Both limbs of the fold are exposed at Högfonna, and yet directly opposite, at Jokulskarvet, only the north-western limb is preserved, implying a change in fold axis orientation. Unfortunately, the restricted outcrop extent and limited nature of the data sets renders the positioning of the fold axial trace for the northern syncline highly subjective. In addition, faulting associated with the D_2 event has crosscut the area, apparently resulting in displacement of the north-east section of the northern syncline.

Locally, overturned bedding is recorded from an isolated locality near Stridbukken, indicated by inverted way-up indicators (including cross-stratification and water escape structures). Within this zone of overturned strata, the bedding is orientated on average 002°/72°, and the overturning is regarded as indicative of the presence of a minor thrust, which may have developed as an accommodation structure within the syncline.

Axial planar cleavage within the folds is generally divergent, dipping across the fold limbs at a high angle. A factor commonly responsible for the development of divergent cleavage orientations is that of competency contrasts: within a fold, the axial planar cleavage tends to be refracted as it passes through lithologies of differing competencies (Hobbs, Means and

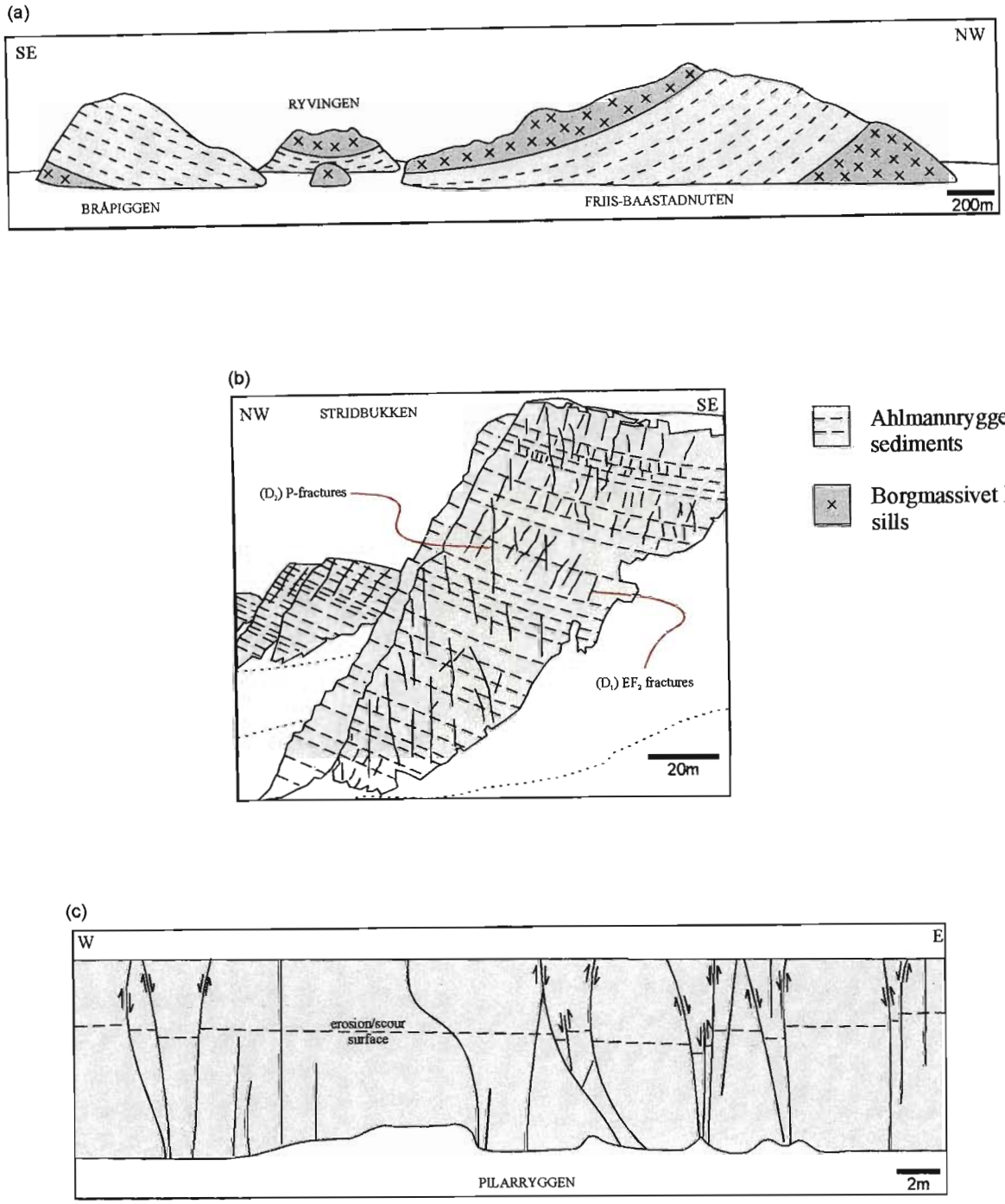

Figure 3.2: Simplified sketches of the main structural features resulting from the D_1 and D_2 deformational events recorded in the Borgmassivet and Ahlmannryggen regions. (a) Looking down plunge along a syncline, exposed across Bråpiggen, Ryvingen and Friis-Baastadnuten, formed during the early stages of the NNW-SSE compressive event (after Minnaar, 1975). (b) Sketch of the up-plunge view of the southern syncline exposed at Stridbukken, where deformation associated with both the D_1 and D_2 events is observed. Inclined extension/dilational fractures (EF_2) associated with the development of large buckle folds are seen to be cross-cut by steeply dipping, NE-SW trending P-shear fractures which developed during the strike-slip deformation event. (c) D_2 sinistral strike-slip deformation has resulted in the formation of numerous small-scale negative flower-structures and faults at Pilarryggen, exhibiting contrasting senses of movement.

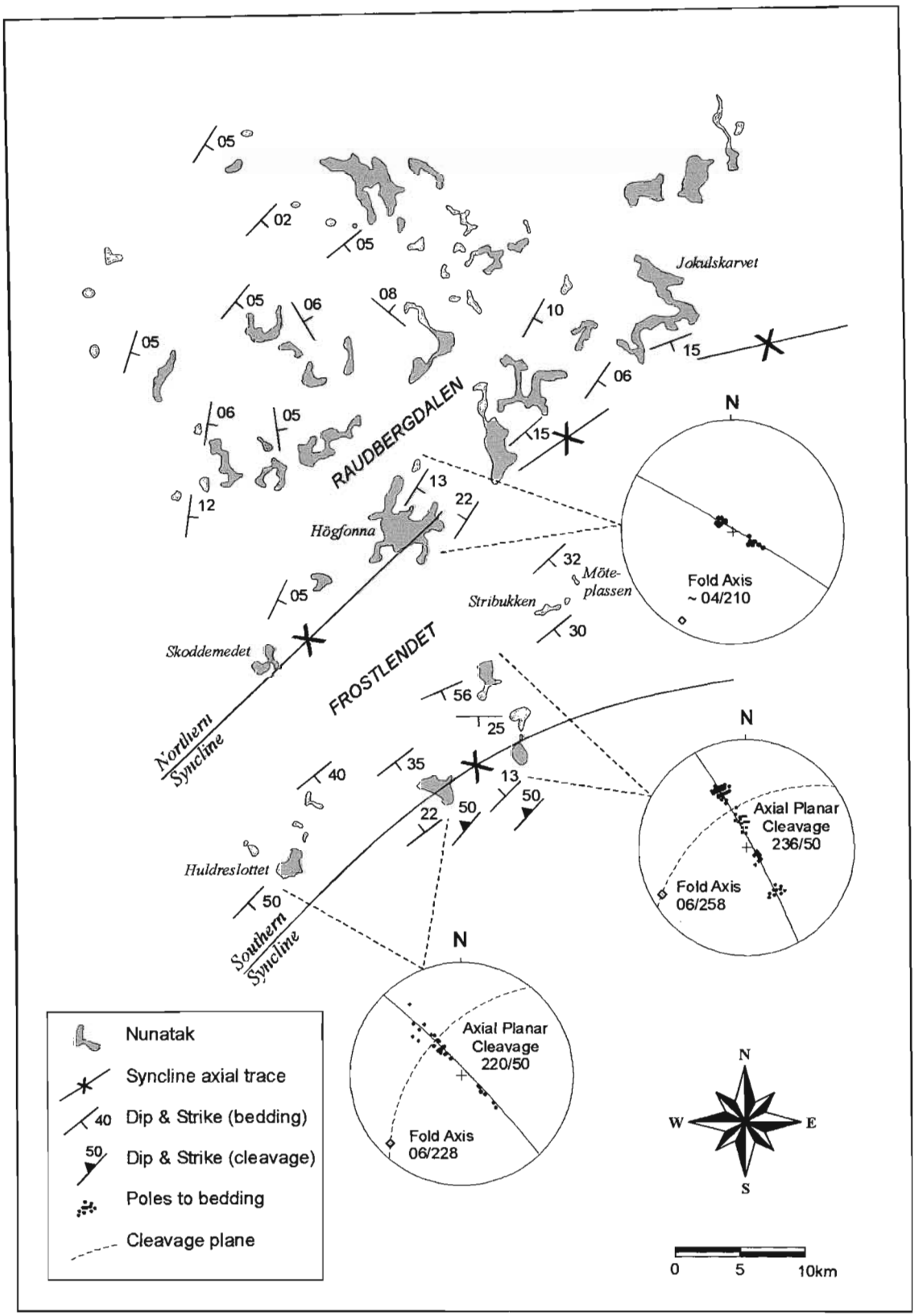

Figure 3.3: Simplified map and selected stereonets from the Borgmassivet region, with the nunataks indicated in grey. Two synclines, both of which exhibit arcuate axial traces, are exposed in the SE, along the Skoddemedet-Jokulskarvet and Huldreslottet-Möteplassen mountain ranges. The linking anticline is obscured by the Frostlendet glacier.

Williams, 1976; Ramsey and Huber, 1987). Considering that the cleavage orientations were preferentially recorded from fine-grained mudrocks (which exhibited a far more prominent cleavage than associated sandstones), refraction due to competency contrast is regarded as a likely explanation for the apparently divergent attitude of the cleavage.

The D_1 folding is attributed to the development of large buckle folds during north-northwest – south-southeast to north – south orientated compression. Price and Cosgrove (1990) define large buckle folds as large-scale structures exhibiting wavelengths of between several hundred metres and several kilometres, which develop in the upper levels of the crust. They consider folds such as these an important component of cover rock deformation during tectonic disturbance of the basement.

3.2.1.2 Fractures

Two distinct sets are present in the D_1 fracture generation, the occurrence of which is restricted to the folded region in the south-east Borgmassivet. These include extension fractures exhibiting an orthogonal relationship (labelled EF_1 and EF_2) and conjugate shear fractures (labelled SF_1 and SF_2) (Figure 3.4).

Despite these sets representing the primary fractures, they are not the master sets in the regional pattern. Sets $EF_{1\&2}$ and $SF_{1\&2}$ tend to be closely spaced and are of limited lateral and vertical extent (often being confined to within individual bedding layers), and are considered to be a combination of major and minor fractures. The extensional fractures typically exhibit a spacing of between 8-12cm, and are characterised by uneven surfaces occasionally marked by plumose or hackle structures. Occasionally, set EF_1 contains minor quartz infill. The shear fractures are slightly wider spaced (averaging between 10-20cm apart), and generally exhibit smooth surfaces with no distinctive features.

Fracture set EF_1 is invariably steeply dipping to vertical, and is consistently orientated perpendicular to the fold axes, such that variations in the fold axis trends are mimicked by changes in the orientation of set EF_1. Set EF_2 is orientated parallel to the fold axes, with slight changes in trend also closely related to the arcuate shape of the folds. Data sets were primarily collected from the north-western limbs of the two synclines, where set EF_2 dips steeply between the north-northwest and north-west. Difficulties in access limited the collection of data from the south-eastern limbs of the folds, however it was established that the equivalent of set EF_2 on the south-east limb of the southern syncline also trended parallel to the fold axis but dipped steeply in the opposite direction.

As sets $EF_{1\&2}$ are extension fractures, it is expected that at the instant of development the least principal stress (σ_3) acted at right angles to the fracture plane (Price and Cosgrove, 1990). The contrasting principal stress orientations required for the formation of these sets indicates that EF_1 and EF_2 could not have developed simultaneously, however σ_3 was apparently consistently orientated parallel to bedding during their formation.

Conjugate shear fractures SF_1 and SF_2 are recorded from the limbs of both synclines, although displacement across these structures is only rarely observed and the term 'shear' is applied with caution. As for the extensional fractures, these conjugate sets also exhibit variations in orientation in relation to changes in the fold axial trend, and consistently maintain a high angle of incidence with respect to the fold axes. For interpretation of the shear fractures in terms of stress orientation, the Navier-Coulomb criterion of failure is applied. Accordingly, it can be established that the maximum principal compressive stress (σ_1) was predominantly orientated north-northwest – south-southeast, with minor variations recorded along the length of the folds. Minimum principal compressive stress (σ_3) consistently remained orientated parallel to the bedding, while the intermediate compressive stress (σ_2) was orientated perpendicular to the fold limbs.

3.2.1.3 Interpretation

Both the large-scale folds and associated fracture sets $EF_{1\&2}$ and $SF_{1\&2}$ developed within a predominantly north-northwest – south-southeast orientated stress regime. Slight variations in the orientation of σ_1 resulted in the rotation of the folds and associated fractures, and the development of arcuate synclinal structures. Minimum principal compressive stress (σ_3) remained consistently orientated parallel to the bedding, while σ_2 was orientated vertically.

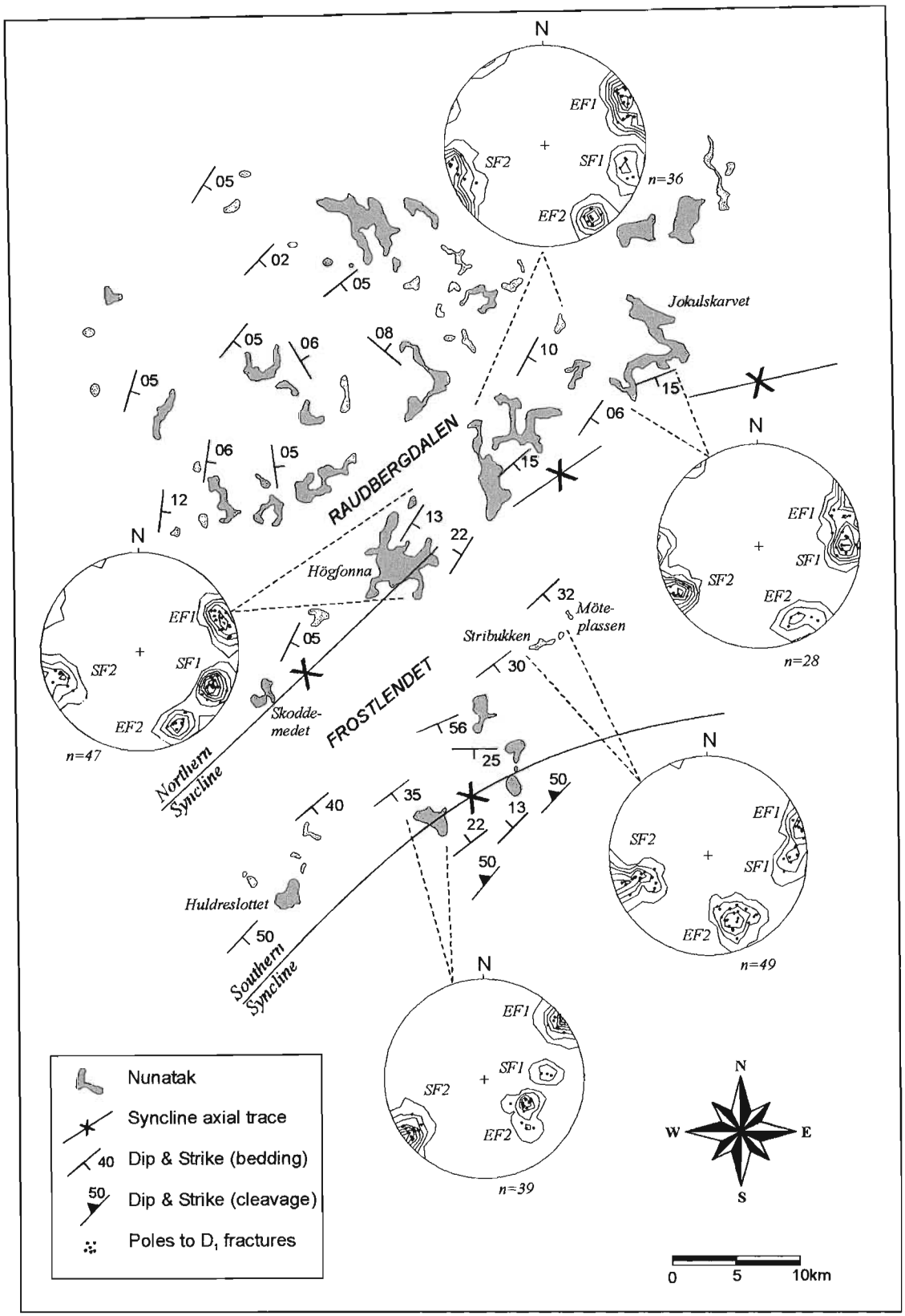

Figure 3.4: Simplified map and selected stereonets recording the primary fracture sets exposed in the SE Borgmassivet. Fracture sets consist of both conjugate shear fractures (sets SF_1 and SF_2) and orthogonal dilational fractures (sets EF_1 and EF_2). These fracture sets are related to the folding observed in this region and changes in the fracture orientations can be linked to the arcuate shape of the fold axes.

The ideal fracture patterns commonly associated with large buckle folds are presented in Figure 3.5a. These ideal fracture patterns can be closely matched to the primary fracture system recorded in the south-east Borgmassivet. Fracture sets EF_1 and EF_2 are similar in nature to the D_1 and D_2 dilational fractures, while the conjugate sets correspond closely to the most commonly expected shear fractures in an idealised fold structure (S_1 and S_2-Figure 3.5a). Shear fractures generally exhibit a more complex relationship to the fold geometry than dilational fractures. Figure 3a illustrates the expected orientations of shear fractures relative to the limbs of a fold, of which only the most commonly occurring sets are recorded from the south-east Borgmassivet. This may be an effect of sampling bias, as data were mainly collected from isolated localities on the limbs of the synclines and more detailed investigation may establish the presence of additional shear fracture sets. According to Price and Cosgrove (1990), the shear fractures may take the form of normal, thrust, strike-slip and oblique-slip faults. Where observed, movement along shear fractures SF_1 and SF_2 is generally strike-slip in nature. However, the occasional presence of locally overturned beds within the southern syncline indicates that small-scale reverse faulting/ thrusting has also taken place, suggesting the presence of low-angle fractures from Price and Cosgrove's (1990) 'rare' fracture grouping.

Changes in the orientation of the stress field during folding represents a likely explanation for the slight deviation of the observed fracture pattern from that expected in an ideal system. Theoretically, the orthogonal extension/dilation fractures (EF_1 and EF_2) should bisect shear fractures SF_1 and SF_2, as illustrated in Figure 3.5b. However, sets EF_1 and EF_2 are consistently rotated away from this 'ideal' orientation (by between 10° and 30° to the west). This suggests that the fracture sets did not develop simultaneously, and slight variations in the orientation of the stress field during the development of the folds are considered responsible for the deviation from an 'ideal' relationship.

3.2.2 D_2 Event

The folds and fracture sets developed during the D_1 event are crosscut and sometimes re-activated by a second deformational episode which resulted in the development of an extensive fracture system throughout the Borgmassivet and Ahlmannryggen regions. Overall, the D_2 fractures are more widely spaced than those associated with the D_1 event, are more persistent, and are regarded as the master sets in the regional pattern (Figure 3.2b).

3.2.2.1 Fractures

Five distinct fracture sets developed during the D_2 event (Figure 3.6). These fracture sets are all steeply dipping and, with the exception of a few minor variations, display highly consistent trends. The majority of the D_2 sets are shear fractures, however an extensional set (designated set T) is also present. This extensional T set exhibits a similar orientation to set EF_1 from the south-east Borgmassivet, suggesting that the north-northwest – south-southeast compressive regime of D_1 was maintained during the D_2 event. The only notable distinction between sets EF_1 and T is the variation in fracture intensity, with set T being notably less intense and characterised by a fracture spacing of between 50cm and 2m. Both sets occasionally contain quartz infill, a testament to their dilational mode of development.

The shear fractures (sets R, R', P and X) are characterised by smooth surfaces, and set P occasionally exhibits small 'feather fractures' indicative of a sinistral shear sense. Occasionally, set R may show evidence of pressure solution veining. Adjacent to the Pencksökket-Jutulstraumen boundary, hybrid shear fractures from set R' are often readily identifiable due to intense brecciation of quartz infilling, occasionally sufficiently severe to result in the incorporation of centimetre long fragments of wall-rock. This brecciated veining is also locally accompanied by malachite staining.

The fracture spacing in the shear sets varies from 10cm to over 1m but averages approximately 50cm. Unlike the sets associated with the D_1 folding event, the D_2 fractures tend to be highly persistent, extending through multiple bedding layers and often continuing for several metres along strike. Sets R and P contain the most persistent fractures of all the sets, often cross-cutting associated D_2 fractures, and strike-slip movement along these fractures has often resulted in left-lateral displacement of sets T/EF_1, EF_2, X and R'.

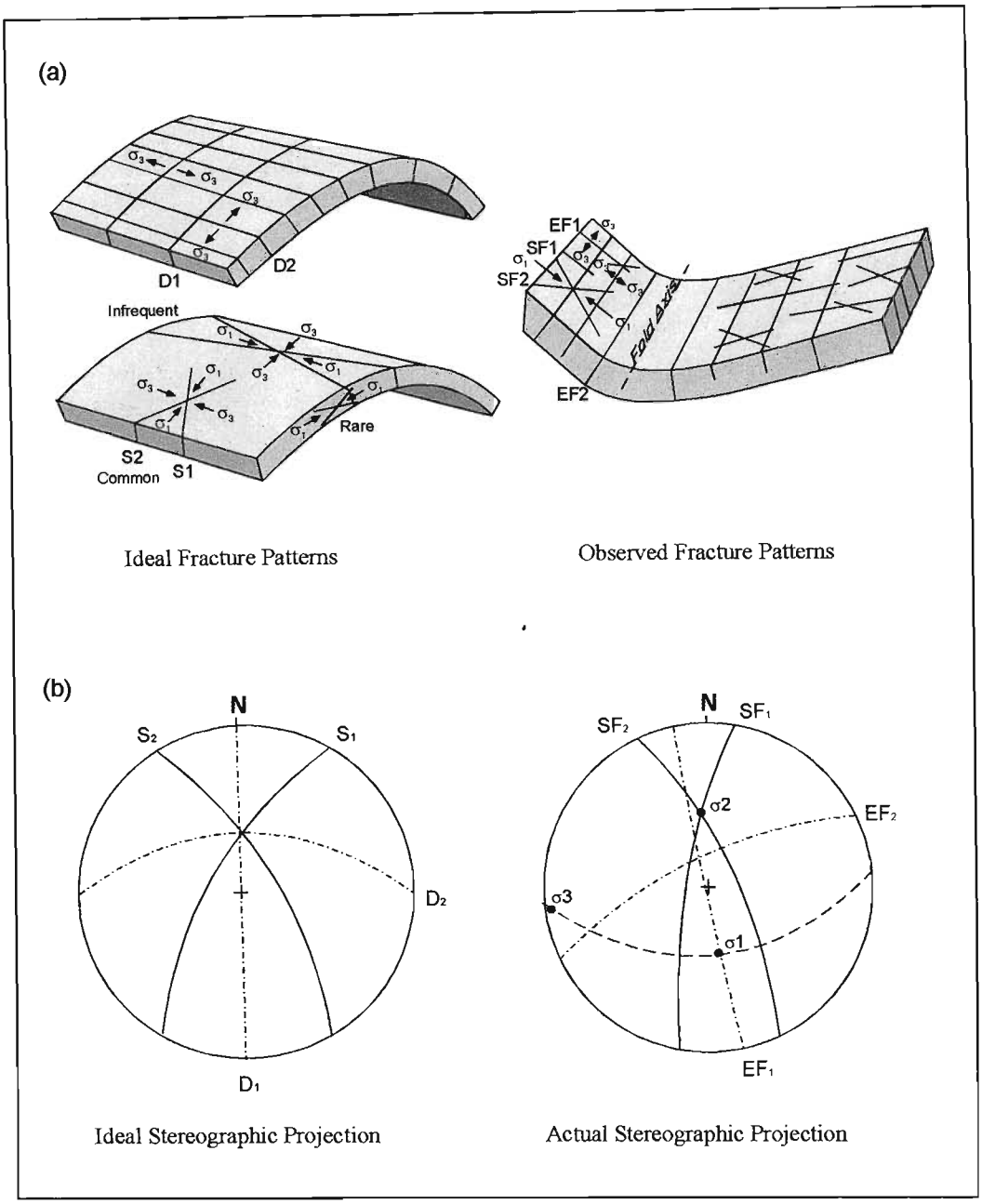

Figure 3.5: (a) The primary fracture orientations recorded from the limbs of the synclines in the SE Borgmassivet correspond closely to the ideal models of Price and Cosgrove (1990). (b) A stereographic projection of the observed fracture relationships differs slightly from that expected in Price's (1966) ideal fold system, due to changes in the orientation of the stress field during the progressive deformation, resulting in the rotation of the fracture sets away from an 'ideal' position.

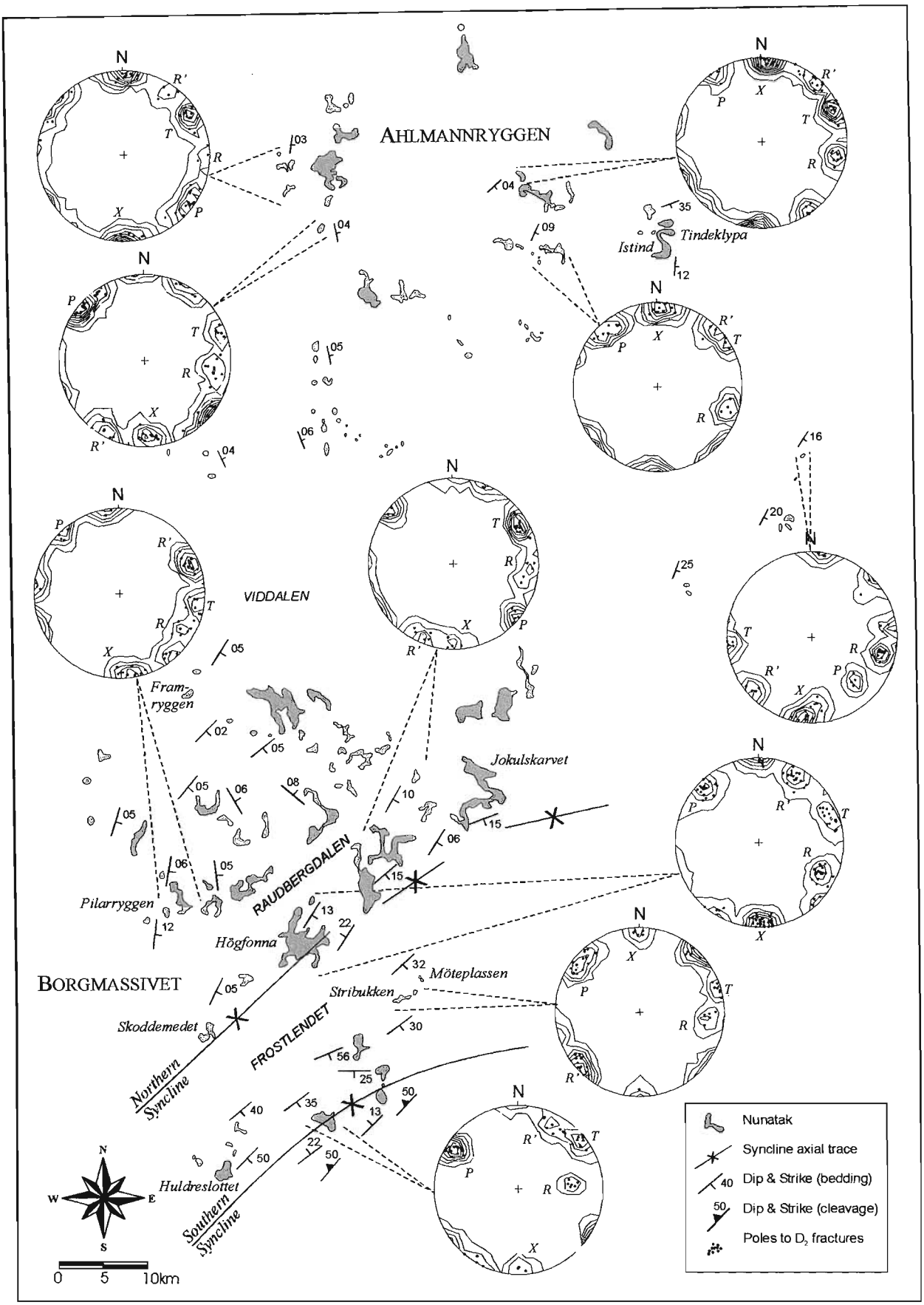

Figure 3.6: Simplified map and selected stereonets recording the master D_2 fracture sets exposed in the Ahlmannryggen and Borgmassivet regions. Five distinct fracture sets (R, R`, P, X and T) developed during D_2 tectonism, all of which display consistent orientations across the entire area. The development of these D_2 fracture sets caused offset and re-activation of the primary D_1 fractures in the SE Borgmassivet.

The D_2 shear fractures are best developed adjacent to the Jutulstraumen-Pencksökket boundary, and fracture intensity decreases slightly to the west. The extent of shear displacement across the fractures also decreases to the west, and the fracture planes tend to assume a distinct anastomosing character away from the main bounding glaciers. This westerly decrease in the D_2 deformation intensity, away from the Jutulstraumen-Pencksökket glaciers, suggests that this boundary system represents the locus of deformation for the D_2 event.

3.2.2.2 Interpretation

The regional D_2 fracture pattern within the Borgmassivet and Ahlmannryggen closely resembles that expected in a strike-slip system with a sinistral sense of movement (Figure 3.7a,b). As Price and Cosgrove (1990) describe, even if it is not directly observed, the presence of a strike-slip system can be inferred from the nature of the secondary fractures in the region. These are associated with movement along the main first order basement fault and have been modelled experimentally by a number of researchers (e.g. Tchalenko, 1968). Fractures which developed in these experiments include Riedel Shears (R and R'), Y-shears, X-shears, P-shears and extensional T-fractures.

As described by McClay (1987), strike-slip faulting is initiated by the development of Reidel shears (R and R') orientated at ~30° to σ_1. Movement tends to be concentrated along one Reidel system (R), which is synthetic to the direction of maximum resolved shear stress. The Y-shear represents the main shear plane in the basement, but is not always observed in the cover rocks. In some systems, synthetic P- and antithetic X-shears, typically orientated at 45° to σ_1, may also develop. The T-fracture is an extensional feature, which develops parallel to σ_1. It is often orientated at about 45° to the Y-shear, and does not necessarily exhibit a component of movement.

With the exception of the Y-shear, all fractures sets expected to form during strike-slip deformation are represented in the Grunehogna Province cover rocks. When the Navier-Coulomb criterion of failure is applied to the fractures sets regarded as equivalent to the Reidel Shears, it becomes obvious that the maximum principal compressive stress responsible for D_2 brittle faulting maintained the same north-northwest – south-southeast orientation as observed for the D_1 event (Figure 3.7b). The orientations of the fracture sets do exhibit minor variations across the region, possibly an effect of slight rotations of the principal stresses during the D_2 event. The main fault planes and zones of displacement associated with this strike-slip dominated D_2 event are not encountered in outcrop, but are inferred along the glacial valleys crosscutting the region.

Major strike-slip faults often exhibit a curvilinear Principle Displacement Zone (PDZ), identifiable from a curved or kinked trace at the surface (Price and Cosgrove, 1990; Figure 3.7c). Horizontal movement along such a non-linear fault plane will create either zones of compression or zones of extension, where voids or overlaps try to develop. In such fault systems, the T-fracture may develop into a normal fault at releasing bends, permitting the formation of grabens (Figure 3.7d), while horsts may develop in regions subject to compression.

The development of grabens within zones of localised transtension along curvilinear strike-slip faults is considered responsible for the juxtapositioning of the rhomb-shaped glacier-bounded blocks of Jutulstraumen Group volcaniclastics with outcrops of the Ahlmannryggen Group. The formation of negative flower structures – observed on a small scale at Pilarryggen (Figure 3.2c) – is characteristic of strike-slip systems with localised regions of transtension (Twiss and Moores, 1992), and provides supporting evidence for this interpretation. A left-stepping sinistral strike-slip fault is inferred adjacent to the Istind-Tindeklypa block in the eastern Ahlmannryggen. Continuation of this inferred fault zone into the north-western Borgmassivet would account for the slight offsets that apparently exist between some of the nunataks in this region, however, as this fault is not encountered in outcrop, this inference is highly subjective. The development of a duplex structure along a releasing bend located in the eastern Borgmassivet is suspected to be responsible for the formation of the two adjacent rhomb-shaped grabens encountered in this area. The northernmost graben exhibits the greatest offset, and juxtaposes Ahlmannryggen and Jutulstraumen Group sequences, while the second, southerly graben apparently experienced only minor displacement and resulted in a slight

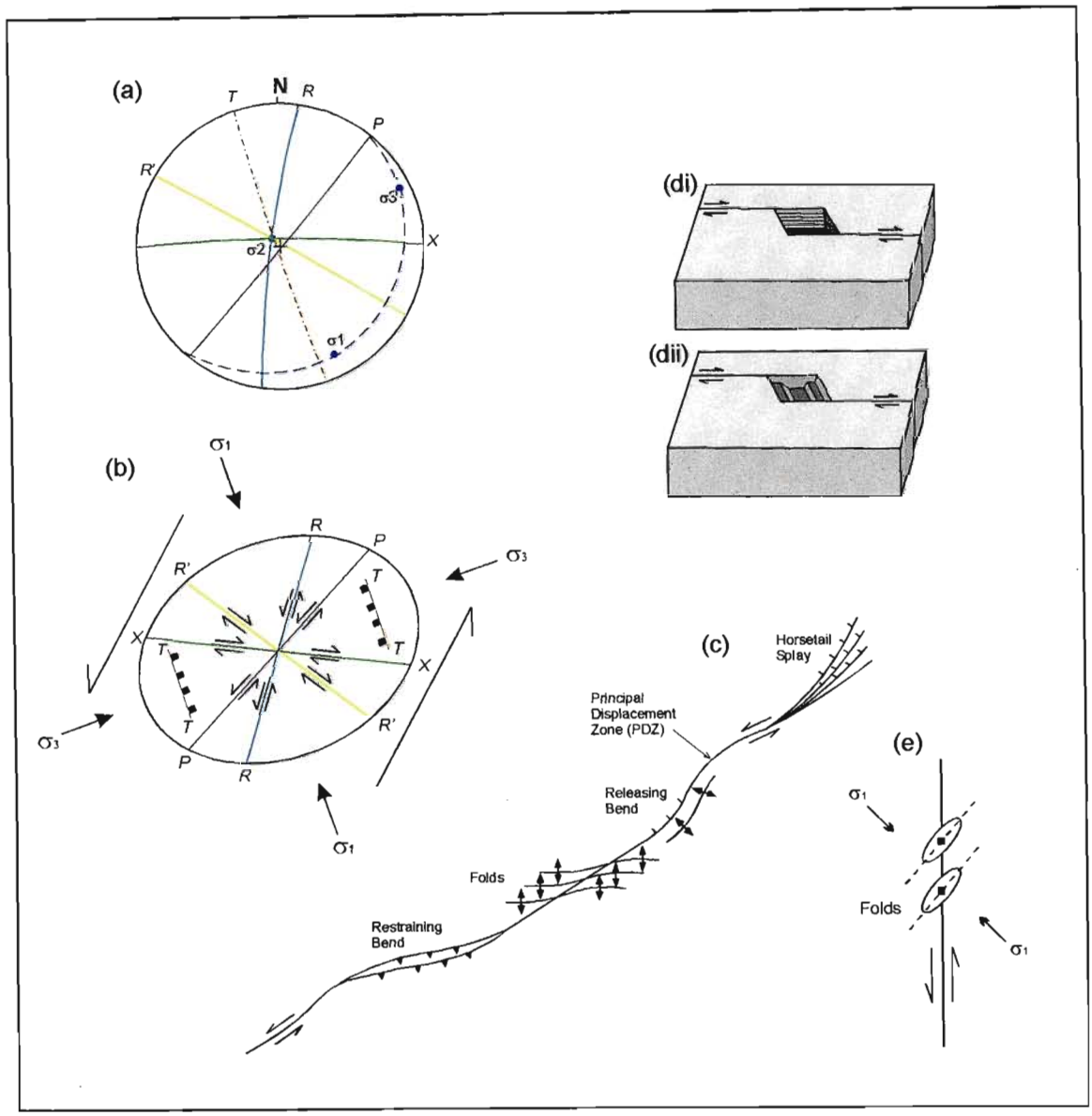

Figure 3.7: (a) Stereonet depicting the general orientation of the master fracture sets identified in the Ahlmannryggen and Borgmassivet regions. The observed D2 fracture pattern corresponds to the fractures expected to develop in a sinistral strike-slip system, as shown in the strain ellipse in (b) (adapted from McClay, 1987). (c) Typical structures associated with a curvi-linear Principal Displacement Zone (PDZ) include horsts, which develop in restraining bends; grabens, which form within releasing bends; *en echelon* folds with rotated fold axes and horsetail splays near fault terminations (adapted from Christie-Blick and Biddle, 1985). Other secondary features commonly associated with a first order basement fault include secondary faults and fissures. The strike-slip deformation within the Grunehogna Province can be attributed to faulting along either secondary minor faults or splay faults originating from a PDZ located within the Jutulstaumen-Pencksökket dislocation. Grabens form within localised regions of transtension via either an opening mode (di) or shearing mode (dii), with the latter involving oblique slip and normal faulting components (Aydin and Nur, 1985). (e) Shear in the basement will induce compression in the cover rocks, leading to the development of *en echelon* folds. Initially these are orientated at ~45° to the first order fault, however continued shearing will result in rotation of the fold axes, until they are near parallel with the first order fault (Price and Cosgrove, 1990), as seen in the southeast Borgmassivet.

offset of the Ahlmannryggen Group strata. The presence of a third fault zone, in the central Ahlmannryggen, is suggested by the left-lateral displacement encountered at Grunehogna. All three of these inferred fault zones are regarded as secondary faults originating from a first-order basement fault located within the Pencksökket-Jutulstraumen dislocation.

3.2.3 D_3 Event

WDML was situated near South Africa and the Agulhas Plateau prior to Gondwana fragmentation (Grantham *et al.*, 1988; Groenewald *et al.*, 1991). Limited examination of Jurassic dyke orientations and associated fracture patterns was undertaken, in an attempt to constrain the nature of deformation associated with Gondwana fragmentation. Steeply dipping fracture sets, striking 152°, 300°, 203°, 356° and 228° were recorded in Jurassic intrusions in the northwestern Borgmassivet. These orientations correspond to those of pre-existing fracture sets developed in the Grunehogna Province during D_1 and D_2 tectonism, suggesting that deformation of the Grunehogna Province during Gondwana fragmentation was restricted to re-activation of/displacement along pre-existing structures. The orientations of the dykes also correspond closely to the D_2 fracture orientations, implying exploitation of these pre-existing weaknesses during the intrusive event.

Late stage normal faulting (possibly accentuated by the presence of pre-existing fracture planes) is thought to be related to Gondwana fragmentation. Extension during this event is considered responsible for the development of the large-scale faults recognised to the west of the Ahlmannryggen, which produce a series of blocks that are stepped down to the west and northwest (Hinz and Krause, 1982). Down-faulting due to Jurassic-aged extension is also recognised within the Pencksökket-Jutulstraumen divide (Grantham and Hunter, 1991), and represents a likely explanation for the down-faulting of Straumsnutane Group lavas within the Straumsnutane region, on the western margin of the Jutulstraumen glacier.

3.3 DISCUSSION

Based on the folding and regional fracture pattern exposed in the cover rocks of the Grunehogna Province, it is possible to identify two main deformational episodes. The first involved progressive ductile to brittle deformation within a north-northwest – south-southeast compressive setting, leading to the formation of large-scale buckle folds (D_1), followed by development of extensive brittle strike-slip faulting (D_2) (Figure 3.8). The second event to have affected the Grunehogna Province is Gondwana fragmentation (D_3), which apparently resulted in the re-activation of many pre-existing fracture sets and displacement along these pre-existing planes of weakness.

Price and Cosgrove (1990) separate strike-slip faults into two main groups. The first consists of relatively small structures in the upper levels of the crust, with extents not usually exceeding a few tens of kilometres. The second, and more important group, comprises strike-slip faults that are of regional or continental extent. These major features extend through the crust and tend to develop at present or ancient plate boundaries. Based on its regional extent and location along the eastern margin of the Grunehogna Province, the inferred strike-slip fault system is considered to fall within this latter category. The presence of strike-slip deformation was first noted by Aucamp (1972), who reported a series of small-scale, locally occurring north-northeast – south-southwest trending sinistral strike-slip faults at Grunehogna, with a total horizontal displacement of 55m. However, he interpreted these structures in a local context and did not consider that these faults may be part of a far more extensive, regional strike-slip deformation event.

Despite a lack of direct evidence, the existence of a regionally extensive strike-slip system within the Grunehogna Province can be inferred on the basis of the regional fracture pattern and the nature of the ductile folding and the small-scale brittle structures exposed locally. When a major strike-slip fault in the basement is covered by a sequence of sediments, movement along the fault will induce compression and extension in the cover rocks, leading to the formation of folds and a variety of different fractures. Folds formed in such a setting tend to display an initial orientation as indicated in Figure 2.7e, with the fold axes striking at ~45° to the first order basement fault, and orientated at 90° to σ_1 (Price and Cosgrove, 1990). However, continued shearing in the basement will result in rotation of the fold structures, until they are almost parallel to the main fault, as observed along the

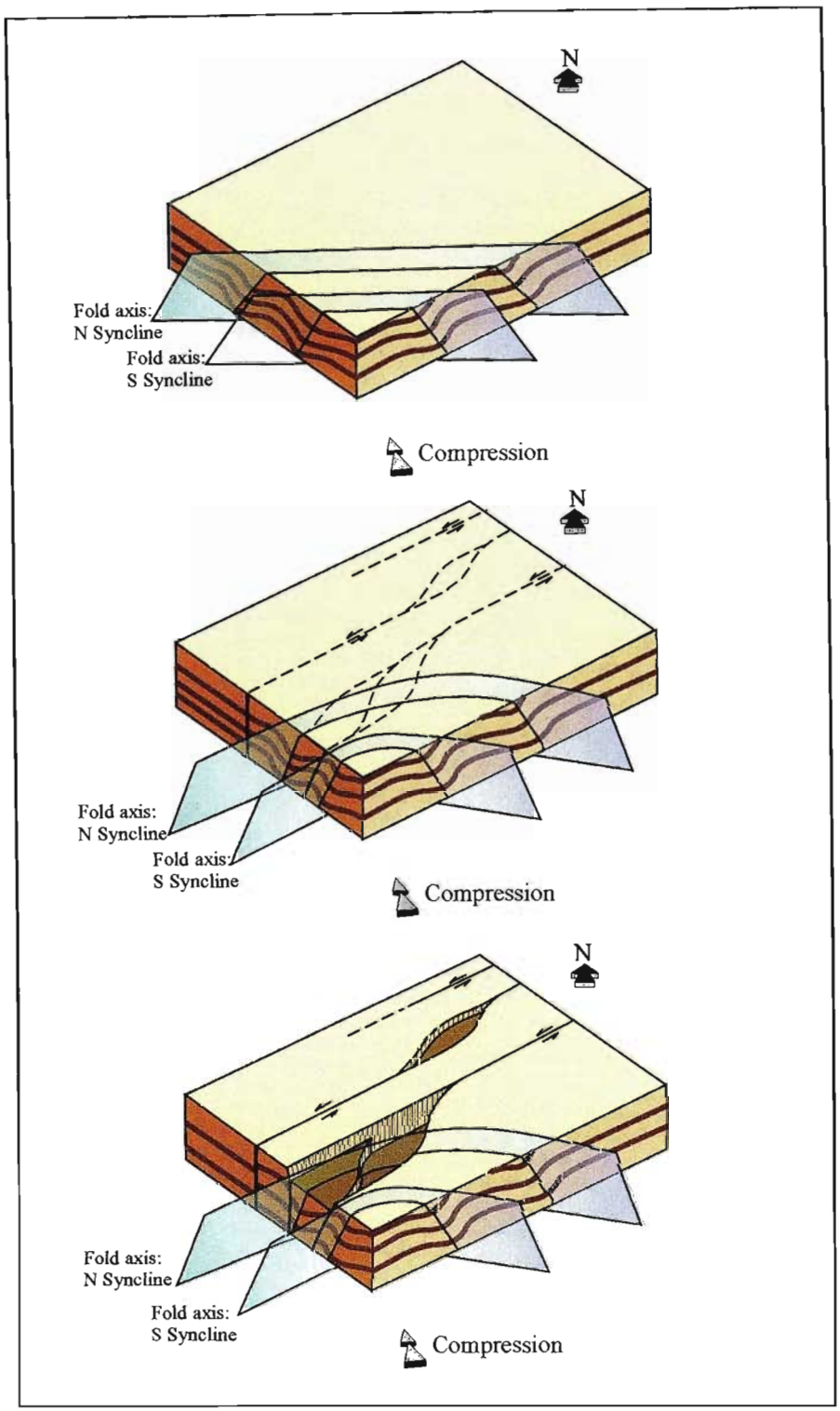

Figure 3.8: Simplified block diagrams depicting deformation of the Ahlmannryggen and Borgmassivet regions due to progressive NNW-SSE transpression. Initial folding (D_1) was followed by left-lateral strike-slip deformation (D_2). The development of rhomb-shaped grabens within localised regions of transtension at releasing bends resulted in the juxtapositioning of Ahlmannryggen Group sediments and Jutulstraumen Group volcaniclastics.

Inglewood Fault in southern California (Price and Cosgrove, 1990). An equally applicable model, which must also be considered, is one in which the NNW-SSE compression may have induced initial disharmonic folding in the cover sequence prior to any strike-slip movement in the basement. However, in both scenarios, the arcuate shape of the fold axes is considered to result from progressive shearing in the basement, which resulted in the rotation of originally east-northeast trending folds (and associated fracture sets) to a north-east – south-west orientation.

The presence of a previously unrecognised regional strike-slip system in the Grunehogna Province effectively explains the inconsistent nature of the faulting encountered in the Borgmassivet and Ahlmannryggen. Juxta-positioning of Ahlmannryggen Group and Jutulstraumen Group outcrops is also explained by this model. In addition, strike-slip displacement can account for the lack of vertical offset across the Schyttbreen glacier located to the west. The presence of Ahlmannryggen Group sediments on both sides of this lineament may preclude extensive normal/reverse faulting, but does not eliminate the possibility of strike-slip displacement. Difficulties in establishing the temporal relationship between the major Type 1 and minor Type 2 faults of Krynauw (1986) are also resolved. Whereas Krynauw (1986) considered the formation of these structures to be related to the same tectonic event, it is suggested here that they formed during two entirely separate periods of tectonism. His Type 2 faults correspond to the inferred secondary faults of the D_2 strike-slip system, while the Type 1 faults can be explained by normal faulting during Gondwana fragmentation.

3.4 REGIONAL IMPLICATIONS

The thermo-magmatic effects of Pan-African overprinting in WDML are well documented, whilst the tectonic expression of this event is controversial. Conflicting models have been developed which alternatively propose either pervasive reworking (Grantham *et al.*, 1995; Groenewald *et al.*, 1995) or limit effects to thermal overprinting (Moyes *et al.*, 1993; Groenewald, 1995).

Within the southern Kirwanveggen, development of a strike-slip fault system at *ca.* 550Ma is considered responsible for the formation of the Urfjell Group, which was deposited in a pull-apart basin located within a releasing bend along a north-east trending left-lateral strike-slip system (Croaker, 1999; Croaker *et al.*, 1999). Croaker (1999) interprets significant and rapid uplift along a linked system of thrusts and left lateral transpressive zones at approximately 550Ma, during which time top-to-north thrusting was experienced within the southern Kirwanveggen (Helferich *et al.*, 1999). Within this overall transpressive framework, localised tension could have been produced at releasing bends along key transcurrent strike-slip zone/s. At the surface, these tensional domains may have developed into extensional pull-apart basins of limited extent, forming small depositories which would have rapidly filled with detritus from the emergent orogen. Continued north-northwest – south-southeast to north-northeast – south-southwest transpression resulted in the subsequent deformation of the Urfjell Group within the multiphase strike-slip system at *ca.* 530Ma (Moyes *et al.*, 1995b; 1997).

Given the close similarities between the nature of the D_1/D_2 deformation observed in the Grunehogna Province, and the strike-slip faulting recorded in the southern Kirwanveggen, coeval development within a regional north-northwest – south-southeast Pan-African compressional regime is considered likely. The faulting within the Borgmassivet, Ahlmannryggen and Kirwanveggen regions can be attributed to the formation of secondary and splay faults originating from a PDZ located along the Pencksökket-Jutulstraumen divide (Figure 3.9), the existence of which was first postulated by Allen (1991), based on structures exposed in the H U Sverdrupfjella.

Further support for a Pan-African age for the strike-slip deformation comes from studies of the shearing in the Straumsnutane area (Peters *et al.*, 1991). In simple shear models, the shear boundaries are generally orientated at 45° to σ_1. The angle between the shearing recorded in the Straumsnutane area (027°/65°) and the orientation of σ_1 during D_1 and D_2 is approximately 45°, raising the possibility that the deformation observed in the Straumsnutane area is related to the strike-slip deformation affecting the Borgmassivet and Ahlmannryggen regions. Folding is also documented in the Straumsnutane area, characterised by roughly north-northeast

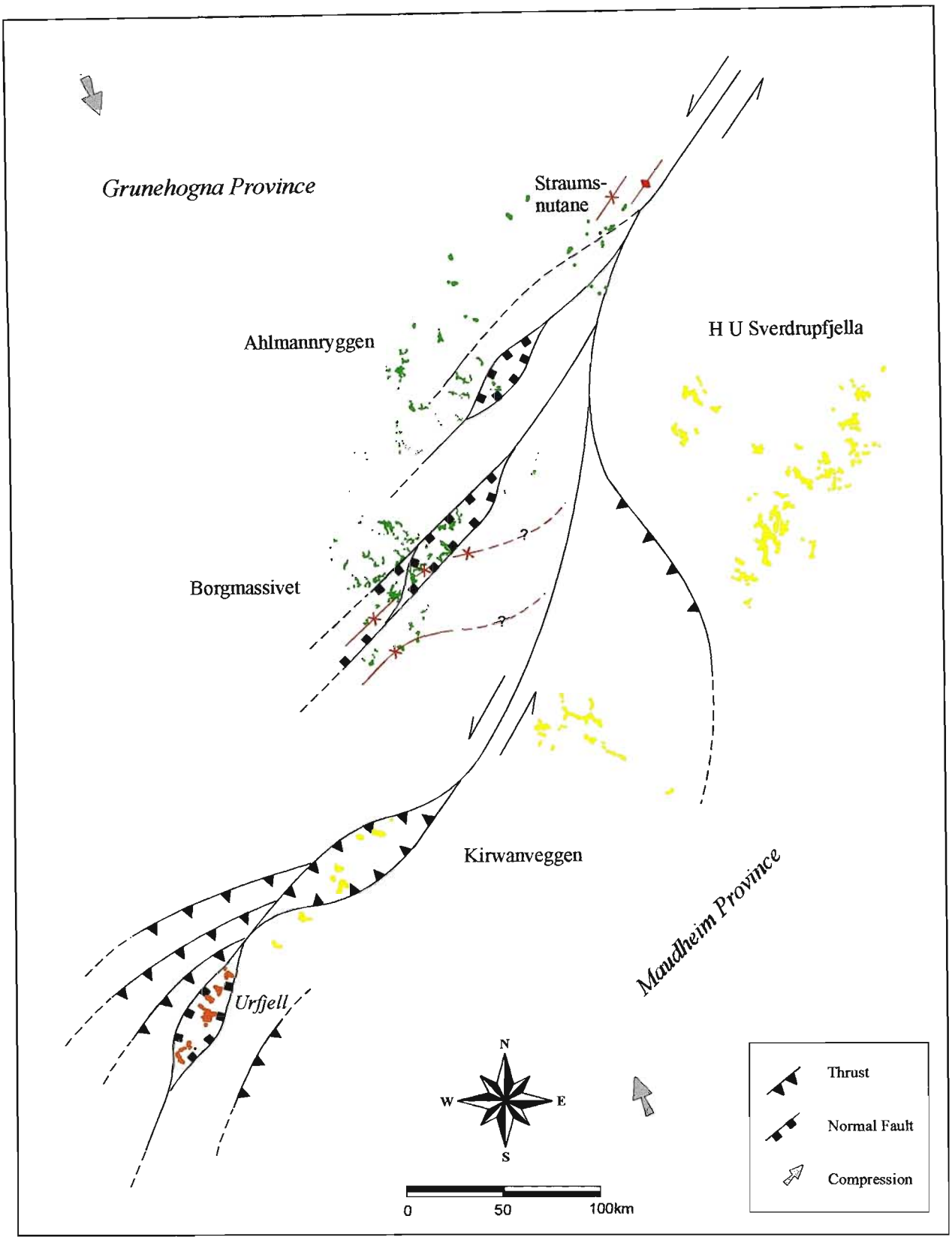

Figure 3.9: Extensive left-lateral strike-slip deformation is present in both the Maudheim Province and the Grunehogna Province, associated with ca 520Ma NNW-SSE transpression. Deformation in the Borgmassivet and Ahlmann-ryggen is considered to be an extension of the strike-slip faulting identified by Croaker (1999) and Moyes *et al.* (1995; 1997) in the southern Kirwanveggen.

trending axes. This closely parallels the orientation of the shearing and the orientation of the inferred principal strike-slip faults. The Straumsnutane shearing is characterised by strongly orientated flakes of white mica, which yield K-Ar isotopic ages of 522 ±11 and 526 ±11Ma (Peters *et al.*, 1991), which closely approximates the age of the strike-slip deformation observed in the southern Kirwanveggen.

A Pan-African age is therefore favoured for the D_1 and D_2 strike-slip tectonism observed in the Ahlmannryggen and Borgmassivet regions, based on close similarities in stress orientations and deformation style with the ca. 520Ma shearing observed in the Straumsnutane, the *ca.* 550-530Ma strike-slip faulting in the southern Kirwanveggen.

The presence of regional Pan-African strike-slip tectonism within the Grunehogna Province and Kirwanveggen has important implications regarding local plate reconstructions and tectonic styles, and suggests extensive 'Pan-African' aged reworking of the 'Grenvillian' Dronning Maud Belt. This will be expanded on in Section D – Regional Tectonics.

SECTION D

1-BASIN EVOLUTION
2-REGIONAL TECTONICS
3-CONCLUSIONS

Overview:

This final section presents a comprehensive basin evolution model, drawing on observations from the lithostratigraphic, sedimentological, provenance and age investigations, and considers the evolution of the Ahlmannryggen Group sedimentary basin within the geological framework of WDML.

In addition, the formation and deformation of the sedimentary sequence are considered in relation to regional tectonic events, including the amalgamation of Rodinia and Gondwana, with refinements to local styles of plate assembly suggested. A summary of the conclusions resulting from this study is also presented.

1. BASIN EVOLUTION

1.1 INTRODUCTION

The Ahlmannryggen Group preserves a unique record of basin formation during the 'Kibaran' orogenic event in WDML and provides an opportunity to examine the nature of this extensive episode of tectonism from a cratonic perspective. The nature of the Ahlmannryggen sedimentary basin provides important insights into the local plate tectonic configuration and tectonic styles, and provides evidence in support of an originally more extensive cratonic province. Determination of the nature and evolution of the Ahlmannryggen Group basin necessitates integration of the lithostratigraphic, sedimentological, geochemical and geochronological data sets. The following section will place constraints on the tectonic setting of the basin and will examine the evolution of the basin within the broader framework of WDML.

1.2 THE AHLMANNRYGGEN BASIN

1.2.1 Regional Framework

Aeromagnetic data from WDML (Corner, 1994, Figure 1.1) reveals that the Ahlmannryggen sedimentary basin developed along the southern margin of the Grunehogna Province, adjacent to the high-grade Maudheim Province. This aeromagnetic data provides a far more accurate reflection of the extent and trend of the Maudheim Province belt than the outcrop pattern in the region, which suggests an overall NE-SW orientation. Examination of the aeromagnetic data reveals the trend of the belt is instead dominantly E-W, except in the H U Sverdrupfjella region, where the trend changes to NE-SW before returning to an E-W orientation in central DML (not included in Figure 1.1).

The variation in the trend through the H U Sverdrupfjella is attributed to shearing during NNW-SSE orientated Pan-African compression, which is considered to have resulted in the development of a regionally extensive strike-slip system and partial rotation of the belt. Removal of the effects of this Pan-African reworking permits tentative reconstruction of the local plate tectonic configuration during the Kibaran orogenic episode, and suggests that the fold-thrust belt originally exhibited a somewhat more linear, possibly E-W trend along the southern margin of a more extensive Grunehogna Province. A model incorporating an extended cratonic province would account for both the formation of a E-W linear fold-thrust belt and the positioning of the Ahlmannryggen basin depo-centre out to the east of the current outcrop area. The nature of the Pan-African and Kibaran tectonism within WDML, and their effect on the Grunehogna Province are considered in greater detail in Section D: 2.

1.2.2 Age

The *ca.* 1130Ma age determined for the volcanic zircon populations in the Ahlmannryggen Group is considered to approximate the timing of deposition of the Grunehogna/Högfonna and Bråpiggen Formations of the Ahlmannryggen Group. This timing of sedimentation within the Ahlmannryggen Group basin implies a close relationship with Mesoproterozoic tectonism in the adjacent Maudheim Province. The earliest recorded phases of a prolonged stage of plate convergence involving folding, thrusting and high-grade metamorphism of this island arc terrain are documented at *ca.* 1135Ma (Jacobs *et al.*, 1996). The Ahlmannryggen Group basin was evidently well established by this stage, implying that docking of the island arc against the margin of the Grunehogna Province must have been initiated prior to 1130Ma. Unfortunately, the lack of exposure of underlying basin fill sequences precludes determination of the timing of basin formation.

1.2.3 Palaeogeography

The original extent of the Ahlmannryggen sedimentary basin is difficult to determine, as the present outcrop exposure is interpreted to represent the central/medial portion of the basin only. In addition, the limited aeromagnetic data available for the Borgmassivet region (the Ahlmannryggen area has not been surveyed) is apparently strongly influenced by the geomorphology of the area and cannot be used to establish the basin margins. Accordingly, only a minimum estimated width of ~130km and length of 150km can be determined from the outcrop pattern. The original basin is considered to have been far more extensive in nature, and possibly

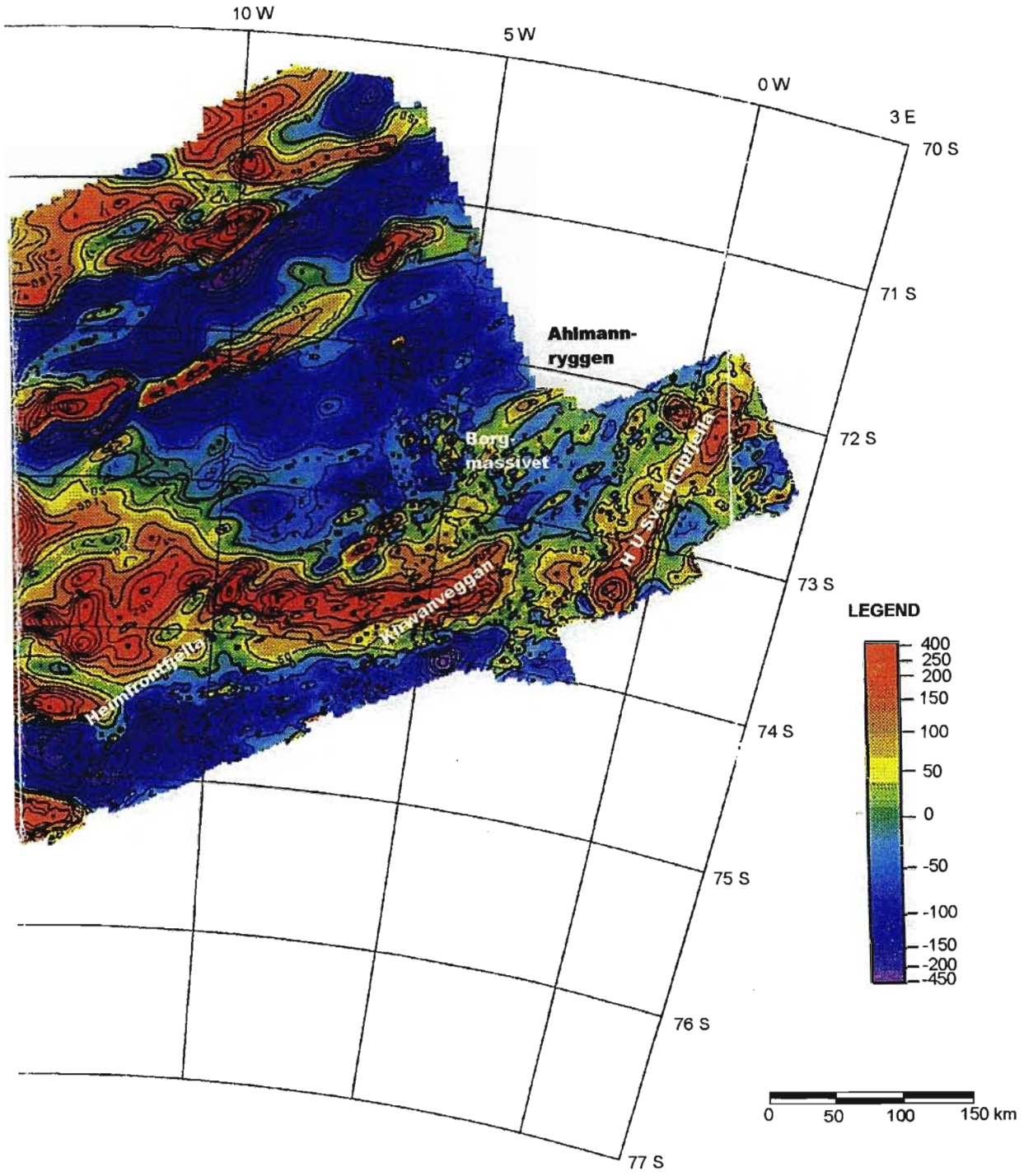

Figure 1.1: The regional aeromagnetic map of WDML (from Corner, 1994) reveals the nature and extent of the Kibaran Maudheim Province fold-thrust belt. Outcrop patterns must not be regarded as an accurate reflection of the trend of the belt, which is dominantly E-W, except in the H U Sverdrupfjella region, where the trend changes to NE-SW. This curvature is attributed to shearing during NNW-SSE orientated Pan-African compression. The Ahlmannryggen Group is regarded as having been deposited in a peripheral foreland basin located along the southern margin of the Grunehogna Province, due to collision with the continental island arc system of the Maudheim Province.

extended for more than 400km along the length of the Grunehogna Province.

Based on sedimentological and palaeocurrent evidence, sedimentation within the Ahlmannryggen basin is regarded as having occurred in both a northeasterly flowing transverse drainage system and a southeasterly flowing longitudinal drainage system. The basin is regarded as having developed in response to tectonism along a linear orogenic belt located to the south/southwest, with the trend of the basin reflecting the orientation of the regional structural grain in the fold-thrust belt. Palaeocurrent orientations suggest that the longitudinal drainage systems entered a depo-centre located some distance to the east/southeast (in the area currently occupied by the H U Sverdrupfjella region of the high-grade Maudheim Province). This easterly location/positioning of the Ahlmannryggen basin depo-centre provides strong evidence in favour of an extended cratonic province, with an orogenic belt originally restricted to its southern margin.

1.2.4 Tectonic Setting and Sediment Fill

Determination of the tectonic setting of the sedimentary basin has been problematic, often due to poor age constraints during initial studies. Early interpretations suggested an epeirogenic intracontinental setting, considerably older than the Kibaran collisional event (Wolmarans and Kent, 1982). When improved age constraints revealed an association with Kibaran orogenesis, Barton *et al.* (1987) and Groenewald *et al.* (1995) suggested that the Ritscherflya Supergroup accumulated in a foreland basin setting, while Moyes *et al.* (1995a) suggested development in fault bounded intracratonic basins resulting from isostatic uplift following Kibaran age orogenesis. More recently, Moyes and Harris, (1996) suggested that deposition occurred in either a retroarc or peripheral foreland basin setting.

Based on its age, location and sedimentological characteristics, a peripheral foreland basin model is favoured for the Ahlmannryggen Group. The sedimentary sequence is considered to have accumulated in an elongate basin formed on the margin of the Grunehogna Province in response to docking of the Maudheim Province island arc terrain. In such a setting, the subsiding peripheral foreland basin would have received a combination of detritus shed from the arc terrain and the Grunehogna Province basement and pre-existing cover rocks. This interpretation is supported by numerous tectonic discrimination schemes, which reveal that an active continental margin signature dominates in the Ahlmann-ryggen Group. The minor passive margin signature observed on some of the discrimination diagrams is attributed to input from an extensive sedimentary source terrain, while the presence of abundant volcaniclastic material, derived from the contemporaneously active arc system, accounts for the island arc signature identified in some discrimination schemes. A peripheral foreland basin model is also supported by results of a gravity survey (Corner, 1994), which reveals a profile consistent with those obtained over other boundaries between stable cratons and younger accreted terrains (e.g. the Alps, Figure 1.2).

Foreland basins are characteristically elongate, rapidly subsiding troughs that form adjacent to orogenic belts, where crustal loading causes down-warping of the adjacent lithosphere (Beaumont, 1981; Watts *et al.*, 1982). As described by Sinclair and Allen (1992), during the early stages of foreland basin evolution, rapid subsidence overwhelms the sedimentation rate, leading to an underfilled phase of deep marine sedimentation (Figure 1.3). The available accommodation space is gradually consumed by sedimentation as the basin evolves into a filled phase of shallow marine deposition. Non-marine sedimentation dominates the final, overfilled phase of the basin. The sandstone to fine-grained dominated, fluvial braidplain/delta plain sequences of the Ahlmannryggen Group are considered to have accumulated during this final overfilled phase. Unfortunately, the extensive ice cover prohibits determination of the nature of the underlying rocks, and as such it is impossible to confirm the presence of underlying marine sequences.

The fluvial styles interpreted in Section B indicate perennial streams, with more or less constant discharge. Under these constant discharge conditions, the change from braidplain to delta plain environments suggests a tectonic control on accommodation and sedimentation. As such, the sedimentation patterns in the Ahlmannryggen Group may be explained in terms of tectonic cycles of orogenic loading and unloading (Figure 1.3):

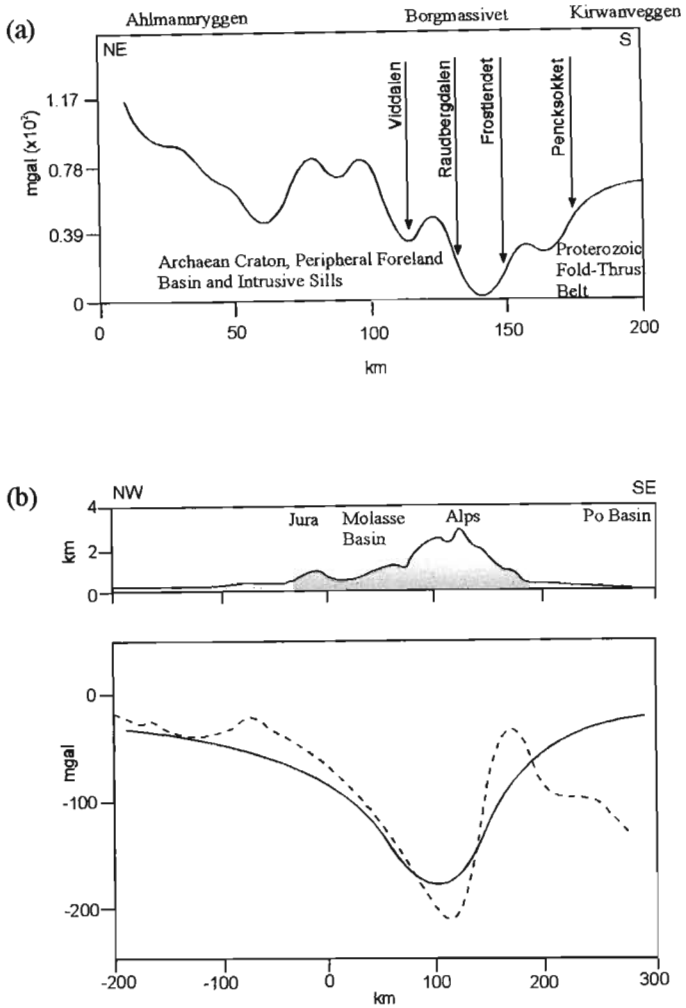

Figure 1.2: (a) Observed Bouguer gravity data, corrected for ice thickness, along a profile extending from the northern Ahlmannryggen, through the central Borgmassivet to the central Kirwanveggen (from Corner, 1994). This gravity profile is similar to profiles obtained over other boundaries between stable cratons and younger, accreted terrains, e.g. the Alps, as shown in (b). (b) Topography and measured Bouger anomalies (dotted line, lacking terrain corrections) along a NW-SE section across the Alps and North Alpine Foreland Basin. Solid line represents the computed Bouguer anomaly assuming local (Airy) isostatic equilibrium (adapted from Allen and Allen, 1990).

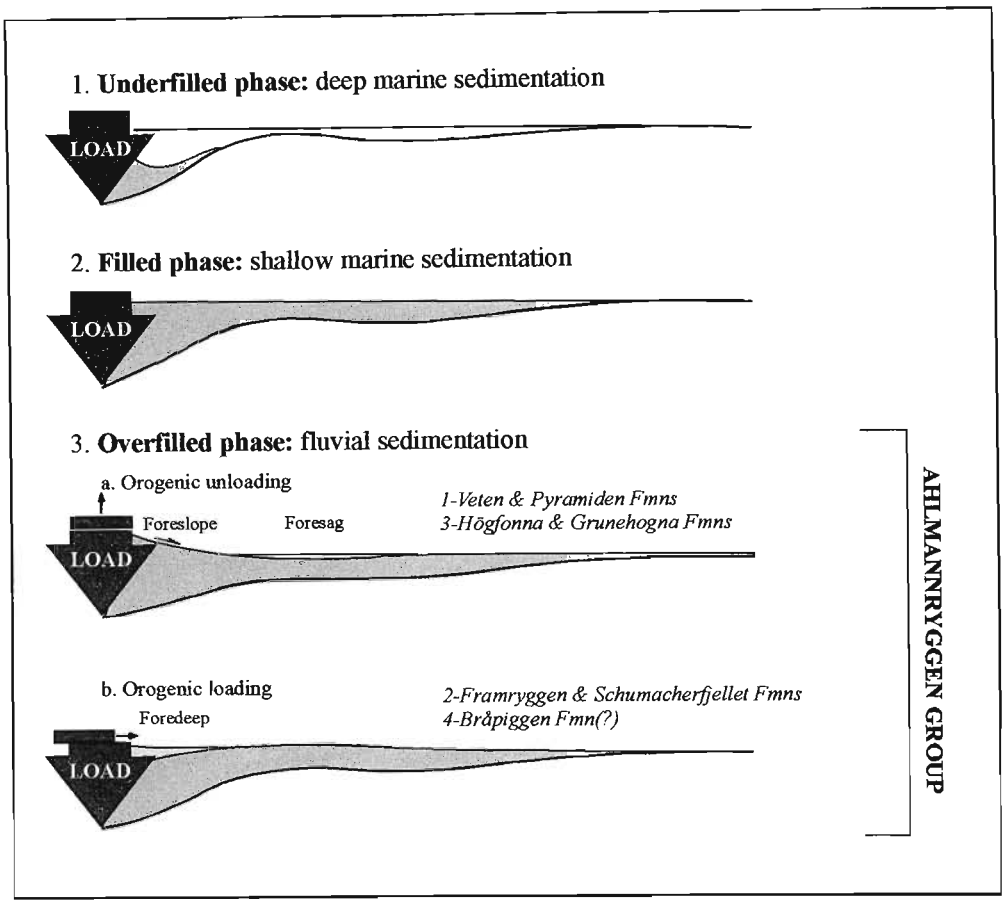

Figure 1.3: Sedimentation relative to accommodation in a foreland system (after Sinclair and Allen, 1992; Catuneanu and Elango, 2001). During early stages of basin evolution, rapid subsidence overwhelms sedimentation rates, resulting in an underfilled phase of deep marine sedimentation. As the available accommodation space is consumed, the basin evolves into a filled phase of shallow marine sedimentation. Nonmarine sedimentation dominates in the final, overfilled phase of basin evolution. The Ahlmannryggen Group is regarded as having accumulated within the foresag and foredeep during this final overfilled stage, with variations in the sedimentation pattern reflecting episodes of orogenic loading and unloading. Orogenic unloading results in flexural uplift and steepening of the topographic slope, while orogenic loading leads to differential subsidence and lowering of the topographic gradient. The depocentre migrates between the foredeep (during loading) and the foresag (during unloading).

- the coarse-grained Veten and Pyramiden Formations accumulated in transverse fluvial braidplains that extended across both the Borgmassivet and Ahlmannryggen regions (Stage 1 of Section B4), and are regarded as representing deposition during orogenic unloading.
- the overlying Framryggen and Schumacher-fjellet Formations indicate a change to distal, delta plain conditions and migration of the longitudinal drainage system towards the orogenic front (Stage 2 of Section B4). The change in the sedimentation pattern is attributed to orogenic loading, and an associated migration of the basin axis towards the foredeep (e.g. Sinclair and Allen, 1992; Catuneanu and Elango, 2001).
- the Högfonna and Grunehogna Formations record a return to conditions dominated by orogenic unloading, and deposition of coarse-grained sediment and anti-tectonic gravels on a fluvial braidplain (e.g. Blair and Bilodeau, 1988; Heller and Frost, 1988; Heller and Paola, 1992) (Stage 3 of Section B4).
- a final episode of orogenic loading is possibly recorded in the Bråpiggen Formation, although limited exposure prohibits definite recognition (Stage 4 of Section B4).

Within most foreland basin systems, high energy fluvial systems tend to extend further away, in a distal direction, from the thrust front with time, in response to progradation of the orogenic front (e.g. Beaumont, 1981; Raynolds and Jonson, 1985; Puigdefrabregas *et al.*, 1986; Sinclair and Allen, 1992; Catuneanu and Elango, 2001). This pattern is not observed in the Ahlmannryggen Group basin, and instead a gradual southward migration, towards the thrust belt, is suggested. This may be due to the limited nature of the exposed basin fill (only ~1600m), which may not record such higher order variations. Alternatively, the rheological properties of the underlying lithosphere may have been affected by magmatic influences related to the establishment of the source for the Borgmassivet Suite, which was emplaced prior to consolidation of the sediments (Krynauw *et al.*, 1988). Heat flow from this source may have lowered the flexural rigidity of the lithosphere, resulting in a narrowing of the foreland basin.

1.2.5 Source Terrains

Apart from providing a record of the Kibaran and Pan-African evolution of the Grunehogna Province, the Ahlmannryggen Group also provides insights into the Archaean and Proterozoic lithological configuration of the region through an understanding of its provenance characteristics. Detritus entering the basin was sourced from a wide variety of terrains, imparting a complicated provenance signature to the Ahlmannryggen Group sediments. An integrated provenance study revealed that sediment originated either directly or indirectly from at least seven distinct sources.

Contemporaneous volcanicity in the Maudheim Province island arc terrain is considered a likely source for the *ca.* 1130Ma volcaniclastics present in the Ahlmannryggen Group, with the highest abundances recorded from the more southerly/ proximal regions of the Borgmassivet. Uplifted portions of this island arc terrain represent a probable source for the metamorphic component, which is also best represented in the more proximal exposures of the Borgmassivet. A number of magmatic sources, aged between 1600Ma and 3400Ma, are represented in part by the Annandagstoppane basement granite, presently outcropping to the west of the preserved basin sequence. Contributions from a sedimentary terrain dominated by a banded ironstone association are clearly indicated by the ubiquitous presence of abundant chert and quartzite clasts and rare magnetite pebbles in the gravel deposits. Unfortunately, no likely sedimentary source is currently exposed in WDML, however this association may represent an early platform sequence developed along a passive margin of the Grunehogna Province prior to the onset of Kibaran orogenesis. Two separate metamorphic terrains, with ages of *ca.* 1335Ma and *ca.* 2600Ma, are also recognised, but are not exposed.

The generally immature nature of the Ahlmannryggen Group sediments suggests rapid erosion rates and limited chemical weathering predominated within the source terrains. Although many of the inferred provenance terrains are not exposed in WDML, a local source for the detritus entering the basin is evidenced by the abundance of unstable lithic and mineral grains, including volcanic, schistose metamorphic and feldspar grains.

2. REGIONAL TECTONICS

2.1 INTRODUCTION

The Grunehogna Province cover rocks provide insight into the two main episodes of tectonism to have affected this Archaean fragment since the Proterozoic. The first resulted in the formation of a peripheral foreland basin and accumulation of the Ahlmannryggen Group. The second event involved progressive ductile to brittle strike-slip deformation of the cover sequence and rotation of the adjacent orogenic belt. These events are considered directly related supercontinental amalgamation.

2.2 SUPERCONTINENT AMALGAMATION

2.2.1 Rodinia

The life cycle of the Rodinia supercontinent is represented by its birth in a series of Meso- to Neoproterozoic collisions lumped under the terms 'Grenvillian' and 'Kibaran', and by its break-up recorded in late Neoproterozoic rifting and passive margin successions (Dewey and Burke, 1973; Bond *et al.*, 1984; Dalziel, 1991, 1992; Moores, 1991; Hoffman, 1991; Powell *et al.*, 1993). The accretion of the Maudheim Province island arc terrain onto the southern margin of the Grunehogna Province represents one of the numerous collisional events marking the gradual assembly of this supercontinent.

During the Mesoproterozoic, subduction occurred under a fragment of crust referred to as the 'East Antarctic Craton' by Groenewald *et al.* (1995), resulting in the formation of a volcanic arc and back-arc/marginal basin (Moyes *et al.*, 1993; Groenewald *et al.*, 1995; Grantham *et al.*, 1995). By *ca.* 1130Ma, collision of this crustal fragment with the Grunehogna Province had resulted in accretion of the arc-basin terrain and the formation of a linear, Kibaran-age orogenic belt (Arndt *et al.*, 1991; Groenewald *et al.*, 1995). There is no direct evidence supporting the existence of the 'East Antarctic Craton', which is apparently masked by the extensive ice cover encountered on the Antarctic plateau, however its presence in the region between WDML and the Shackleton Range is inferred based on isotopic studies (e.g. Arndt *et al.*, 1991).

The tectonic expression of this collisional event on the under-riding portion of crust involved the formation of a peripheral foreland basin on the Grunehogna Province, in which the Ahlmannryggen Group accumulated. Earlier interpretations of this volcano-sedimentary sequence had suggested an epeirogenic intracontinental basin setting, considerably older than the Kibaran collisional event (Wolmarans and Kent, 1982). However improved age constraints and provenance studies indicate that the development of the Ahlmannryggen Group basin is closely linked to the evolution of the adjacent high-grade belt, and deposition was contemporaneous with the development of the Mesoproterozoic orogenic Maudheim Province.

The subsequent emplacement of the Borgmassivet Suite is possibly related to a large-scale mantle thermal anomaly, rather than the local style of plate assembly as was suggested by Moyes and Harris (1996). A widespread igneous event at *ca.* 1105Ma apparently affected both Laurentia and the Zimbabwe/Kaapvaal Cratons of southern Africa, as evidenced by the coeval development of the Keweenawan and Umkondo igneous suites (Hanson *et al.*, 1998; Powell *et al.*, 2001; Wingate, 2001). Similar aged mafic intrusions are also recorded in Australia (1116 ±12Ma; Tanaka and Idnurm, 1994). Considering that palaeomagnetic data indicate a juxtapositioning of the Grunehogna Province with the Zimbabwe/Kaapvaal Cratons at this stage (Gose *et al.*, 1997) and that a pre-1080ma age is favoured for the Borgmassivet Suite, the generation of this voluminous igneous suite may have resulted from the same widespread event.

2.2.2 Gondwana

The break-up of Rodinia and subsequent assembly of Gondwana took place during the late Precambrian and early Palaeozoic, between ~0.7Ga and ~0.5Ga (e.g. Moores, 1991; Hoffman, 1991; Kröner *et al.*, 1992). These events were characterised by the opening of the Pacific Ocean basin, while the Mozambique Ocean, which originally separated East and West Gondwana, was consumed (Burke and Dewey, 1972; Kröner, 1979; 1991).

The location of the final suture zone between East and West Gondwana is controversial, however it is considered by a number of researchers to extend from the East African Orogen into central Dronning Maud Land (CDML) and ultimately to the Shackleton Range (e.g. Jacobs *et al.*, 1995; Wilson *et al.*, 1997; Gose *et al.*, 1997; Jacobs and Thomas, 1999; Board, 2001). Shackleton (1996) had interpreted the Pencksökket-Jutulstraumen divide as representing a possible East-West Gondwana suture zone, however numerous studies describe the tectonic continuity of the Proterozoic high-grade Maudheim Province across this dislocation (e.g. Groenewald *et al.*, 1991; Grantham *et al.*, 1995; Groenewald *et al.*, 1995). In addition, the Grunehogna Province is also thought to extend east of the Pencksökket-Jutulstraumen system (this study-Section D1), providing a further basis for rejecting Shackleton's interpretation. This feature is instead attributed to Pan-African reactivation of the original Proterozoic suture zone between the Grunehogna Province and the Maudheim Province.

The thermo-magmatic effects of Pan-African overprinting in WDML are well documented, however the tectonic expression of this event is often controversial. Conflicting models have been developed which alternatively propose pervasive reworking (e.g. Grantham *et al.*, 1995; Groenewald *et al.*, 1995) or limit effects to thermal overprinting (e.g. Moyes *et al.*, 1993; Groenewald, 1995). However the presence of an extensive Pan-African strike-slip system along the margin of the Grunehogna Province and within the Kirwanveggen region suggests significant reworking of the Kibaran Maudheim Province during Gondwana amalgamation. As suggested by Allen (1991) and this study, sinistral displacement along a PDZ located within the Pencksökket-Jutulstraumen divide may account for the juxtapositioning of the high-grade belt of the Maudheim Province against the presently defined eastern margin of the Grunehogna Province. Palaeocurrent evidence from the Ahlmannryggen Group indicates that during the Proterozoic evolution of this peripheral foreland basin, the basin depo-centre was located some distance to the east or south-east of the currently exposed sequence, in an region presently occupied by the H. U. Sverdrupfjella portion of the Maudheim Province. This inferred easterly extension of the original basin provides evidence in favour of a more extensive cratonic province, with a high-grade belt initially restricted to its southern margin and the current positioning only achieved during the compressive Pan-African event, due to shearing and strike-slip displacement.

2.3 PALAEOGEOGRAPHIC RECONSTRUCTIONS

The juxtapositioning of the Grunehogna Province with the Kaapvaal/Zimbabwe Cratons of southern Africa, which had initially been achieved during Rodinia amalgamation, appears to have been maintained during the assembly of Gondwana. However, a major problem in palaeogeographic reconstructions is the precise relative positioning of the African and Antarctic landmasses. The contact regions are masked by a thick Cretaceous-Tertiary sequence in Mozambique, and by ice in Antarctica, while marine geophysical anomalies are not definitive, resulting in both 'loose fit' (e.g. De Wit *et al.*, 1988) and 'tight fit' models being proposed (e.g. Roeser *et al.*, 1996). The Pan-African sinistral strike-slip system identified in WDML (Section C3) has important implications regarding the validity of these different refit models.

'Tight-fit' reconstructions such as those of Grantham *et al.* (1988), Groenewald *et al.* (1991) and Roeser *et al.* (1996) suggest that the Grunehogna Province was positioned close against the present eastern edge of the Kaapvaal Craton and generally consider it to represent a fragmented portion of the Craton (Figure 2.1). In such a scenario, the Lebombo and Explora Escarpments form conjugate facing continental margins, and separation of the Grunehogna Province from the Kaapvaal Craton is attributed to Jurassic-aged rifting during the break-up of Gondwana. In these models, the Proterozoic Maudheim Province is a continuation of the Natal and Mozambique Belts, while the Ahlmannryggen Group may be linked to the Umkondo Group of Mozambique/Zimbabwe, possibly representing medial to distal depositories within the same system.

Problems with such a 'tight-fit' model arise when the Pan-African strike-slip deformation in WDML is taken into consideration. This large-scale, regionally extensive strike-slip system can be expected to have extended beyond the immediate vicinity of the Grunehogna Province,

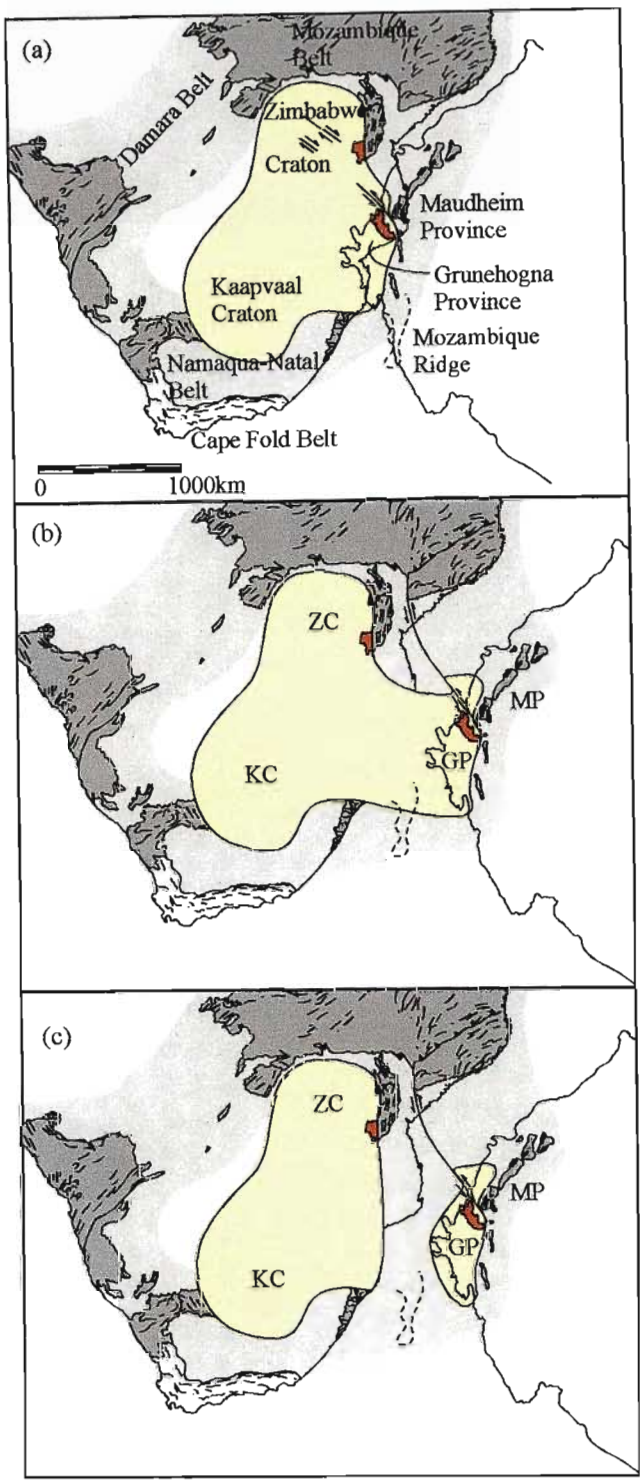

Figure 2.1:(a) A 'tight-fit' Gondwana reconstruction (e.g. Roeser *et al.*, 1996), in which the Grunehogna Province represents a fragment of the Kaapvaal Craton, is rejected based on the nature of the Pan-African strike-slip system identified in WDML. (b) A 'loose-fit' (e.g. De Wit *et al.*, 1988), extended Kaapvaal Craton model is also rejected, as this necessitates a dramatic change in orientation of the N-S striking Mozambique Belt. (c) A 'loose-fit' model in which the Grunehogna Province exists as a separate micro-plate is favoured, implying that the region between the Kaapvaal Craton and Grunehogna Province is occupied by Proterozoic crust.

and continuation into adjacent regions is highly probable. In the 'tight-fit' model, continuation of the PDZ inferred along the Pencksökket-Jutulstraumen dislocation requires the presence of north-west to south-east trending faults within the Zimbabwe Craton region. However, the only suitably orientated strike-slip faults were last active during the Proterozoic and are dextral in nature (Wilson, 1990). Additional complications with the 'tight-fit' model are revealed when the Mozambique Ridge is taken into account. This section of submerged crust is often neglected in palaeogeographic reconstructions (e.g. Groenewald *et al.*, 1991; Roeser *et al.*, 1996). According to Mougenot *et al.* (1991) the Mozambique Ridge consists of Archaean crust which had been reworked in the Proterozoic, and tholeiitic basalts of Karoo affinity, suggesting that this segment of crust is a continental fragment of Africa. A position between the Falkland Plateau (to the west) and the Explora Escarpment of the Antarctica margin (to the east) is therefore favoured by Mougenot *et al.* (1991), a location difficult to accommodate in a 'tight-fit' model.

An alternative is to consider the Grunehogna Province as an extension of the Kaapvaal Craton, but in an overall 'loose-fit' scenario in which these two terrains are arranged in pre-Gondwana break-up positions similar to those suggested by De Wit *et al.* (1988) (Figure 2.1b). A 'loose-fit' model such as this implies the existence of an extensive region of Archaean crust, which originally linked the Kaapvaal Craton and Grunehogna Province. In such a reconstruction, the Mozambique Ridge can be accommodated relatively easily and, in addition, the Pan-African strike-slip deformation in WDML can be correlated with structures exposed in northern Mozambique. However, the distinct north – south trend of the southern portion of the Mozambique Belt represents an obvious restriction in such a model as this orogenic province would apparently trend/strike directly into the extended Archaean crust unless a dramatic >90° swing in the orientation of the belt occurs. Considering the highly consistent north-south structural trends observed in the Mozambique Belt, such a possibility seems unlikely.

A final option is to retain the 'loose-fit' reconstruction of De Wit *et al.* (1988), but with the Grunehogna Province recognised as a discrete microplate, separate from the Kaapvaal Craton (Figure 2.1c). In such a model, the pre-Gondwana break-up position of the Grunehogna Province would have been attained during Rodinia amalgamation, implying that the region between the Archaean microplate and the Kaapvaal Craton was occupied by Proterozoic crust. Palaeomagnetic data clearly indicate that the Grunehogna Province and Kaapvaal Craton were closely juxtapositioned by 1.1Ga (Gose *et al.*, 1997), suggesting that the closure of any dividing ocean basin must have been completed by this stage. Evidence for the subduction of oceanic crust beneath the Kaapvaal Craton in the period 1.4-1.2Ga is provided by the numerous alkali complexes of this age found in the north-eastern regions of South Africa (Tankard *et al.*, 1982), and the presence of *ca.* 1.2Ga xenocrystic zircons in the Lebombo rhyolites (Van Niekerk, 1968). The presence of Proterozoic crust accreted along the eastern margin of the Kaapvaal Craton during Rodinia amalgamation is also implied by Basson (2000), based on a tectonic history of the Kibaran collision between the Kaapvaal Craton and Natal Metamorphic Province, which indicates that the Kaapvaal Craton did not extend significantly further eastwards from the present margin. It is therefore proposed that a continuation of the north-south trending Mozambique Belt may represent a suture zone between the Grunehogna Province microplate and the Kaapvaal Craton. Unfortunately, this region is masked by thick Cretaceous-Tertiary cover, which effectively obscures the nature of the underlying crust.

Further implications of this final model are that the Ritscherflya Supergroup and Umkondo Group basins developed in isolation, which would account for the sedimentological variations observed between these two systems (e.g. Swanepoel, 1995). In addition, the Mozambique Ridge is readily accommodated, while continuation of the strike-slip system into adjacent regions can be accounted for - a northward projection of the PDZ inferred along the Pencksökket-Jutulstraumen dislocation extends to the western edge of the ENE-WSW trending Lurio Belt of northern Mozambique, which according to Pinna *et al.* (1993), swings southwards to merge with sinistral Pan-African shear zones.

2.4 TWO-PHASE GONDWANA ASSEMBLY

The assembly of the Gondwana supercontinent apparently consisted of two distinct phases. Investigations in Kenya, Tanzania and Madagascar reveal an early collision event, between 650Ma and 750Ma (Mosley, 1993; Muhongo, 1997; Nedelec *et al.*, 2000), while elsewhere, a later ~550Ma event is recognised (e.g. Shiraishi *et al.*, 1994). The first event involved island arc accretion, ophiolite obduction and the development of the extensive ~N-S trending fold axes and thrust zones in the region of the East African Orogen (Stern, 1994; Shackleton, 1996). Slightly more enigmatic is the later NW-SE transpressive event, which resulted in the development of extensive sinistral strike-slip faults and shear zones in east Africa (e.g. Pinna *et al.*, 1993), Madagascar (e.g. Kriegsman, 1995; Nedelec *et al.*, 2000), India (e.g. Drury *et al.*, 1984), CDML (e.g. Jacobs *et al.*, 1998) and WDML. The first event is considered a result of the closure of the Mozambique Ocean and suturing of East and West Gondwana prior to 600Ma (e.g. Shackleton, 1996; Nedelec *et al.*, 2000), while the later strike-slip event may be related to escape tectonics developing between 550Ma and 520Ma, in response to the Ross Orogeny along the southern margin of East Antarctica (Figure 2.2).

The Cental Asian collision zone of India and Eurasia provides an attractive modern analogy for the late stage strike-slip tectonism recorded in Antarctica and Africa. India represents a rigid indentor driven into the Asian continent, resulting in a combination of thrust and strike-slip displacements (Molnar and Tapponnier, 1975; Tapponnier and Molnar, 1976). As a result of the northward progress of the India block, two wedges of Asian crust, the Indo-China block and the China block, have escaped to the southeast (Tapponnier *et al.*, 1985). A similar tectonic regime is envisaged during the later stages of Gondwana amalgamation, where northeast directed collision during the Cambro-Ordovician Ross Orogeny (Gunn and Warren, 1962) may have resulted in a wedge of East Antarctic lithosphere escaping to the north/northwest. The movement of this escaping block along the strike-slip system identified in WDML can explain enigmatic Pan-African shortening observed in the Lurio Belt of Mozambique, while the Shackleton Range in Antarctica can be equated to the Pamir "Knot" in the Himalayan collision, where three intersecting orogenic belts also occur. The physiographic divide between the Archaean Grunehogna Province and the Proterozoic high-grade Maudheim Province represents a pre-existing crustal boundary preferentially exploited as a zone of weakness during this event.

In addition, the northwest movement of the escaping block may have resulted in large-scale uplift and the formation of a late Pan-African aged plateau region in SE Africa, erosion of which could have supplied detritus to the 490Ma Natal Group exposed in the Kwa-Zulu Natal province of South Africa. According to Thomas *et al.* (1992), palaeocurrent and K-Ar/^{40}Ar-^{39}Ar age data indicate that the source region for the Natal Group was an elevated area bearing a Pan-African signature, probably located in southern Mozambique. Immature detritus was sourced from this elevated region, and transported south and southwestwards by fluvial systems. Thomas *et al.* (1992) therefore conclude that the Natal Group represents a continental, post-orogenic molasse deposit, derived from rapid erosion of an elevated Pan-African mountain chain adjacent to SE Africa. The escape tectonics model proposed here provides a possible explanation for the development of this elevated terrain.

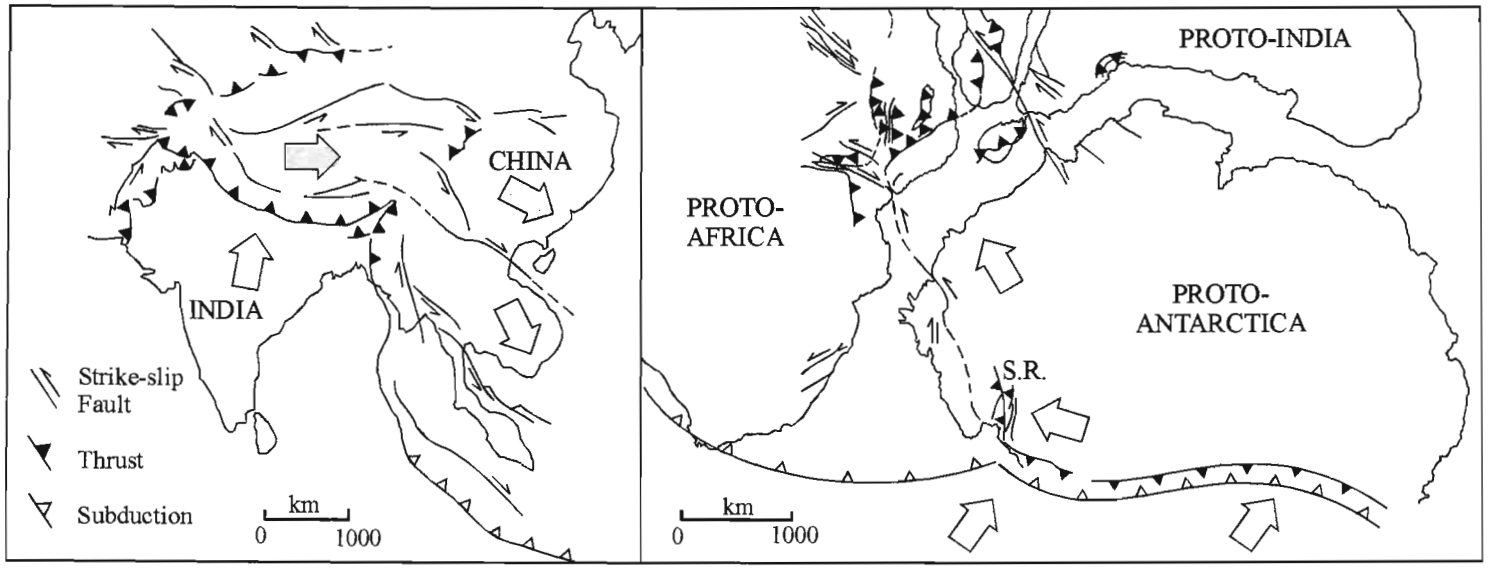

Figure 2.2: During the final stages of Gondwana amalgamation, NE directed collision along the Ross Orogen may have resulted in a wedge of proto-Antarctic lithosphere escaping to the N/NW. This is almost a mirror image of the present-day escape tectonics occurring around India, where the northward progress of the India block has resulted in two wedges of Asian crust, the Indo-China block and the China block, escaping to the SE (Tapponnier *et al.*, 1985).

3. CONCLUSIONS

The Mesoproterozoic Ritscherflya Supergroup forms an extensive volcano-sedimentary cover sequence on the Archaean Grunehogna Province of WDML, Antarctica. Investigations into the nature of the older, predominantly sedimentary successions, which are assigned to the Ahlmannryggen Group, revealed that:

- the lithostratigraphy of the Ahlmann-ryggen Group is best represented by separate subdivisions for the two geographical areas in which exposures crop out. These include the Pyramiden (>600m), Schumacherfjellet (*ca.* 390m) and Grunehogna (>500m) Formations, to which exposures within the Ahlmannryggen region are assigned, and the Veten (>175m), Framryggen (*ca.* 600m), Högfonna (*ca.* 300m) and Bråpiggen (>490m) Formations, defined for exposures in the Borgmassivet region.

- overall, broadly similar lithostratigraphic characteristics are displayed in both regions, and although the two sequences have been assigned separate subdivisions, they are considered to represent contemporaneous sedimentation in different portions of the same basin, under similar depositional conditions.

- the Ahlmannryggen Group is a sandstone to fine-grained dominated sequence containing minor gravel deposits, with the presently preserved exposures representing deposition in the medial portion of the basin only. Based on a combination of vertical section and lateral profile analysis, the depositional conditions are interpreted to have varied between braided fluvial and braid delta plain environments. palaeocurrent orientations suggest the presence of both transverse and longitudinal drainage systems, with the main depo-centre of the basin located to the east/southeast of the exposed sequence.

- detritus entering the basin was sourced either directly or indirectly from at least seven different terrains. These included equivalents of the presently exposed basement of the Maudheim Province and Archaean basement granites of the Grunehogna Province. Contemporaneous volcanic activity within the Maudheim Province island arc terrain represented a likely source for the volcaniclastic material present in the sequence. Additional source terrains included a banded ironstone association, at least two further magmatic provinces and two separate metamorphic terrains, none of which are presently exposed in WDML.

- the development of the basin can be attributed to continental collision and the accretion of the Maudheim Province island arc terrain onto the margin of the Grunehogna Province during the Mesoproterozoic, resulting in flexing of the under-riding crust to form a peripheral foreland basin.

- the presently exposed portion of the Ahlmannryggen Group represents deposition during the final, overfilled phase of the peripheral foreland basin, with variations in sedimentation patterns attributable to periods of orogenic loading and unloading.

- the Grunehogna Province cover rocks, often considered to be relatively undisturbed (e.g. Grantham and Hunter, 1991; Moyes *et al.*, 1993; Krynauw, 1996), have been affected by a combination of ductile and brittle deformation. This deformation is attributed to the development of a regionally extensive strike-slip system during the Pan-African, and can be correlated with strike-slip deformation observed in the southern Kirwanveggen (Croaker, 1999; Croaker *et al.*, 1999).

- sinistral displacement along secondary faults originating from the principal displacement zone located in the Pencksökket-Jutulstraumen divide resulted in the formation and rotation of large-scale buckle folds (D_1), and brittle strike-slip faulting (D_2) of the cover sequence. The

development of rhomb-shaped grabens in regions of transtension is considered responsible for the localised juxtapositioning of overlying Jutulstraumen Group volcaniclastics with the Ahlmannryggen Group sediments.

- within a regional tectonic framework, the development of the Maudheim Province fold-thrust belt and the formation of the Ahlmannryggen Group peripheral foreland basin can be attributed to continental collision during the early stages of the assembly of the supercontinent Rodinia.

- the Pan-African strike-slip deformation is related to Gondwana amalgamation. The assembly of the Gondwana supercontinent consisted of two distinct stages. The first phase is commonly attributed to the closure of the Mozambique ocean and suturing of East and West Gondwana between 750Ma and 650Ma, and was characterised by ophiolite obduction, island arc accretion and the development of extensive north-south trending fold axes and thrust zones (e.g. Stern, 1994; Shackleton, 1996; Nedelec *et al.*, 2000). The second stage was apparently characterised by the development development of extensive strike-slip faults and shear zones in east Africa, Madagascar, India, CDML and WDML at ~550Ma (e.g. Drury *et al.*, 1984; Pinna *et al.*, 1993; Kriegsman, 1995; Jacobs *et al.*, 1998; Nedelec *et al.*, 2000). This later event may be related to escape tectonics developing in response to the Ross orogeny and the suturing of east and west Antarctica.

- the Grunehogna Province represents an isolated microplate, as proposed by Barton *et al.* (1987), rather that a fragmented extension of the Kaapvaal Craton of southern Africa, as suggested by Groenewald *et al.* (1995). Juxtapositioning of these crustal blocks is considered to have been achieved during the early stages of Rodinia amalgamation, and an overall lose fit arrangement with southern Africa, such as that proposed by De Wit *et al.* (1988), is favoured. The Ahlmannryggen Group is therefore not considered to be an extension of sedimentary sequences exposed in southern Africa (such as the Umkondo Group of Mozambique/Zimbabwe), but is instead regarded as a localised basin, the development of which was restricted to the southern margin of the Grunehogna Province.

REFERENCES

Abbey, S. (1989). The evaluation of reference material for rock analysis. In: Ahmedali, S. T. (Ed.), *X-ray fluorescence analysis in the geological sciences: Advances in methodology.* Geol. Assoc. Canada: Short Course 7, 38pp.

Allen, A. R. (1991) The tectonic and metamorphic evolution of H.U. Sverdrupfjella, western Dronning Maud Land, Antarctica. In: Thomson, M. R. A., Crame, J. A. and Thomson, J. W. (Eds.), *Geological evolution of Antarctica*, Cambridge University Press, Cambridge, 53-60.

Allen, J. R. L. (1964). Studies in fluviatile sedimentation: six cyclothems from the Lower Old Red Sandstone, Anglo-Welsh basin. *Sediment.*, **3**, 163-198.

Allen, J. R. L. (1983). Studies in fluviatile sedimentation: bars, bar complexes and sandstone sheets (low sinousity braided streams) in the Brownstones (L.Devonian), Welsh Borders. *Sediment. Geol.*, **33,** 237-293.

Allen, J. R. L. (1984). *Sedimentary structures: their character and physical basis.* Elsevier, Amsterdam, 663pp.

Allen, P. A. and Allen, J. R. (1990). *Basin analysis: Principles and applications.* Blackwell Science, Great Britain.

Arndt, N. T.,Todt, W., Chauvel, C., Tapfer, M. and Weber, K. (1991). U/Pb zircon age and Nd isotopic composition of granitoids, charnockites and supracrustal rocks from Heimefrontfjella, Antarctica. *Geol. Rundsch.*, **80,** 759-777.

Ashley, A. (1990). Classification of large-scale subaqueous bedforms: a new look at an old problem. *J. Sediment. Petrol.*, **60,** 160-172.

Aucamp, A. P. H. (1972). The geology of Grunehonga, Ahlmannrtggen, western Dronning Maud Land. *S. Afr. J. Antarct. Res.*, **2,** 16-22.

Aydin, A. and Nur, A. (1982). Evolution of pull-apart basins and their scale independence. *Tectonics*, **1**, 91-105.

Baker, J. C., Fielding, C. R., Caritat, P. and Wilkinson, M. M. (1993). Permian evolution of sandstone composition in a complex back-arc extensional to foreland basin: the Bowen Basin, eastern Australia. *J. Sediment. Petrol.*, **63**, 881-893.

Barrett, P. J. and Fitzgerald, P. G. (1985). Deposition of the lower Feather Conglomerate, a Permian braided river deposit in southern Victoria Land, Antarctica, with notes on the regional paleogeography. *Sediment. Geol.*, **45**, 189-208.

Barton, J. M., Klemd, R., Allsopp, H. L., Auret, S. H. and Copperthwaite, Y. E. (1987). The geology and geochronology of the Annandagstoppane granite, western Dronning Maud Land, Antarctica. *Contrib. Mineral. Petrol.*, **97,** 488-496.

Basson, I. J. (2000) *The structural, metamorphic and tectonic context of selected sub-economic veining in the Natal Thrust Front and Natal Nappe Zone, northern Kwazulu-Natal.* Ph.D. thesis, University of Natal, Durban, 362 pp.

Basu, A., Young, S. W., Suttner, L. J., James, W. C. and Mack, G. H. (1975). Re-evaluation of the use of undulatory extinction and polycrystallinity in detrital quartz for provenance determination. *J. Sediment. Petrol.*, **45**, 873-882.

Beaumont, C. (1981). Foreland basins. *Geophys. J. R. Astr. Soc.*, **65**, 291-329

Beukes, N. J. and Klein, C. (1990). Geochemistry and sedimentology of a facies transition-from microbanded to granular iron-formation in the early Proterozoic Transvaal Supergroup, South Africa. *Precamb. Res.*, **47**, 99-139.

Bhatia, M. R. (1981). *Petrology, geochemistry and tectonic setting of some flysch deposits.* PhD thesis, Australian National University, Canberra, 382pp.

Bhatia, M. R. (1983). Plate tectonics and geochemical composition of sandstones. *J. Geol.*, **91**, 611-627.

Bhatia, M. R. and Crook, K. A. W. (1986). Trace elements characteristics of graywackes and tectonic setting discrimination of sedimentary basins. *Contrib. Mineral. Petrol.*, **92**, 181-193.

Blair, T. C. and Bilodeau, W. L. (1988). Development of tectonic cyclotherms in rift, pull-apart and foreland basins: sedimentary response to episodic tectonism. *Geology*, **16**, 517-520.

Blatt, H. (1967). Provenance determination and the recycling of sediments. *J. Sediment. Petrol.*, **37**, 1031-1044.

Blatt, H., Middleton, G. and Murray, R. (1980). *Origin of Sedimentary Rocks.* Prentice-Hall, Inc., New Jersey, 782pp.

Board, W. (2001). *Tectonothermal evolution of selected areas of the eastern H.U. Sverdrupfjella, western Dronning Maud Land, Antarctica.* Final project report submitted to the South African National Antarctic Programme, Department of

Environment and Tourism Directorate: Antarctica and Islands, South Africa, 16 pp.

Bond, G. C., Nickeson, P. A. and Kominz, M. A. (1984). Breakup of a supercontinent between 625 and 555Ma: new evidence and implications for continental histories. *Earth Planet. Sci. Lett.*, **70**, 325-345.

Boothroyd, J. C. and Ashley, G. M. (1975). Process, bar morphology and sedimentary structures on braided outwash fans, North-eastern gulf of Alaska. In: Jopling, A. V. and McDonald, B. C. (Eds.), Glaciofluvial and glaciolacustrine sedimentation. *Spec. Publ. Soc. Econ. Paleont. Miner.*, **23**, 193-222.

Brandl, G. (1983). *The geology of the Pietersburg Area: Expl. Sheet 2328 (Pietersburg).* Geol. Surv. S. Afr., 43pp.

Bredell, J. H. (1977). The Precambrian sedimentary-volcanic sequence and associated intrusive rocks of the Ahlmannryggen, western Dronning Maud Land: a new interpretation. *3rd Symposium on Antarctic geology and geophysics*, U.S.A.

Bridge, J. S. (1993). Description and interpretation of fluvial deposits: a critical perspective. *Sediment.*, **40,** 801-810.

Brodzikowski, K. and Haluszczak, A. (1987). Flame structures and associated deformations in Quaternary glaciolacustrine and glaciodeltaic deposits: examples from central Poland. In: Jones, M. E. and Preston, M. F. (Eds.), *Deformation of sediments and sedimentary rocks.* Geological Society Special Publication 29, Blackwell Scientific Publications, Great Britain, 11-24.

Bromley, M. H. (1991). Variations in fluvial style as revealed by architectural elements, Kayenta Formation, Mesa Creek, Colorado, USA: evidence for both ephemeral and perennial fluvial processes. In: Miall, A. D. and Tyler, N. (Eds.), *The three-dimensional facies architecture of terrigenous clastic sediments and it implications for hydrocarbon discovery and recovery.* SEPM Concepts in sedimentology and palaeontology, **3**, 94-103.

Burke, K. C. A. and Dewey, J. F. (1972). Orogeny in Africa. In: Dessauvagie, T. J. F. and Whiteman, A. J. (Eds), *African Geology.* Univ. Ibadan, Nigeria, 583-608.

Byrd, R. E. (1947). Our navy explores Antarctica. *The National Geographic Magazine*, XCII(4).

Caby, R., Dostal, J. and Dupuy, C. (1977). Upper Proterozoic volcanic greywackes from northern Hoggar (Algeria). *Precamb. Res.*, **5**, 283-597.

Cant, D. J. and Walker, R. G. (1978). Fluvial processes and facies sequences in the sandy braided South Saskatchewan River, Canada. *Sediment.*, **25,** 625-648.

Catuneanu, O. and Elango, H. N. (2001). Tectonic control on fluvial styles: the Balfour Formation of the Karoo Basin, South Africa. *Sediment. Geol.*, **140**, 291-313.

Christie-Blick, N. and Biddle, K. T. (1985). Deformation and basin formation along strike-slip faults. In: Biddle, K.T. and Christie-Blick, N. (Eds). Strike-slip deformation, basin formation, and sedimentation. *Soc. Econ. Paleont. Mineral. Spec. Publ.*, **37,** 1-34.

Church, M. (1983). Pattern of instability in a wandering gravel bed channel. In: Collinson, J. D. and Lewin, J. (Eds.), Modern and Ancient fluvial Systems. *Int. Assoc. Sediment. Spec. Publ.*, **6,** 169-180.

Collinson, J. D. (1968a). Deltaic sedimentation units in the Upper Carboniferous of northern England. *Sediment.*, **10**, 233-254.

Collinson, J. D. (1968b). The sedimentology of the Grindslow Shales and the Kinderscout Grit: a deltaic complex in the Namurian of northern England. *J. Sediment. Petrol.*, **39**, 194-221.

Collinson, J. D. (1970). Bedforms of the Tana river, Norway. *Geogr. Ann.*, **52A**, 31-55.

Colquhoun, G. P., Fergusson, C. L. and Tye, S. C. (1999). Provenance of early Palaeozoic sandstones, southeastern Australia, Part 2: cratonic to arc switching. *Sediment. Geol.*, **125**, 153-163.

Compston, W., Williams, I. S. and Meyer, C. (1984). U-Pb chronology of zircons from lunar breccia 73217 using sensitive high mass-resolution ion microprobe. In: Proceedings of the 14th Lunar Science Conference. *J. Geophys. Res. Suppl.*, **89**, B525-B354.

Condie, K. C., Wilks, M., Rosen, D. M. and Zolbin, V. L. (1991). Geochemistry of metasediments from the Precambrian Hapschan Series, eastern Anabar Shield, Siberia. *Precamb. Res.*, **50**, 37-47.

Corner, B. (1994). *Geological Evolution of Western Dronning Maud Land within a Gondwana Framework: Geophysics Subprogramme.* Final project report submitted to the South African National Antarctic Programme, Department of Environment and Tourism Directorate: Antarctica and Islands, South Africa, 21 pp.

Cowan, E. J. (1991). The large-scale architecture of the fluvial Westwater Canyon Member, Morrison Formation (Jurassic), San Juan Basin, New Mexico. In Miall A. D., Tyler, N. (Eds), The three-dimensional facies

architecture of terrigenous clastic sediments, and its implication for hydrocarbon discovery and recovery. *Soc. Econ. Paleont. Mineral.*, **3**, 80-93.

Cowen, E. J. (1993). Longitudinal fluvial drainage patterns within a foreland basin-fill: Permo-Triassic Sydney Basin, Australia. *Sediment. Geol.*, **85**, 557-577.

Cox, R. and Lowe, D. R. (1995). A conceptual review of regional-scale controls on the composition of clastic sediment and the co-evolution of continental blocks and their sedimentary cover. *J. Sediment. Res.*, **A65**, 1-12.

Cox, R. and Lowe, D. R. (1996). Quantification of the effects of secondary matrix on the analysis of sandstone composition, and a petrographic-chemical technique for retrieving original framework grain modes of altered sandstones. *J. Sediment. Res.*, **66**, 548-558.

Croaker, M. (1999) *Geological constraints on the evolution of the Urfjell Group, southern Kirwanveggen, western Dronning Maud Land, Antarctica.* M.Sc. thesis, University of Natal, South Africa, 181 pp.

Croaker, M., Jackson, C., Armstrong, A., Whitmore, G., Lindsay, P. and Mare, L. (1999) The Cambrian Urfjell Group, western Dronning Maud Land – sedimentology, structure, isotope and geochemical constraints on the evolution of a strike-slip basin. *Proc. 8th Int. Symp. Antarct. Earth Sci.*, Wellington, 12.

Crook, K. A. W. (1974). Lithogenesis and geotectonics: the significance of compositional variation in flysch arenites (graywackes), In: Dott, R.H., and Shaver, R.H. (Eds.), Modern and ancient geosynclinal sedimentation. *SEPM Spec. Publ.*, **19**, 304-310.

Crowley, K. D. (1983). Large scale bed configuration (macroforms), Platte River basin, Colorado and Nedbraska: primary structures and formative processes. *Geol. Soc. Amer. Bul.*, **94**, 117-133.

Cummings, G. L. and Richards, J. R. (1975). Ore lead isotope ratios in a continuously changing Earth. *Earth Planet. Sci. Letters*, **28,** 155-171.

Cummins, W. A. (1962). The greywacke problem. Liverpool and Manchester *Geol. J.*, **3**, 51-72.

Dalziel, I. W. D. (1991). Pacific margins of Laurentia and East Antarctica-Australia as a conjugate rift pair: evidence and implications for an Eocambrian supercontinent. *Geol.*, **19**, 598-601.

Dalziel, I. W. D. (1992). On the organisation of the American plates in the Neoproterozoic and the breakout of Laurentia. *GSA Today*, **2**, 237-241.

De Ridder, E. (1970). *The sedimentary succession exposed in part of the Borg Massif, western Queen Maud Land, Antarctica.* MSc thesis, University of Pretoria, South Africa.

De Wit, M., Jeffery, M., Bergh, H. and Nicolaysen, L. (1988). *Geological map of sectors of Gondwana, reconstructed to their disposition ~150Ma.* Bernard Price Institute of Geophysical Research, University of the Witwatersrand, South Africa.

Dewey, J. F. and Burke, K. C. A. (1973). Tibetan, Variscan and Precambrian basement reactivation: products of continental collision. *J. Geol.*, **81**, 683-692.

Dickinson, W.R. (1970). Interpreting detrital modes of graywacke and arkose. *J. Sediment. Petrol.*, **40**, 695-707.

Dickinson, W.R. (1985). Interpreting provenance relations from detrital modes of sandstones. In: Zuffa, G.G. (Eds.), *Provenance of arenites.* Proceeding of the NATO Advanced Study Institute on Reading Provenance from Arenites, Cosenza, Itlay, 333-362.

Dickinson, W. R., Beard, L. S., Brakenridge, G. R., Erjavec, J. L., Ferguson, R. C., Inwan, K. F., Knepp, R. A., Lindberg, F. A. and Ryberg, P. T. (1983). Provenance of North American Phanerozoic sandstones in relation to tectonic setting. *Geol. Soc. Amer. Bul.*, **94**, 222-235.

Dickinson, W.R. and Suczek, C.A, (1979). Plate tectonics and sandstone composition. *Amer. Assoc. Petrol. Geol. Bul.*, **63**, 2164-2182.

Dodson, M. H., Compston, W., Williams, I. S. and Wilson, J. F. (1988). A search for ancient detrital zircons in Zimbabwe sediments. *J. Geol. Soc. Lond.*, **145**, 977-983.

Dreyer, T., Corregidor, J., Arbues, P. and Puigdefabregas, C. (1999). Architecture of the tectonically influenced Sobrarbe deltaic complex in the Ainsa Basin, northern Spain. *Sediment. Geol.*, **127**, 127-169.

Drury, S. A., Harris, N. B. W., Holt, R. W., Reeves-Smith, G. J. and Wrightman, R. T. (1984). Precambrian tectonics and crustal evolution in South India. *J. Geol.*, **92**, 3-20.

Duncan, R.A., Hooper, P.R., Rehacek, J., Marsh, J.S. and Duncan, A.R. (1997). The timing and duration of the Karoo igneous event, southern Gondwana. *J. geophys. Res.*, **102**, 18127-18138.

Encarnación, J., Flemming, T.H., Elliot, D.H. and Eales, H.V. (1996). Synchronous emplacement of Ferrar and Karoo dolerites and the early breakup of Gondwana. *Geol.*, **24**, 535-538.

Eriksson, P. G., Condie, K. C., Tirsgaard, H., Mueller, W. U., Altermann, W., Miall, A. D., Aspler, L. B., Catuneanu, O. and Chiarenzelli, J. R. (1998). Precambrian clastic sedimentation systems. *Sediment. Geol.*, **120**, 5-53.

Ferreira, E. P. (1986). *'n Sedimentologies-stratigrafiese ondersoek van die sedimentere gesteentes in die Ahlmannryggen, Antarktika.* M.Sc. thesis, University of Stellenbosch, South Africa, 193 pp.

Fielding, C.R. (1993). A review of recent research in fluvial sedimentology. *Sediment. Geol.*, **85**, 3-14.

Fleuty, M. J. (1964). The description of folds. *Proc. Geol. Assoc.*, **75**, 461-489.

Floyd, P. A., Winchester, J. A. and Park, R. G. (1989). Geochemistry and tectonic setting of Lewisian clastic metasediments from the Early Proterozoic Loch Maree Group of Gairloch, NW Scotland. *Precamb. Res.*, **45**, 203-214.

Folk, R. L. (1980). *Petrology of Sedimentary Rocks*, Hemphill, Austin, Texas. 182pp.

Frimmel, H. E. (2000). New U-Pb zircon ages for the Kuboos pluton in the Pan-African Gariep Belt, South Africa: Cambrain mantle plume or far field collisional effect. *S. Afr. J. Geol.*, **103**, 207-214.

Gose, W. A., Helper, M. A., Connelly, F. E., Hutson, F. E. and Dalziel, I. W. D. (1997). Paleomagnetic data and U-Pb isotopic age determinations from Coates Land, Antarctica: Implications for late Proterozoic plate reconstructions. *J. Geophys. Res.*, **102**, 7887-7902.

Graham, J. (1988). Collection and analysis of field data: In :Tucker, M.E. (Ed.), *Techniques in Sedimentology*. Blackwell Scientific Publications. 5-62.

Graham, S. A., Ingersoll, R. V. and Dickinson, W. R. (1976). Common provenance for lithic grains in Carboniferous sandstones from Ouachita Mountains and Black Warrior Basin. *J. Sediment. Petrol.*, **46**, 620-632.

Grantham, G. H. (1992). *Geological evolution of western H.U. Sverdrupfjella, Dronning Maud Land, Antarctica.* PhD thesis, University of Natal, South Africa.

Grantham, G. H., Groenewald, P. B. and Hunter, D. R. (1988). Geology of the northern H.U. Sverdrupfjella, western Dronning Maud Land and implications for Gondwana reconstructions. *S. Afr. J. Antarct. Res.*, **18**, 2-10.

Grantham, G. H. and Hunter, D. R. (1991). The timing and nature of faulting and jointing adjacent to the Pencksökket, western Dronning Maud Land, Antarctica. In: Thomson, M.R.A., Crame, J.A. and Thomson, J.A. (Eds.), *Geological evolution of Antarctica.* Cambridge, Cambridge University Press, 47-51.

Grantham, G. H., Jackson, C., Moyes, A. B., Groenewald, P. B., Harris, P. D., Ferrar, G. and Krynauw, J. R. (1995). The tectonothermal evolution of the Kirwanveggen-H.U. Sverdrupfjella areas, Dronning Maud Land, Antarctica. *Precamb. Res.*, **75**, 209-229.

Groenewald, P. B. (1995). *The geology of northern H.U. Sverdrupfjella and its bearing on crustal evolution in Dronning Maud Land, Antarctica.* PhD thesis, University of Natal, South Africa, 320pp.

Groenewald, P. B., Grantham, G. H. and Watkeys, M. K. (1991). Geological evidence for a Proterozoic to Mesozoic link between southeastern Africa and Dronning Maud Land, Antarctica. *J. Geol. Soc. Lond.*, **148**, 1115-1123.

Groenewald, P. B., Moyes, A. B., Grantham, G. H. and Krynauw, J. R. (1995). East Antarctica crustal evolution: geological constraints and modelling in western Dronning Maud Land, Antarctica. *Precamb. Res.*, **75**, 231-250.

Gromet, L. P., Dymek, R. F., Haskin, L. A. and Korotev, R. L. (1984). The "North American Shale Composite": its compilation, major and trace element characteristics. *Geochim. Cosmochim. Acta*, **48**, 2469-2482.

Gunn, B. M. and Warren, G. (1962). The geology of Victoria Land between the Mawson and Mulock Glaciers, Antarctica. *N.Z. Geol. Surv. Bul.*, **71**, 1-157.

Halpern, M. (1970). Rubidium-strontium date of possibly 3 billion years for a granitic rock from Antarctica. *Science*, **169,** 977-978.

Hanson, R. E., Martin, M. W., Bowring, S. A. and Munyantiwa, H. (1998). U-Pb zircon age for the Umkondo dolerites, eastern Zimbabwe: 1.1Ga large igneous province in southern Africa – East Antarctica and possible Rodinia correlations. *Geology*, **26**, 1143-1146.

Harms, J. C. (1975). Stratification produced by migrating bedforms. In: Depositional environments as interpreted from primary sedimentary structures and stratification sequences. *Soc. Econ. Paleont. Short Course*, **2**, 45-61.

Harms, J. C. and Fahnestock, R. K. (1965). Stratification, bedforms, and flow phenomena (with an example from the Rio Grande). In: Middleton, G. V. (Eds.), Primary sedimentary structures and their

hydrocarbon interpretation. *Soc. Econ. Palaeont. Mineral.* Spec. Publ., **12**, 84-115.

Harms, J. C., Southhard, J. B., Spearing, D. R. and Walker, R.G. (1975). Depositional environments as interpreted from primary sedimentary structures and stratification sequences. *Soc. Econ. Palaeont. Mineral., Short Course*, **2**, 161pp.

Harris, P. D. (1999). *The geological evolution of the northern Kirwanveggan*, PhD thesis, University of Witswaterand, South Africa.

Harris, P. D., Moyes, A. B., Fanning, C. M. and Armstrong, R. A. (1995a). Zircon Ion Microprobe constraints on Deformation of High Grade Gneisses in the northern Kirwanveggan, western Dronning Maud Land, Antarctica. *Abstracts Volume, VIIth International Symposium on Antarctic Earth Sciences*, Siena, Italy, 183.

Harris, P. D., Moyes, A. B., Fanning, C. M. and Armstrong, R. A. (1995b). Zircon Ion microprobe results from the Maudheim high-grade gneiss terrane, western Dronning Maud Land, Antarctica. *Extended Abstracts, Centennial Geocongress*, Rand Afrikaans University, Johannesburg, 648-651.

Harwood, G. (1988). Microscopical techniques: II. Principles of sedimentary petrography. In: Tucker, M. (Eds.), *Techniques in Sedimentology*. Blackwell, Oxford, 108-173.

Haskin, M. A. and Haskin, L. A. (1966). Rare earths in European shales: a redetermination. *Science*, **154**, 507-509.

Haszeldine, R. S. (1983a). Fluvial bars reconstructed from a deep, straight channel, Upper Carboniferous coalfield of northeast England. *J. Sediment. Petrol.*, **53**, 1233-1248.

Haszeldine, R. S. (1983b). Descending tabular cross-beds sets and bounding surfaces from a fluvial channel in the Upper Carboniferous coalfield of northeast England. In: Collinson, J. D. and Lewin, J. (Eds.), Modern and ancient fluvial systems. *Int. Assoc. Sediment.* Spec. Publ., **6**, 449-456.

Hedberg, H. D. (1976). *International stratigraphic guide: a guide to stratigraphic classification, terminology and proceedure. International Subcommission on Stratigraphic Classification of IUGS Commission on Stratigraphy*. John Wiley and Sons, Inc., USA.

Hein, F. J. and Walker, R. G. (1977). Bar evolution and development of stratification in the gravelly, braided, Kicking Horse River, British Columbia. *Can. J. Earth Sci.*, **4**, 562-570.

Helferich, S., Henjes-Kunst, F., Kleinschmidt, G. (1999). New geochemical and geochronological data from southern most Kirwanveggen, Dronning Maud Land, Antarctica – Evidence for a Pan-African thrust system. *Abstracts of proceedings, 8th international Symposium on Antarctic Earth Science*, Wellington.

Heller, P. L., Angevine, C. L., Winslow, N. S. and Paola, C. (1988). Two-phase stratigraphic model of foreland basin sequences. *Geology*, **16**, 501-504.

Heller, P. L. and Frost, C. D. (1988). Isotopic provenance of clastic deposits: Application of geochemistry to sedimentary provenance studies. In: Kleinspehn, K.L. and Paola, C. (Eds.), *New perspectives in basin analysis*. Springer-Verlag, New York, 27-42.

Heller, P. L. and Paola, C. (1992). The large scale dynamics of grain-size variation in alluvial basins. 2. Application to syntectonic conglomerate. *Basin Res.*, **4**, 91-102.

Herron, M. M. (1988). Geochemical classification of terrigenous sands and shales from core or log data. *J. Sediment. Petrol.*, **58**, 820-829.

Hinz, K. and Krause, W. (1982). The continental margin of Queen Maud Land/Antarctica: seismic sequences, structural elements and geological development. *Geologische Jahrbuch*, **E23**, 17-41.

Hjellbakk, A. (1997). Facies and fluival architecture of a high-energy braided river: the Upper Proterozoic Seglodden Member, Varanger Peninsula, northern Norway. *Sediment. Geol.*, **114**, 131-161.

Hobbs, B. E., Means, W. D., Williams, P. F. (1976). *An outline of structural geology*. Wiley, New York.

Hodgkinson, G. R. (1989). *Palaeomagnetic studies in western Dronning Maud Land, Antarctica*. MSc thesis, University of Witwatersrand, South Africa, 134pp.

Hoffman, P. F. (1991). Did the breakout of Laurentia turn Gondwanaland inside-out? *Science*, **252**, 1409-1412.

Huddleston, P. J. (1973). Fold morphology and some geometrical implications of theories of fold development. *Tectonophys.*, **16**, 1-46.

Ingersoll, R. V. (1978). Petrofacies and petrologic evolution of late Cretaceous fore-arc basin, northern and central California. *J. Geol.*, **86**, 335-352.

Ingersoll, R. V., Bullard, T. F., Ford, R. L., Grimm, J. P., Pickle, J. D. and Sares, S. W. (1984). The effect of grain size on detrital modes: A test of the Gazzi-Dickinson point-counting method. *J. Sediment. Petrol.*, **54**, 103-116.

Jackson, C. (1997). *Characterization of Mesoproterozoic to Palaeozoic Crustal Evolution of western Dronning Maud Land – Study three: Deformation history and thermochronology of the central Kirwanveggan*. Progress Report submitted to the South African National Antarctic Programme, Department of Environment and Tourism Directorate: Antarctica and Islands, South Africa, 40 pp.

Jackson, C. and Armstrong, R. A. (1997). The tectonic evolution of the central Kirwanveggan, Dronning Maud Land, Antarctica: Temporal resolution of deformation episodes using SHRIMP U-Pb zircon geochronlogy. *T-Dogs Xiiith Anniversary conference*, University of Witwatersrand, Johannesburg.

Jacobs, J., Ahrendt, H., Kreutzer, H. and Weber, K. (1995). K-Ar and 40 Ar-39Ar and apatite fission track evidence for Neoproterozoic and Mesozoic basement rejuvenation events in the Heimefrontfjella and Mannefallknausane (east Antarctica). *Precamb. Res.*, **75**, 251-262.

Jacobs, J., Bauer, W., Spaeth, G., Thomas, R.J. and Weber, K. (1996). Lithology and structure of the Grenville-aged (1.1Ga) basement of Heimefrontfjella (East Antarctica). *Geol. Rundsch.*, **85**, 800-821.

Jacobs, J., Fanning, C. M., Henjes-Kunst, F., Olesch, M. and Paech, H.-S. (1998). Continuation of the Mozambique Belt into East Antarctica: Grenville-age metamorphism and ployphase Pan-African high-grade events in central Dronning Maud Land. *J. Geol.*, **106**, 385-406.

Jacobs, J. and Thomas, R. J. (1999). From Rodinia to Gondwana, the East-Antarctic perspective. *Gondwana Res.*, **2**, 567.

Jones, P. C. (1972). Quartzarenite and litharenite facies in the fluvial foreland deposits of the Trenchard Group (Westphalian), Forest of Dean, England. *Sediment. Geol.*, **8**, 177-198.

Jones, S. J., Frostick, L. E. and Astin, T. R. (2001). Braided stream and flood plain architecture: the Rio Vero Formation, Spanish Pyrenees. *Sediment. Geol.*, **139**, 229-260.

Karpeta, W. P. (1993). Sedimentology and gravel bar morphology in an Archaean braided river sequence: the Witpan Conglomerate Member (Witwatersrand Supergroup) in the Welkom Goldfield, South Africa. In: Best, J. L. and Bristow, C. S. (Eds). *Braided Rivers*. Geol. Soc. Spec. Publ., **75**, 369-388.

Kriegsman, L. M. (1995). The Pan-African event in East Antarctica: a view from Sri Lanka and the Mozambique Belt. *Precamb. Res.*, **75**, 263-277.

Kröner, A. (1979). Pan-African plate tectonics and its repercussions on the crust of northeast Africa. *Geol. Rundsch.*, **68**, 656-583.

Kröner, A. (1991). African linkage of Precambrian Sri Lanka. *Geol. Rundsch.*, **80**, 429-440.

Kröner, A. Todt, W., Hussein, I. M., Mansour, M. and Rashwan, A. A. (1992). Dating of late Proterozoic ophiolites in Egypt and the Sudan using the single grain zircon evaporation technique. *Precamb. Res.*, **59**, 15-32.

Kröner, A. and Williams, I. S. (1993). Age of metamorphism in the high-grade rocks of Sri Lanka. *J. Geol.*, **101**, 513-521.

Krynauw,J.R. (1986). *The petrology and geochemistry of intrusions at selected nunataks in the Ahlmannryggen and Gaeverryggen, western Dronning Maud Land, Antarctica*. Ph.D thesis, University of Natal, South Africa.

Krynauw, J. R. (1996a). A review of the Geology of East Antarctica, with special Reference to the c. 1000 Ma and c. 500 Ma Events. *Terra Antarct.*, **3**, 77-89.

Krynauw, J. R. (1996b). *Geological evolution of western Dronning Maud Land within a Gondwana Framework*. Final Report submitted to the South African National Antarctic Programme, Department of Environment and Tourism Directorate: Antarctica and Islands, South Africa, 24 pp.

Krynauw, J. R., Behr, H. J. and Van Den Kerkhof, A. M. (1994). Sill emplacement in wet sediments: fluid inclusion and cathodluminescence studies at Grunehogna, western Dronning Maud Land, Antarctica. *J. Geol. Soc. Lond.*, **151**, 777-794.

Krynauw, J. R., Hunter, D. R. and Wilson, A. H. (1987). A review of the field relationships, petrology and geochemistry of the Borgmassivet intrusions in the Grunehogna Province, western Dronning Maud Land, Antarctica. *5th International Symposium on Antarctic Earth Sciences*, Cambridge.

Krynauw, J. R., Hunter, D. R. and Wilson, A. H. (1990). A reassessment of the Nils Jorgennutane suite in the Ahlmannryggen. *S. Afr. J. Antarct. Res.*, **20**, 2-8.

Krynauw, J. R., Jackson, C., Harris, P. D., Knoper, M. W., Harris, C. and Grantham, G. H. (1996). *Characterization of the Mesoproterpzoic to Palaeozoic Crustal Evolution of Western Dronning Maud Land*. Earth Science Programme 1996-2001, Sub-Programme Proposal, South African National Antarctic Programme.

Krynauw, J. R., Watters, B. R., Hunter, D. R. and Wilson, A. H. (1988). Emplacement of sills into wet sediments at Grunehonga, western Dronning Maud Land, Antarctica. *J. Geol. Soc. Lond.*, **145**, 1019-1032.

Krynauw, J. R., Watters, B. R., Hunter, D. R. and Wilson, A. H. (1991). A review of the field relations, petrology and geochemistry of the Borgmassivet intrusions in the Grunehonga Province, western Dronning Maud Land. In: Thomson, M.R.A., Crame, J.A. and Thomson, J.A. (Eds.), *Geological evolution of Antarctica*. Cambridge University Press, Cambridge, 33-39.

Le Maitre, R. W., Bateman, P., Dudek, A., Keller, J., Lameyre Le Bas, M. J., Sabine, P. A., Schmid, R., Sorensen, H., Streckeisen, A., Woolley, A. R. and Zanettin, B. (1989). *A classification of igneous rocks and glossary of terms*. Blackwell, Oxford.

Leopold, L. B. and Wolman, M. G. (1957). River channel patterns; braided, meandering, and straight. *US Geological Survey* professional paper, **282-B**.

Long, D. G. F. (1978). Proterozoic stream deposits: some problems of recognition and interpretation of ancient sandy fluvial systems. In: Miall, A.D. (Ed.), Fluvial Sedimentology. *Can. Soc. Petrol. Geol. Memoir.*, **5**, 313-342.

Lopez Gamundi, O., Espejo, I. S. and Alonso, M. S. (1990). Sandstone composition changes and palaeocurrent reversal in the Upper Palaeozoic and Triassic deposits of the Huaco area, western Panganzo Basin, west-central Argentina. *Sediment. Geol.*, **66**, 99-111.

Ludwig, K.R. (1999). *Isoplot/Exversion 2.00: A geochronological Toolkit for Microsoft Excel*. Berkley Geochronological CenterSpecial Publication, No. 1a, 46pp.

MacNaughton, R. B, Dalrymple, R. W. and Narbonne, G. M. (1997). Early Cambrian braid-delta deposits, MacKenzie Mountains, north-western Canada. *Sediment.*, **44**, 587-609.

Martin, P. K. and Hartnady, C. (1986). Plate tectonic development of the southwest Indian Ocean: a revised reconstruction of East Antarctica and Africa. *J. Geophys. Res.*, **91**, 4767-4785.

McClay, K. R. (1987). *The mapping of geological structures*. Geological Society of London Handbook. John Wiley & Sons, England.

McCulloch, M. T. and Wasserburg, G. J. (1978). Sm-Nd and Rb-Sr geochronlogy of continental crust formation. *Science*, **200**, 1003-1011.

McKee, E. D., Crosby, E. J. and Berryhill, H. L. (1967). Flash flood deposits, Bijou Creek, Colorado, June 1965. *J. Sediment. Petrol.*, **37**, 829-851.

McLennan, S. M. (1989). Rare earth elements in sedimentary rocks: influence of provenance and sedimentary processes, In: Lipin, B.R. and McKay, G.A. (Eds.), *Geochemistry and Mineralogy of Rare Earth Elements*. Mineralogical Society of America, Washington, 169-200.

McLennan, S. M., Hemmimg, S., McDaniel, D. K. and Hanson, G. N. (1993). Geochemical approaches to sedimentation, provenance, and tectonics. In: Johnsson, M.J., and Basu, A. (Eds.), Processes Controlling the Composition of Clastic Sediments: Boulder, Colorado. *Geological Society of America* Special Paper, **284,** 21-40.

Meckel, L. D. (1967). Origin of Pottsville Conglomerates (Pennsylvanian) in the Central Appalachians. *Geol. Soc. Amer. Bul.*, **78**, 223-258.

Metz, R. (1981). Why not raindrop impressions? *J. Sedimen. Petrol.*, **51(1)**, 265-268.

Miall, A. D. (1977). A review of the braided river depositional environment. *Earth Sci. Rev.*, **13**, 1-62

Miall, A. D. (1978). Lithofacies types and vertical profile models in braided river deposits: a summary. In: Miall, A.D. (Ed.), *Fluvial Sedimentology*. Can. Soc.Petrol.Geol. Mem., **5**, 597-604.

Miall, A. D. (1985). Architectural element analysis: A new method of facies analysis applied to fluvial deposits. *Earth Sci. Rev.*, **22**, 261-308.

Miall, A. D. (1988a). Reservoir heterogeneities in fluvial sandstone: lessons from outcrop studies. *Amer. Assoc. Petrol. Geol. Bul.*, **72**, 682-697.

Miall, A. D. (1988b). Architectural elements and bounding surfaces in fluvial deposits: anatomy of the Kayenta Formation (Lower Jurassic), southwest Colorado. *Sediment. Geol.*, **55**, 233-262.

Miall, A. D. (1990). *Principles of sedimentary basin analysis*. 2nd Edition, Springer-Verlag, New York, 668pp.

Miall, A. D. (1993). The architecture of fluvial-deltaic sequences in the Upper Mesaverde Group (Upper Cretaceous), Book Cliffs, Utah. In: Best, J.L. and Bristow, C. S. (Eds.), *Braided rivers*. Geol. Soc. Lond. Spec. Publ., **75**, 305-332.

Miall, A. D. (1994). Reconstructing fluvial macroform architecture from two-dimensional outcrops: examples from the Castlegate Sandstone, Book Cliffs, Utah. *J. Sediment. Res.*, **B64**, 146-158.

Miall, A. D. (1996). *The geology of fluvial deposits – sedimentary facies, basin analysis and*

petroleum geology. Springer, Berlin, 582pp.

Miall, A. D. and Gibling, M. R. (1978). The Siluro-Devonian clastic wedge of somerset Island, Arctic Canada, and some regional paleogeographic implications. *Sediment. Geol.*, **21**, 85-127.

Minnaar, C. L. J. (1975). Some field and petrographical data on the volcaniclastics of Bråpiggen. *Unpubl. Report Geol. Surv.*, Pretoria, South Africa.

Molnar, P. and Tapponnier, P. (1975). Cenozoic tectonics of Asia: effects of a continental collision. *Science*, **189**, 419-426.

Moore, P. S. (1979). Deltaic sedimentation-Cambrian of south Australia. *J. Sediment. Petrol.*, **49**, 1229-1244.

Moores, E. M. (1991). Southwest U.S. – East Antarctic (SWEAT) connection: a hypothesis. *Geology*, **19**, 425-428.

Morton, A. C., Claoue-Long, J. C. and Berge, C. (1996). SHRIMP constraints on sediment provenance and transport history in the Mesozoic Statfjord Formation, North Sea. *J. Geol. Soc. Lon.*, **153**, 915-929.

Mosley, P. N. (1993). Geological evolution of the late Proterozoic "Mozambique Belt" of Kenya. *Tectonophys.*, **221**, 223-250.

Mougenot, D., Gennesseaux, M., Hernandez, J., Lepvrier, C., Malod, J.-A., Raillard, S., Vanney, J.-R. and Villeneuve. (1991). La ride du Mozambique (Ocean Indien): un fragment continental individualise lors du coulissement de l'Amerique et de l'Antarctique le long de l'Afrique de l'Est? *C. R. Acad. Sci. Paris*, **312(II)**, 655-662.

Moyes, A. B. and Barton, J. M. Jr. (1990). A review of the isotopic data from western Dronning Maud Land, Antarctica. *Zentralblatt für Geologie und Palaontologie.*,Teil I. **(1/2),** 19-31.

Moyes, A. B., Barton, J. M. Jr. and Groenewald, P. B. (1993). Late Proterozoic to Early Palaeozoic tectonism in Dronning Maud Land, Antarctica: supercontinental fragmentation and amalgamation. *J. Geol. Soc. Lon.*, **150**, 833-842.

Moyes, A. B. and Harris, P. D. (1996). *Final Project Report of the Radiogenic Isotopes Project on the Geological Evolution of Western Dronning Maud Land within a Gondwana Framework*. Final Report submitted to the South African National Antarctic Programme, Department of Environment and Tourism Directorate: Antarctica and Islands, South Africa, 38 pp.

Moyes, A. B., Krynauw, J. R. and Barton, J. M. Jnr. (1995a). The age of the Ritscherflya Supergroup and Borgmassivet Intrusions, Dronning Maud Land, Antarctica. *Antarct. Sci.*, 7, 87-97.

Moyes, A. B., Knoper, M. W. and Harris, P. D. (1995b). The age and significance of the Urfjell Group, western Dronning Maud Land, Antarctica. Abstracts volume, *VII th International Symposium on Antarctic Earth Sciences*, Siena, Italy, 277.

Moyes, A. B., Knoper, M. W. and Harris, P. D. (1997). The age and significance of the Urfjell Group, Western Dronning Maud Land, Antarctica. In: Ricci, C.A. (Eds.), *The Antarctic Region: Geological Evolution and Processes*. Terra Antarctica Publication, Siena, 31-36.

Muhongo, S. (1997). Tectonic fabrics and metamorphism in the Mozambique orogenic belt in Tanzania: Implications for Proterozoic collisional sutures in Gondwanaland. *Gondwana Res. Misc. Publ.*, **5**, 57-58.

Nance, W. B. and Taylor, S. R. (1976). Rare earth element patterns and crustal evolution – I. Australian post-Archean sedimentary rocks. *Geochim. Cosmochim. Acta*, **40**, 1539-1551.

Nedelec, A., Ralison, B., Bouchez, J. L. and Gregoire, V. (2000). Structure and metamorphism of the granite basement around Antananarivo: A key to the Pan-African history of central Madagascar and its Gondwana connections. *Tectonics*, **19(5)**, 997-1020.

Neethling, D. C. (1970). *South African earth science exploration of western Queen Maud Land, Antarctica*. MSc thesis, University of Natal, South Africa.

Norrish, K. and Chappel, B. W. (1977). X-ray fluorescence spectrometry. In: Zussman, J. (Ed.), *Physical methods in determinative mineralogy*, Academic Press, New York, 235-237 and 257-262.

Norrish, K. and Hutton, J. T. (1969). An accurate X-ray spectographic method for the analysis of a wide range of geological samples. *Geochim. Cosmochim. Acta*, **33**, 431-435.

North, C. P and Taylor, K. S. (1996). Ephemeral-fluvial deposits: integrated outcrop and simulation studies reveal complexity. *Amer. Assoc. Petrol. Geol. Bul.*, **80**, 811-830.

Owen, G. (1987). Deformation processes in unconsolidated sands. In: Jones, M. E. and Preston, M. F. (Eds.), *Deformation of sediments and sedimentary rocks*. Geological Society Special Publication 29, Blackwell Scientific Publications, Great Britain, 11-24.

Paces, J. B. and Miller, J. D. (1989). Precise U-Pb ages of Duluth Complex and related mafic

intrusions, Northeastern Minnesota: Geochronological insights to physical, petrogenic, , paleomagnetic and tectonomagmatic processes associated with the 1.1 Ga midcontinent rift system. *J. Geophys. Res.*, **98B**, 13997-14013.

Peters, M. (1989). Igneous rocks in western and central Neuschwabenland, Vestfjella and Ahlmannryggen, Antarctica: Petrography, geochemistry, geochronology, paleomagnetism, geotectonic implications. *Beri. Polarforschung.*, **61**, 186.

Peters, M, Haverkamp, B., Emmermann, R., Kohnen, H., Webber, K. (1991). Palaeomagnetism, K-Ar dating and geodynamic setting of igneous rocks in western and central Neuschwabenland, Antarctica. In: Thomson, M.R.A., Crame, J.A., Thomson, J.W. (Eds.), *Geological evolution of Antarctica.* Cambridge University Press, Cambridge, 41-46.

Pettijohn, F. J., Potter, P. E. and Siever, R. (1972). *Sand and Sandstone.* Springer-Verlag, New York.

Pettijohn, F. J., Potter, P. E. and Siever, R. (1987). *Sand and Sandstone.* Second Edition, Springer-Verlag, New York, 553pp.

Pinna, P., Jourde, G., Caluez, J.-Y., Mroz, J. P. and Marques, J. M. (1993). The Mozambique Belt in northern Mozambique: Neoproterozoic (1100-850Ma) crustal growth and tectogenesis, and superimposed Pan-African (800-550Ma) tectonism. *Precamb. Res.*, **62**, 1-59.

Pittman, E. D. (1979). Recent advances in sandstone diagenesis. *Ann. Review. Earth Planet. Sci.*, 7, 39-62.

Potts, P. J. (1987). Inductively coupled plasma-mass spectrometry. In: *A handbook of silicate rock analysis.* Blackie, Glasgow, 575-586.

Powell, C. McA., McElhinny, M. W., Li, Z. X., Meert, J. G. and Park, J. K. (1993). Palaeomagnetic constraints on timing of the Neoproterozoic breakup of Rodinia and the Cambrian formation of Gondwana. *Geology,* **21**, 889-892.

Powell, C. McA., Jones, D. L., Pisarevsky, S. and Wingate, M. T. D. (2001). Palaeomagnetic constraints on the position of the Kalahari craton in Rodinia. *Precamb. Res.,* **110**, 33-46.

Price, N. J. (1966). *Fault and joint development in brittle and semi-brittle rocks.* Pergamon, London.

Price, N. J., Cosgrove, J. W. (1990). *Analysis of geological structures.* Cambridge University Press, Great Britain.

Puigdefabregas, C., Munoz, J. A. and Marzo, M. (1986). thrust belt development in the eastern Pyrenees and related depositional sequences in the southern foreland basin. In: Allen, P. A. and Homewood, P. (Eds.), *Foreland Basins.* International Association of Sedimentologists Special Publication 8, 229-246.

Ramsey, J. G. and Huber, M. I. (1987). *The Techniques of Modern Structural Geology. Volume 2: Folds and Fractures.* Academic Press, London.

Raynolds, R. G. H. and Johnson, G. D. (1985). Rates of Neogene depositional and deformational processes, north-west Himalayan foredeep margin, Pakistan. In: Snelling, N. J. (Ed.), *The chronology of the geological record.* Geological Society of London Memoir **10**, 297-311.

Reid, D. L., Welke, H. J., Betton, P. J. and Erland (1987). Composition, age and tectonic setting of amphibolites in the central Bushmanland Group. *Precamb. Res.,* **36**, 99-126.

Reineck, H. E. (1960). Uber Zeitlucken in rezenten Flachsee-sedimenten. *Geol. Rundschau*, **49**, 149-161.

Reineck, H. E. and Wunderlich, R. (1968). Classification and origin of flaser and lenticular bedding. *Sediment.,* **11**, 99-104.

Roe, S. L. and Hermansen, M. (1993). Processes and products of large, late Precambrian sandy rivers in northernNorway. In: Marzo, M., Puigdefabregas, C. (Eds.), *Alluvial sedimentation.* Int. Assoc. Sediment. Spec. Publ., **17,** 151-166.

Roeser, H. A., Fritsch, J. and Hinz, K. (1996). The development of the crust off Dronning Maud Land, East Antarctica. In: Storey, B. C., King, E. C. and Livermore, R. A., (Eds.), *Weddell Sea Tectonics and Gondwana Break-up.* Geol. Soc. Lon. Spec. Publ., **108**, 243-264.

Roots, E. F. (1953). Preliminary notes on the geology of western Dronning Maud Land. *Norsk Geologisk Tidskrift,* **32,** 18-33.

Roots, E. F. (1969). Geology of western Queen Maud Land. In: Bushell, V. C. and Craddock, C. (Eds.), *Geologic maps of Antarctica, Antarctic Map Folio Series,* **12,** P1. VI.

Roser, B. P., Cooper, R. A., Nathan, S., and Tulloch, A. J. (1996). Reconnaissance sadnstone geochemistry, provenance, and tectonic setting of the lower Paleozoic terranes of the West Coast and Nelson, New Zealand. *N. Z. J. Geol. Geophys.*, **39**, 1-16.

Roser, B. P. and Korsch, R. J. (1986). Determination of tectonic setting of sandstone-mudstone suites using SiO2 content and K2O/Na2O ratio. *J. Geol.*, **94**, 635-650.

Roser, B. P. and Korsch, R. J. (1988). Provenance signatures of sandstone-mudstone suites determined using discriminant function analysis of major element data. *Chem. Geol.*, **67**, 119-139.

Rust, B. R. (1972). Structure and process in a braided river. *Sediment.*, **18**, 221-245.

Rust, B. R. and Gibling, M. R. (1990). Braidplain evolution in the Pennsylvanian South Bar Formation, Sydney Basin, Nova Scotia, Canada. *J. Sediment. Petrol.*, **60**, 59-72.

Rust, B. R. and Koster, E. H. (1984). Course alluvial deposits. In: Walker, R. G. (Ed.), *Facies models*. 2nd Edition, Geoscience Canada, 53-69.

Sambridge, M. S. and Compston, W. (1994). Mixture modelling of multi-component data sets with application to ion-probe zircon ages. *Earth Planet. Sci. Let.*, **128**, 373-390.

Selley, R. C. (1985). *Ancient sedimentary environments*. 3rd edition. Chapman and Hall, London, 317pp.

Shackleton, R. M. (1996). The final collision zone between East and West Gondwana: where is it? *J. Afr. Earth Sci.*, **23**, 271-287.

Shiraishi, S., Hiroi, Y., Ellis, D. J., Fanning, C. M., Motoyoshi, Y. and Nakai, Y. (1994). Cambrian orogenic belt in East Antarctica and Sri Lanka: implications for Gondwana assembly. *J. Geol.*, **102**, 47-65.

Sinclair, H. D. and Allen, P. A. (1992). Vertical versus horizontal motions in the Alpine orogenic wedge: stratigraphic response in the foreland Basin. *Basin Res.*, **4**, 215-232.

Sircombe, K. N. (1999). Tracing provenance through the isotopic ages of littoral and sedimentary detrital zircon, eastern Australia. *Sediment. Geol.*, **124**, 47-67.

Smith, N. D. (1970). The braided stream depositional environment: comparison of the Platte River with some Silurian clastic rocks, north central Appalachians. *Geol. Soc. Amer. Bul.*, **81**, 2993-3014.

Smith, N. D. (1971). Transverse bars and braiding in the lower Platte River, Nebraska. *Geol. Soc. Amer. Bul.*, **82**, 3407-3420.

Smith, N. D. (1972). Some Sedimentological aspects of planar cross-stratification in a sandy braided river. *J. Sediment. Petrol.*, **42**, 624-634.

Smith, N. D. (1986). Proglacial fluvial environment. In: Ashley, G. M. (Ed.), Glacial sedimentary environments. *SEMP Short Course*, **16**, 85-134.

Sonderholm, M. and Tirsgaard, H. (1998). Proterozoic fluvial styles: response to changes in accommodation space (Rivieradal sandstone, eastern North Greenland), *Sediment. Geol.*, **120**, 257-254.

Stacey, J. S. and Kramers, J. D. (1975). Approximation of terrestrial lead isotope evolution by a two-stage model. *Earth Planet. Sci. Let.*, **26**, 207-221.

Stern, R. J. (1994). Arc assembly and continental collision in the Neoproterozoic East African Orogen: Implications for the consolidation of Gondwana. *Rev. Earth Planet. Sci.*, **2**, 319-351.

Suttner, L. J. and Basu, A. (1985). The effect of grain size on detrital modes: a test of the Gazzi-Dickinson point-counting method – Discussion. *J. Sediment. Petrol.*, **55**, 616-627.

Suttner, L. J., Basu, A. and Mack, G. H. (1981). Climate and the origin of quartz arenites. J. *Sediment. Petrol.*, **51**, 1235-1246.

Swanepoel, J. J. P. (1988). *Die stratigrafie en sedimentologie van die Ahlmannryggengroep in die Borgmassivet, Wes Koningin Maudland, Antarktika*. MSc thesis, University of Stellenbosch, South Africa.

Swanepoel, J. J. P. (1995). Stratigraphy and sedimentology of the Ahlmannryggen Group in the Borgmassivet, western Dronning Maud Land. *S. Afr. J. Antarct. Res.*, **25**, 17-50.

Tanaka, H. and Idnurm, M. (1994). Palaeomagnetism of Proterozoic mafic intrusions and host rocks of the Mt Isa inlier, Australia: revisited. *Precamb. Res.*, **69**, 241-258.

Tankard, A. J., Jackson, M. P. A., Eriksson, K. A., Hobday, D. K., Hunter, D. R. and Minter, W. E. L. (1982). *Crustal evolution of southern Africa, 3.8 billion years of Earth history*. Spinger-Verlag, New York, 523 pp.

Tapponnier, P. and Molnar, P. (1976). Slip line field theory and large scale continental tectonics. *Nature*, **264**, 319-324.

Tapponnier, P., Peltzer, G. and Armijo, R. (1985). On the mechanics of collision between India and Asia. In: Coward, M. P. and Ries, A. (Eds.), *Collision Tectonics*. Geol. Soc. Lond. Spec. Publ., 19, 115-157.

Taylor, S. R. and McLennan, S. M. (1985). *The Continental Crust: Its Composition and Evolution*. Blackwell. London, 312pp.

Tchalenko, J. S. (1968). The evolution of kink bands and the development of compression textures in sheared clays. *Tectonophys.*, **6**, 159-174.

Thomas, R. J., Marshall, C. G. A., Watkeys, M. K., Fitch, F. J. and Miller, J. A. (1992). K-Ar and 40Ar/39Ar dating of the Natal Group, Southeast Africa: a post Pan-African molasse? *J. Afr. Earth Sci.*, **15**, 453-471.

Todd, S. P. and Went, D. J. (1991). Lateral migration of sand-bed rivers: examples from the Devonian Glashabeg Formation, SW Ireland and the Cambrian Alderney Sandstone Formation, Channel Islands. *Sediment.*, **38**, 997-1020.

Tucker, M. E. (1981). *Sedimentology and Petrology – An introduction to the origin of Sedimentary Rocks.* Geological Series, University of Durham, Blackwell Scientific Publications, London.

Turnbridge, I. P. (1981). Sandy high-energy flood sedimentation – some criteria for recognition, with an example from the Devonian of SW England. *Sediment. Geol.*, **28**, 79-96.

Twiss, R. J., and Moores, E. M. (1992). *Structural Geology.* W. H. Freeman and Company, U.S.A.

Van Niekerk, C. B. (1968) *The suitability of extrusive rocks for U-Pb radiometric dating.* Ph.D. thesis, University of Cape Town, South Africa, 320 p.

Vicars, R. G. and Breyer, J. A. (1981). Sedimentary facies in air-fall pyroclastic debris, Arikaree Group (Miocene), Northwest Nebraska, U.S.A. *J. Sediment. Petrol.*, **51**, 909-921.

Visser, D. J. L. (1998). *The geotectonic evolution of South Africa and offshore areas.* Geol. Surv. S. Afr., 319pp.

Walraven, F., Armstrong, R. A. and Kruger, F. J. (1990). A chronostratigraphic framework for the north-central Kaapvaal Craton, the Bushveld Complex and the Vredefort Structure. *Tectonophys.*, **171**, 23-48.

Watters, B. R., Krynauw, J. R. and Hunter, D. R. (1991). Volcanic rocks of the Proterozoic Jutulstraumen Group in western Dronning Maud Land, Antarctica. In: Thomson, M.R.A., Crame, J.A., Thomson, J.W. (Eds.), *Geological evolution of Antarctica.* Cambridge University Press, Cambridge, 41-46.

Watts, A. B., Cochran, J. R., Bodine, J. H. and Steckler, M. S. (1982). Lithospheric flexure. *Int. Geol. Congr. Abstr.*, **26**, 1375.

Williams, G. E. (1971). Flood deposits of the sand-bed ephermal streams of central Australia. *Sediment.*, **17**, 1-40.

Williams, I. S., Buick, J. S. and Cartwright, I. (1996). An extended episode of early Proterozoic metamorphic fluid flow in the Reynolds Range, central Australia. *J. Metamorph. Geol.*, **14**, 29-47.

Williams, I. S. and Claesson, S. (1987). Isotopic evidence for the Precambrian provenance and Caledonian metamorphism of high-grade paragneisses from the Seve Nappes, Scandinavian Caledonides. II. Ion microprobe zircon U-Th-Pb. *Contrib. Mineral. Petrol.*, **97**, 205-221.

Williams, P. F. and Rust, B. R. (1969). The sedimentology of a braided river. *J. Sediment. Petrol.*, **39**, 649-679.

Wilson, J. F. (1990). A craton and its cracks; some of the behaviour of the Zimbabwe Block from the late Archaean to the Mesozoic in response to horizontal movements, and the significance of some of its mafic dyke fracture patterns. *J. Afr. Earth Sci.*, **10(3)**, 483-501.

Wilson, T. J., Grunow, A. M. and Hanson, R. E. (1997). Gondwana assembly: The view from southern Africa and east Gondwana. *J. Geodyn.*, **23**, 263-286.

Wingate, M. T. D. (2001). SHRIMP baddeleyite and zircon ages for an Umkondo dolerite sill, Nyanga Mountains, Eastern Zimbabwe. *S. Afr. J. Geol.*, **104**, 13-22.

Wizevich, M. C. (1992). Photomosaics of outcrops: useful photographic techniques. In: Miall, A.D. and Tyler, N. (Eds.), The three dimensional facies architecture of terrigenous clastic sediments, and its implications for hydrocarbon discovery and recovery. *SEMP- Concepts in Sedimentology and Palaeotology*, **3**, 22-24.

Wolmarans, L. G. and Kent, L. E. (1982). Geological investigations in western Dronning Maud Land, Antarctica - a synthesis. *S. Afr. J. Antarct. Res. Suppl.*, **2**, 93pp.

Wolmarans, L. G. and Krynauw, J. R. (1981). *Reconnaissence geological map of the Ahlmannryggen area, western Dronning Maud Land, Antarctica*: Sheet 1 of 3, Pretoria; SASCAR.

Wronkiewicz, D. J. and Condie, K. C. (1989). Geochemistry of sediments from the Pongola Supergroup, South Africa: evidence for a 3Ga-old evolved continental craton. *Geochim. Cosmochim. Acta*, **53**, 1537-1549.

Wronkiewicz, D. J. and Condie, K. C. (1990). Geochemistry and mineralogy of sediments from the Ventersdorp and Transvaal Supergroups, South Africa: Cratonic evolution during the early Proterozoic. *Geochim. Cosmochim. Acta.*, **54**, 343-354.

APPENDIX 1
METHODOLOGY

METHODOLOGY

This section provides a brief description of the various analytical techniques and methods used to meet the aims of the study.

MAPPING

A *ca.* 1:280 000 regional geological map, created by combining 1:250 000 topographic maps and aerial photos, was constructed. Field location and photogeological interpretation work used a combination of *ca.* 1:15 000 and 1:50 000 aerial photos flown in 1983/1984 and 1989 by the German Government. The completed Regional Geological Map of the Ahlmannryggen and Borgmassivet (this study) represent a compilation of work carried out as part of this study. The base map was constructed from previous SANAP geological maps and Index maps published by the Norsk Polarinstitutt in 1962.

Mapping incorporated measured sections, traverses and the construction of detailed lateral profiles from cliff face exposures. Structural and palaeocurrent measurements were recorded using a Breithaupt Kassel compass, corrected for magnetic declination. Palaeocurrent readings were taken from a range of sedimentary structures. When the direct measurement of the axis of a trough cross-bed was not possible, small three-dimensional exposures were used. Adjustment for tectonic tilting was carried out for bedding dipping at greater than 7.5°, for tilting less than this, adjustment is not necessary (Graham, 1988). Extensive photography of cliff faces was completed in order to produce photo-mosaics, following the guidelines of Wizeich (1992) in order to maximise resolution and minimise geometric distortion.

PETROLOGY

Fifty-eight thin sections were prepared by Mukesh Seyambu of the University of Natal, School of Geological and Computer Sciences, and described using techniques outlined by Tucker (1981), Folk (1980) and Pettijohn *et al.* (1987). Modal estimates of 26 selected sandstone thin sections were determined using a Swift automatic point counter, according to the Gazzi-Dickinson point counting method (Dickinson, 1970; Dickinson and Suczek, 1979; Ingersoll *et al.*, 1984). The samples were all counted to 1000 points.

XRF WHOLE-ROCK CHEMISTRY

Fifty-one whole-rock analyses of samples from the Ahlmannryggen Group were performed at the University of Natal School of Geological and Computer Sciences by X-ray fluorescence spectrometry. These analyses were undertaken in order to identify possible geochemical stratigraphic variations and to constrain the provenance of the Ahlmannryggen Group. Analyses by x-ray fluorescence spectrometry were done using Philips PW1404 and X-UNIQUE spectrometers at the University of Natal, Durban. Instrument calibration was controlled with international standards and internal synthetic standards and blanks. International standards used were DTS-1, PCC-1, GSP-1, W-1, BCR-1, G-2, AGV, NIM-G, NIM-P,NIM-D, NIM-S, NIM-L, BHVO, and DRN. Internationally accepted standards are from Abbey (1989). Prof. A.H. Wilson of the Department of Geology, University of Natal, Durban compiled the computer programs for reduction of count data and calculation of mass absorption coefficients.

One or two kg of sample was cleaned and fine crushed in a jaw crusher. The crush was statistically split to 100g and milled. Part of the milled sample was used for preparation of fusion discs and pressed powder pellets, part was used for ICP-MS analysis and the remainder has been stored for possible future use. Major and minor elements were analysed using the lithium tetraborate fusion method of Norrish and Hutton (1969).

Preparation of Norrish Fusion Discs

Silica crucibles were cleaned in a diluted solution of HCl. Approximately 0.5g of sample was weighed into the silica crucibles and dried at 100°C. These crucibles were placed in a furnace at 1000°C for 4 hrs, then removed and allowed to cool in the desiccator. The spectroflux used for the fusion discs was preheated in Pt crucibles at 1000°C, and approximately 0.4g of the ashed

sample was added as close to the ratio weight sample/weight flux = 2.2 as possible. The samples were fused at 1000°C and the product cast in a brass die maintained at 250°C. Discs were annealed for approximately 3 hours on a heated asbestos plate and then allowed to cool gradually. The flux was Johnson Matthey Spectroflux 105. Each new batch of flux was homogenized and a new set of standards made up. Fusion discs were stored separately in sealed plastic bags.

Pressed Powder Pellets

Approximately 8g of finely milled sample was mixed with 0.6 Mowiol and homogenized using an agate mortar and pestle. The sample was place in a metal die (position cylinder), and compressed to a pellet *ca.* 5mm thick under a pressure of 8 tonnes for *ca.* 10 seconds. The pellets were hardened in an oven at 110°C for 3-4 hours. Ragged edges on the pellets were trimmed. Contact with the surface to be radiated was avoided. Pellets separated by cardboard discs, were stored in airtight containers.

Precision of XRF Analyses

Precision of major and trace element analyses by XRF is as follows;

	Detection Limits	Analytical Accuracy (%)	Tube Anode
SiO2	0.004%	0.2	Sc/Mo
Al2O3	0.005%	0.5	Sc/Mo
Fe2O3	0.001%	0.5	Sc/Mo
MnO	0.001%	0.5	Sc/Mo
MgO	0.011%	0.3	Sc/Mo
CaO	0.0003%	0.2	Sc/Mo
K2O	0.0003%	0.2	Sc/Mo
TiO2	0.0004%	0.2	Sc/Mo
P2O5	0.001%	0.2	Sc/Mo
Na2O	0.018%	2	Sc/Mo
Sc	0.3ppm	10	Cr
Ba	1ppm	20	Cr
Zn	0.3ppm	5	Au
Cu	0.2ppm	5	Au
Ni	0.1ppm	5	Au
Cr	0.6ppm	5	Au
V	0.5ppm	10	Au
La	1.5ppm	15	Au
Zr	0.3ppm	3	Rh
Sr	0.3ppm	3	Rh
Nb	0.1ppm	3	Rh
Y	0.3ppm	3	Rh
Rb	0.4ppm	2	Rh
U	0.1ppm	20	Rh
Th	0.5ppm	20	Rh
Pb	1ppm	10	Au
Ga	0.2ppm	10	Au
Co	1ppm	10	Au
Ce	0.13ppm	5	Au
Nd	0.3ppm	5	Au
As	0.001ppm	10	Au
S	0.001ppm	10	Cr
F	2ppm	10	Cr
Cl	1ppm	10	Cr
Sn	2ppm	10	Au
W	0.5ppm	10	Au
Mo	1ppm	10	Au
Cd	0.6ppm	10	Au
Ta	3ppm	10	Rh

ICP-MS TRACE ELEMENT CHEMISTRY

Trace elements, including the rare earth elements, were analysed using inductively coupled plasma-mass spectrometry (ICP-MS). Approximately 100mg of powder from selected samples was sent to the Department of Geology at the University of Cape Town, where ICP-MS analysis was conducted by Dr A. Spath, using techniques described in Potts (1987).

Laboratory Procedures

Sample preparation involved digesting 50mg of sample powder in closed, heated teflon beakers using HF and HNO_3. The digested samples were analysed in 5% HNO_3 using a Perkin Elmer/ Sciex Elan 6000 ICP-MS. 103Rh, 115In, 187Re and 209Bi were used as internal standards, whereas calibration was achieved using synthetic multi-element standard solutions. Only high purity bottle-distilled acids and water were used. The instrument was optimised to minimise the formation of doubly-charged ions (++Ba/Ba = 0.019) and oxides (CeO/Ce = 0.025). Instrument sensitivity: 34903 cps/ppb 103 Rh.

Instrument operating conditions:

- Nebuliser gas flow: 0.85 L/min
- Main gas flow: ~15 L/min
- Auxiliary gas flow: ~0.75 L/min
- ICP RF power: 1100 W
- Autolens voltages: 9Be = 6.8V; 59Co = 7.4V; 115In = 8.6V
- Vacuum: 2.77e-5 Torr.

U/Pb DETRITAL ZIRCON SHRIMP ANALYSIS

Three rock samples (A.GH.5, B.HF.6 and B.MA.4) were selected from the Ahlmannryggen Group for U/Pb analysis of detrital zircons. The samples all consisted of medium-grained, moderately sorted sandstones with distinct heavy mineral laminae associated with cross beds. The samples were pulverised and a zircon concentrate produced using standard heavy liquid and magnetic separation. Zircon grains were picked

under a binocular microscope and mounted in epoxy, together with fragments of RSES standard SL13 and zircon standard AS 3 (Duluth Complex gabbroic anorthosite; Paces and Miller, 1989). The zircons were then sectioned roughly in half to expose their cores, polished and photographed. All samples were then examined by cathodluminescence imaging, a procedure that allows the ion micro-probe primary beam to be accurately placed in an area of the zircon which will yield the best result. The zircons were analysed by the SHRIMP I ion micro-probe at the Research School of Earth Science at the Australian National University, using techniques described in detail by Compston *et al.* (1984) and William and Claesson (1987). In order to achieve the best coverage of the overall U/Pb age distributions in the samples, between 51 and 60 individual zircon grains were analysed in each sample, using a four scan data collection routine.

The data have been reduced in a manner similar to that described by Compston *et al.* (1984) and William and Claesson (1987). U/Pb in the unknowns were normalised to a $^{206}Pb/^{238}U$ value of 0.1859 (equivalent to an age of 1099 Ma) for AS 3 (Paces and Miller, 1989). The U and Th concentrations were determined relative to those measured in the SL 13 standard. Common Pb corrections were made using the measured $^{204}Pb/^{206}Pb$ composition and the relevant model Pb composition from Cumming and Richards (1975). Uncertainties in the isotopic ratios and ages in the data tables (and in the error bars in the plotted data) are reported at the 1σ level, but unless otherwise stated in the text, the final weighted mean ages are reported as 95% confidence limits. All age calculations and statistical assessments of the final data have been carried out with the software Isoplot/Ex of Ludwig (1999).

U/Pb MINERAL ISOTOPE ANALYSIS

Conventional zircon dissolution was carried out on zircon grains from two tuff samples for the purpose of accurately constraining the age of the Ahlmannryggen Group and contemporaneous volcanic activity. Two tuff layers exhibiting only minor evidence of sedimentary reworking were sampled for the purpose of zircon extraction. The zircon crystals were separated from the two samples using standard heavy liquid and magnetic separation techniques. Four zircon crystals were selected from each sample and analysed at the Department of Geological Sciences, University of Cape town by Professor H. Frimmel, using the techniques described in Frimmel *et al.* (2000).

APPENDIX 2
PREVIOUS STRATIGRAPHIC SUBDIVISIONS FOR THE AHLMANNRYGGEN GROUP

LITHOSTRATIGRAPHY OF THE AHLMANNRYGGEN GROUP

PREVIOUS STRATIGRAPHIC SUBDIVISIONS

Eight researchers have investigated the stratigraphy of the Ahlmannryggen Group since 1949. A summary and comparison of their stratigraphic subdivisions is outlined below.

Roots (1969)
The Ahlmannryggen and Borgmassivet regions were first investigated by E. F. Roots and A. Reece, geologists with the Norwegian-British-Swedish Antarctic Expedition, between 1949 and 1952. Roots (1969) assigned the sedimentary sequence exposed west of the Jutul Glacier (present day Jutulstraumen Glacier) to the Ahlmannrygg Group, and estimated a thickness of at least 1600m for this sequence.

According to Roots (1953), the base of the group appeared to be represented by banded yellow and grey quartzites and a thin mud-chip conglomerate that lies with an angular unconformity on the smooth, apparently eroded surface of the metamorphic complex in the southern part of the Kirwan Escarpment (present day Kirwanveggan). The relationship of these rocks to exposures in the Ahlmann Ridge (present day Borgmassivet and Ahlmannryggen areas) was stated to be unknown. Roots' subdivision of the Almannrygg Group represents the first proposed stratigraphy for the region. He recognised four conformable formations in the Borg Massif (present day Borgmassivet area):

- A basal Fram Formation (>550m): well bedded quartzites, siltstones and mudstones, with the proportion of mudstone increasing vertically from less than 10% to greater than 50% near the top.
- Lower Borg Formation (300m): conspicuously banded quartzites and graywackes with mudstones, siltstones and thin bands of shale.
- Upper Borg Formation (200m): fine-grained quartzites with approximately 15% thinly bedded mudstones and siltstones with a few beds of angular conglomerate.
- An upper Raudberg Formation (>500m): a uniform succession of fine-grained red quartzite with thin layers of mudchip breccia and thin sheets of quartz pebble conglomerate.

De Ridder (1970)
E. De Ridder investigated the geology of the Borg Massif area from 1966 to 1967. He agreed with Roots' 1969 four-fold subdivision, but identified discrepancies in the thicknesses of individual formations. De Ridder defined the lower most formation in the area as the Framryggen Formation, which occurred at Framryggen nunatak and the small nunataks south of Borga (1810, 1885 and 1910). The type locality at Framryggen was described as a cyclic succession of black siliceous argillite and grey to greenish-grey, red banded arenites. The total sequence was inferred to be approximately 250m thick. The small nunataks, 1810, 1885 and 1910, were correlated to the upper part of the sequence exposed at Framryggen.

De Ridder (1970) divided the overlying Högfonna Formation, a jasper-bearing conglomeratic succession, into two conformable members. He identified exposures of this formation in the central part of the Borgmassivet, and proposed a conformable relationship to the underlying Framryggen Formation, despite the absence of an observable contact. The upper contact of the formation was taken to be represented by an 8m thick conglomerate exposed at Högfonna Nunatak, where it is conformably overlain by sediments he assigned to the Raudberg formation.

The Lower Högfonna Member was characterised by a partly cyclic sequence of reddish-grey to grey arenites and purple-brown argillite, approximately 450m thick. De Ridder identified other outcrops of the lower member of the Högfonna Formation at Nalegga, Borga, Fingeren, and Hogskavlen. The Upper Högfonna Member was identified as a 350m thick sequence of well-developed tuff bands and local red beds,

exposed at Högfonna, in the south-eastern Borgmassivet. He correlated this member to other exposures at Fasetfjellet, Soyla, Domen, Hogskavlen and Pilarryggen.

De Ridder investigated two outcrops of his proposed Raudberg formation, the first was some 150m of sediment overlying the Högfonna formation at Högfonna nunatak, the second, an approximately 350m thick succession at Raudberg nunatak. He reported a succession of thinly and thickly bedded, fine-grained red arenites and siliceous red argillites with subordinate intraformational conglomerate overlying the upper member of the Högfonna Formation at Högfonna nunatak, with a similar succession exposed at Raudberget.

Neethling (1970)

Concurrent to De Ridder's investigations in the Borgmassivet, D. C. Neethling carried out numerous studies of the geology of the Ahlmannryggen area. He tentatively proposed an alternative subdivision of the Ahlmannrygg Group, as well as suggesting a greater total thickness for the succession, of between 1700m and 1900m.

Neethling (1970) also retained a four-fold subdivision for the Ahlmannrygg Group, which he modified to include a lower Pyramiden Formation (300m), overlain by the Schumacher Formation (450m), followed by the Högfonna Formation (650m), and finally, the upper Raudberget Formation (300m to 500m). As previously mentioned, Roots (1969) had suggested that the base of the Ahlammrygg Group was exposed as quartzitic and conglomeritic beds unconformably overlying basement rocks at Kuven Hill and Tunga Spur in the Kirwan Escarpment. This however was refuted by Neethling, who concluded these outcrops represented much younger, and unrelated deposits.

Neethling's basal Pyramiden Formation had neither the upper nor lower contact exposed, and the proposed total thickness of 300m was considered to be a minimum estimate. The Pyramiden Formation consisted of well-bedded and thin greenish-gray sub-graywackes and siltstone with intercalated, dark muddy layers and rare monomict conglomerate. The overlying Schumacher Formation was considered to comprise mainly thinly bedded sub-graywackes and purplish mudstone and argillite, cyclically deposited and containing rare intraformational conglomerate. Neethling retained De Ridder's upper Högfonna and Raudberg Formations. The Högfonna Formation he considered conformable with his underlying Schumacher Formation, with the contact exposed at Grunehogna. Neethling did not identify any correlatives to De Ridder's Raudberg Formation in the Ahlmannryggen, but did however retain the formation name in his proposed revision of the stratigraphy.

Aucamp (1972)

A. P. H. Aucamp carried out the first detailed geological mapping of the Grunehogna nunatak group in the Ahlmannryggen area, during the 1968 – 1969 summer. He described a 300m thick sequence of typically low grade metamorphosed sediments, representing the top portion of Neethling's Schumacher Formation and De Ridder's overlying Högfonna Formation.

He was in agreement with Neethling's description of the Schumacher Formation, but suggested additional correlatives at Schumacherfjellet, Veten, and Framryggen nunataks. Aucamp (1972) proposed a three-fold subdivision of the Högfonna Formation, demarcated by two jasper-bearing conglomerates, as apposed to De Ridder's two-fold division. He postulated correlations with a wide number of other sequences, including exposures at Nils Jorgennutane, Jekselen, Fasettfjellet, Vindegga, Stridbukken, Framrabben, Trioen and the upper part of Veten.

Bredell (1977)

J. H. Bredell also briefly investigated the geology of the Ahlmannryggen area, during the summer of 1970 – 1971. He too modified Neethling's proposed subdivisions, but still recognised a four fold subdivision of the Ahlmannrygg Group; a lower Pyramiden Formation, followed by the Grunehogna Formation, the Högfonna Formation and an upper Raudberget Formation, restricted to the Borgmassivet.

Bredell (1977) extended the distribution of the Pyramiden Formation to include outcrops at Nashornet and Viddalskollen nunataks as well as Babordsranten and Kjolrabben. A two-fold subdivision into a lower and upper member was proposed for the sequence exposed in the Nashornet-Viddalskollen area.

Bredell (1977) renamed Neethling's Schumacher Formation the Grunehogna Formation, considering the nunatak of this name to contain a more representative sequence. He regarded the Grunehogna Formation to be the most widely distributed sedimentary unit in the Ahlmannryggen area, and agreed with Neethling's discription as alternating persistent beds of light coloured arenites and dark coloured argillites.

Bredell accepted De Ridder's two-fold subdivision of the Högfonna Formation for sequences exposed in the Borgmassivet, but could find no corresponding division in the successions exposed in the Ahlmannryggen. In addition, Bredell described correlatives from Jekselen and Tindeklypa nunataks, which he believed to constitute the upper part of the Högfonna Formation. As a result, he suggested an alternative subdivision, namely a lower Borgmassivet Member (including all sedimentary rocks assigned by De Ridder to the origionally defined Högfonna formation as well as the lithologically similar rocks from the Ahlmannryggen), and an upper Jekselen Member (includes all arenaceous, jasper-bearing, calcareous sedimentray rocks occurring at Jekselen and Tindeklypa).

Wolmarans and Kent (1982)

In 1982, L. G. Wolmarans and L. E. Kent summarised the past work done in the Borgmassivet and Ahlmannryggen areas in an attempt to resolve the controversy regarding the stratigraphy of the Ritscherflya Supergroup. Their proposed stratigraphic subdivisions represent the currently accepted stratigraphy of the area. Wolmarans and Kent (1982) subdivided the Ahlmannryggen Group into six formations. In ascending order, the Ahlmannryggen Group was divided into the Pyramiden, Framryggen, Schumacherfjellet, Högfonna, Raudberget and Jekselen Formations. These are summarised below from Wolmarans and Kent (1982).

The Pyramiden Formation is exposed at nunataks Pyramiden, Sphinksen, Knallen, Babordsranten, Kjolrabben Peak 1611, Nashornet, Viddalskollen, and Nashornkalvane in the Ahlmannryggen area, with nether the upper nor lower contacts exposed. The type area consists essentially of thin and evenly bedded feldspathic greywacke alternating with dark grey siltstone.

The Framryggen Formation is restricted to the north-western part of the Borgmassivet, and apart from the type locality (Framryggen nunatak) only occurs at Trioen, Framrabben, and Borga 1810, 1885, 1910. This formation comprises a succession of alternating mudstones and greywackes, and although there is no exposure of the upper or lower contacts, it is inferred to have a conformable relationship with both the underlying Pyramiden, and overlying Högfonna Formations.

The Schumacherfjellet Formation, consisting of a sequence of alternating light coloured arenites and dark coloured argillites, is restricted to the Ahlmannryggen area, with occurences recorded from nunataks Shumacherfjellet, Grunehogna, Lyftingen, Kjollrabben, Styrbordsknattane, Ovenuten, Flarjuven, Flarjuvnutten and Klumpane. The top of the formation is exposed at Grunehogna, where it is conformably overlain by sediments of the Högfonna Formation. However, the base is nowhere exposed, and the supposed contact with the underlying Pyramiden Formation has not been proved in outcrop.

The Högfonna Formation is described as comprising a conglomeritic and jasper-bearing succession of quartzites, mudstones and shales, with red beds and tuff layers occurring towards the top of the formation. Wolmarans and Kent subdivided the Högfonna Formation into the Grunehogna, Veten and Högfonnaksla members. The Högfonna Formation shows the widest distribution of all the formations within the Ahlmannryggen Group, occuring virtually throughout the Borgmassivet, but is limited to the Grunehogna nunatak in the Ahlmannryggen area, where it conformably overlies the Schumacherfjellet Formation.

The Jekselen Formation is described as detached blocks / xenoliths of steeply dipping arenaceous sediment in diorite of the Borgmassivet Intrusives. The occurrence of this formation is restricted to the type locality, Jekselen nunatak, and isolated exposures at Tindeklypa. The sequence consists predominantly of calcareous sandstone units with well developed cross-bedding, and lesser amounts of shale and conglomerate.

The upper most formation of the Ahlmannryggen Group, the Raudberget Formation, comprises a red-bed succession of quartzite and mudstone interbedded with volcaniclastic material and

minor conglomerates. It conformably overlies the Högfonna Formation, but the upper contact is not exposed. The distribution of this formation is confined to the Borgmassivet. The base of the formation is marked by a prominent 8m thick conglomerate at Högfonna nunatak , which is overlain by dark red quartzites alternating with siliceous mudstones

Ferreira (1986)

The Ahlmannryggen area was again investigated by E. Ferreira from 1983 to 1985, who recognised the same five-fold subdivision as outlined in Wolmarans and Kent (1982) (the occurrence of the Raudberg Formation being restricted to the Borgmassivet area), but interpreted slightly different depositional settings.

Swanepoel (1982)

Concurrent to the investigations of Ferriera, J. J. P. Swanepoel examined outcrops of the Ahlmannryggen Group in the Borgmassivet area. Swanepoel (1982) suggested drastic revisions to the stratigraphic subdivisions developed by Wolmarans and Kent (1982). He proposed a three-fold subdivision of the Ahlmannryggen Group, into a lower, coarsening-upwards Friis-Baastadnuten Formation, a middle, fining-upwards Veten Formation, and an upper, coarse grained Grunehogna Formation.

APPENDIX 3
DETAILED LITHOFACIES DESCRIPTIONS

LITHOFACIES OF THE AHLMANNRYGGEN GROUP

GRAVEL LITHOFACIES

Massive Gravel (Gm_{1-2})

Stratification and grading are entirely absent from the massive gravel lithofacies, which may occur as a poorly sorted matrix-, or clast-supported gravel. In all cases, the matrix is medium- to very coarse-grained, and often quartz dominated, although a high proportion of lithic and feldspathic grains may be present. The clasts show a high degree of variability, ranging in size from 2mm to over 200mm, with an average between 10mm to 60mm. Clasts vary from being highly angular with a low sphericity, to well rounded with a moderate sphericity. Clast types include brilliant red jasper, less abundant black and white chert, quartz, red sandstone, quartzite, black and green mudstone, and rare orthogneiss. Clast imbrication is rare, but has been observed in a limited number of outcrops. Bed thickness varies from less than 0.2m to a maximum of 2.0m, and may contain discontinuous layers and lenses of sandstone containing scattered clasts and gravel stringers. The basal surface of the massive gravel units is invariably erosional , while the upper contacts are often transitional. Mud / silt rip-up clasts may be present in the otherwise exotic / extraformational clast dominated gravel. Overall, Gm lithofacies are rare in the Ahlmannryggen Group, constituting only 1.5% of the total sequence observed.

Gravel lithofacies may owe their origin to a number of different depositional processes, and may be formed under a wide range of physical conditions (Allen, 1983). As marked variations were noted between some of the Gm facies exposures, a two-fold subdivision of facies Gm was considered necessary. Sub-facies Gm_1 is generally matrix supported, and the clasts lack imbrication, suggesting a flood depositional origin (Bridge, 1993 and Miall, 1996). Sub-facies Gm_2 is typically clast supported, and may show imbrication of the clasts consistent with other associated palaeoflow indicators. This sub-facies probably owes its origins to the migration of longitudinal bars or low-density bedload sheets (Bridge, 1993 and Todd and Went, 1991).

Flat Lying Gravel (Gfl)

Flat lying gravels represent a very minor percent (< 0.5%) of the total lithofacies recorded for the Ahlmannryggen Group. Facies Gfl is poorly to moderately sorted, generally matrix supported, with a quartz dominated, medium- to coarse-grained matrix. Clasts vary in size from 10mm to 60mm, and may be sub-angular to well rounded. Stratification is flat lying, with no imbrication of the clasts observed. The basal contact is generally erosional, and the beds (which reach a maximum thickness of 0.2m) may be normally or inversely graded. Mud / silt rip-up clasts may be present in the otherwise exotic / extraformational clast dominated gravel. Facies Gfl exhibits a slightly different clast assemblage from the other gravel lithofacies in that it contains a lower proportion of quartz and sandstone clasts, and no quartzite or gneiss clasts were identified.

Facies Gfl is interpreted as representing horizontally stratified gravel sheets, which may develop in association with longitudinal bars (Miall, 1993), and can show either an upward increase or decrease in clast size, depending on the mode of accretion. Clast accumulation in place tends to result in an upward fining trend, as the deposit builds to shallower water levels. However, these deposits also tend to migrate downstream, and in such cases, the upper, coarser deposits may migrate over the finer basal deposits (Miall, 1996).

Stratified Gravel with Planar Cross-beds (Gp)

Planar cross-stratified gravel varies from clast to matrix supported, with clast sizes reaching a maximum of 80mm. The matrix is medium grained to gritty, and is quartz dominated, but with a significant proportion of lithic and feldspathic grains. Clast types are the same as discussed for Gm lithofacies. The clast shape varies from sub-angular to well rounded, and overall, facies Gp varies from poorly to moderately sorted. Facies Gp shows distinctive planar cross-stratification, with foreset dips varying from 15° to 35°. Bed thicknesses are typically limited to between 0.5m to 1.5m, and in rare cases show indistinct normal grading. Clasts may be imbricate, and the basal surface is generally erosional. Occasionally, Gp facies contain horizons of planar cross-stratified sandstone. Within the Ahlmannryggen Group, Gp lithofacies are only present in a few isolated horizons, forming 0.1% of the exposed sequence.

In most cases (e.g. Miall, 1977; Karpeta, 1993; Williams, 1971 and Rust, 1972) the formation of Gp lithofacies can been attributed to the migration of large gravelly bedforms under high flow regime conditions.

Stratified Gravel with Trough Cross-beds (Gt)
Trough cross-bedded gravels have a limited distribution in the Ahlmannryggen Group, forming only 4% of the total sequence. Facies Gt varies from clast to matrix supported, with a typically very coarse grained to gritty matrix. Clasts sizes are highly variable, reaching a maximum of 60mm. A common feature of this facies is the alternation of matrix and clast supported horizons. An erosively based, clast supported lower region generally grades up into a matrix supported region, that often contains heavy mineral laminae. There is no imbrication visible in the clast arrangement, and bed thicknesses reach a maximum of 2m. This lithofacies often grades vertically into St lithofacies within the same coset.

As is the case for Gp, Gt lithofacies also represent a deposit formed under high flow regime conditions. Karpeta (1993) provides a broad interpretation of the mode of formation this lithofacies type, and attributes the origin of Gt to the migration of large, gravelly 3-D bedforms, while William and Rust (1969) also propose a channel scour origin.

SANDSTONE LITHOFACIES

Massive Sandstone (Sm)
Massive sandstone lithofacies in the Ahlmannryggen Group are highly variable, and may be fine- to very coarse-grained. Facies Sm is generally moderately to well sorted, but may contain scattered exotic and intraformational clasts up to 60mm in size (predominantly less than 10mm). No stratification is visible in this facies, which may have an erosional base characterised by the presence of Se lithofacies, or alternatively, may exhibit a simple, sharp lower contact. The upper surface may be transitional to erosional. The occurrence of Sm lithofacies is diverse, but despite its widespread distribution throughout the Ahlmannryggen Group, forms only 3% of the sequence.

Massive sandstone beds may form in a variety of depositional environments. Smith (1986) suggested that short-lived mass flows were responsible for the dumping of sediment at a rate too fast for hydraulic sorting processes to work effectively. The relatively short transport distances (suggested by the presence of mud rip-up clasts) and the rapid deposition of the sediment load may be attributed to velocity changes, which would reduce the dispersive pressure and turbulence below a critical value, permitting rapid deposition of the load. The occurrence of thin, isolated units of Sm lithofacies in sequences otherwise dominated by fine-grained lithofacies, may also represent the periodic introduction of coarser-grained, current-borne sediment into a system otherwise dominated by suspension fall-out.

Horizontally Laminated Sandstone ($Sh_{1,2}$)
Lithofacies Sh may be fine- to coarse-grained, and is generally moderately to well sorted. Occasionally, Sh lithofacies contain gritty stringers and scattered clasts (intra- and extra-formational). Stratification within this lithofacies is limited to laminations orientated at up to 5°, and rare evidence of parting lineations on bedding plane surfaces. The restricted occurrence of parting lineations may be ascribed to pervasive alteration of the sediments, and limited bedding plane exposures. Heavy mineral laminae may be present. The basal contact may be sharp, or may be marked by the development of Facies Se. Lithofacies Sh is widely distributed, yet only constitutes 2% of the Ahlmannryggen Group.

Two contrasting modes of occurrence were noted for Sh lithofacies, and as a result, division into sub-facies is suggested. Sub-facies Sh_1 is coarser grained (typically medium- to coarse-grained), may contain scattered clasts and occasionally displays parting lineations. This sub-facies is generally associated with a variety of other sandstone lithofacies, and commonly shows an upward transition into either planar or trough cross-stratified sandstone. A popular explanation for the formation of this facies is described in Harms and Fahnestock (1965), Allen (1964), Collinson (1968) and Miall (1977), who all attribute the formation of a plane bed configuration to the presence of upper flow regime conditions, during which the sediment forms a traction carpet, with virtually continuous particle movement.

Alternatively, the horizontally bedded sandstones with the Ahlmannryggen Group may be fine to

medium grained, devoid of parting lineations and commonly showing an upward transition into a fine grained, mud dominated facies (sub-facies Sh_2), suggesting deposition under lower flow regime conditions (Moore, 1979 and Harms *et al.*, 1975). According to Miall (1977), shallow water and low flow velocities can combine to create very low amplitude sand waves, leading to the development of horizontally bedded sandstones under low flow regime conditions.

Planar Cross-Stratified Sandstone (high angle) (Sph)

A wide variety of high angle planar cross-stratified sandstones occurs in the Ahlmannryggen Group, forming one of the dominant lithofacies types, and constituting over 11% of the total sequence.

Facies Sph shows a wide variety of grains sizes, from fine- to very coarse-grained, and may contain scattered clasts up to 10mm in size. Heavy mineral laminae may also be present. Generally however, this facies is medium grained and moderately sorted. Occasionally, Sph lithofacies may be normally graded, and may show a decrease in cross-bed scale vertically, however this is not the norm. Foreset thicknesses vary from under 0.1m to 1.5m, with dips of between 16° and 35°, and may be asymptotically shaped. The lower contacts are generally erosional, often with facies Se developed at the base, while upper contacts are transitional to sharp or erosional.

According to a number of authors (e.g. Bridge, 1993 and Harms *et al.*, 1975) the development of planar cross-stratification can be attributed to the migration of straight crested (two-dimensional) dunes or sand waves under lower flow regime conditions. An alternative explanation for the development of planar cross-beds in the fluvial environment, is the migration of transverse or slip faces bars (Smith, 1972 and Todd and Went, 1991). The presence of asymptotically shaped cross-beds may be ascribed to the presence of strong separation eddies during the high water stage (Miall, 1977), while the rare normal grading and vertically decreasing cross-bed scale may be attributed to waning flow conditions. The smaller scale cross-beds may owe their origin to the generation of small, repetitive sand waves, formed in relatively low velocity currents (Todd and Went, 1991).

Planar Cross-Stratified Sandstone (low angle) (Spl)

Low angle planar cross-stratified sandstone forms approximately 8% of the lithofacies within the Ahlmannryggen Group. Facies Spl may be medium- to very coarse-grained, and occasionally contains scattered extra- and/or intra-formational clasts up to 10mm in size. Commonly however, Spl lithofacies are medium grained and moderately to well sorted. Foreset thickness ranges from under 0.2m to 2.5m, and the foresets dip at between 5° to 15°. Basal contacts are typically sharp to erosional, and may have a basal Se lithofacies layer developed, while the upper contacts vary from erosional to transitional in nature. Heavy mineral laminae may be present.

According to a number of authors (e.g. Smith, 1972, Moore, 1979 and Todd and Went, 1991), low angle planar cross-stratification represents deposition on the inclined surface of side, lateral or point bars, with the lower foreset angle attributed to increasing depth and flow strength on the bar surface.

Trough Cross-Stratified Sandstone (St)

Trough cross-stratified sandstone forms a significant proportion (31%) of the lithofacies present in the Ahlmannryggen Group. St lithofacies vary from medium- to very coarse-grained and are generally well sorted, but may contain scattered extra- and intra-formational clasts up to 10mm. The cross-beds range from small- to large-scale, with trough depths of between 0.05m to 2.5m and may form cosets of several meters. The basal, erosional surface may be marked by the development of Facies Se, and rarely, the units may be normally graded. Heavy mineral laminae may also be present.

It is generally accepted that trough cross-beds are formed by migrating sinuous crested (three-dimensional) dunes under low to high flow regime conditions (Harms *et al.*, 1975). Occasional normal grading of the lithofacies may be attributed to deposition under waning flow conditions.

Sandstone with Ripple Marks ($Sr_{1,2}$)

Sandstone units with preserved ripple bedforms (Facies Sr) are common in the Ahlmannryggen Group, but overall only constitutes 0.2% of the observed sequence. Facies Sr consists of fine to medium-grained, moderately to well sorted

sandstone ripple casts, which may occur as solitary trains, or more rarely, as interference sets. This lithofacies can be subdivided into two groups based on the morphology of the ripples.

Sub-facies Sr_1 is typified by almost symmetrical ripple crests, either straight or slightly sinuous, and rarely bifurcate. Ripple amplitude is between 2mm and 10mm, while wave length varies from 10mm to 80mm. These small scale wave ripples are regarded as having formed by currents operating in the lower part of the lower flow regime (Allen, 1964). The occurrence of Facies Sr_1 is wide spread, and it essential to examine each occurrence in context with the associated lithofacies types, in order to constrain the environment of formation.

Sub-facies Sr_2 consists of ripples with a pronounced asymmetrical morphology. The ripple crests vary from straight or sinuous to linguoid, with an amplitude of between 3mm and 6mm, and a wavelength varying from 15mm to 33mm. These current ripples are formed during low flow regime conditions, and are widely known from a variety of depositional settings, including river and tidal channels, and are also shaped by deep-sea currents (Allen, 1984). As is the case with Sr_1 lithofacies, it is essential to treat each occurrence individually, and examine in detail the associated lithofacies types in order to constrain the environment of formation.

Basal Scour Sandstone / Mudchip Breccia (Se)
This is not a true, discrete lithofacies in the same sense as the other facies described here, but does represent a recognisable 'state' within the sedimentary sequence, and is therefore dealt with separately. Facies Se is a typically medium- to coarse-grained sandstone, with a well-developed mud-chip breccia, and in some cases, exotic gravel clasts. In most instances, a thin layer (usually about 0.25m thick) of massive sandstone containing an intra- and/or extra-formational gravel layer, overlies a generally well pronounced erosional / scoured basal surface. Facies Se passes transitionally into either Sp or St, and more rarely, into Sm and Sh lithofacies. Facies Se is common throughout the Ahlmannryggen Group, but forms only 0.5% of the observed sequence.

This facies represents the initial scouring action of a current, which is responsible for eroding into the underlying, generally finer grained layers, often ripping up angular mud / silt clasts. If subsequent deposition occurs relatively rapidly thereafter, the mud / silt flakes may be preserved, and deposited as a mud-chip breccia overlying the erosional surface. Longer transport distances / duration may result in the destruction of the mud-chips, in which case the mud-chip breccia may be poorly developed to absent.

Scour Fill Sandstone (Ss)
Scour fill sandstone is a relatively uncommon facies type in the Ahlmannryggen Group, constituting only 1% of the total lithofacies present. This facies type typically forms scoop-shaped or concave-up deposits consisting of coarse-grained sandstone, and may contain sub-angular to rounded extra- and/or intra-formational gravel clasts. Where these clasts are exceptionally abundant, as is common near the basal contact, Ss lithofacies may consist of a matrix or clast supported gravel. Internal stratification may take the form of horizontal to low angle laminations, and the scours are typified by a pronounced basal erosion surface extending to a maximum depth of 1.2m, and ranging from 1.0m to 10m in width.

Scouring may form at channel confluences, or may be related to the action of strong separation eddies, or to the development of local votices around obstructions. The erosion of the scour hollow and its subsequent infilling do not represent simultaneous events. Larger scours may represent small channels formed by avulsion during high water stage, or by bar dissection during falling water conditions (Miall, 1977).

Ripple Cross-Laminated Sandstone (Srl)
Facies Srl consists predominantly of fine-grained, well-sorted sandstone displaying abundant small-scale internal stratification, and occasionally occurring as sets of climbing ripples. This is a relatively uncommon facies type in the Ahlmannryggen Group, forming only 1% of the observed sequence.

According to Miall (1977), ripples continue to migrate across surfaces during low energy level periods, even at extremely shallow depths, and in so doing, form small-scale cross-stratified deposits. These deposits are typically considered indicative of sediment migration during the lower part of the lower flow regime (Allen, 1964) and have been recorded from a number of contrasting depositional settings, including

fluvial, deltaic and marginal marine environments (Moore, 1979 and Allen, 1964).

Flaser Bedded Sandstone – Mudstone (SFf)
Flaser bedded sandstone forms only 0.5% of the lithofacies present in the Ahlmannryggen Group. Facies SFf consists of very fine- to fine-grained, moderately sorted sandstone with lesser amounts of mudstone. This lithofacies is easily recognisable, with small-scale cross-bedded to ripple cross-laminated sandstone containing intercalated fine grained mud/silt flasers. The nature of the flasers in variable, with a continuum from wavy to bifurcate wavy recorded. Wavy flaser bedding contains discontinuous concave and convex mud flasers, while the bifurcate wavy flaser bedding is similar in appearance, but has the added characteristic of regular bifurcations resulting from the contact of a partially exposed flaser of an earlier generation with younger flasers.

Flaser bedding represents a type of interbedding of contrasting lithologies, and owes its origins to the alternation of current or wave action and slack water. The current or wave action forms the sand into ripples, while the mud is deposited from suspension during times of slack water (Rieneck and Wunderlich, 1968).

Wavy Bedded Sandstone - Mudstone (SFw)
Facies SFw is similar to SFf lithofacies in many respects, and merely represents another stage in a continuum from cross-bedded sandstone with isolated flasers to lenticular bedding (Rieneck and Wunderlich, 1968). Facies SFw contains a regular alternation of fine- to medium-grained, moderately sorted sandstone and mudstone. The sandstone is ripple cross-laminated, with mud/silt layers overlying the ripple crests and filling the ripple troughs. As a result, the upper surface of the mud layer takes on the curvature of the underlying sandstone ripples to a limited degree; the thicker the mud layer, the more reduced the surface undulations. Although constituting only 8% of the lithofacies present in the Ahlmannryggen Group, SFw lithofacies show a wide distribution.

As with SFf lithofacies, the formation of SFw requires the sorting of sediment into two distinct lithologies. The formation of ripples indicates that currents in the lower part of the lower flow regime operated during certain stages of deposition, alternating with slack water conditions, however with a greater build-up of mud than for flaser bedding (bedding (Rieneck and Wunderlich, 1968).

FINE-GRAINED LITHOFACIES

Massive Mudstone (Fm)
This lithofacies type lacks internal stratification, and consists entirely of massive, moderately sorted mud/silt. Unit thicknesses range from a few centimeters to 1.5m, with non-erosional lower contacts and erosional upper contacts. Facies Fm may occur as either laterally extensive sheets, or isolated, discontinuous lenses. Fm is a relatively common lithofacies type in the Ahlmannryggen Group, forming 10% of the observed sequence.

The absence of any features indicative of current activity, and the fine grained nature of this lithofacies suggests deposition took place largely from suspension, with little or no current activity (Collinson, 1968).

Mudstone with Desiccation Cracks (Fd)
Lithofacies Fd is not a true lithofacies in the same sense as the other facies types described here, in that it merely represents a modification of other fine-grained facies such as the massive mudstone (Fm) and rippled mudstone (Fr) lithofacies. However, Facies Fd has significant environmental implications, and as such will be dealt with separately. The critical factor distinguishing Facies Fd is the presence of desiccation cracks on the bedding plane surface of a fine-grained unit. Lithofacies Fd, although constituting only 0.2% of the Ahlmannryggen Group, is wide spread.

It is a well documented fact that shrinkage cracks form due to temporary subaerial exposure, and can occur in many continental and coastal environments. However, there are few, if any detectable differences between the fractures developed in these different settings, and as such Facies Fd in not particularly indicative of deposition setting (Allen, 1984). On the other hand, Facies Fd does provide convincing evidence of shallow water / temporary subareal conditions, and when considered in relation to the associated facies types, may provide important constraints on the nature of the depositional environment.

Mudstone with Raindrop Impressions (Frd)
Facies Frd also represents the modification of a pre-existing fine-grained lithofacies type, but in a manner sufficiently significant to warrant inclusion as a separate lithofacies type. In the case of Facies Frd, the diagnostic characteristic is the presence of raindrop imprints on the upper surface of a fine-grained unit, again indicative of temporary sub-aerial exposure (Allen, 1984 and Metz, 1981). The distribution of Frd lithofacies is limited, forming less than 0.1% of the observed sequence.

Horizontally Laminated Mudstone (Fh)
Lithofacies Fh consists predominantly of moderately sorted mud/silt, often with thin, very fine- to fine-grained sandstone laminae. Facies Fh is relatively wide spread, but overall, only constitutes 5% of the observed sequence. Basal contacts are generally transitional, and upper contacts transitional to erosional. This facies is interpreted as a low energy deposit that accumulated in an environment where the dominant sedimentary process was suspension fall out of fine-grained material, accompanied by the periodic input of current transported sands (Hjellbakk, 1997). The fluctuating grain size may also be attributed to fluctuating sediment supply, possibly related to climatic factors (Collinson, 1968). This lithofacies type has been reported from a wide range of depositional settings, and considered in isolation is not environmentally indicative.

Ripple Cross-Laminated Mudstone (Frl)
This is a finer grained version of Facies Srl, dominated by silt and mud as opposed to fine-grained sand, although the internal stratification and interpretation of the mode of formation are consistent with that previously given. Lithofacies Frl forms 10% of the observed sequence.

Mudstone with Ripples ($Fr_{1,2}$)
As is the case with the above mentioned lithofacies type, facies Fr shares many similarities with a previously described facies type, notably facies $Sr_{1,2}$, with the exception that facies Fr is mud and silt dominated, as opposed to sand dominated. The general lithofacies descriptions and interpretations given for $Sr_{1,2}$ therefore apply. Lithofacies Fr constitutes less than 0.5% of the observed sequence.

VOLCANICLASTIC LITHOFACIES

Volcaniclastic lithofacies are relatively uncommon in the Ahlmannryggen Group, constituting only 3% of the total sequence. Volcaniclastic sediments are composed chiefly of grains of volcanic origin, derived from comtemporaneous volcanicity, and depending on mode of occurrence can be classified as primary or reworked. Massive primary pyroclastics, consisting of fallout deposits are extremely rare in the Ahlmannryggen Group, while reworked volcanogenic deposits are more common, with examples occurring virtually throughout the succession. These deposits result from the subsequent reworking of volcaniclastic material in the sedimentary environment, in the same way as any other clastic material. Thus many of the depositional sedimentary structures described in the above mentioned lithofacies can be found in reworked volcaniclastic deposits (Tucker, 1981).

Massive Volcaniclastic (Vm)
Facies Vm is restricted to a few units near the top of the Ahlmannryygen Group. According to Wolamrans and Kent (1982), these volcaniclastics can be subdivided according to textural variations, into four categories: vitroclastic tuffs, laminated tuffs, pisolitic tuffs and welded tuffs.

Epiclastic Lithofacies (V)
There are a number of reworked volcaniclastic horizons within the Ahlmannryggen Group, which combined constitute approximately 3% of the observed sequence. These units represent reworking of volcaniclastic material under the same conditions that formed the equivalent sandstone / fine-grained facies, and the reader is referred to the relevant examples described under these sections for description and interpretation. The presence of reworked volcaniclastic material in a previously described lithofacies is denoted by the use of the letter V as a suffix.

APPENDIX 4
SEDIMENTARY LOGS

Appendix 4: Additional vertical profiles from the Schumacherfjellet Formation

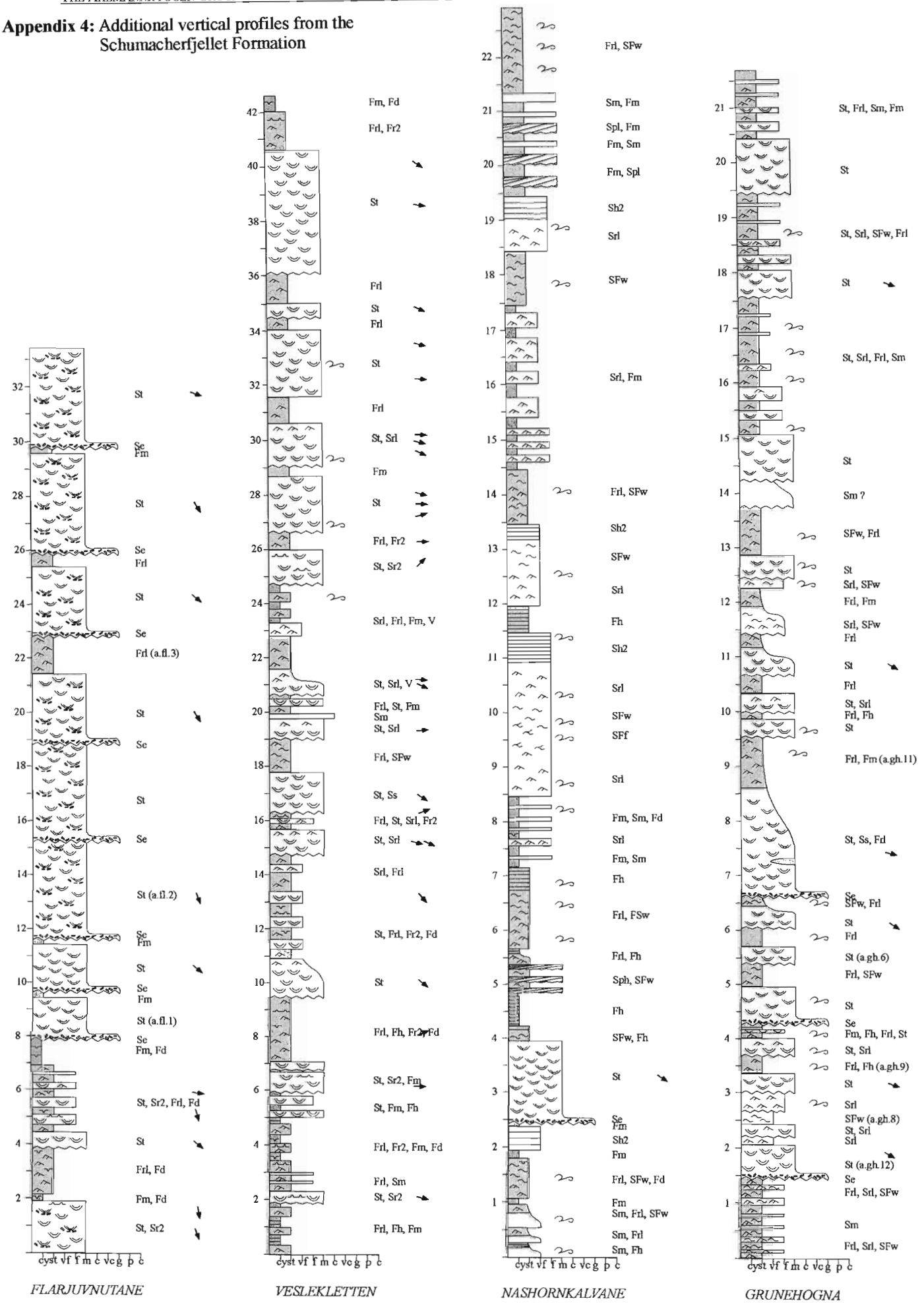

Appendix 4: Additional vertical profiles from the Grunehogna Formation

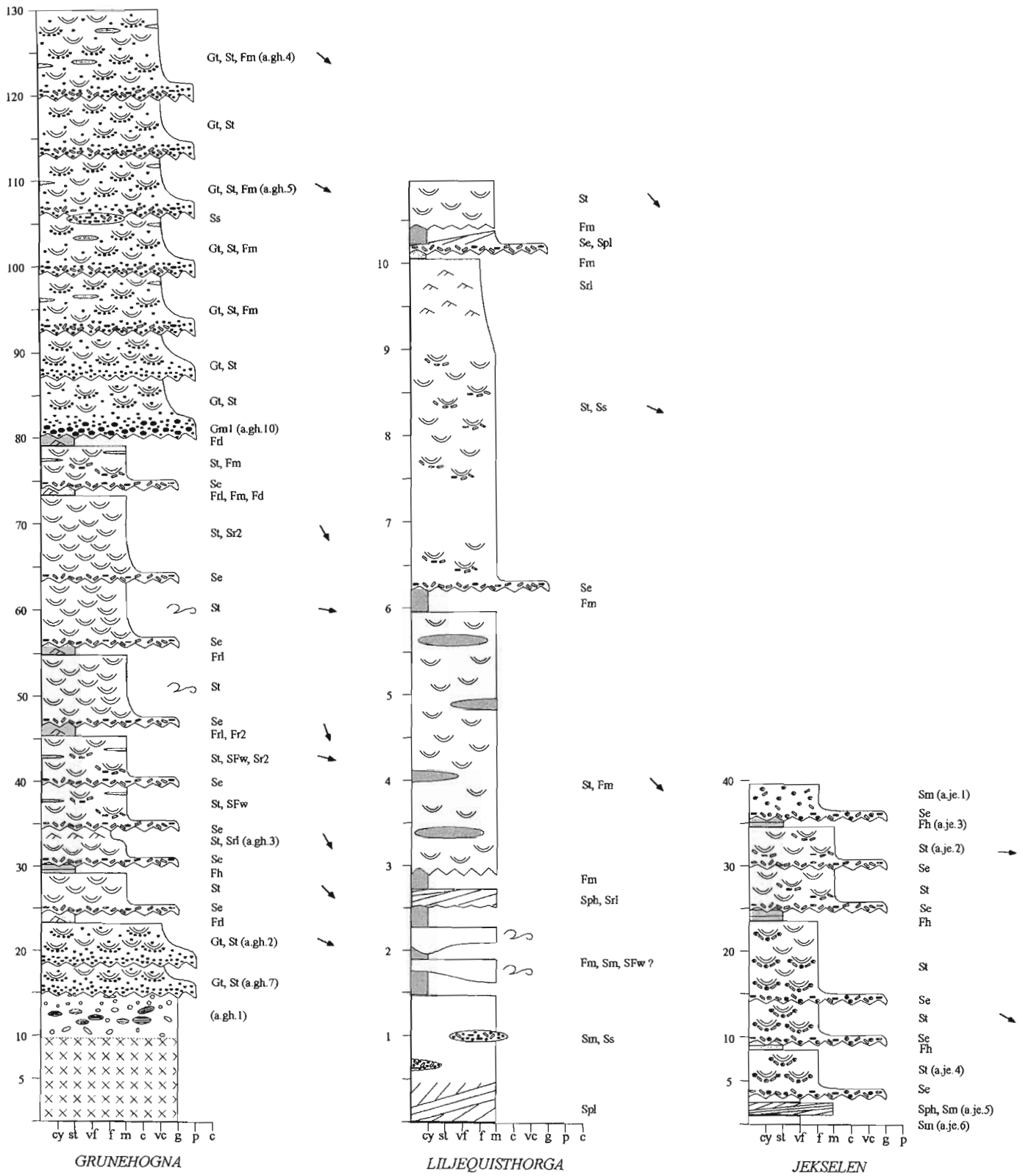

Appendix 4: Additional vertical profiles from the Veten Formation

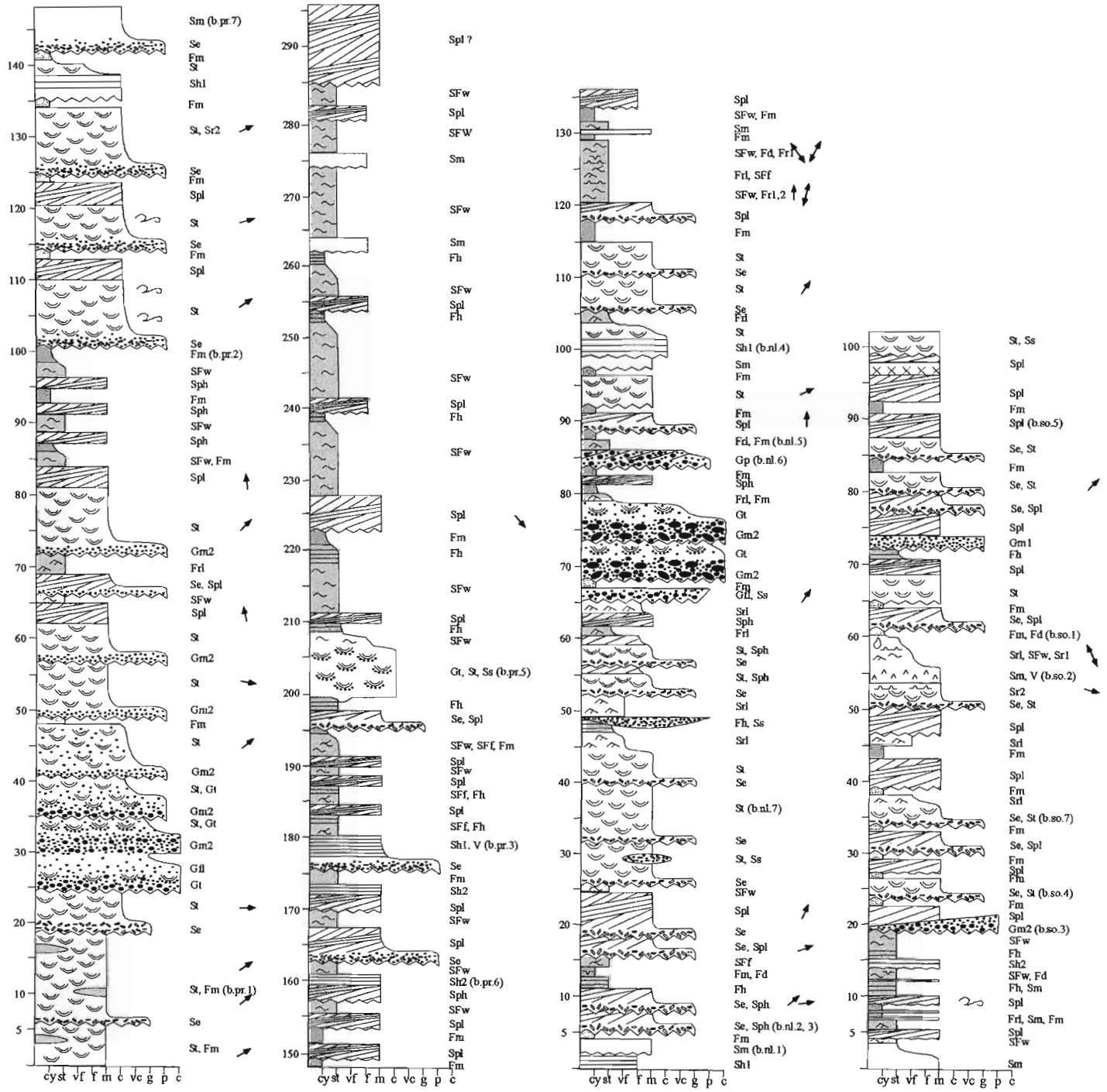

Appendix 4: Additional vertical profiles from the Veten (0m-120m) and Framryggen (120m-480m) Formations

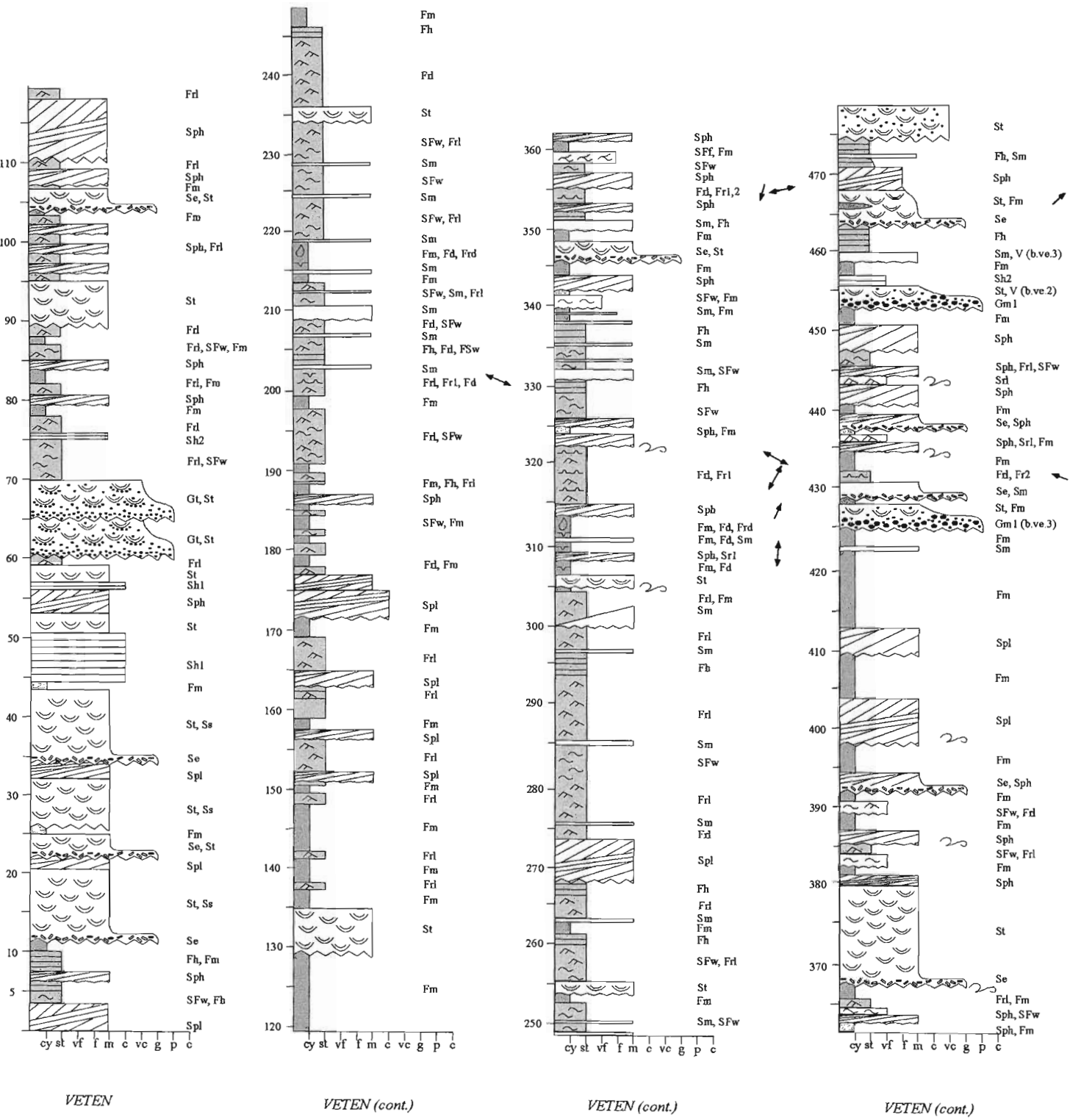

Appendix 4: Additional vertical profiles from the Framryggen Formation

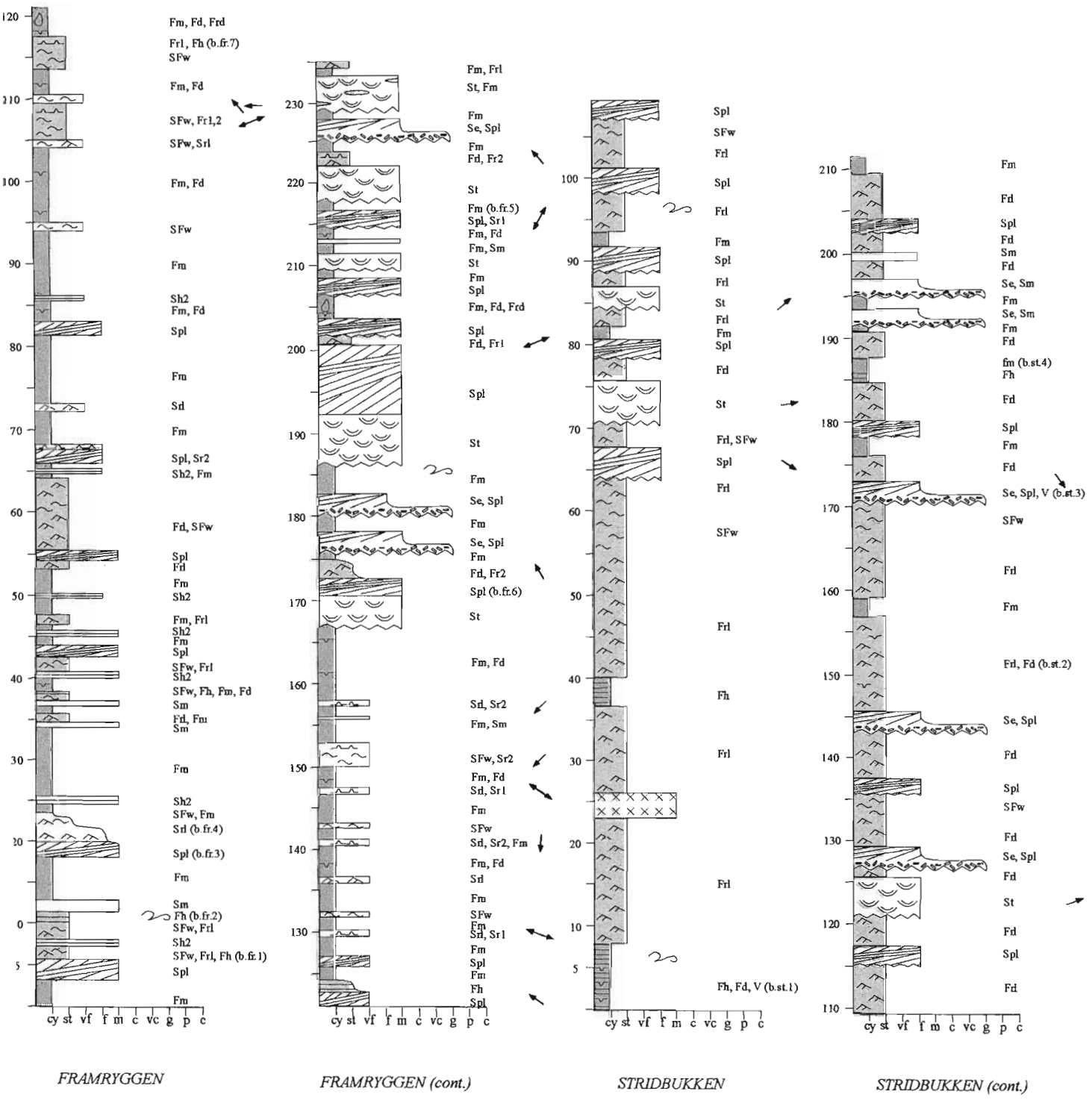

Appendix 4: Additional vertical profiles from the Framryggen Formation

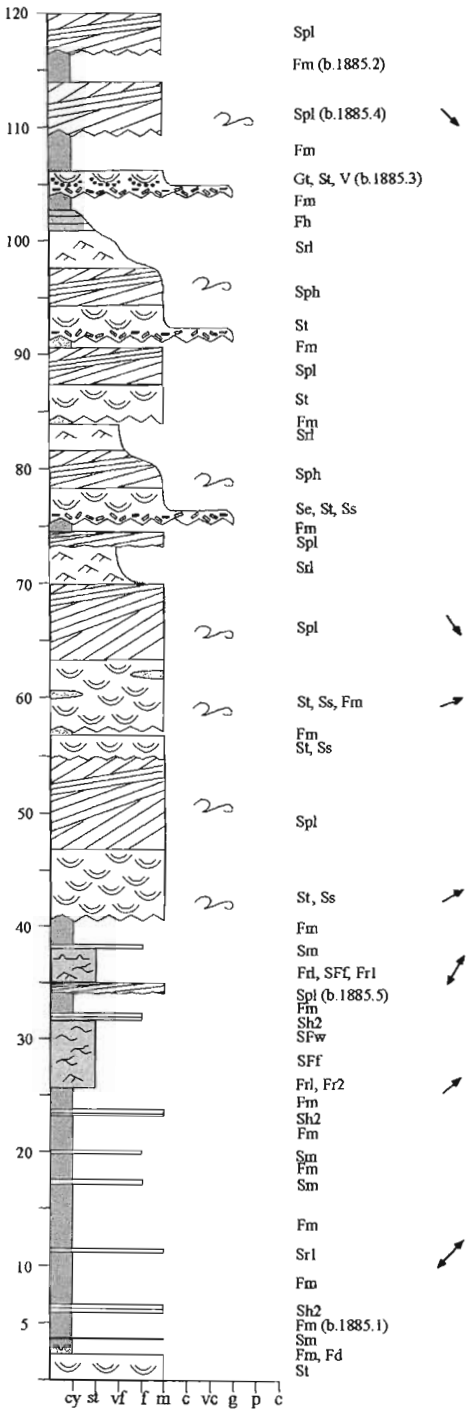

NUNATAK 1885

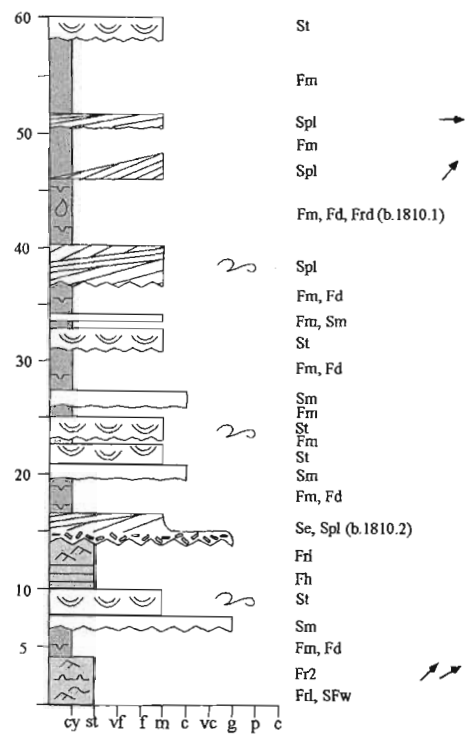

NUNATAK 1810

Appendix 4: Additional vertical profiles from the Högfonna Formation

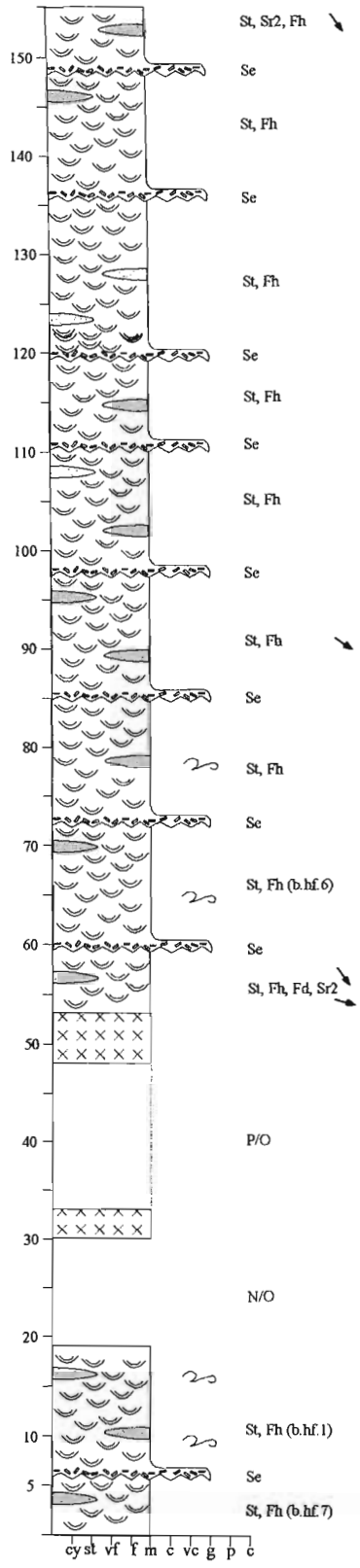

HÖGFONNA

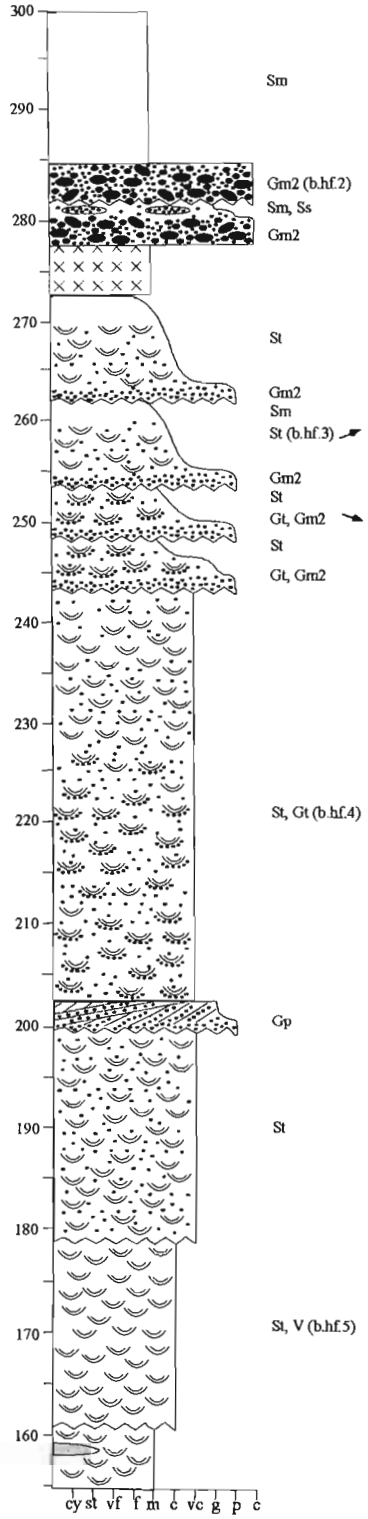

HÖGFONNA (cont.)

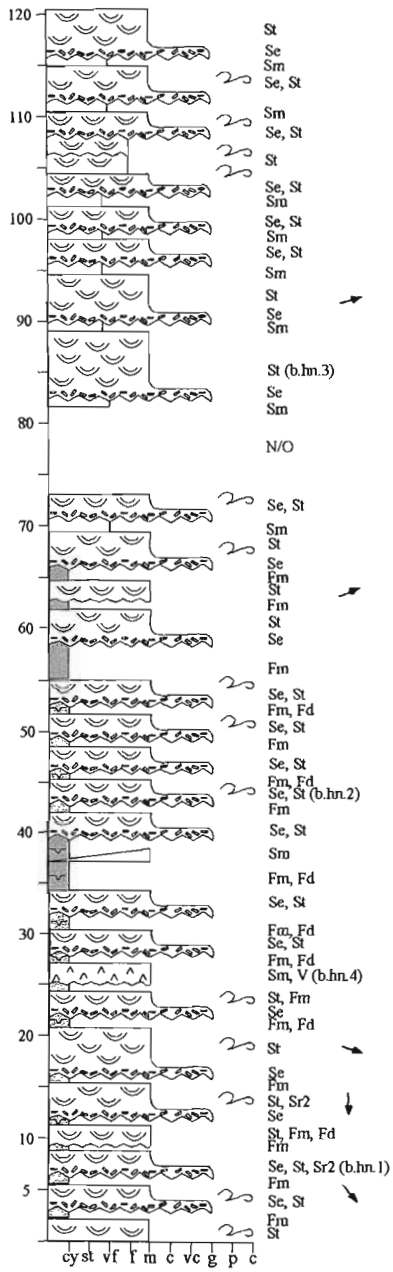

HÖGFONNA- 2130

Appendix 4: Additional vertical profiles from the Högfonna Formation

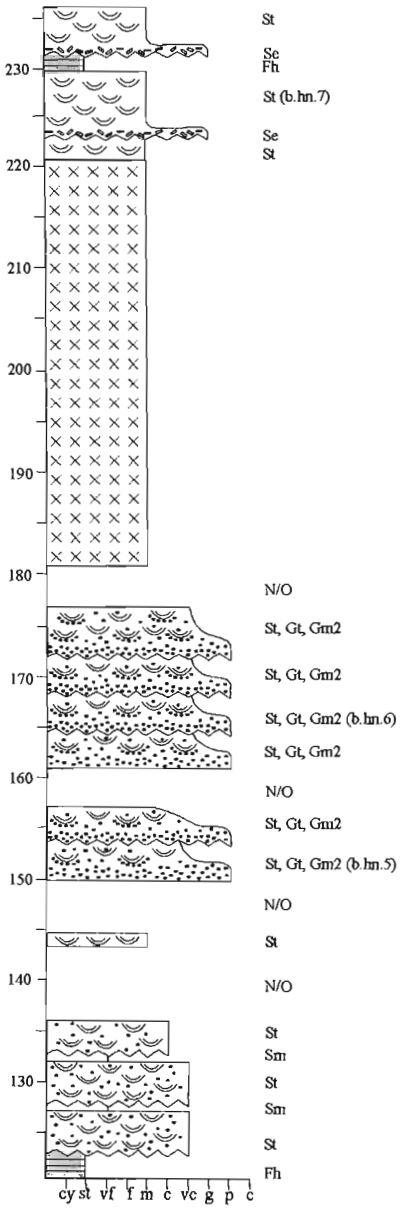

HÖGFONNA- 2130 (cont.)

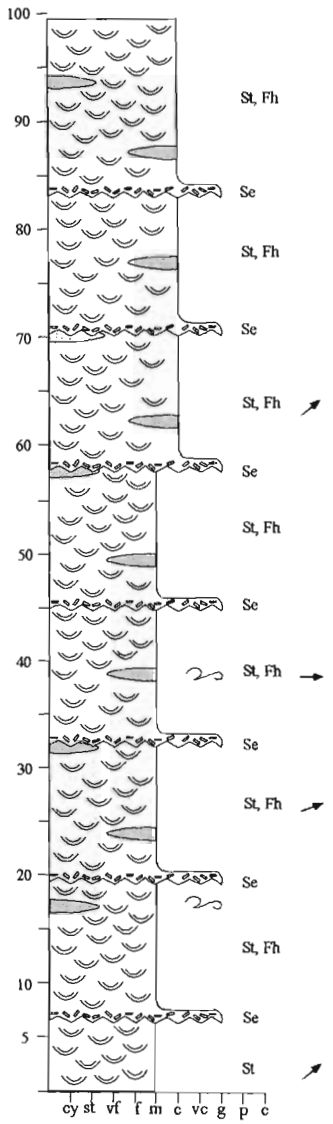

RAUDBERGET

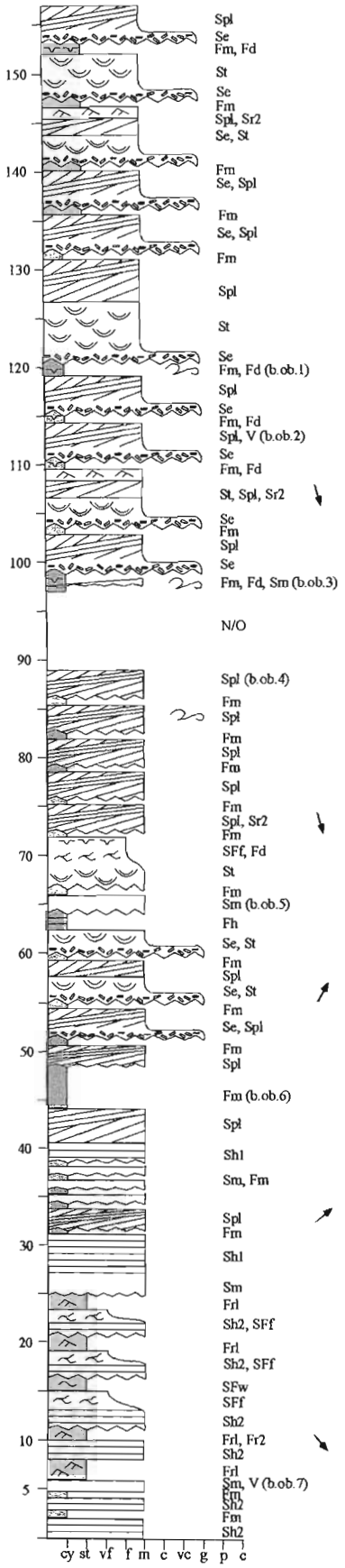

OVBRATTEN

Appendix 4: Additional vertical profiles from the Högfonna Formation

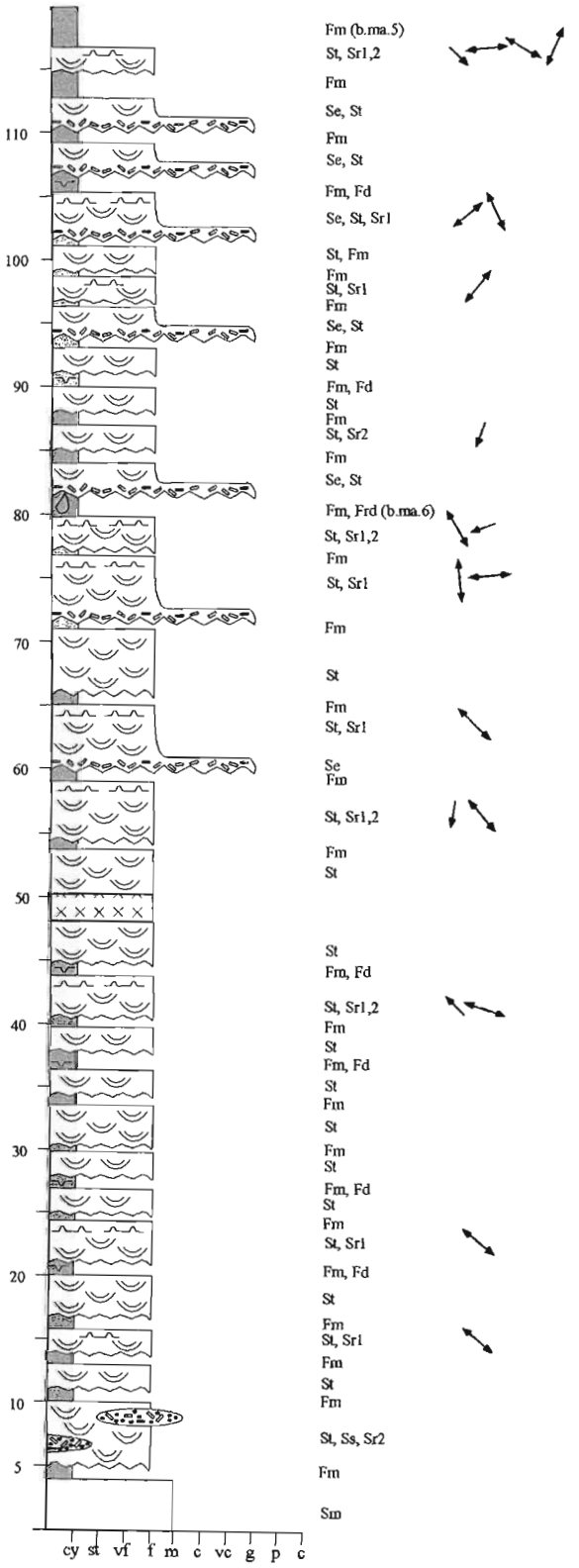

MANA

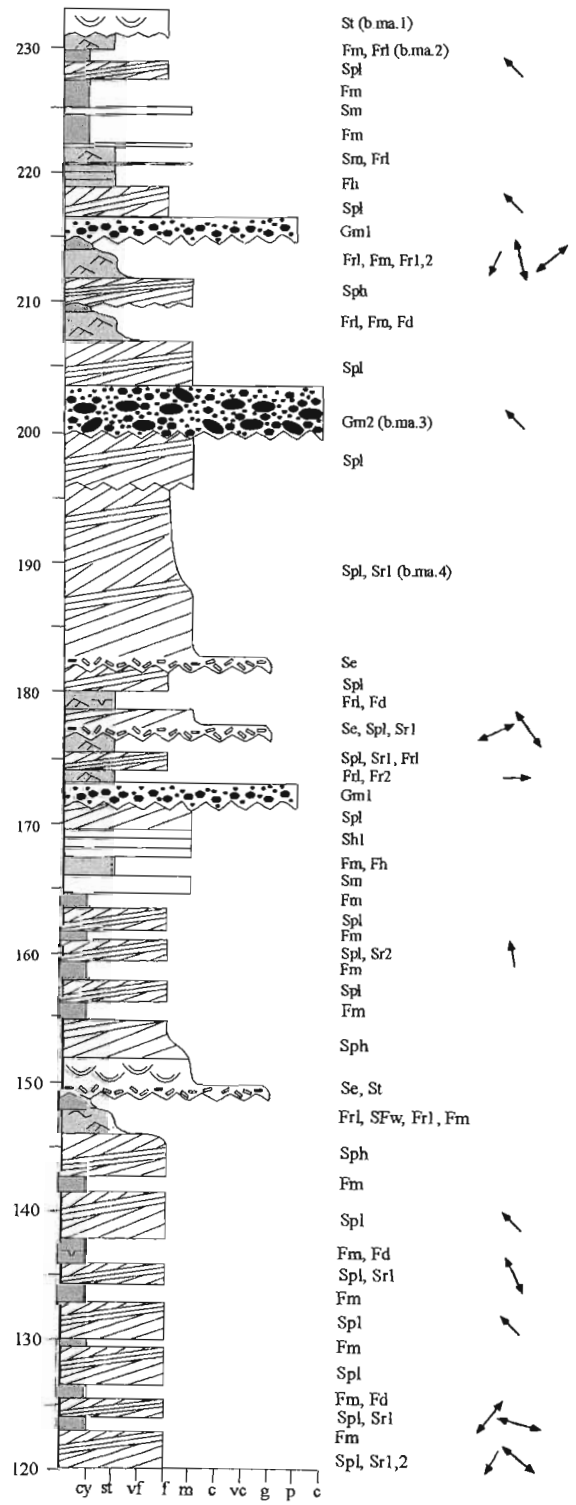

MANA (cont.)

Appendix 4: Additional vertical profiles from the Bråpiggen Formation

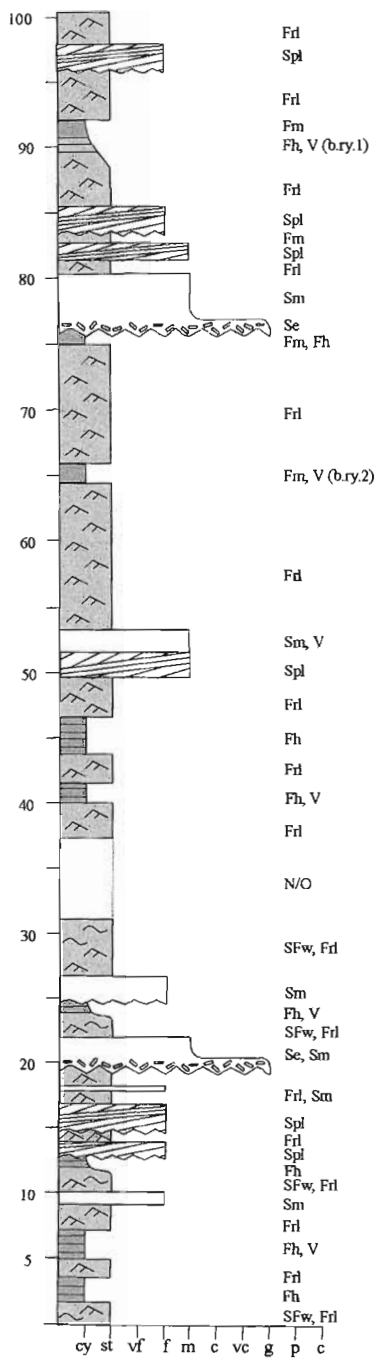

RYVINGEN

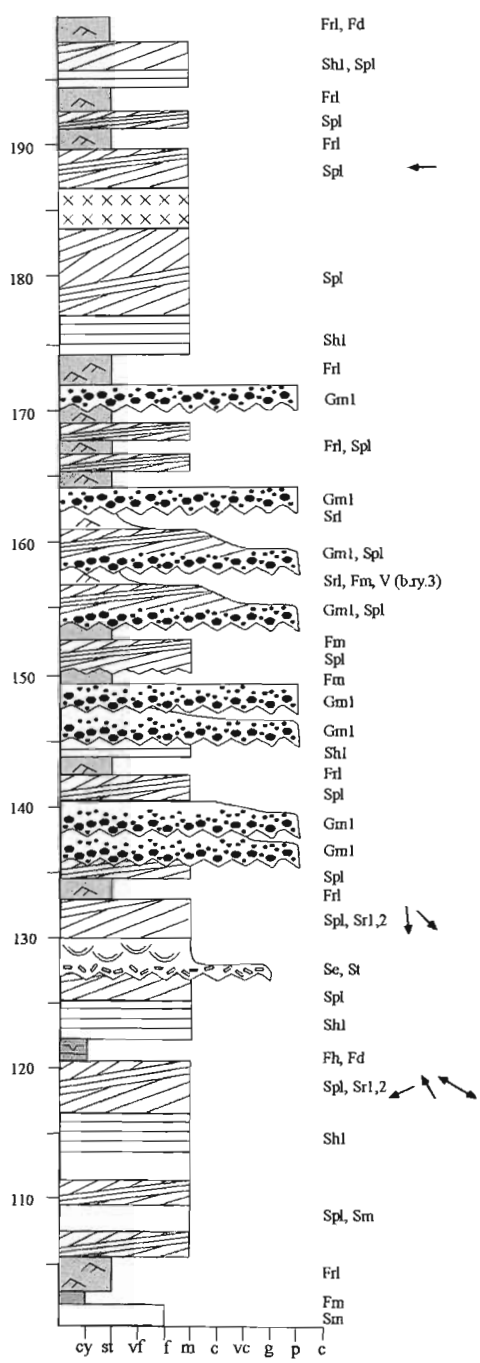

RYVINGEN (cont.)

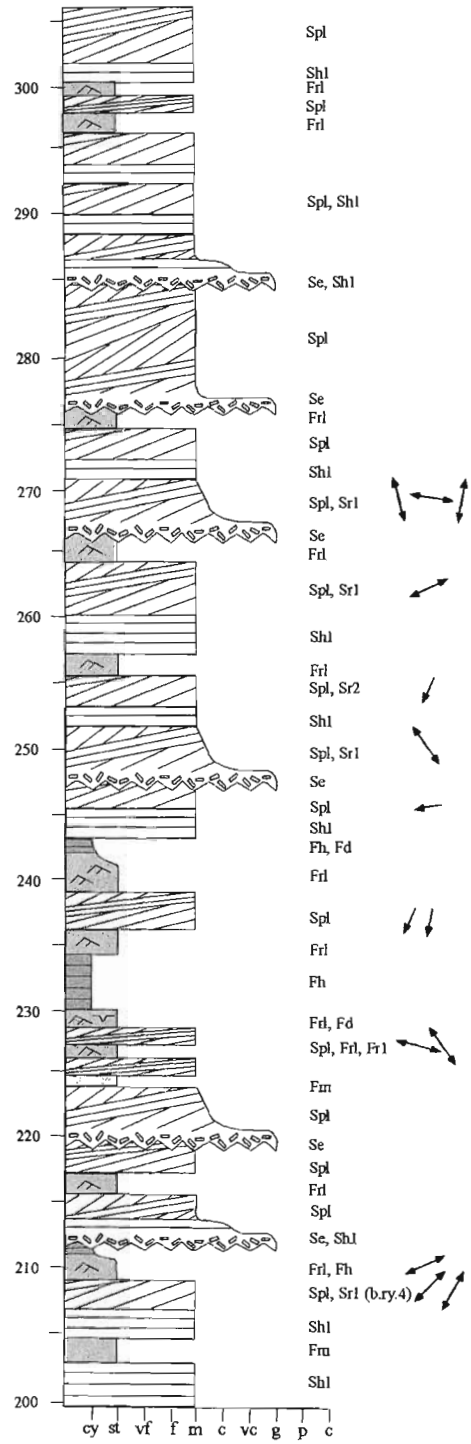

RYVINGEN (cont.)

Appendix 4: Additional vertical profiles from the Bråpiggen Formation

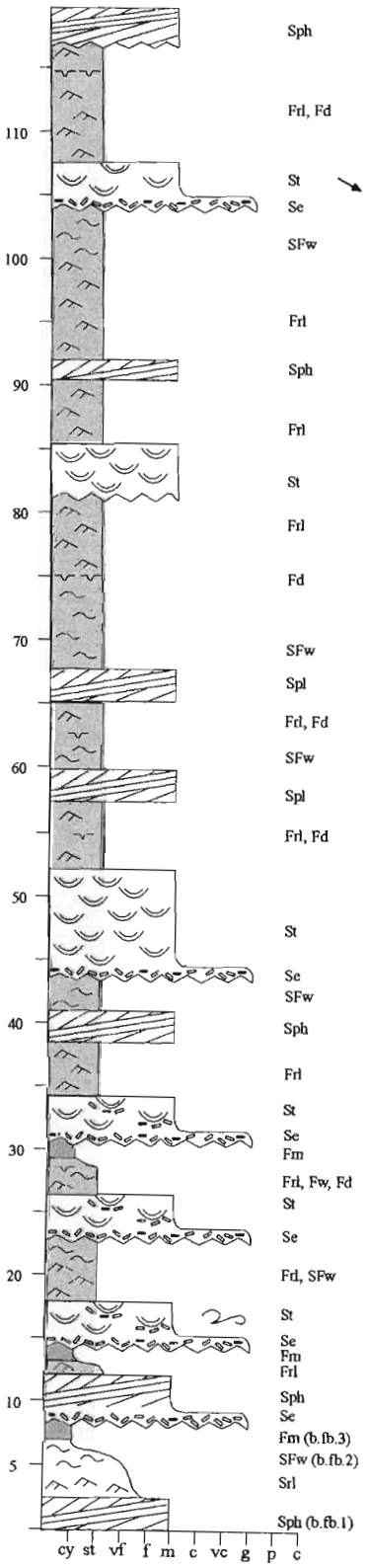

FRIIS-BAASTADNUTEN

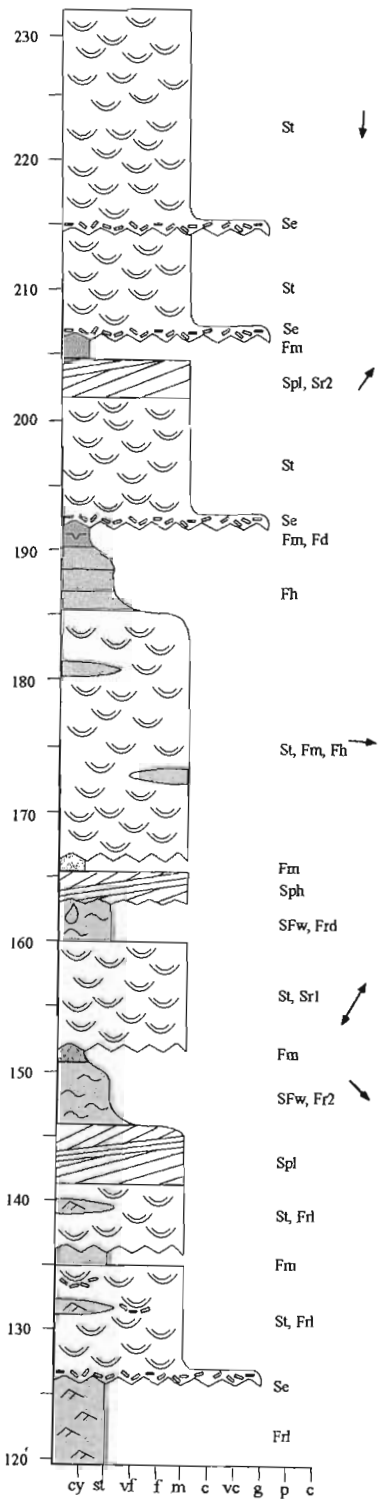

FRIIS-BAASTADNUTEN (cont.)

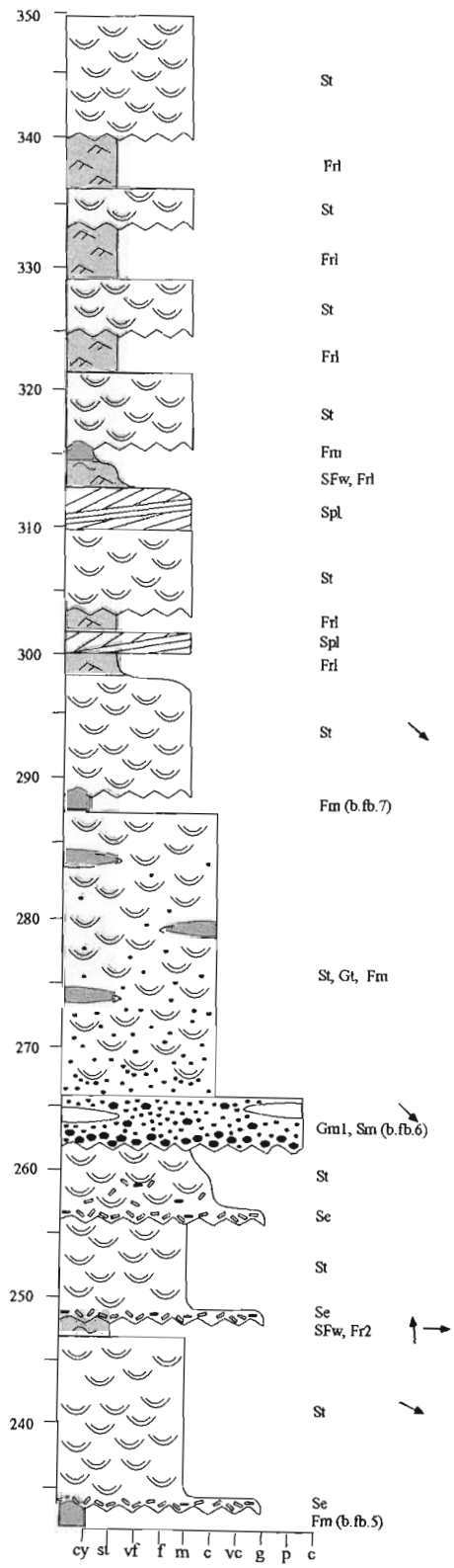

FRIIS-BAASTADNUTEN (cont.)

Appendix 4: Additional vertical profiles from the Bråpiggen Formation

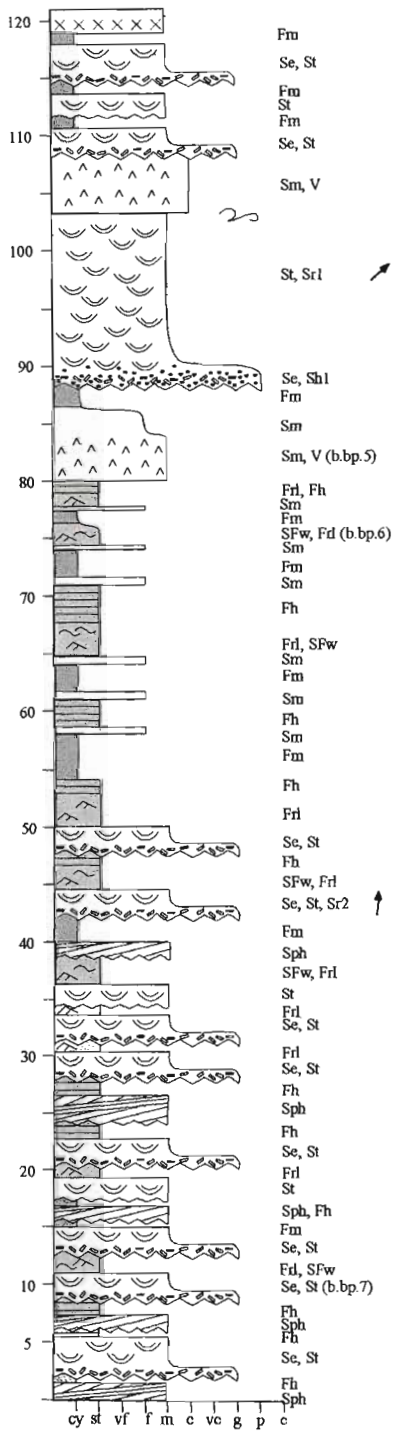

BRÅPIGGEN

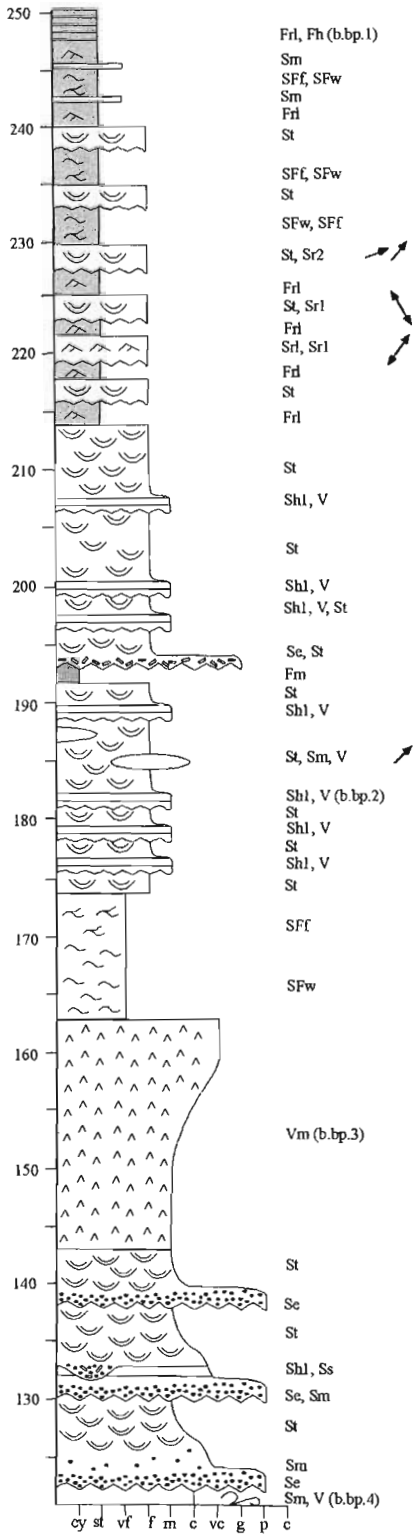

BRÅPIGGEN (cont.)

APPENDIX 5
SAMPLE DESCRIPTIONS

Formation	Sample No	Location	Sample Description	Thin Sect.	Geochem.	Geochron.
Pyramiden Fmn	A.PM.1	North face of Pyramiden nunatak, 2.5m up section.	Fine to med. grained sandstone, fresh: light grey, weathered: dark grey. Small scale planar cross-bedding.			
	A.PM.2	North face of Pyramiden nunatak, 25m up section.	Silicified mudstone, fresh: very dark grey, weathered: dark red. Thin sandy laminae, wavy bedding.	Y	ICP-MS, X-RF	
	A.PM.3	North face of Pyramiden nunatak, 25.5m up section.	Fine to med. grained sandstone, fresh: light grey, weathered: dark grey. Small scale planer cross-bedding, mudstone rip-up clasts.	Y		
	A.PM.4	North face of Pyramiden nunatak, 34m up section.	Med. grained sandstone, light to very light biege colour, heavy mineral enriched. Small scale soft sediment deformation (load structures) abundant.			
	A.PM.5	North face of Pyramiden nunatak, 33m up section.	Fine to med. grained sandstone, light grey colour. Massive to deformed due to load structures.	Y		
	A.PM.6	North face of Pyramiden nunatak, 1m up section.	Med. grained sandstone, weathered: reddish-brown, fresh: light grey. Massive.	Y	X-RF	
Schumacherfjellet Fmn	A.GH.8	Northeastern face of Grunehogna nunatak Peak 1285, 2.5m up section.	Thinly interbedded, fine grained graded sandstone and wavy bedded to horizontally laminated silty mudstone.	Y		
	A.GH.9	Northeastern face of Grunehogna nunatak Peak 1285, 3.5m up section.	Silty mudstone, ripple cross-laminated to horizontally laminated, soft sediment deformation		ICP-MS, X-RF	
	A.GH.6	Northeastern face of Grunehogna nunatak Peak 1285, 5.7m up section.	Med. grained sandstone with trough cross-beds, light brown colour.	Y	X-RF	
	A.GH.11	Northeastern face of Grunehogna nunatak Peak 1285, 9m up section.	Light grey silty mudstone, ripple cross-laminated to massive. Sandy laminae abundant in lower rippled portion.			
	A.GH.12	Northeastern face of Grunehogna nunatak Peak 1285, 1.7m up section.	Med. grained sandstone with trough cross-beds, light brown colour. Mudstone rip-up clasts.			
Grunehogna Fmn	A.GH.1	Southwest ridge of Grunehogna nunatak Peak 1285, 10m up section.	Sediment-sill interaction zone. Fine grained reconsituted sediment with small vugs and ovoid bodies. Orange-red colour. Ovoid bodies often light green in colour due to the presence of epidote.			
	A.GH.2	Southwest ridge of Grunehogna nunatak Peak 1285, 20m up section.	Coarse grained sandstone with gravel stringers concentrated along trough cross-bed foresets. Clast include mudchip rip-ups, quartz, jasper, chert, quartzite; sub-angular to rounded.			

Formation	Sample No	Location	Sample Description	Thin Sect.	Geochem.	Geochron.
Grunehogna Fmn	A.GH.3	Southwest ridge of Grunehogna nunatak Peak 1285, 32m up section.	Silty mudstone, ripple cross-laminated. Muddy laminae are dark grey, sandy/silty laminae: light brown to green (due to epidote).			
	A.GH.4	Southwest ridge of Grunehogna nunatak Peak 1285, 125m up section.	Mudstone, dark greyish purple, massive.		ICP-MS, X-RF	
	A.GH.5	Southwest ridge of Grunehogna nunatak Peak 1285, 110m up section.	Med grained to gritty sandstone with gravel stringers conc. along trough cross-bed foresets. Heavy mineral laminae.	Y		SHRIMP
	A.GH.10	Southwest ridge of Grunehogna nunatak Peak 1285, 80m up section.	Massive gravel, clast types include quartz, jasper, chert, quartzite, mudstone rip-ups. Matrix dark greyish green, gritty. Clasts up to 15mm in diameter. Moderately sorted.			
	A.GH.7	Southwest ridge of Grunehogna nunatak Peak 1285, 16m up section.	Medium grained sandstone with gravel stringers concentrated along trough cross-bed foresets. Clasts average 5-10mm. Heavy mineral laminae.	Y	X-RF	
	A.JE.1	Southeast face of Jekselen nunatak, 37m up section.	Dark greenish-grey sandstone containing shperical concretions between 2-5mm in diameter.	Y	X-RF	
	A.JE.2	Southeast face of Jekselen nunatak, 30m up section.	Greenish-grey to buff coloured calcareous sandstone			
	A.JE.3	Southeast face of Jekselen nunatak, 25m up section.	Greenish-grey sandstone with numerous angular, flat mudstone rip-up clasts and clacite inclusions.	Y	X-RF	
	A.JE.4	Southeast face of Jekselen nunatak, 12m up section.	Greenish-grey, medium grained sandstone, calcareous.			
	A.JE.5	Southeast face of Jekselen nunatak, 6m up section.	Buff-coloured sandstone with dark brown mudstone rip-up clasts.	Y	X-RF	
	A.JE.6	Southeast face of Jekselen nunatak, 1m up section.	Cream coloured to light grey sandy shale, with minor calcite concentrated along fractures.			
Veten Fmn	B.NL.1	Northwest face of Nalegga nunatak, 3m up section.	Med. grained sandstone, light tan colour, massive.	Y	X-RF	
	B.NL.2	Northwest face of Nalegga nunatak, 7m up section.	Med. grained sandstone, planar cross-bedded with prominent heavy mineral laminae (~3mm thick) concentrated along foresets.	Y		
	B.NL.3	Northwest face of Nalegga nunatak, 7m up section.	Thick (~2cm) heavy mineral enriched band within the planar cross-bedded sandstone unit.			
	B.NL.4	Northwest face of Nalegga nunatak, 100m up section.	Very coarse grained sandstone, horizontally bedded. Light green colouration due to epidote.			
	B.NL.5	Northwest face of Nalegga nunatak, 87m up section.	Mudstone, dark grey colour. Ripple cross-laminated to massive. Silty to very fine grained sandtone laminae in ripple c-l.		ICP-MS, X-RF	

Formation	Sample No	Location	Sample Description	Thin Sect.	Geochem.	Geochron.
Veten Fmn	B.NL.6	Northwest face of Nalegga nunatak, 85m up section.	Gravel with planar cross-beds. Varies from matrix to clast supported. Matrix very coarse grained to gritty. Moderately sorted, clasts vary from 5mm to 60mm (ave ~10mm).			
	B.NL.7	Northwest face of Nalegga nunatak, 35m up section.	Sandstone, med. grained with trough cross-beds. Heavy mineral lamine, scattered mudstone rip-up clasts (dark brown to green).	Y	X-RF	
	B.SO.1	Northwest ridge of Soyla nunatak, 60m up section.	Mudstone, dark grey colour. Massive.		ICP-MS, X-RF	
	B.SO.2	Northwest ridge of Soyla nunatak, 55m up section.	Highly altered, light green sandstone with abunadant epidote and volcaniclastics. Massive.			
	B.SO.3	Northwest ridge of Soyla nunatak, 20m up section.	Massive gravel, poorly sorted. Coarse-grained to gritty, epidote rich matrix. Clasts up th 25mm in diameter, but average <10mm.			
	B.SO.4	Northwest ridge of Soyla nunatak, 25m up section.	Med. grained sandstone, weathers reddish-orange. Trough cross-bedded with heavy mineral laminae.	Y	X-RF	
	B.SO.5	Northwest ridge of Soyla nunatak, 90m up section.	Medium grained sandstone with planar cross-beds. Highly altered with notable green colouration due to the presence of epidote.	Y		
	B.SO.7	Northwest ridge of Soyla nunatak, 35m up section.	Medium grained sandstone with trough cross-beds and scattered dark brown mudstone rip-up clasts.			
	B.PR.1	Southeast ridge of Pilaryggen nunatak, 11m up section.	Med. grained sandstone, fresh: greenish-grey, weathered: reddish-orange. Green tinge due to epidote. Scattered mudstone rip-up clasts of intraformational origin.	Y	X-RF	
	B.PR.2	Southeast ridge of Pilaryggen nunatak, 102m up section.	Mudstone, dark purplish-red, massive.		ICP-MS, X-RF	
	B.PR.3	Southeast ridge of Pilaryggen nunatak, 178m up section.	Horizontally laminated med. grained sandstone with volcaniclastic enrichment. Speckled light greenish-beige colour.	Y		
	B.PR.5	Southeast ridge of Pilaryggen nunatak, 200m up section.	Med. grained sandstone, weathered: light reddish-tan, fresh: light grey. Trough cross-bedded with scattered mudchip rip-up clasts.			
	B.PR.6	Southeast ridge of Pilaryggen nunatak, 167m up section.	Med. grained sandstone, horizontally laminated with soft sediment deformation due to load structures.			
	B.PR.7	Southeast ridge of Pilaryggen nunatak, 145m up section.	Pyroclastic layer, weathered: green (due to epidote), fresh: light grey. Massive.	Y	X-RF	
Framryggen Fmn	B.FR.1	Southwestern ridge of Framryggen nunatak, 6m up section.	Mudstone, horizontal laminated to ripple cross-laminated, with silty laminae.		ICP-MS, X-RF	

Formation	Sample No	Location	Sample Description	Thin Sect.	Geochem.	Geochron.
Framryggen Fmn	B.FR.2	Southwestern ridge of Framryggen nunatak, 10m up section.	Mudstone, horizontally laminated with greenish fine-grained to silty laminae (green tinge due to alteration-epidote).			
	B.FR.3	Southwestern ridge of Framryggen nunatak, 19m up section.	Medium grained, grey siliceous sst with pinkish-red banding along planar cross-bed foresets.	Y	X-RF	
	B.FR.4	Southwestern ridge of Framryggen nunatak, 22m up section.	Highly altered, dark grey to green, ripple cross-laminated to wavy bedded, fine-grained muddy sandstone.			
	B.FR.5	Southwestern ridge of Framryggen nunatak, 217m up section.	Mudstone, dark grey, massive.		ICP-MS, X-RF	
	B.FR.6	Southwestern ridge of Framryggen nunatak, 172m up section.	Med. grained sandstone with heavy mineral laminae concentrated along planar cross-bed foresets. Weathered: reddish orange to green.	Y	X-RF	
	B.FR.7	Southwestern ridge of Framryggen nunatak, 115m up section.	Mudstone, horizontal laminations.			
	B.1810.1	Nunatak 1810, south of Borga, 42m up section.	Silty mudstone with thin sandy laminae, wavy bedded. Small scale soft sediment deformation (load structures) with overlying sandy layer.			
	B.1810.2	Nunatak 1810, south of Borga, 15m up section.	Coarse to medium grained, highly altered sandstone. Fines upwards, pale green colour due to epidote. Scattered pale-green mudstone rip-up clasts.			
	B.1885.1	Northwest ridge of Nunatak 1885, south of Borga, 5m up section.	Mudstone, dark marron-brown colour, thinly laminated.		ICP-MS, X-RF	
	B.1885.2	Northwest ridge of Nunatak 1885, south of Borga, 115m up section.	Massive mudstone.			
	B.1885.3	Northwest ridge of Nunatak 1885, south of Borga, 105m up section.	Coarse sandstone with gravel stringers concentrated along trough cross-bed foresets. Clasts (ave. 5mm in diameter) incl quartz, jasper, chert, mudstone, quartzite, feldspar.	Y	X-RF	
	B.1885.4	Northwest ridge of Nunatak 1885, south of Borga, 113m up section.	Medium grained sandstone with heavy mineral laminae concentrated along cross-bed foresets.	Y		
	B.1885.5	Northwest ridge of Nunatak 1885, south of Borga, 34m up section.	Fine to medium grained sandstone with poorly developed planar cross-stratification. Light red colour, thin heavy mineral laminae.	Y		
	B.ST.1	Northeastern face of the central ridge at Stridbukken, 4m along section.	Silty mudstone, horizontally laminated with occasional soft sediment deformation. Minor volcaniclastic content (including volcanic glass fragments).	Y		

Formation	Sample No	Location	Sample Description	Thin Sect.	Geochem.	Geochron.
Framryggen Fmn	B.ST.2	Northeastern face of the central ridge at Stridbukken, 150m along section.	Mudstone, ripple cross-laminated, thin silty laminae.			
	B.ST.3	Northeastern face of the central ridge at Stridbukken, 172m along section.	Fine-grained sandstone containing heavy mineral laminae. Light green colour.	Y	X-RF	
	B.ST.4	Northeastern face of the central ridge at Stridbukken, 185m along section.	Mudstone, massive.		ICP-MS, X-RF	
	B.VE.1	Southwest face of Veten nunatak, 458m up section.	Massive tuff, pale tan to green colour with dark spots. Abundant volcaniclastics, including volcanic glass fragments.	Y		Conv. zircon dissolution
	B.VE.2	Southwest face of Veten nunatak, 454m up section.	Gritty sandstone with scattered gravel clasts averaging 5mm in diameter, and thin calcite veins.	Y		
	B.VE.3	Southwest face of Veten nunatak, 425m up section.	Poorly sorted, coarse-grained sandstone with scattered gravel clasts and mudchips. Fines up to a medium grained sandstone.	Y	X-RF	
	B.VE.4	Southwest face of Veten nunatak, 205m up section.	Silty mudstone, dark marron brown with light tan to greenish sandy laminae. Wavy bedded to horizontally laminated.		ICP-MS, X-RF	
Hogfonna Fmn	B.RB.1	Northeastern ridge of Raudberget, 5m up section.	Sandstone, fresh: tan, weathered: light red. Well sorted, medium grained with heavy mineral laminae concentrated along through cross-bed foresets.	Y	X-RF	
	B.RB.2	Northeastern ridge of Raudberget, 90m up section.	Coarse grained sandstone, weathers reddish-orange. Heavy mineral laminae concetrated along trough cross-bed foresets. Exhibits slight spheroidal weathering. Scattered mudchip rip up clasts.	Y		
	B.OB.1	Western ridge of Ovebratten nuntatak, 120m up section.	Mudstone exhibiting intensive small scale soft sediment deformation with overlying fine-grained sandstone. Ball-and pillow structures common.			
	B.OB.2	Western ridge of Ovebratten nuntatak, 112m up section.	Medium grained sandstone with heavy mineral laminae and possible volcaniclastic fragments (including volcanic glass).			
	B.OB.3	Western ridge of Ovebratten nuntatak, 97m up section.	Mudstone, massive. Dark reddish-brown colour.		ICP-MS, X-RF	
	B.OB.4	Western ridge of Ovebratten nuntatak, 87m up section.	2cm thick heavy mineral band in medium grained sandstone, broken into distinct sections by soft sediment deformation of the sandstone and underlying mustone layer.			
	B.OB.5	Western ridge of Ovebratten nuntatak, 65m up section.	Medium grained sandstone, moderately sorted, mudchip breccia at the base.	Y	X-RF	

Formation	Sample No	Location	Sample Description	Thin Sect.	Geochem.	Geochron.
Hogfonna Fmn	B.OB.6	Western ridge of Ovebratten nuntatak, 45m up section.	Mudstone, massive. Dark reddish-brown colour.		ICP-MS, X-RF	
	B.OB.7	Western ridge of Ovebratten nuntatak, 5m up section.	Sandstone, medium grained, massive. Well sorted, possibly with a minor volcaniclastic content.	Y	X-RF	
	B.Hh.1	Small nunatak to the north-northeast of Hogfonna, 8m up section.	Sandstone, medium grained with scattered mudchip rip up clasts. Weathers a distinctive red colour.	Y	X-RF	
	B.Hh.2	Small nunatak to the north-northeast of Hogfonna, 16m up section.	Pyroclastic layer. Bright red with small circular, pale-pink protuberances (up to 20mm in diameter) giving the rock a knobbly appearance - altered lapilli ?	Y	X-RF	
	B.Hh.2(b)	Small nunatak to the north-northeast of Hogfonna, 44m up section.	Medium grained sandstone, weathers red. Heavy mineral laminae concentrated along trough cross-bed foresets. Soft sediment deformation.			
	B.Hh.3	Small nunatak to the north-northeast of Hogfonna, 85m up section.	Sandstone, weathers dark reddish brown and tends to exhibit spheroidal weathering. Scattered mudchip rip-up clasts and thin heavy mineral laminae.	Y	X-RF	
	B.Hh.3(b)	Small nunatak to the north-northeast of Hogfonna, 150m up section.	Coarse grained sandstone, weathers a reddish-brown colour. Thin gravel stringers concentrated along trough cross-bed foresets.			
	B.Hh.4	Small nunatak to the north-northeast of Hogfonna, 165m up section.	Coarse grained to gritty sandstone, weathers a reddish-brown colour. Thin gravel stringers concentrated along trough cross-bed foresets.	Y		
	B.Hh.5	Small nunatak to the north-northeast of Hogfonna, 225m up section.	Fine to medium grained sandstone, moderately to well sorted, weathers dark red. Thin heavy mineral laminae.	Y	X-RF	
	B.HF.1	Nothern ridge of Hogfonna nunatak, 15m up section.	Medium grained sandstone with heavy mineral laminae concentrated along cross-bed foresets.	Y		
	B.HF.2	Nothern ridge of Hogfonna nunatak, 280m up section.	Massive gravel, moderately sorted, clasts up to 60mm in diameter (ave 20-30mm) Clast types include quartz, chert, jasper, mudstone, quartzite.			
	B.HF.3	Nothern ridge of Hogfonna nunatak, 255m up section.	Gritty to coarse grained sandstone with scattered gravel clasts. Weathered: reddish orange, fresh: greenish-grey.	Y		
	B.HF.4	Nothern ridge of Hogfonna nunatak, 205m up section.	Coarse grained sandtone with scattered gravel clasts and gravel stringers concentrated along trough cross-bed foresets.	Y		
	B.HF.5	Nothern ridge of Hogfonna nunatak, 170m up section.	Coarse grained sandstone, moderately sorted, slight spheroidal weathering. Thin heavy mineral laminae.	Y		
	B.HF.6	Nothern ridge of Hogfonna nunatak, 58m up section.	Medium grained sandstone, weathers a light pinkish-purple. Thin heavy mineral laminae.	Y		SHRIMP

Formation	Sample No	Location	Sample Description	Thin Sect.	Geochem.	Geochron.
Hogfonna Fmn	B.HF.7	Nothern ridge of Hogfonna nunatak, 5m up section.	Medium grained sandstone, weathers red, slight spheroidal weathering.			
	B.HF.8	Nothern ridge of Hogfonna nunatak, 100m above base, north-western face.	Tuff layer. Bright red with small circular, pale-pink protuberances (up to 20mm in diameter) giving the rock a knobbly appearance - altered lapilli ?	Y		
	B.HF.9	Nothern ridge of Hogfonna nunatak, 102m above base, northwestern face.	Tuff layer, as for B.HF.8.	Y	X-RF	
	B.HF.10.0	Nothern ridge of Hogfonna nunatak, 4m above base, northwestern face.	Medium grained sandstone, weathers reddish, fresh: greenish-grey. Contains thin muddy laminae, wavy bedded to ripple-cross-laminated.	Y		
	B.HF.10.1(a)	Nothern ridge of Hogfonna nunatak, 9m above base, northwestern face.	Medium- to fine-grained, ripple cross-laminated sst. Contains abundant small volcanic glass shards and small pale feldspar crystals.	Y	X-RF	
	B.HF.10.1(b)	Nothern ridge of Hogfonna nunatak, 16m above base, northwestern face.	Silty mudstone, wavy bedded to ripple cross-laminated.	Y		
	B.HF.10.2	Nothern ridge of Hogfonna nunatak, 18m above base, northwestern face.	Massive mudstone.		ICP-MS, X-RF	
	B.HF.10.3	Nothern ridge of Hogfonna nunatak, 25m above base, northwestern face.	Moderately to well sorted,fine to med grained sandstone. Possibly tuffaceous. Light green colour.	Y	X-RF	
Brapiggen Fmn	B.MA.1	Southern ridge of Mana nunatak, 232m up section across the crest of the ridge.	Fine to medium grained sandstone, moderately sorted, small scale trough cross-bedding.	Y	X-RF	
	B.MA.2	Southern ridge of Mana nunatak, 230m up section across the crest of the ridge.	Massive mudstone.		ICP-MS, X-RF	
	B.MA.3	Southern ridge of Mana nunatak, 200m up section across the crest of the ridge.	Massive gravel, clast supported, polymictic. Clast diameter up to 20cm, averages ~ 5cm. Clast types incl jasper, chert, quartz, quartzite, feldspar phenocrysts, gneiss, mudstone, and rare magnetite.			
	B.MA.4	Southern ridge of Mana nunatak, 190m up section across the crest of the ridge.	Medium grained sandstone, planar cross-bedded with heavy mineral laminae concentrated along foresets.	Y		SHRIMP
	B.MA.5	Southern ridge of Mana nunatak, 120m up section across the crest of the ridge.	Massive mudstone.			
	B.RY.1	Northeast ridge on Ryvingen nunatak, 85m up section.	Volcaniclastic sandstone, fine-grained. Contains glass shards and small feldspar phenocrysts.	Y	X-RF	

Formation	Sample No	Location	Sample Description	Thin Sect.	Geochem.	Geochron.
Brapiggen Fmn	B.RY.2	Northeast ridge on Ryvingen nunatak, 53m up section.	Medium grained sandstone, appears massive with scattered mudchip rip-up clasts, but contains small glass shards and feldspar phenocryts suggesting it contains reworked volcaniclastics.	Y	X-RF	
	B.RY.3	Northeast ridge on Ryvingen nunatak, 160m up section.	Medium grained sandstone with abundant small euhedral feldspar phenocrysts(?). Soft sediment deformation.	Y		
	B.RY.4	Northeast ridge on Ryvingen nunatak, 250m up section.	Medium grained sandstone , moderately to well sorted.			
	B.RY.5	Northeast ridge on Ryvingen nunatak, 275m up section.	Mudstone with thin silty laminae, wavy bedded to ripple cross-laminated.			
	B.FB.1	Northeastern ridge of Friis-Baastadnuten nunatak, 2m up section.	Medium to coarse grained sandstone, moderately sorted.			
	B.FB.2	Northeastern ridge of Friis-Baastadnuten nunatak, 7m up section.	Massive mudstone.			
	B.FB.3	Northeastern ridge of Friis-Baastadnuten nunatak, 5m up section.	Wavy bedded mudstone and fine-grained sandstone.			
	B.FB.5	Northeastern ridge of Friis-Baastadnuten nunatak, 232m up section.	Massive mudstone.		ICP-MS, X-RF	
	B.FB.6	Northeastern ridge of Friis-Baastadnuten nunatak, 264m up section.	Massive gravel, clast supported, polymictic. Clast diameter up to 80mm, averages <10mm. Clasts imbricate. Clast types include jasper, chert, quartz, sandstone and mudstone.			
	B.FB.7	Northeastern ridge of Friis-Baastadnuten nunatak, 287m up section.	Massive mudstone.		ICP-MS, X-RF	
	B.BP.1	Northern ridge of Brapiggen nunatak, 250m up section.	Silty mudstone, ripple cross-laminated.		ICP-MS, X-RF	
	B.BP.2	Northern ridge of Brapiggen nunatak, 182m up section.	Reworked, horizontally laminated volcaniclastic sandstone.	Y		
	B.BP.3	Northern ridge of Brapiggen nunatak, 150m up section.	Massive tuff, pale green colour with dark spots. Minerals and rock fragments are disseminated in a groundmass of glass shards and volcanic ash.	Y		Conv. zircon dissolution
	B.BP.4	Northern ridge of Brapiggen nunatak, 122m up section.	Pyroclastic layer, highly altered vitric crystal tuff containing feldpsar phenocrysts. Minor soft sediment deformation.	Y	X-RF	
	B.BP.5	Northern ridge of Brapiggen nunatak, 82m up section.	Pyroclastic layer containing abundant feldspar phenocrysts. Pale green colour.	Y	X-RF	

Formation	Sample No	Location	Sample Description	Thin Sect.	Geochem.	Geochron.
Brapiggen Fmn	B.BP.6	Northern ridge of Brapiggen nunatak, 75m up section.	Silty mudstone, wavy bedded to ripple cross-laminated.		ICP-MS, X-RF	
	B.BP.7	Northern ridge of Brapiggen nunatak, 12m up section.	Mudstone, ripple cross-laminated with silty to fine-grained sandy laminae. Well developed cleavage: 312/28.			

APPENDIX 6
GEOCHEMICAL DATA

Appendix 6a: Major and trace element geochemistry for sandstone samples from the Ahlmannryggen Group, determined by X-RF.

Fmn	Pyramiden	Schumacher.	Grunehogna	Grunehogna	Grunehogna	Grunehogna	Veten	Veten	Veten	Veten	Framryggen	Framryggen	Framryggen
Sample	A.PM.6	A.GH.6	A.GH.7HM	A.JE.1	A.JE.3	A.JE.5	B.NL.1	B.NL.7 H.M.	B.SO.4HM	B.PR.1	B.ST.3 H.M.	B.VE.3	B.FR.3
SiO2	68.64	85.99	78.98	71.17	69.66	81.26	80.84	78.44	67.28	64.09	66.85	69.64	84.43
Al2O3	10.19	5.51	8.69	12.84	14.14	8.59	8.37	9.77	13.60	16.80	10.49	11.81	8.08
Fe2O3	6.32	3.60	5.76	4.42	4.62	1.12	1.81	3.01	6.16	4.74	11.17	6.47	0.96
MnO	0.12	0.02	0.05	0.06	0.07	0.01	0.02	0.02	0.05	0.08	0.12	0.19	0.03
MgO	5.83	0.87	1.27	2.32	2.28	0.44	1.19	1.20	1.99	2.64	1.51	1.98	0.97
CaO	3.12	0.88	0.42	2.63	2.45	2.57	2.13	1.90	4.08	4.09	5.08	6.27	0.96
Na2O	2.30	0.00	0.85	3.53	3.32	4.36	2.23	1.98	2.71	3.98	2.26	2.50	3.41
K2O	1.06	1.83	2.52	1.56	2.48	0.12	2.69	2.66	2.84	2.63	0.66	0.02	0.17
TiO2	0.67	0.29	0.60	0.52	0.56	0.44	0.22	0.41	0.64	0.50	1.26	0.62	0.27
P2O5	0.14	0.17	0.11	0.21	0.21	0.14	0.09	0.13	0.21	0.19	0.25	0.18	0.05
Nb	8.20	7.30	12.00	9.70	11.60	9.10	3.80	7.50	9.20	12.20	11.20	6.50	10.00
Y	26.30	28.30	24.10	33.20	34.50	30.40	15.70	24.00	30.10	27.30	27.20	23.70	16.20
Rb	35.90	71.90	92.40	42.90	67.70	4.90	65.20	70.50	66.50	91.50	27.20	0.90	5.70
Zr	159.30	105.20	168.00	205.40	199.80	289.30	72.70	121.60	138.90	144.10	130.60	99.80	168.80
Sr	162.10	7.50	40.30	214.10	179.90	84.60	78.70	158.90	404.80	462.90	333.30	981,80	120.40
U	3.80	1.90	1.70	4.40	2.00	2.90	2.60	2.20	2.90	4.50	3.00	4.60	4.00
Th	10.20	9.40	11.70	12.20	12.80	9.30	7.00	8.20	8.80	12.60	8.10	5.40	14.50
Zn	57.70	13.10	48.10	50.10	50.60	5.80	10.50	18.20	28.00	56.00	61.60	68.70	35.20
Cu	4.60	1.60	1.40	2.50	1.50	1.10	4.80	1.80	10.50	4.20	4.30	30.70	2.90
Ni	248.50	25.10	41.20	33.70	35.00	6.60	49.50	36.40	45.40	14.50	45.90	87.70	15.40
Cr	68.10	49.00	32.70	11.70	18.50	75.40	56.40	42.50	9.60	42.60	87.70	59.00	70.60
V	104.00	68.00	101.80	81.00	98.30	29.30	42.10	69.20	113.60	91.60	211.70	148.00	39.00
La	12.80	47.20	13.40	59.20	25.20	23.10	0.00	14.70	14.10	20.90	20.50	13.10	18.00
Pb	0.00	0.00	0.00	17.91	8.71	0.00	1.90	3.90	7.61	17.61	27.11	26.41	58.70
Ga	9.40	6.10	9.50	2.10	4.20	5.80	6.50	6.40	2.60	4.90	4.30	0.70	6.10
Co	61.00	96.50	74.30	42.10	35.40	67.30	85.40	80.90	56.20	32.90	79.30	80.80	105.40
Ce	34.50	92.30	53.20	99.90	65.70	59.60	11.60	25.60	42.60	39.60	54.40	37.70	49.70
Nd	6.10	65.10	21.50	44.10	29.30	26.70	2.30	15.10	13.50	13.20	18.90	14.50	18.00
As	0.00	0.00	0.40	3.60	4.00	0.00	0.00	1.10	7.30	7.80	7.10	14.80	25.50
Ba	568.00	530.10	832.10	1073.10	857.20	26.90	747.50	892.30	1023.50	651.80	268.00	72.90	64.10
Sc	18.00	6.80	9.80	16.10	16.40	6.40	5.50	7.30	14.20	12.00	18.00	13.40	5.70

Fmn	Framryggen	Framryggen	Hogfonna	Hogfonna	Hogfonna	Hogfonna	Hogfonna	Hogfonna	Hogfonna	Hogfonna	Hogfonna	Brapiggen	Brapiggen
Sample	B.FR.6 H.M.	B.1885.3	B.MA.1	B.OB.5A	B.OB.7	B.RB.1 H.M.	B.Hh.1	B.Hh.3 H.M.	B.Hh.5 HM	B.HF.101A	B.HF.103	B.RY.1	B.RY.2
SiO2	68.01	69.63	82.94	79.33	72.21	88.90	72.22	62.92	77.55	66.63	76.99	71.17	64.08
Al2O3	13.41	13.30	7.10	10.39	13.91	5.10	12.46	10.51	8.97	16.40	11.11	14.56	15.66
Fe2O3	5.86	5.80	2.01	2.20	2.98	1.59	3.36	12.32	3.80	5.50	3.06	2.97	6.72
MnO	0.13	0.13	0.05	0.22	0.04	0.01	0.06	0.15	0.07	0.05	0.04	0.06	0.04
MgO	3.20	1.95	1.28	0.62	1.47	0.54	0.97	1.86	1.17	2.82	0.62	1.45	3.59
CaO	2.61	2.94	2.01	2.22	2.95	0.37	4.28	4.75	2.61	1.55	2.97	3.26	0.92
Na2O	3.61	4.05	2.24	2.11	2.70	0.72	3.16	1.77	1.43	2.11	2.19	2.68	1.05
K2O	1.73	0.74	0.53	2.35	2.40	1.65	2.43	2.13	2.07	3.60	1.94	2.73	6.81
TiO2	0.58	0.64	0.23	0.21	0.45	0.16	0.40	2.40	1.18	0.66	0.38	0.38	0.66
P2O5	0.15	0.17	0.90	0.10	0.14	0.08	0.13	0.22	0.26	0.14	0.12	0.13	0.17
Nb	10.60	7.70	4.80	7.00	11.10	2.60	9.80	34.20	20.00	15.00	9.10	9.20	13.30
Y	28.40	21.70	40.50	23.00	33.40	17.80	23.60	34.30	62.10	37.10	30.20	29.40	37.60
Rb	52.10	28.00	19.70	59.50	88.50	51.30	54.70	79.00	77.60	145.10	47.50	91.30	237.50
Zr	166.20	128.80	128.20	108.70	147.00	87.90	141.00	363.40	127.60	233.20	158.00	176.20	164.50
Sr	243.40	564.90	145.90	240.30	263.30	21.00	363.20	330.40	147.90	135.20	188.50	359.10	99.60
U	4.70	2.70	4.40	3.60	4.30	2.40	2.30	3.90	5.80	2.80	2.20	2.70	3.60
Th	11.50	5.70	5.70	8.10	11.80	4.60	10.10	15.00	27.20	13.70	10.20	13.00	12.20
Zn	65.80	87.80	35.00	9.00	21.00	6.90	35.50	129.20	58.30	26.40	17.40	36.60	50.10
Cu	3.40	84.20	7.30	9.70	0.30	22.40	2.70	13.90	10.60	3.90	1.30	6.20	0.90
Ni	125.30	72.00	15.20	26.40	40.80	10.50	18.10	53.10	22.10	50.50	26.20	17.30	85.30
Cr	87.90	53.10	57.10	55.40	7.90	38.40	36.20	49.70	95.80	59.00	5.20	93.00	43.30
V	113.30	144.70	32.70	66.80	58.50	40.30	52.50	301.70	92.40	95.10	66.80	63.90	78.50
La	12.80	13.80	11.10	5.00	1.90	9.60	18.10	62.70	38.90	13.20	12.70	37.70	21.50
Pb	0.21	13.81	0.00	0.01	1.01	0.00	4.71	46.11	18.10	4.61	2.10	12.61	12.22
Ga	4.40	2.40	6.90	0.20	2.10	5.60	0.60	0.60	9.00	8.30	8.50	4.40	1.90
Co	59.90	87.60	112.90	90.50	64.20	120.90	60.30	45.50	65.40	36.80	81.20	52.20	37.10
Ce	55.10	29.00	35.20	40.40	42.80	32.50	35.70	85.20	131.00	57.80	54.60	65.20	69.90
Nd	18.60	135.00	28.30	12.30	15.80	12.90	11.00	30.90	61.10	21.60	26.40	30.60	31.80
As	0.00	12.40	0.60	0.00	2.90	0.00	7.80	12.00	10.40	1.00	2.30	3.30	2.20
Ba	771.10	697.20	237.90	530.60	678.60	397.10	899.50	717.70	858.10	705.70	553.50	1089.10	1545.80
Sc	15.00	16.90	6.10	4.90	9.00	3.60	9.40	30.00	11.80	19.00	5.30	9.30	23.20

Appendix 6b: Major and trace element geochemistry for pyroclastic samples from the Ahlmannryggen Group, determined by X-RF.

Fmn	Framryggen	Hogfonna	Hogfonna	Brapiggen	Brapiggen
Sample	B.PR.7*	B.Hh.2*	B.HF.9*	B.BP.4*	B.BP.5*
SiO2	76.85	68.99	74.91	63.95	73.16
Al2O3	12.35	16.61	12.62	16.22	14.49
Fe2O3	1.57	3.32	2.11	4.62	2.33
MnO	0.03	0.03	0.04	0.11	0.06
MgO	0.41	1.77	1.00	2.07	1.38
CaO	2.34	0.80	3.06	5.44	3.03
Na2O	4.27	2.09	3.56	3.14	1.80
K2O	0.98	5.58	1.83	3.50	2.79
TiO2	0.25	0.26	0.24	0.60	0.30
P2O5	0.08	0.06	0.08	0.15	0.11
Nb	8.70	18.60	11.00	9.80	28.60
Y	32.50	63.80	50.10	27.40	30.40
Rb	33.70	236.50	75.90	121.80	106.10
Zr	138.00	245.70	172.50	145.80	194.40
Sr	578.30	167.60	470.70	356.00	291.20
U	4.90	4.60	4.20	4.40	6.50
Th	13.40	30.00	18.70	9.40	23.80
Zn	19.70	54.10	38.20	71.50	39.80
Cu	50.20	4.10	0.70	11.10	62.80
Ni	1.60	9.20	10.40	7.90	2.70
Cr	10.70	23.20	44.70	64.20	30.10
V	19.90	57.40	48.70	88.00	29.00
La	19.90	36.40	27.10	24.30	38.50
Pb	12.51	2.72	16.71	8.91	13.11
Ga	0.10	1.30	2.00	4.80	3.40
Co	71.00	16.40	61.70	31.60	30.90
Ce	66.50	104.10	61.80	62.30	96.50
Nd	30.20	41.90	33.80	26.80	43.10
As	5.50	16.20	11.70	6.40	4.70
Ba	865.10	1404.20	745.80	1131.00	1359.50
Sc	6.10	13.30	8.60	9.70	6.00

Appendix 6c: Major and trace element geochemistry for fine-grained samples from the Ahlmannryggen Group, determined by X-RF.

Fmn	Pyramiden	Schumacher.	Grunehogna	Veten	Veten	Veten	Framryggen	Framryggen	Framryggen	Framryggen	Framryggen	Hogfonna	Hogfonna
Sample	A.PM.2	A.GH.9	A.GH.4	B.NL.5	B.SO.1	B.PR.2	B.ST.4	B.VE.4	B.FR.1	B.FR.5	B.1885.1	B.MA.2	B.OB.3
SiO_2	57.47	63.41	69.98	65.25	62.82	64.73	63.79	61.92	63.54	65.58	77.03	68.55	63.39
Al_2O_3	14.51	17.33	13.94	16.09	16.85	16.79	16.73	18.52	18.01	15.61	11.24	14.87	17.17
Fe_2O_3	11.19	6.96	6.82	7.71	7.43	7.75	7.65	8.86	8.01	7.56	3.77	6.70	7.84
MnO	0.12	0.06	0.06	0.06	0.02	0.11	0.10	0.07	0.10	0.11	0.07	0.04	0.04
MgO	9.75	3.22	2.19	2.56	3.15	2.96	2.29	2.68	2.16	3.52	1.63	2.25	3.92
CaO	0.84	1.03	0.34	0.69	2.01	1.20	2.33	0.79	0.63	1.27	0.98	0.96	0.57
Na_2O	1.54	1.44	0.10	0.88	1.88	1.13	1.98	0.92	1.02	1.71	2.24	1.54	0.43
K_2O	3.33	5.06	4.60	5.28	4.51	4.22	3.51	4.83	5.03	3.58	1.82	3.50	5.55
TiO_2	0.64	0.77	1.03	0.73	0.78	0.70	0.75	0.88	0.87	0.80	0.52	0.74	0.72
P_2O_5	0.15	0.15	0.07	0.14	0.17	0.09	0.21	0.04	0.17	0.11	0.08	0.18	0.15
Nb	9.20	14.00	14.60	14.50	18.40	12.40	18.60	15.30	15.50	14.10	9.26	13.90	16.60
Y	26.10	33.00	28.40	28.30	30.00	24.60	34.30	26.70	48.30	28.30	18.50	31.70	26.60
Rb	121.60	186.00	164.00	201.00	193.00	160.00	136.00	212.00	210.20	145.00	84.00	138.00	221.00
Zr	128.50	180.50	460.20	195.70	235.30	166.20	197.20	183.70	235.10	208.70	167.50	254.60	186.20
Sr	94.40	72.90	16.90	97.90	235.00	109.00	255.00	95.60	73.50	160.00	160.00	156.00	47.40
U	2.30	3.00	4.34	3.54	2.61	3.69	4.09	3.84	5.50	3.20	2.41	4.01	3.51
Th	8.06	11.70	15.30	12.00	12.80	10.50	14.30	13.20	17.20	11.20	8.52	12.50	12.00
Zn	66.20	50.50	33.90	34.10	21.60	100.90	80.30	54.70	51.00	92.10	50.10	31.40	30.50
Cu	77.10	4.52	3.40	2.63	2.96	400.00	16.90	5.42	0.60	4.58	10.00	3.18	2.84
Ni	297.00	64.10	51.50	70.10	61.10	65.40	51.10	95.20	48.80	97.30	45.40	55.40	74.30
Cr	158.10	57.50	115.00	68.70	52.00	58.40	44.50	83.20	39.40	74.50	40.10	66.30	68.70
V	54.30	46.20	39.40	52.70	43.20	58.00	38.60	65.00	150.10	47.00	28.70	50.90	51.30
La	25.00	33.90	39.60	34.30	46.80	34.50	46.80	52.90	18.50	33.20	21.90	44.70	28.30
Pb	4.35	7.31	3.39	6.41	9.75	21.60	37.70	6.27	7.52	11.70	8.06	3.61	6.42
Ga	6.70	0.20	4.60	0.30	8.60	0.40	0.10	3.50	3.00	7.60	0.50	6.70	5.20
Co	44.80	28.40	28.50	28.30	22.80	21.90	27.40	29.30	32.20	38.50	42.70	35.70	20.60
Ce	51.60	63.60	90.80	73.00	94.00	68.10	92.70	113.00	80.30	64.20	46.90	91.30	74.70
Nd	22.20	28.00	36.30	31.50	38.30	29.40	35.30	43.70	34.90	25.40	20.30	38.10	25.10
As	0.00	1.20	0.00	1.80	0.00	20.90	16.00	0.00	2.60	5.40	0.40	0.00	0.00
Ba	915.00	732.00	747.00	980.00	792.00	813.00	961.00	787.00	692.80	550.00	512.00	590.00	618.00
Sc	18.90	16.00	12.70	15.60	15.20	15.70	15.20	18.40	26.00	16.30	8.70	14.90	15.00

Fmn	Hogfonna	Hogfonna	Brapiggen	Brapiggen	Brapiggen	Brapiggen
Sample	B.OB.6	B.HF.102	B.FB.5	B.FB.7	B.BP.1	B.BP.6
SiO_2	63.96	63.29	62.94	65.71	64.55	60.47
Al_2O_3	16.78	16.87	16.23	17.06	16.64	17.87
Fe_2O_3	7.91	7.47	8.41	4.89	7.86	9.26
MnO	0.03	0.05	0.09	0.06	0.08	0.09
MgO	3.01	2.75	3.53	3.24	2.19	2.30
CaO	0.81	0.91	1.27	2.63	1.65	2.60
Na_2O	1.06	0.98	1.34	1.29	1.87	1.21
K_2O	4.97	6.29	4.67	4.16	4.05	4.58
TiO_2	0.77	0.86	0.80	0.35	0.72	0.73
P_2O_5	0.16	0.10	0.20	0.14	0.13	0.53
Nb	14.70	16.80	23.80	7.62	13.70	11.80
Y	31.30	26.30	25.60	17.20	22.80	31.90
Rb	212.00	213.00	186.00	156.00	130.00	168.00
Zr	187.10	236.50	178.50	92.80	187.60	177.50
Sr	116.00	128.00	201.00	1319.00	157.00	223.00
U	3.62	3.76	3.41	1.85	3.24	3.52
Th	11.70	13.50	13.00	5.76	9.32	10.30
Zn	43.90	44.90	125.10	45.50	87.30	87.70
Cu	3.22	3.35	11.90	2.59	3.95	6.17
Ni	80.30	66.70	96.00	82.80	67.00	94.20
Cr	69.10	73.70	66.20	37.10	62.60	68.90
V	50.20	48.10	59.60	23.50	41.60	73.10
La	38.40	22.50	40.30	21.90	29.50	39.30
Pb	11.90	15.20	14.00	16.00	24.30	24.30
Ga	0.00	9.20	0.70	1.90	9.60	0.80
Co	28.80	24.80	31.20	25.80	28.70	28.80
Ce	77.00	51.20	79.90	43.20	63.00	87.50
Nd	33.10	18.90	31.60	18.40	26.10	41.10
As	6.10	2.20	4.80	11.30	17.40	22.10
Ba	745.00	1551.00	1153.00	2387.00	882.00	906.00
Sc	17.40	15.20	18.10	9.22	11.50	17.40

Appendix 6d: Trace element geochemistry for fine-grained samples from the Ahlmannryggen Group, determined by ICP-MS.

Fmn	Pyramiden	Schumacher.	Grunehogna	Veten	Veten	Veten	Framryggen	Framryggen	Framryggen	Framryggen	Hogfonna	Hogfonna	Hogfonna
Sample	**A.PM.2**	**A.GH.9**	**A.GH.4**	**B.NL.5**	**B.SO.1**	**B.PR.2**	**B.ST.4**	**B.VE.4**	**B.FR.5**	**B.1885.1**	**B.MA.2**	**B.OB.3**	**B.OB.6**
Cs	10.90	6.91	5.94	5.22	6.90	10.50	7.84	6.76	11.30	3.14	4.59	6.88	8.43
Pr	5.89	7.58	10.10	8.44	10.50	7.92	9.88	12.50	6.94	5.46	10.40	6.80	8.84
Sm	4.24	5.55	6.50	5.94	6.91	5.55	6.73	6.78	4.86	4.03	7.29	5.14	6.41
Eu	1.18	1.30	1.33	1.22	1.54	1.15	1.65	1.33	1.10	0.89	1.57	1.19	1.43
Gd	3.95	5.12	5.35	5.24	6.04	4.97	6.40	5.27	4.69	3.54	6.40	4.74	5.85
Tb	0.62	0.80	0.83	0.84	0.93	0.76	1.00	0.80	0.76	0.56	0.98	0.77	0.92
Dy	3.74	4.85	5.16	5.13	5.52	4.42	6.03	4.79	4.74	3.34	5.80	4.66	5.47
Ho	0.75	0.99	1.07	1.04	1.10	0.88	1.22	0.98	0.99	0.66	1.15	0.94	1.11
Er	2.18	2.29	3.26	3.06	3.18	2.49	3.51	2.91	2.95	1.92	3.26	2.69	3.18
Tm	0.32	0.43	0.50	0.46	0.46	0.37	0.51	0.44	0.44	0.29	0.47	0.40	0.47
Yb	2.08	2.81	3.37	3.01	3.02	2.43	3.30	2.91	2.93	1.91	3.09	2.64	3.07
Lu	0.32	0.43	0.53	0.47	0.46	0.37	0.50	0.44	0.44	0.29	0.48	0.39	0.46
Hf	3.07	4.51	8.98	4.47	5.34	3.99	4.86	4.42	4.69	3.69	5.16	4.60	4.49
Ta	0.76	1.19	1.24	1.18	1.17	0.91	1.50	1.14	1.21	1.05	1.24	1.21	1.11

Fmn	Hogfonna	Brapiggen	Brapiggen	Brapiggen	Brapiggen
Sample	B.HF.102	B.FB.5	B.FB.7	B.BP.1	B.BP.6
Cs	6.16	14.00	8.61	7.85	9.42
Pr	5.22	8.77	4.98	6.98	10.60
Sm	3.88	5.62	3.30	5.21	8.11
Eu	0.91	1.30	0.95	1.27	1.71
Gd	3.95	4.96	3.18	4.69	7.10
Tb	0.72	0.75	0.49	0.74	1.05
Dy	4.78	4.47	2.92	4.54	6.01
Ho	1.02	0.89	0.59	0.92	1.17
Er	3.12	2.57	1.68	2.71	3.21
Tm	0.48	0.38	0.24	0.40	0.45
Yb	3.29	2.51	1.59	2.61	2.83
Lu	0.51	0.38	0.24	0.39	0.43
Hf	5.66	4.07	2.11	4.32	4.16
Ta	1.22	1.76	0.67	1.00	0.73

Appendix 6e: Correlation matrix of chemical elements for the Ahlmannryggen Group sandstone samples.

	SiO_2	Al_2O_3	Fe_2O_3	MnO	MgO	CaO	Na_2O	K_2O	TiO_2	P_2O_5	Nb	Y	Rb	Zr	Sr	U	Th	Zn	Cu	Ni	Cr	V	La	Pb	Ga	Co	Ce	Nd	As	Ba	Sc
SiO_2	1.000																														
Al_2O_3	-0.815	1.000																													
Fe_2O_3	-0.696	0.202	1.000																												
MnO	-0.452	0.158	0.547	1.000																											
MgO	-0.647	0.403	0.516	0.350	1.000																										
CaO	-0.119	0.138	-0.025	0.037	-0.078	1.000																									
Na_2O	-0.284	0.402	-0.127	0.117	0.048	0.273	1.000																								
K_2O	-0.368	0.547	0.035	-0.235	0.207	-0.108	-0.358	1.000																							
TiO_2	-0.529	0.045	0.849	0.442	0.277	-0.013	-0.110	-0.044	1.000																						
P_2O_5	0.041	-0.206	0.124	0.096	0.063	-0.086	-0.050	-0.233	0.132	1.000																					
Nb	-0.446	0.317	0.445	0.168	0.129	0.030	-0.138	0.277	0.655	-0.065	1.000																				
Y	-0.202	0.295	0.009	-0.153	0.039	0.273	-0.071	0.370	0.156	0.206	0.437	1.000																			
Rb	-0.380	0.561	0.069	-0.227	0.227	-0.068	-0.366	0.961	-0.002	-0.211	0.374	0.498	1.000																		
Zr	-0.400	0.273	0.390	0.063	0.200	0.026	0.193	0.089	0.541	-0.024	0.698	0.328	0.192	1.000																	
Sr	-0.426	0.394	0.204	0.490	0.013	0.388	0.470	-0.264	0.111	-0.044	-0.001	-0.057	-0.247	-0.128	1.000																
U	-0.238	0.306	-0.046	0.251	0.147	0.162	0.218	-0.008	0.088	0.138	0.447	0.438	0.103	0.117	0.323	1.000															
Th	-0.165	0.349	-0.088	-0.184	-0.004	0.151	-0.065	0.404	0.111	-0.214	0.680	0.769	0.528	0.386	-0.106	0.552	1.000														
Zn	-0.684	0.314	0.778	0.591	0.481	0.095	0.126	-0.019	0.769	0.156	0.572	0.170	0.066	0.466	0.358	0.292	0.173	1.000													
Cu	-0.025	0.101	-0.041	0.212	-0.125	-0.054	0.176	-0.212	-0.030	-0.069	0.130	-0.156	-0.164	-0.146	0.492	0.292	-0.004	0.200	1.000												
Ni	-0.346	0.015	0.443	0.423	0.831	-0.083	-0.050	-0.086	0.245	-0.017	-0.075	-0.171	-0.094	-0.010	0.035	-0.016	-0.223	0.330	-0.047	1.000											
Cr	-0.040	-0.190	0.243	0.376	0.206	0.008	0.011	-0.276	0.285	0.154	0.022	-0.037	-0.205	0.067	-0.056	0.105	-0.044	0.286	-0.119	0.250	1.000										
V	-0.578	0.087	0.942	0.616	0.372	0.009	-0.052	-0.136	0.878	0.112	0.457	-0.031	-0.096	0.446	0.238	-0.047	-0.105	0.805	0.006	0.346	0.313	1.000									
La	-0.180	0.087	0.219	-0.039	-0.032	0.088	-0.114	0.123	0.417	-0.006	0.593	0.409	0.201	0.490	-0.020	0.248	0.502	0.385	0.021	-0.219	-0.026	0.219	1.000								
Pb	-0.170	0.010	0.277	0.195	-0.065	0.163	0.167	-0.224	0.458	-0.082	0.387	-0.048	-0.168	0.225	0.326	0.282	0.193	0.458	0.135	-0.109	0.155	0.342	0.407	1.000							
Ga	0.337	-0.387	-0.130	-0.325	0.132	-0.237	-0.324	-0.122	-0.071	0.152	-0.169	-0.053	-0.106	-0.137	-0.574	-0.265	-0.044	-0.221	-0.300	0.199	0.281	-0.158	-0.189	-0.226	1.000						
Co	0.760	-0.844	-0.261	-0.033	-0.426	-0.096	-0.206	-0.616	-0.235	0.237	-0.570	-0.455	-0.644	-0.504	-0.131	-0.320	-0.572	-0.358	0.078	-0.028	0.180	-0.126	-0.425	-0.022	0.238	1.000					
Ce	-0.109	0.161	0.060	-0.110	-0.069	0.001	-0.211	0.274	0.267	-0.054	0.614	0.697	0.388	0.385	-0.147	0.446	0.775	0.214	-0.002	-0.261	-0.022	0.020	0.806	0.217	-0.054	-0.471	1.000				
Nd	-0.008	0.059	0.022	0.029	-0.100	0.009	0.050	-0.046	0.080	0.063	0.145	0.242	0.047	0.022	0.128	0.059	0.184	0.287	0.610	-0.112	0.002	0.066	0.368	0.093	-0.089	-0.002	0.368	1.000			
As	-0.156	0.169	0.070	0.122	-0.122	0.250	0.267	-0.107	0.184	-0.163	0.281	0.198	-0.015	0.129	0.442	0.330	0.392	0.402	0.218	-0.186	0.029	0.156	0.247	0.786	-0.322	-0.088	0.209	0.242	1.000		
Ba	-0.397	0.594	-0.017	-0.218	0.179	-0.017	-0.150	0.819	-0.048	-0.243	0.345	0.370	0.768	0.054	-0.062	0.181	0.497	0.086	0.105	-0.085	-0.375	-0.184	0.347	-0.155	-0.227	-0.691	0.427	0.184	-0.058	1.000	
Sc	-0.760	0.372	0.879	0.440	0.668	-0.020	0.018	0.183	0.775	0.102	0.510	0.196	0.231	0.585	0.118	0.049	0.084	0.785	-0.061	0.474	0.209	0.831	0.286	0.252	-0.198	-0.440	0.161	0.105	0.108	0.122	1.000

Appendix 6f: Correlation matrix of chemical elements for the Ahlmannryggen Group fine-grained samples.

	SiO_2	Al_2O_3	Fe_2O_3	MnO	MgO	CaO	Na_2O	K_2O	TiO_2	P_2O_5	Nb	Y	Rb	Zr	Sr	U	Th	Zn	Cu	Ni	Cr	V	La	Pb	Ga	Co	Ce	Nd	As	Ba	Sc
SiO_2	1.000																														
Al_2O_3	-0.717	1.000																													
Fe_2O_3	-0.862	0.426	1.000																												
MnO	-0.250	-0.033	0.407	1.000																											
MgO	-0.560	-0.098	0.604	0.342	1.000																										
CaO	-0.190	0.269	-0.103	0.128	-0.126	1.000																									
Na_2O	0.157	-0.282	-0.207	0.241	0.027	0.503	1.000																								
K_2O	-0.491	0.696	0.309	-0.372	-0.099	-0.229	-0.694	1.000																							
TiO_2	-0.166	0.206	0.394	-0.042	-0.188	-0.494	-0.462	0.468	1.000																						
P_2O_5	-0.365	0.290	0.313	0.122	-0.040	0.573	0.098	0.050	-0.085	1.000																					
Nb	-0.226	0.318	0.238	-0.105	-0.216	-0.116	-0.120	0.438	0.605	0.023	1.000																				
Y	-0.301	0.401	0.344	0.125	-0.132	-0.177	-0.154	0.305	0.559	0.296	0.354	1.000																			
Rb	-0.456	0.715	0.288	-0.411	-0.126	-0.280	-0.656	0.923	0.467	0.009	0.502	0.400	1.000																		
Zr	0.319	-0.233	-0.084	-0.251	-0.332	-0.418	-0.465	0.181	0.756	-0.172	0.296	0.305	0.125	1.000																	
Sr	0.046	0.119	-0.420	-0.079	-0.023	0.652	0.165	-0.138	-0.717	0.077	-0.378	-0.415	-0.163	-0.427	1.000																
U	-0.037	0.304	0.217	0.118	-0.416	-0.396	-0.448	0.382	0.735	0.043	0.447	0.759	0.415	0.553	-0.512	1.000															
Th	-0.057	0.258	0.186	-0.070	-0.354	-0.412	-0.384	0.446	0.855	-0.059	0.699	0.756	0.523	0.663	-0.561	0.870	1.000														
Zn	-0.239	0.105	0.316	0.767	0.090	0.314	0.290	-0.217	-0.025	0.259	0.196	-0.107	-0.280	-0.314	-0.026	0.000	-0.145	1.000													
Cu	-0.069	0.019	0.129	0.440	0.145	-0.024	-0.033	-0.110	-0.109	-0.154	-0.183	-0.160	-0.140	-0.174	-0.091	0.008	-0.171	0.384	1.000												
Ni	-0.561	-0.108	0.662	0.429	0.955	-0.063	0.063	-0.173	-0.185	0.067	-0.296	-0.158	-0.204	-0.355	-0.020	-0.398	-0.403	0.189	0.097	1.000											
Cr	-0.361	-0.237	0.635	0.212	0.737	-0.409	-0.324	0.011	0.300	-0.102	-0.142	-0.100	-0.080	0.244	-0.352	-0.083	-0.054	-0.003	0.046	0.781	1.000										
V	-0.326	0.425	0.399	0.324	-0.046	-0.255	-0.248	0.306	0.391	0.229	0.190	0.791	0.411	0.071	-0.318	0.697	0.558	0.088	0.028	-0.010	-0.077	1.000									
La	-0.154	0.221	0.235	-0.160	-0.200	0.147	0.000	0.016	0.413	0.139	0.463	0.119	0.148	0.258	-0.220	0.171	0.323	0.058	-0.024	-0.151	0.063	-0.173	1.000								
Pb	-0.180	0.296	0.045	0.373	-0.251	0.719	0.376	-0.105	-0.176	0.400	0.133	-0.031	-0.220	-0.273	0.236	0.030	-0.101	0.566	0.226	-0.195	-0.380	-0.134	0.133	1.000							
Ga	-0.142	-0.041	0.177	-0.173	0.222	-0.096	0.074	0.079	0.228	-0.230	0.054	-0.086	-0.039	0.254	-0.121	-0.065	0.030	-0.202	-0.204	0.189	0.322	-0.079	-0.098	-0.190	1.000						
Co	0.227	-0.643	0.050	0.417	0.390	-0.204	0.438	-0.687	-0.163	-0.058	-0.367	-0.038	-0.635	-0.105	-0.142	-0.196	-0.240	0.150	-0.190	0.508	0.379	0.039	-0.220	-0.312	0.061	1.000					
Ce	-0.188	0.365	0.317	-0.135	-0.305	-0.043	-0.249	0.195	0.623	0.187	0.531	0.477	0.370	0.432	-0.360	0.562	0.648	-0.075	-0.124	-0.253	0.015	0.290	0.845	0.005	-0.065	-0.268	1.000				
Nd	-0.192	0.354	0.327	-0.077	-0.319	0.035	-0.185	0.136	0.561	0.345	0.388	0.537	0.301	0.384	-0.333	0.539	0.569	-0.034	-0.077	-0.227	-0.006	0.370	0.802	0.018	-0.169	-0.187	0.953	1.000			
As	-0.187	0.315	0.099	0.435	-0.217	0.673	0.208	-0.110	-0.250	0.497	-0.151	-0.090	-0.239	-0.303	0.268	0.004	-0.287	0.621	0.449	-0.119	-0.290	-0.026	0.047	0.859	-0.253	-0.295	-0.051	0.057	1.000		
Ba	-0.182	0.253	-0.183	-0.067	0.071	0.486	-0.072	0.235	-0.476	0.030	-0.173	-0.393	0.089	-0.334	0.837	-0.370	-0.389	0.023	-0.057	0.075	-0.151	-0.252	-0.289	0.263	-0.035	-0.291	-0.408	-0.411	0.230	1.000	
Sc	-0.601	0.499	0.679	0.352	0.233	-0.288	-0.240	0.384	0.509	0.221	0.365	0.807	0.511	0.021	-0.432	0.610	0.588	0.154	0.034	0.244	0.173	0.874	0.072	-0.145	-0.065	0.067	0.394	0.437	-0.122	-0.294	1.000

	SiO_2	Al_2O_3	Fe_2O_3	MnO	MgO	CaO	Na_2O	K_2O	TiO_2	P_2O_5	Nb	Y	Rb	Zr	Sr	U	Th	Zn	Cu	Ni	Cr	V	La	Pb	Ga	Co	Ce	Nd	As	Ba	Sc
Cs	-0.585	0.320	0.543	0.637	0.455	0.268	0.039	0.054	-0.003	0.257	0.240	0.007	0.049	-0.325	0.121	-0.121	-0.150	0.783	0.309	0.468	0.224	0.381	0.034	0.305	-0.074	0.035	-0.063	-0.044	0.392	0.187	0.504
Pr	-0.167	0.329	0.302	-0.121	-0.311	0.035	-0.177	0.118	0.574	0.262	0.420	0.620	0.288	0.396	-0.320	0.591	0.618	-0.034	-0.077	-0.223	0.033	0.513	0.964	0.021	-0.145	-0.205	0.973	0.994	0.025	-0.389	0.453
Sm	-0.176	0.305	0.319	-0.134	-0.332	0.114	-0.127	0.117	0.524	0.505	0.365	0.747	0.232	0.378	-0.384	0.606	0.564	-0.020	-0.068	-0.251	-0.015	0.552	0.865	0.124	-0.170	-0.216	0.883	0.957	0.170	-0.469	0.444
Eu	-0.332	0.341	0.397	-0.051	-0.147	0.308	0.045	0.040	0.372	0.611	0.363	0.786	0.122	0.231	-0.241	0.452	0.444	0.040	-0.143	-0.095	0.001	0.435	0.798	0.279	-0.127	-0.171	0.779	0.848	0.249	-0.345	0.443
Gd	-0.233	0.341	0.332	-0.103	-0.309	0.201	-0.049	0.137	0.483	0.590	0.399	0.837	0.221	0.319	-0.364	0.603	0.558	0.021	-0.069	-0.255	-0.074	0.518	0.803	0.252	-0.161	-0.242	0.798	0.874	0.250	-0.436	0.465
Tb	-0.238	0.352	0.332	-0.161	-0.325	0.135	-0.080	0.228	0.552	0.539	0.456	0.883	0.290	0.367	-0.426	0.667	0.640	-0.039	-0.108	-0.290	-0.071	0.497	0.759	0.252	-0.083	-0.281	0.765	0.815	0.198	-0.439	0.476
Dy	-0.229	0.343	0.326	-0.194	-0.336	0.065	-0.119	0.300	0.637	0.459	0.509	0.901	0.333	0.446	-0.471	0.722	0.721	-0.079	-0.162	-0.313	-0.038	0.456	0.725	0.234	0.003	-0.296	0.739	0.762	0.133	-0.424	0.470
Ho	-0.226	0.349	0.319	-0.210	-0.340	0.011	-0.160	0.353	0.694	0.382	0.531	0.902	0.372	0.494	-0.488	0.755	0.769	-0.103	-0.187	-0.325	-0.013	0.424	0.701	0.216	0.051	-0.309	0.717	0.721	0.089	-0.405	0.468
Er	-0.166	0.258	0.317	-0.189	-0.334	-0.050	-0.213	0.333	0.734	0.259	0.549	0.764	0.350	0.578	-0.476	0.792	0.795	-0.112	-0.196	-0.299	0.068	0.375	0.663	0.201	0.184	-0.276	0.711	0.675	0.049	-0.354	0.410
Tm	-0.152	0.279	0.277	-0.245	-0.348	-0.184	-0.264	0.433	0.828	0.149	0.574	0.835	0.427	0.632	-0.569	0.812	0.872	-0.166	-0.218	-0.347	0.075	0.346	0.635	0.104	0.141	-0.300	0.667	0.628	-0.065	-0.402	0.429
Yb	-0.119	0.252	0.243	-0.271	-0.350	-0.239	-0.298	0.460	0.852	0.068	0.585	0.791	0.445	0.671	-0.567	0.817	0.893	-0.193	-0.221	-0.360	0.091	0.306	0.598	0.060	0.188	-0.305	0.635	0.578	-0.121	-0.375	0.401
Lu	-0.094	0.211	0.226	-0.273	-0.343	-0.259	-0.316	0.453	0.854	0.055	0.558	0.778	0.425	0.705	-0.560	0.814	0.893	-0.219	-0.213	-0.350	0.120	0.291	0.582	0.025	0.186	-0.284	0.618	0.570	-0.146	-0.354	0.382
Hf	0.241	-0.160	-0.027	-0.306	-0.335	-0.417	-0.469	0.276	0.830	-0.167	0.388	0.430	0.212	0.981	-0.505	0.683	0.797	-0.302	-0.164	-0.374	0.253	0.006	0.362	-0.199	0.262	-0.208	0.465	0.393	-0.282	-0.360	0.021
Ta	0.119	-0.029	-0.028	-0.076	-0.272	-0.276	-0.018	0.172	0.533	-0.187	0.886	0.370	0.247	0.360	-0.387	0.509	0.752	0.153	-0.250	-0.356	-0.154	0.048	0.434	0.018	-0.056	-0.097	0.402	0.244	-0.316	-0.260	0.236

	Cs	Pr	Sm	Eu	Gd	Tb	Dy	Ho	Er	Tm	Yb	Lu	Hf	Ta
Cs	1.000													
Pr	-0.055	1.000												
Sm	-0.067	0.928	1.000											
Eu	0.066	0.815	0.924	1.000										
Gd	-0.012	0.836	0.968	0.950	1.000									
Tb	-0.068	0.781	0.926	0.904	0.981	1.000								
Dy	-0.107	0.737	0.872	0.845	0.938	0.985	1.000							
Ho	-0.122	0.704	0.822	0.787	0.891	0.956	0.992	1.000						
Er	-0.128	0.671	0.741	0.678	0.790	0.871	0.927	0.950	1.000					
Tm	-0.192	0.631	0.692	0.613	0.741	0.836	0.914	0.955	0.949	1.000				
Yb	-0.209	0.589	0.629	0.538	0.673	0.780	0.870	0.922	0.933	0.994	1.000			
Lu	-0.238	0.581	0.618	0.519	0.656	0.761	0.854	0.907	0.922	0.987	0.996	1.000		
Hf	-0.320	0.416	0.406	0.262	0.367	0.437	0.528	0.584	0.654	0.729	0.768	0.792	1.000	
Ta	0.067	0.298	0.221	0.203	0.248	0.308	0.375	0.409	0.428	0.497	0.521	0.509	0.421	1.000

APPENDIX 7
NORMATIVE QtF*L*, QmF*Lt*
METHODS AND DATA

METHODOLOGY

The following methodology was used to construct the QF*L* diagrams (Cox and Lowe, 1996):

- Point-count data (volume %) are converted to weight % by multiplying each component by its density to get weight/volume, and then normalising to 100%.
- Chemical data (weight %) are re-calculated volatile free by subtracting LOI and normalising to 100%.
- The weight % values for both point-count and chemical data are converted to moles by dividing by molecular weights.
- The weight % values for framework quartz from the point-count data (Q + Lc + silica cement) are subtracted from the weight % SiO_2 from the chemical analysis. This quantity (minus the silica cement) is Qt. The remaining SiO_2 plus all other constituents is the sum of feldspar + lithics + other minerals.
- A normative mineralogy is constructed using the following methods:
  - All K_2O plus amounts of Al_2O_3 and SiO_2 in the ratio 1:1:6 are assigned to K-feldspar.
  - All MgO is assigned to chlorite, using MgO, Al_2O_3 and SiO_2 in the ratio 5:1:3.
  - All Na_2O plus amounts of Al_2O_3 and SiO_2 in the ratio 1:1:6 are assigned to albite.
  - CaO is assigned to anorthite, using the following protocol- if $CaO < Al_2O_3$, use all CaO; if $CaO > Al_2O_3$, use an amount of CaO equal to the amount of Al_2O_3 remaining. In either case, CaO, Al_2O_3 and SiO_2 in the ratio 1:1:2.
  - If in above, $CaO > Al_2O_3$, assign excess CaO to calcite.
  - All Fe_2O_3 goes to Fe oxide.
  - Any remaining Al_2O_3 goes to kaolinite, using Al_2O_3 and SiO_2 in the ratio 1:2,
  - Any remaining SiO_2 is assigned to quartz.
- The molar quantities of the normative minerals are converted to weight % by multiplying by molecular weight. The quantity F* is the sum of normative K-feldspar + anorthite + albite. The quantity L* is the sum of all other components. Minor phases (MnO, S, P_2O_5, TiO_2) are ignored.

Appendix 7: Re-calculated normative QtF*L* and QmF*Lt* modes for the Ahlmannryggen Group sandstone samples, after the methods of Cox and Lowe (1996).

Sample	Fmn	Qt	F*	L*	Qm	F*	Lt*
A.PM.6	Pyramiden	47.3	26.7	26.0	44.5	26.7	28.8
A.GH.6	Schumacher.	46.2	14.0	39.8	26.0	14.0	60.0
A.GH.7	Grunehogna	51.1	24.8	24.1	36.5	24.8	38.7
A.JE.1	Grunehogna	38.8	40.9	20.3	38.0	40.9	21.1
A.JE.3	Grunehogna	32.5	46.7	20.8	27.3	46.7	26.0
A.JE.5	Grunehogna	66.1	28.9	5.0	62.1	28.9	9.0
B.NL.1	Veten	84.2	2.9	12.9	53.7	2.9	43.4
B.NL.7	Veten	44.7	40.0	15.3	40.7	40.0	19.3
B.SO.4	Veten	15.3	54.6	30.1	9.0	54.6	36.4
B.PR.1	Veten	19.9	64.0	16.1	15.9	64.0	20.1
B.ST.3	Framryggen	42.8	37.2	20.0	38.4	37.2	24.4
B.VE.3	Framryggen	23.8	40.3	35.9	14.4	40.3	45.3
B.FR.3	Framryggen	65.3	30.2	4.5	63.5	30.2	6.3
B.FR.6	Framryggen	28.7	52.4	18.9	23.5	52.4	24.1
B.1885.3	Framryggen	20.8	53.0	26.2	13.7	53.0	33.3
B.MA.1	Hogfonna	58.3	28.6	13.1	47.3	28.6	24.1
B.OB.5	Hogfonna	39.6	43.6	16.8	35.4	43.6	21.0
B.OB.7	Hogfonna	40.1	52.9	7.0	39.8	52.9	7.3
B.RB.1	Hogfonna	56.3	17.9	25.8	50.4	17.9	31.7
B.Hh.1	Hogfonna	26.7	54.0	19.3	18.5	54.0	27.5
B.Hh.3	Hogfonna	30.0	40.9	29.1	15.9	40.9	43.2
B.Hh.5	Hogfonna	24.7	25.4	49.9	12.9	25.4	61.7
B.HF.101	Hogfonna	43.6	40.6	15.8	42.3	40.6	17.1
B.HF.103	Hogfonna	42.3	45.2	12.5	39.9	45.2	14.9
B.RY.1	Brapiggen	35.5	56.5	8.0	29.3	56.5	14.2
B.RY.2	Brapiggen	41.0	40.3	18.7	40.1	40.3	19.6

APPENDIX 8
SHRIMP ANALYTICAL RESULTS

Appendix 8a: Summary of SHRIMP U-Th-Pb zircon results for sample A.GH.5.

Grain. spot	U (ppm)	Th (ppm)	Th/U	Pb* (ppm)	$^{204}Pb/^{206}Pb$	f_{206} %	Radiogenic Ratios $^{206}Pb/^{238}U$	±	$^{207}Pb/^{235}U$	±	$^{207}Pb/^{206}Pb$	±	Ages (in Ma) $^{206}Pb/^{238}U$	±	$^{207}Pb/^{235}U$	±	$^{207}Pb/^{206}Pb$	±	Conc. %
1.1	76	33	0.429	32	0.000154	0.26	0.3872	0.0160	6.925	0.329	0.1297	0.0025	2110	75	2102	43	2094	34	101
2.1	507	194	0.382	101	0.000010	0.02	0.1939	0.0047	2.077	0.056	0.0777	0.0007	1143	26	1141	19	1139	17	100
4.1	196	113	0.575	38	0.000086	0.15	0.1808	0.0049	1.909	0.062	0.0766	0.0011	1072	27	1084	22	1109	30	97
3.1	227	148	0.65	40	0.000299	0.51	0.1668	0.0047	1.753	0.079	0.0762	0.0025	995	26	1028	30	1101	66	90
5.1	237	140	0.591	102	0.000008	0.01	0.3827	0.0120	7.008	0.229	0.1328	0.0008	2089	56	2112	29	2136	10	98
6.1	137	58	0.427	84	0.000001	0.00	0.5403	0.0177	15.051	0.509	0.2020	0.0011	2785	74	2818	33	2843	9	98
7.1	394	60	0.151	229	0.000054	0.09	0.5451	0.0139	15.509	0.413	0.2063	0.0011	2805	58	2847	26	2877	8	98
8.1	101	49	0.484	21	0.000113	0.19	0.1986	0.0060	2.090	0.099	0.0763	0.0025	1168	33	1146	33	1104	66	106
9.1	736	15	0.021	377	0.000010	0.02	0.5040	0.0123	12.452	0.318	0.1792	0.0009	2631	53	2639	24	2645	9	99
10.1	379	191	0.505	74	0.000147	0.25	0.1853	0.0046	1.985	0.057	0.0777	0.0009	1096	25	1111	20	1139	24	96
12.1	561	235	0.418	107	0.000298	0.50	0.1846	0.0045	1.958	0.064	0.0769	0.0014	1092	25	1101	22	1119	38	98
11.2	287	132	0.461	58	0.000271	0.46	0.1940	0.0054	2.086	0.073	0.0780	0.0014	1143	29	1144	24	1147	37	100
13.1	273	267	0.98	58	0.000143	0.24	0.1828	0.0054	1.961	0.079	0.0778	0.0018	1082	30	1102	27	1142	48	95
14.1	266	90	0.34	188	0.000020	0.03	0.6208	0.0174	20.274	0.595	0.2369	0.0014	3113	69	3105	29	3099	10	101
15.2	59	44	0.74	47	0.000010	0.02	0.6333	0.0287	20.365	0.988	0.2332	0.0030	3163	114	3109	48	3074	20	103
16.1	1016	569	0.56	260	0.000202	0.34	0.2251	0.0054	5.230	0.131	0.1685	0.0009	1309	28	1858	22	2543	9	52
18.1	605	394	0.65	120	0.000010	0.02	0.1827	0.0044	1.966	0.053	0.0780	0.0007	1082	24	1104	18	1148	19	94
19.1	1019	357	0.35	144	0.001007	1.70	0.1448	0.0036	1.716	0.054	0.0860	0.0014	872	20	1014	20	1337	32	65
17.1	668	361	0.54	222	0.000218	0.37	0.3115	0.0078	6.622	0.174	0.1542	0.0009	1748	38	2062	23	2393	10	73
20.1	663	188	0.28	111	0.000325	0.55	0.1681	0.0040	1.795	0.050	0.0774	0.0009	1002	22	1044	18	1133	23	88
21.1	1511	682	0.45	146	0.002660	4.49	0.0916	0.0021	0.813	0.038	0.0644	0.0024	565	13	604	22	754	82	75
22.1	336	201	0.60	69	0.000010	0.02	0.1903	0.0050	2.031	0.058	0.0774	0.0007	1123	27	1126	20	1131	18	99
23.1	1133	290	0.26	206	0.001726	2.91	0.1739	0.0058	2.865	0.105	0.1195	0.0013	1034	32	1373	28	1949	20	53
24.1	679	126	0.19	125	0.000015	0.02	0.1900	0.0049	2.043	0.061	0.0780	0.0009	1121	27	1130	20	1147	23	98
25.1	184	144	0.79	81	0.000010	0.02	0.3988	0.0134	7.123	0.265	0.1296	0.0016	2163	62	2127	34	2092	22	103
26.1	1028	180	0.18	90	0.001100	1.86	0.0877	0.0021	0.904	0.038	0.0748	0.0024	542	12	654	21	1063	66	51
27.1	1210	53	0.04	256	0.000663	1.12	0.2187	0.0052	3.273	0.087	0.1086	0.0011	1275	27	1475	21	1776	18	72
28.1	67	73	1.08	52	0.000010	0.02	0.5903	0.0208	18.620	0.690	0.2288	0.0018	2991	85	3022	36	3044	13	98
29.1	182	112	0.61	97	0.000019	0.03	0.4541	0.0124	11.830	0.356	0.1890	0.0019	2413	55	2591	29	2733	16	88
30.1	394	112	0.28	184	0.000137	0.23	0.4319	0.0110	10.332	0.289	0.1735	0.0015	2314	50	2465	26	2592	15	89
31.1	72	59	0.82	45	0.000030	0.05	0.5212	0.0162	13.607	0.451	0.1893	0.0016	2704	69	2723	32	2736	14	99
32.1	396	205	0.52	78	0.000067	0.11	0.1870	0.0049	2.001	0.061	0.0776	0.0010	1105	27	1116	21	1137	25	97
33.1	264	185	0.70	119	0.000010	0.02	0.3911	0.0114	7.021	0.217	0.1302	0.0009	2128	53	2114	28	2101	13	101
34.1	343	166	0.48	191	0.000025	0.04	0.4914	0.0121	12.553	0.326	0.1853	0.0010	2577	53	2647	25	2701	9	95
35.1	60	36	0.59	44	0.000168	0.28	0.6063	0.0198	22.574	0.823	0.2701	0.0034	3055	80	3209	36	3306	20	92
36.1	319	157	0.49	59	0.000168	0.28	0.1738	0.0047	1.806	0.057	0.0753	0.0010	1033	26	1047	21	1077	27	96
37.1	405	279	0.69	84	0.000040	0.07	0.1888	0.0050	2.011	0.058	0.0773	0.0007	1115	27	1119	20	1129	19	99
38.1	412	163	0.40	41	0.001052	1.78	0.0938	0.0023	1.013	0.039	0.0783	0.0021	578	14	710	20	1155	55	50
39.1	102	62	0.61	20	0.000545	0.92	0.1877	0.0062	1.839	0.113	0.0711	0.0034	1109	33	1060	41	959	101	116
40.1	283	135	0.48	56	0.000240	0.41	0.1901	0.0051	2.043	0.076	0.0780	0.0018	1122	28	1130	26	1146	46	98
41.1	209	102	0.49	41	0.000288	0.49	0.1898	0.0060	2.174	0.097	0.0831	0.0023	1120	32	1173	32	1272	56	88
42.1	162	78	0.48	105	0.000067	0.11	0.5603	0.0154	16.969	0.491	0.2197	0.0014	2868	64	2933	28	2978	10	96
43.1	130	70	0.54	27	0.000036	0.06	0.1910	0.0066	2.062	0.083	0.0783	0.0013	1127	36	1136	28	1154	33	98
44.1	477	311	0.65	90	0.000064	0.11	0.1741	0.0044	1.850	0.052	0.0771	0.0007	1035	24	1063	19	1123	19	92
45.1	251	153	0.61	51	0.000127	0.22	0.1869	0.0050	1.995	0.064	0.0774	0.0011	1105	27	1114	22	1131	29	98
46.1	337	166	0.49	121	0.000042	0.07	0.3336	0.0094	5.728	0.179	0.1246	0.0013	1856	46	1936	27	2022	19	92
47.1	432	166	0.38	83	0.000063	0.11	0.1879	0.0053	2.005	0.068	0.0774	0.0012	1110	29	1117	23	1131	32	98
48.1	172	54	0.31	41	0.000086	0.15	0.2326	0.0068	2.815	0.105	0.0878	0.0018	1348	35	1359	28	1378	39	98
49.1	56	50	0.89	25	0.000683	1.03	0.3758	0.0161	6.563	0.350	0.1267	0.0034	2056	76	2054	48	2052	48	100
50.1	203	71	0.35	115	0.000093	0.13	0.5092	0.0162	13.544	0.447	0.1929	0.0011	2653	70	2718	32	2767	9	96
51.1	1442	369	0.26	98	0.000412	0.70	0.0655	0.0017	0.676	0.021	0.0748	0.0011	409	10	524	13	1064	29	38
52.1	134	83	0.62	27	0.000346	0.58	0.1888	0.0065	1.975	0.108	0.0759	0.0029	1115	36	1107	38	1092	79	102
53.1	104	105	1.01	25	0.000063	0.11	0.1989	0.0081	2.168	0.103	0.0791	0.0016	1169	44	1171	33	1174	39	100

Notes : Uncertainties given at the one σ level; f206 % denotes the percentage of 206Pb that is common Pb; for % Conc., 100% denotes a concordant analysis.

Appendix 8b: Summary of SHRIMP U-Th-Pb zircon results for sample B.HF.6.

Grain. spot	U (ppm)	Th (ppm)	Th/U	Pb* (ppm)	$^{204}Pb/^{206}Pb$	f_{206} %	Radiogenic Ratios $^{206}Pb/^{238}U$	±	$^{207}Pb/^{235}U$	±	$^{207}Pb/^{206}Pb$	±	Ages (in Ma) $^{206}Pb/^{238}U$	±	$^{207}Pb/^{235}U$	±	$^{207}Pb/^{206}Pb$	±	Conc. %
1.1	384	361	0.94	163	0.000030	0.05	0.3548	0.0110	5.929	0.197	0.1212	0.0011	1957	52	1966	29	1974	16	99
2.1	121	71	0.59	25	0.000010	0.02	0.1935	0.0127	2.135	0.152	0.0800	0.0017	1140	69	1160	51	1198	43	95
3.1	965	527	0.55	177	0.000266	0.45	0.1731	0.0048	1.786	0.056	0.0749	0.0008	1029	27	1040	21	1065	22	97
4.1	721	957	1.33	147	0.000698	1.18	0.1624	0.0047	1.683	0.061	0.0752	0.0013	970	26	1002	23	1073	36	90
5.1	579	418	0.72	110	0.000349	0.59	0.1727	0.0049	1.784	0.068	0.0749	0.0017	1027	27	1040	25	1066	45	96
6.1	471	246	0.52	95	0.000047	0.08	0.1893	0.0058	2.013	0.067	0.0771	0.0007	1118	31	1120	23	1124	19	99
7.1	130	92	0.71	28	0.000101	0.17	0.1932	0.0071	2.136	0.107	0.0802	0.0024	1138	38	1161	35	1202	61	95
8.1	108	70	0.65	22	0.000107	0.18	0.1814	0.0067	2.006	0.122	0.0802	0.0035	1075	37	1118	42	1202	89	89
9.1	610	351	0.58	125	0.000225	0.38	0.1887	0.0056	2.282	0.077	0.0877	0.0011	1115	31	1207	24	1376	24	81
10.1	269	179	0.66	53	0.000010	0.02	0.1774	0.0055	1.924	0.065	0.0787	0.0009	1053	30	1089	23	1164	22	90
11.1	622	164	0.26	111	0.000339	0.57	0.1800	0.0052	1.879	0.073	0.0757	0.0017	1067	28	1074	26	1088	46	98
12.1	356	294	0.83	131	0.000016	0.03	0.3199	0.0101	5.103	0.171	0.1157	0.0009	1789	49	1837	29	1891	15	95
13.1	161	172	1.07	37	0.000010	0.02	0.1886	0.0060	2.015	0.079	0.0775	0.0015	1114	32	1121	27	1134	39	98
14.1	230	170	0.74	49	0.000177	0.30	0.1912	0.0061	2.015	0.081	0.0764	0.0016	1128	33	1120	28	1106	43	102
15.1	179	105	0.59	38	0.000041	0.07	0.2008	0.0063	2.182	0.083	0.0788	0.0014	1180	34	1175	27	1168	36	101
16.1	1176	151	0.13	196	0.000425	0.72	0.1748	0.0049	1.814	0.056	0.0753	0.0008	1039	27	1050	20	1075	21	97
17.1	153	100	0.65	31	0.000158	0.27	0.1836	0.0075	1.999	0.094	0.0789	0.0015	1087	41	1115	32	1171	39	93
18.1	309	103	0.33	54	0.000415	0.70	0.1690	0.0104	1.991	0.138	0.0854	0.0022	1007	57	1112	48	1325	50	76
19.1	449	764	1.70	117	0.000326	0.55	0.1897	0.0070	1.984	0.089	0.0759	0.0016	1120	38	1110	31	1091	42	103
20.1	257	198	0.77	52	0.000125	0.21	0.1800	0.0055	1.926	0.083	0.0776	0.0021	1067	30	1090	29	1137	54	94
21.1	226	165	0.73	47	0.000068	0.11	0.1882	0.0055	2.051	0.069	0.0791	0.0010	1112	30	1133	23	1173	26	95
22.1	521	106	0.20	174	0.000684	1.15	0.3201	0.0096	6.405	0.207	0.1451	0.0012	1790	47	2033	29	2289	15	78
23.1	345	61	0.18	66	0.000078	0.13	0.1975	0.0061	2.089	0.074	0.0767	0.0010	1162	33	1145	25	1114	27	104
24.1	152	93	0.61	33	0.000139	0.24	0.1948	0.0066	2.079	0.104	0.0774	0.0025	1147	36	1142	35	1132	67	101
25.1	302	167	0.55	63	0.000090	0.15	0.1961	0.0058	2.111	0.069	0.0781	0.0009	1154	31	1152	23	1148	22	101
26.1	200	131	0.66	44	0.000043	0.07	0.1991	0.0065	2.114	0.078	0.0770	0.0011	1171	35	1153	26	1121	29	104
27.1	388	350	0.90	89	0.000045	0.08	0.1968	0.0059	2.208	0.078	0.0814	0.0012	1158	32	1183	25	1230	30	94
28.1	126	82	0.65	28	0.000010	0.02	0.2008	0.0065	2.180	0.084	0.0787	0.0014	1180	35	1175	27	1165	36	101
29.1	493	327	0.66	82	0.000830	1.40	0.1521	0.0046	1.581	0.077	0.0754	0.0026	913	26	963	31	1079	71	85
30.1	161	118	0.73	35	0.000010	0.02	0.1969	0.0066	2.039	0.078	0.0751	0.0011	1159	35	1129	26	1071	30	108
31.1	389	152	0.39	74	0.000255	0.43	0.1862	0.0055	2.009	0.079	0.0783	0.0018	1101	30	1119	27	1153	46	96
32.1	385	317	0.82	89	0.000010	0.02	0.2038	0.0063	2.166	0.077	0.0771	0.0011	1196	34	1170	25	1124	29	106
33.1	225	93	0.41	46	0.000166	0.28	0.1997	0.0059	2.047	0.071	0.0743	0.0011	1174	32	1131	24	1051	31	112
34.1	143	155	1.08	34	0.000037	0.06	0.1997	0.0061	2.120	0.075	0.0770	0.0011	1174	33	1155	25	1122	29	105
35.1	212	143	0.67	45	0.000010	0.02	0.1908	0.0057	2.035	0.066	0.0774	0.0008	1126	31	1127	22	1131	20	100
36.1	104	65	0.62	22	0.000220	0.37	0.1936	0.0067	2.042	0.109	0.0765	0.0028	1141	36	1130	37	1109	74	103
37.1	113	80	0.71	65	0.000547	0.92	0.4912	0.0153	11.245	0.394	0.1661	0.0021	2576	66	2544	33	2518	21	102
38.1	823	476	0.58	134	0.000725	1.22	0.1523	0.0060	1.492	0.067	0.0711	0.0012	914	34	927	28	959	35	95
39.1	242	69	0.29	64	0.000003	0.01	0.2588	0.0078	3.533	0.140	0.0990	0.0022	1484	40	1535	32	1606	42	92
40.1	3044	410	0.13	299	0.002491	4.21	0.1029	0.0030	0.934	0.076	0.0659	0.0047	631	18	670	40	803	158	79
41.1	257	50	0.20	96	0.000043	0.07	0.3679	0.0114	6.294	0.206	0.1241	0.0009	2020	54	2018	29	2016	13	100
42.1	193	49	0.25	101	0.000010	0.02	0.4940	0.0153	10.776	0.356	0.1582	0.0013	2588	66	2504	31	2437	14	106
43.1	26	108	4.24	21	0.000059	0.10	0.3929	0.0210	6.736	0.477	0.1243	0.0050	2136	98	2077	65	2019	73	106
44.1	154	119	0.77	35	0.000006	0.01	0.2033	0.0062	2.248	0.077	0.0802	0.0010	1193	33	1196	24	1201	24	99
45.1	181	135	0.75	40	0.000365	0.62	0.1963	0.0058	2.048	0.090	0.0757	0.0022	1155	31	1132	30	1086	58	106
46.1	235	209	0.89	53	0.000010	0.02	0.1935	0.0059	2.088	0.070	0.0783	0.0008	1140	32	1145	23	1153	21	99
47.1	173	69	0.40	103	0.000063	0.11	0.5391	0.0162	13.717	0.447	0.1845	0.0017	2780	68	2730	31	2694	16	103
48.1	954	478	0.50	168	0.000475	0.80	0.1675	0.0073	1.718	0.080	0.0744	0.0009	998	40	1015	30	1052	23	95
49.1	188	108	0.57	135	0.000025	0.04	0.6122	0.0219	17.638	0.692	0.2090	0.0026	3079	88	2970	38	2898	20	106
50.1	146	113	0.77	33	0.000134	0.23	0.2057	0.0064	2.196	0.098	0.0774	0.0022	1206	35	1180	31	1132	56	107
51.1	82	39	0.47	32	0.000173	0.29	0.3645	0.0123	6.086	0.228	0.1211	0.0016	2003	58	1988	33	1973	23	102
52.1	21	6	0.28	12	0.000010	0.02	0.5322	0.0261	12.858	0.713	0.1752	0.0036	2751	111	2669	54	2608	34	106
53.1	299	182	0.61	62	0.000722	1.22	0.1880	0.0058	2.068	0.107	0.0798	0.0030	1110	31	1138	36	1192	77	93
54.1	430	167	0.39	83	0.000013	0.02	0.1871	0.0053	2.052	0.062	0.0795	0.0006	1106	29	1133	21	1185	16	93
55.1	651	665	1.02	69	0.003336	5.63	0.0952	0.0044	0.945	0.069	0.0720	0.0037	586	26	675	37	985	108	60
56.1	695	706	1.02	146	0.000213	0.36	0.1777	0.0056	1.912	0.065	0.0781	0.0008	1054	31	1085	23	1148	19	92
57.1	242	130	0.54	49	0.0001022	0.17	0.1903	0.0057	2.016	0.073	0.0769	0.0013	1123	31	1121	25	1117	35	101
58.1	293	200	0.68	62	0.000194	0.33	0.1918	0.0056	1.991	0.070	0.0753	0.0012	1131	31	1113	24	1077	33	105
59.1	132	97	0.74	29	0.000215	0.36	0.1978	0.0069	2.035	0.088	0.0746	0.0016	1164	37	1127	30	1058	45	110
60.1	478	236	0.49	97	0.000066	0.11	0.1929	0.0059	2.088	0.072	0.0785	0.0010	1137	32	1145	24	1160	24	98

Notes : Uncertainties given at the one σ level; f206 % denotes the percentage of 206Pb that is common Pb; for % Conc., 100% denotes a concordant analysis.

Appendix 8c: Summary of SHRIMP U-Th-Pb zircon results for sample B.MA.4.

Grain. spot	U (ppm)	Th (ppm)	Th/U	Pb* (ppm)	$^{204}Pb/^{206}Pb$	f_{206} %	Radiogenic Ratios $^{206}Pb/^{238}U$	±	$^{207}Pb/^{235}U$	±	$^{207}Pb/^{206}Pb$	±	Ages (in Ma) $^{206}Pb/^{238}U$	±	$^{207}Pb/^{235}U$	±	$^{207}Pb/^{206}Pb$	±	Conc. %
1.1	535	30	0.06	114	0.000045	0.07	0.2242	0.0146	2.680	0.179	0.0867	0.0008	1304	77	1323	51	1353	18	96
2.1	73	109	1.50	48	0.000219	0.31	0.4812	0.0158	10.403	0.380	0.1568	0.0020	2532	69	2471	34	2422	21	105
3.1	446	447	1.00	95	0.000229	0.39	0.1821	0.0049	1.956	0.065	0.0779	0.0013	1078	27	1100	23	1144	33	94
4.1	402	384	0.96	91	0.000001	0.00	0.1914	0.0053	2.071	0.061	0.0785	0.0006	1129	29	1139	21	1159	14	97
5.1	1759	778	0.44	214	0.001186	1.98	0.1174	0.0030	1.107	0.035	0.0684	0.0011	716	17	757	17	879	35	81
6.1	485	173	0.36	89	0.000058	0.10	0.1821	0.0049	1.912	0.062	0.0762	0.0012	1078	27	1085	22	1099	31	98
7.1	176	163	0.93	40	0.000106	0.18	0.1964	0.0063	2.106	0.091	0.0778	0.0020	1156	34	1151	30	1141	51	101
8.1	263	224	0.85	57	0.000107	0.18	0.1898	0.0055	2.005	0.066	0.0766	0.0010	1120	30	1117	23	1112	26	101
9.1	38	31	0.81	17	0.000252	0.38	0.3882	0.0165	6.973	0.344	0.1303	0.0027	2114	77	2108	45	2102	36	101
10.1	375	121	0.32	66	0.001101	1.81	0.1810	0.0050	2.139	0.086	0.0857	0.0023	1073	27	1161	28	1331	52	81
12.1	448	273	0.61	92	0.000094	0.16	0.1901	0.0089	2.050	0.102	0.0782	0.0009	1122	48	1132	34	1153	24	97
13.1	151	109	0.72	33	0.000116	0.20	0.1959	0.0057	2.059	0.081	0.0762	0.0018	1153	31	1135	27	1101	48	105
14.1	512	377	0.74	90	0.000457	0.78	0.1591	0.0042	1.614	0.057	0.0736	0.0015	952	24	976	22	1030	41	92
15.1	274	197	0.72	58	0.000086	0.14	0.1917	0.0056	2.075	0.069	0.0785	0.0010	1131	30	1141	23	1159	26	98
16.1	162	111	0.68	34	0.000024	0.04	0.1900	0.0055	2.002	0.070	0.0764	0.0012	1121	30	1116	24	1107	32	101
17.1	92	45	0.50	38	0.000250	0.37	0.3852	0.0118	6.880	0.241	0.1295	0.0017	2101	55	2096	32	2092	24	100
18.1	91	35	0.39	38	0.000209	0.31	0.3898	0.0127	7.129	0.320	0.1326	0.0036	2122	59	2128	41	2133	48	100
19.1	882	219	0.25	178	0.000284	0.47	0.2031	0.0053	2.391	0.070	0.0854	0.0009	1192	29	1240	21	1324	19	90
20.1	79	78	0.99	18	0.000412	0.69	0.1973	0.0074	2.094	0.131	0.0770	0.0035	1161	40	1147	44	1120	94	104
21.1	331	213	0.64	64	0.000151	0.26	0.1772	0.0054	1.856	0.077	0.0760	0.0019	1052	30	1066	28	1095	50	96
22.1	90	62	0.69	48	0.000147	0.21	0.4594	0.0150	9.976	0.362	0.1575	0.0019	2437	67	2433	34	2429	21	100
23.1	98	106	1.07	24	0.000225	0.38	0.1988	0.0062	2.137	0.102	0.0780	0.0025	1169	33	1161	33	1146	66	102
24.1	98	70	0.71	44	1.53E-04	0.23	0.3869	0.0166	7.017	0.325	0.1316	0.0017	2108	77	2114	42	2119	23	100
25.1	237	131	0.55	58	0.000079	0.13	0.2288	0.0063	2.735	0.085	0.0867	0.0010	1328	33	1338	23	1354	22	98
26.1	376	333	0.89	82	0.000010	0.02	0.1892	0.0054	2.051	0.064	0.0786	0.0007	1117	29	1133	21	1162	18	96
27.1	633	39	0.06	135	0.000125	0.20	0.2232	0.0059	2.708	0.078	0.0880	0.0008	1299	31	1331	22	1382	18	94
28.1	627	1058	1.69	159	0.000050	0.08	0.1847	0.0049	2.010	0.057	0.0789	0.0006	1093	27	1119	19	1170	15	93
29.1	376	258	0.69	80	0.000010	0.02	0.1923	0.0051	2.027	0.060	0.0765	0.0007	1134	28	1125	20	1107	19	103
30.1	83	48	0.59	26	0.000275	0.44	0.2868	0.0105	4.012	0.209	0.1015	0.0033	1626	53	1637	43	1651	62	99
31.1	226	134	0.60	76	0.000100	0.16	0.3067	0.0089	4.440	0.143	0.1050	0.0011	1724	44	1720	27	1715	20	101
32.1	360	189	0.52	73	0.000029	0.05	0.1923	0.0051	2.043	0.060	0.0771	0.0007	1134	28	1130	20	1123	19	101
33.1	112	88	0.78	24	0.000404	0.68	0.1895	0.0060	1.963	0.101	0.0751	0.0028	1119	32	1103	35	1071	77	105
34.1	418	241	0.58	91	0.000116	0.20	0.2012	0.0056	2.139	0.067	0.0771	0.0009	1182	30	1161	22	1124	23	105
35.1	193	125	0.65	38	0.000426	0.72	0.1836	0.0052	1.878	0.076	0.0742	0.0019	1087	28	1073	27	1047	53	104
36.1	100	26	0.26	37	0.000044	0.06	0.3491	0.0147	7.629	0.366	0.1585	0.0029	1930	71	2188	44	2440	31	79
37.1	196	161	0.82	42	0.000255	0.43	0.1882	0.0102	1.959	0.118	0.0755	0.0016	1112	56	1102	41	1081	42	103
38.1	304	160	0.52	62	0.000021	0.04	0.1909	0.0053	2.035	0.064	0.0773	0.0009	1126	29	1127	22	1130	24	100
39.1	609	370	0.61	336	0.000019	0.03	0.4736	0.0132	11.881	0.346	0.1820	0.0011	2499	58	2595	28	2671	10	94
40.1	201	183	0.91	43	0.000149	0.25	0.1832	0.0051	1.966	0.066	0.0779	0.0012	1084	28	1104	23	1143	31	95
41.1	369	289	0.78	79	0.000052	0.09	0.1895	0.0081	2.038	0.092	0.0780	0.0007	1119	44	1128	31	1146	18	98
42.1	1731	110	0.06	335	0.000235	0.39	0.2038	0.0052	2.362	0.064	0.0841	0.0005	1196	28	1231	20	1294	12	92
43.1	425	150	0.35	82	0.000056	0.09	0.1901	0.0081	2.012	0.092	0.0768	0.0009	1122	44	1120	31	1116	23	101
44.1	40	57	1.45	10	0.000336	0.56	0.1972	0.0074	2.283	0.139	0.0840	0.0037	1161	40	1207	44	1291	88	90
45.1	104	51	0.49	62	0.000077	0.10	0.5242	0.0159	13.901	0.449	0.1923	0.0015	2717	68	2743	31	2762	13	98
46.1	265	247	0.93	58	0.000075	0.13	0.1879	0.0055	1.955	0.071	0.0755	0.0014	1110	30	1100	25	1082	38	103
47.1	808	401	0.50	317	0.000027	0.04	0.3614	0.0103	6.446	0.217	0.1294	0.0019	1989	49	2039	30	2089	26	95
48.1	352	158	0.45	67	0.000168	0.28	0.1823	0.0052	1.925	0.065	0.0766	0.0012	1080	28	1090	23	1111	31	97
49.1	136	96	0.71	29	0.000010	0.02	0.1888	0.0065	2.087	0.088	0.0802	0.0016	1115	35	1145	29	1201	40	93
50.1	681	664	0.98	144	0.000278	0.47	0.1778	0.0048	1.921	0.059	0.0784	0.0009	1055	26	1088	21	1156	22	91
51.1	481	484	1.01	107	0.000012	0.02	0.1879	0.0049	2.013	0.062	0.0777	0.0010	1110	27	1120	21	1140	26	97
52.1	82	63	0.76	36	0.000060	0.09	0.3788	0.0120	6.766	0.240	0.1295	0.0016	2071	56	2081	32	2092	22	99

Notes : Uncertainties given at the one σ level; f206 % denotes the percentage of 206Pb that is common Pb; for % Conc., 100% denotes a concordant analysis.